VIBRATIONS OF DISORDERED BINARY CHAINS

Thesis for the Degree of Ph. D.
MICHIGAN STATE UNIVERSITY
RONALD D. PAINTER
1973

This is to certify that the

thesis entitled

VIBRATIONS OF DISORDERED BINARY CHAINS

presented by

RONALD DEAN PAINTER

has been accepted towards fulfillment
of the requirements for

Ph.D. degree in Physics

Major professor

Date 3 May 1973

ABSTRACT

VIBRATIONS OF DISORDERED BINARY CHAINS

By

Ronald D. Painter

We have examined the vibrations of harmonic linear disordered atomic chains which include an arbitrary concentration of defects differing only in mass from the host atoms. This study included computer experiments on long chains and configuration average theories for infinite chains.

Using the theory of ergodic Markov chains, we generated disordered binary linear chains with short-range order among the constituents. Nearest-neighbors and second-nearest-neighbor correlations were explicitly introduced. For comparative purposes we also generated random chains. The relationship between the Markov correlation and the Warren-Cowley short-range order parameters was explored. Although a simple analytic relation exists for the first-order Markov chain, correlations generated by the second-order Markov chain cannot be described only by pair correlation functions. We computed the density of vibrational states for various of these chains, in the harmonic approximation with all

force constants equal. The spectra of chains of as many as 100,000 atoms were computed and the effect of short-range order on the spectra was determined. We explicitly computed the eigenvalues and eigenvectors for 1000 atom chains. The localization of normal modes (λ) was studied as a function of energy by calculating $\sum_{\ell} U_{\ell}^{4}(\lambda)$, where U_{ℓ} is the normalized displacement on site ℓ, and also by calculating an exponential decay parameter. We were, therefore, able to describe the region of appreciable amplitude of the eigenvectors as well as the decay rate away from this region. We have studied the vibrational density of states theoretically. Clusters of up to six atoms were firstly embedded in a uniform chain of host atoms, and, secondly, periodically extended to form a periodic chain. In each case the spectra of these chains, averaged over all configurations with short-range order included, were compared to those found experimentally. For defect concentration $\leq .5$ the embedded cluster gave good agreement with experiment in the impurity band especially in random systems, though it did not give information about the spectrum in the host band. The periodically extended cluster gave qualitative agreement with experiment for the whole spectrum for all concentrations of defects and all conditions of short-range order. The periodic cluster theory, however, introduced many spurious singularities in the density of states. Finally a modified self consistent cluster theory (cluster CPA)

was employed to calculate the density of states. For the seven site cluster, the agreement with experimental results was remarkably good. We found noticeable discrepancies between theory and experiment only where high degrees of short-range order were introduced.

VIBRATIONS OF DISORDERED BINARY CHAINS

By

Ronald D. Painter

A THESIS

Submitted to
Michigan State University
in partial fulfillment of the requirements
for the degree of

DOCTOR OF PHILOSOPHY

Department of Physics

1973

DEDICATION

I dedicate this thesis to my wife, Gloria, for her patience and understanding of my virtual absence from my family for the last two years.

ACKNOWLEDGEMENTS

Sincere thanks go to Professor William M. Hartmann for his guidance and friendship without which this thesis would not have been possible. I, also, wish to thank, Dr. Leonard, head of the Propulsion Department, Naval Weapons Center for his support of my receiving this degree. I am indebted to R. L. Bush for his discussions with me on the localization problem and to W. Butler for sending us his preprints. Finally, I wish to express gratitude to the following members of my thesis committee for consenting to critize this work:

Dr. William M. Hartmann

Dr. Thomas A. Kaplan

Dr. Jack Bass

Dr. Frank J. Blatt

Dr. George F. Bertsch

TABLE OF CONTENTS

LIST OF TABLES

LIST OF FIGURES

CHAPTER I

INTRODUCTION

Historical Review

The modern theory of lattice dynamics began in 1912 with the work of Debye[1] and Born and von Karman,[2] although Newton in Principia (C. 1686) began the study of lattices by using a chain of masses connected by harmonic springs to calculate the velocity of sound in air. The first qualitative properties of lattices appeared around 1840 in response to the work of Cauchy on the theory of optical dispersion. Baden-Powell[3] and Hamilton[4] showed that there is a maximum frequency, below which waves can be transmitted through lattices unattenuated and above which, the wave is attenuated. Lord Kelvin[5,6] gave the best discussion of the physical significance of Hamilton's mathematical results. He, also, showed that the diatomic lattice has a forbidden gap in the frequency spectrum.

Lord Rayleigh[7] in the Theory of Sound derived two theorems for a single defect in a monatomic lattice that have a direct relation to defect modes in crystal lattices.

1. "If in a dynamical system composed of an array of masses coupled to each other by Hookeian Springs, a single mass is reduced (increased) by ΔM, all frequencies are unchanged or increased (decreased), but not more than the distance to the next unperturbed frequency."
2. Modes at the band edge may split off and enter the forbidden frequency regions.

These theorems are clearly demonstrated in Appendix I. Although these results were obtained in the 1880's, it was not until 1957 that Bjork[8] gave analytic expressions for the location of the frequency of the mode in the forbidden gap as a function of mass defect and force constant defect for monatomic and diatomic chains. For a detailed history and two and three dimensional applications see Reference (9).

Classical Lattice Dynamics

Classical lattice dynamics formulated by Born and von Karman employed a Hamiltonian with a kinetic energy and a central pair potential. For the one dimensional case

$$H = \sum_{\ell,\alpha} \frac{p_\alpha^2(\ell,t)}{2m_\alpha(\ell)} + \frac{1}{2} \sum_{\ell,\ell'} V(R_{\ell,\ell'}+U_{\ell,\ell'}^{(t)}) \qquad (1.1)$$

$$R_{\ell,\ell'} = R_{\ell} - R_{\ell'} = (\ell - \ell')a$$

$$U_{\ell,\ell'} = U(\ell) - U(\ell')$$

where a is the lattice constant and t is time.

The latin indices indicate unit cells and greek indices refer to different atoms in the unit cell. R denotes unit cell positions and U represents displacements from the mean atomic positions. $P_{\alpha}(\ell,t)$ is the momentum of the atom of mass, m_{α}, at the α^{th} atom in the ℓ^{th} unit cell. V is the pair potential. Expanding the pair potential in a Taylor series about the displacements from equilibrium, we get

$$V(R_{\ell,\ell'}+U_{\ell,\ell'}) = V(R_{\ell,\ell'}) + \sum_{\beta} \frac{\partial V}{\partial U_{\beta}(\ell')}\Big|_{R_{\ell,\ell'}} U_{\beta}(\ell')$$

$$+\frac{1}{2} \sum_{\alpha,\beta} U_{\alpha}(\ell) \frac{\partial^2 V}{\partial U_{\alpha}(\ell)\partial U_{\beta}(\ell')}\Big|_{R_{\ell,\ell'}} U_{\beta}(\ell') + \ldots$$

The first term is an arbitrary constant and the second term is zero for a lattice in equilibrium. To first approximation only the harmonic term remains. The Hamiltonian can be rewritten in the harmonic approximation as

$$H = \sum_{\ell,\alpha} \frac{P_{\alpha}^2(\ell,t)}{m_{\alpha}(\ell)} + \frac{1}{2} \sum_{\substack{\ell\ell' \\ \alpha\beta}} U_{\alpha}(\ell,t)\phi_{\alpha\beta}(\ell,\ell')U_{\beta}(\ell',t) \qquad (1.3)$$

where

$$\phi_{\alpha\beta}(\ell,\ell') = \frac{\partial^2 V}{\partial U_\alpha(\ell)\,\partial U_\beta(\ell')}\Big|_{R_{\ell,\ell'}}$$

Using Hamilton's equations of motion we get

$$m_\alpha(\ell)\ddot{U}_\alpha(\ell,t) = \sum_{\ell',\beta} \phi_{\alpha\beta}(\ell,\ell')U_\beta(\ell',t) \tag{1.4}$$

Fourier transforming Equation (1.4), we have

$$m_\alpha(\ell)\omega^2 U_\alpha(\ell) = -\sum_{\ell'\beta} \phi_{\alpha\beta}(\ell,\ell')U_\beta(\ell') \tag{1.5}$$

where

$$U_\alpha(\ell) = \frac{1}{2\pi}\int_{-\infty}^{\infty} U_\alpha(\ell,t)e^{i\omega t}dt$$

For $m_\alpha(\ell) = m_\alpha$ independent of ℓ, the eigenvalue Equation (1.5) can be diagonalized by expanding the displacements in plane waves.

$$U_\alpha(\ell) = \sum_{k,j} \frac{Q_j(k)}{\sqrt{Nm_\alpha}}\sigma_{\alpha j}(k)\, e^{ik\cdot R_\ell} \tag{1.6}$$

where the $Q_j(k)$'s are the normal coordinates of the lattice and the $\sigma_{\alpha j}(k)$'s are the expansion coefficients, j is the branch index.

Substituting Equation (1.6) into Equation (1.5), we have

$$\frac{m_\alpha}{N}\ \omega^2 \sum_{k,j} Q_j(k)\sigma_{\alpha j}(k)e^{ik\cdot R_\ell} = -\sum_{\ell',\beta} \phi_{\alpha\beta}(\ell,\ell') \sum_{k,j} \frac{Q_j(k)\sigma_{\beta j}(k)}{\sqrt{Nm_\beta}} e^{ik\cdot R_{\ell'}}$$

Multiplying by $e^{-k'\cdot R_\ell}$ and summing over ℓ where

$$\sum_\ell e^{ik\cdot R_\ell} = N\delta(k)$$

and then the LHS over k, we have

$$\sqrt{N\ m_\alpha}\ \omega^2 \sum_j Q_j(k)\sigma_{\alpha j}(k) = -\sum_{\substack{\ell',\ell \\ \beta,jk}} \frac{\phi_{\alpha\beta}(\ell,\ell')}{\sqrt{m_\beta N}} Q_j(k)\sigma_{\beta j}(k)\ e^{i(kR_{\ell'}-k'R_\ell)}$$

Let $D_{\alpha\beta}(k) = \sum_{\ell'} \frac{\phi_{\alpha\beta}(\ell,\ell')}{\sqrt{m_\alpha m_\beta}} e^{ik\cdot(R_{\ell'}-R_\ell)}$ (1.7)

$$\omega^2 \sum_j Q_j(k)\sigma_{\alpha j}(k) = -\frac{1}{N} \sum_{\substack{\ell,\beta \\ jk}} D_{\alpha\beta}(k)Q_j(k)\sigma_{j\beta}(k)e^{i(k-k')R_\ell}$$

summing over ℓ and k and rearranging we get

$$\sum_j Q_j(k)\left[\omega_j^2(k)\sigma_{\alpha j}(k) + \sum_\beta D_{\alpha\beta}(k)\sigma_{\beta j}(k)\right] = 0$$

Since $Q_j(k) \neq 0$, we have

$$\omega_j^2(k)\sigma_{\alpha j}(k) = -\sum_\beta D_{\alpha\beta}(k)\sigma_{\beta j}(k) \qquad (1.8)$$

The $\sigma_{j\alpha}(k)$'s obey the usual closure and completeness conditions

$$\sum_j \sigma^*_{\alpha j}(k)\sigma_{\beta j}(k) = \delta_{\alpha\beta} \qquad (1.9a)$$

$$\sum_{\alpha} \sigma^{*}_{\alpha j}(k)\ \sigma_{\alpha j'}(k) = \delta_{jj'} \qquad (1.9b)$$

For the monatomic linear chain, we have only one atom per unit cell and one branch; therefore

$$\omega_j^2(k) = -D(k)$$

and σ is real

$$D(k) = \sum_{\ell'} \frac{\phi(\ell,\ell')}{m} e^{ika(\ell'-\ell)}$$

since $\phi(\ell,\ell') = \begin{cases} \gamma\delta_{\ell,\ell\pm1} \\ -2\gamma\delta_{\ell,\ell'} \end{cases}$

$$D(k) = \frac{\gamma}{m}(e^{ika}+e^{-ika}-2) = -\frac{4\gamma}{m}\sin^2(\frac{ka}{2})$$

or

$$\omega_j^2(k) = \omega_{max}^2 \sin^2(\frac{ka}{2}) \quad \text{for } k = \frac{2\pi}{aN}n \quad n=0,1,2,\ N-1 \qquad (1.10)$$

The density of states is

$$\nu(\omega) = \frac{a}{\pi}\frac{dk}{d\omega} = \frac{2}{\pi}\frac{1}{(\omega_m^2-\omega^2)^{\frac{1}{2}}}$$

or $$D(\omega^2) = \frac{1}{\pi}\frac{1}{\omega(\omega_m^2-\omega^2)^{\frac{1}{2}}} \quad 0\leq\omega\leq\omega_m \qquad (1.11a)$$

$$= 0 \quad \omega>\omega_m$$

Appendix G gives similar derivations for bases of 2,3,4 and 6 atoms for 2 constituent chains. For convenience Equation (1.11a) is rewritten

$$D(\omega^2) = \frac{1}{\pi} \mathrm{Re}\left(\frac{1}{\omega\sqrt{\omega_m^2 - \omega^2}}\right) \quad \omega > 0 \tag{1.11b}$$

where Re(...) is the real part of (...). For the diatomic chain of masses m_a and m_b with all force constants equal

$$D(\omega^2) = \frac{1}{\pi\omega} \mathrm{Re}\left(\frac{\gamma\left(\frac{1}{m_a} + \frac{1}{m_b}\right) - \omega^2}{\sqrt{\omega^2 - \frac{2\gamma}{m_a}}\sqrt{\omega^2 - \frac{2\gamma}{m_b}}\sqrt{\omega^2 - 2\gamma\left(\frac{1}{m_a} + \frac{1}{m_b}\right)}^{1}}\right) \tag{1.12}$$

where we define $\sqrt{-1} = +i$

Both of these spectra have square root singularities in ω^2. The diatomic spectrum clearly has a gap between $\frac{2\gamma}{m_a}$ and $\frac{2\gamma}{m_b}$.

The frequency spectrum of the monatomic chain was first given by Born and von Karman.[2] Unfortunately, their atomistic approach to lattice dynamics was neglected for approximately thirty years because calculations in three dimensions are difficult. Two approximations were used. In 1907 Einstein[10] proposed treating the lattice as N uncoupled harmonic oscillators of frequency ω_E. The density of states normalized to one is

$$\nu_E(\omega) = \delta(\omega - \omega_E) \tag{1.13}$$

An improved approximation was proposed by Debye,[1] where he related the spectra of allowed frequencies to the properties of the elastic continuum. Debye's 3-dimensional density of states is

$$\nu_D(\omega) = \frac{3}{\omega_{max}^3} \omega^2 \theta(\omega_{max}-\omega) \qquad (1.14)$$

where θ is the unit step function. The 1-dimensional analogy of this density of states is

$$\nu_D(\omega) = \omega_{max}^{-1} \theta(\omega_{max}-\omega) \qquad (1.15)$$

Both of these approximations allow simple calculation of thermodynamic properties but the models are too simplified for accurate calculations, even for thermodynamic calculations.

The spectra of disordered chains were not considered until the 1950's. The first significant work on disordered lattices was by Lifshitz[11] and, independently, by Montroll and Potts.[12] Their work involved the use of classical Green's functions to compute the properties of isolated defects in crystal lattices. Dyson[13] in 1953 had already presented a detailed theoretical approach to finding the density of states of a one-dimensional linear chain with equal nearest neighbor force constants. Unfortunately, Dyson's analytic expressions have not been numerically solved. In 1957, Schmidt[14] derived a functional equation for the random, linear chain which was solved numerically in 1964 by Agacy.[15] The first significant numerical attempts at calculating the spectra of a disordered chain were by the moment-trace method. Maradudin, et al.[16] had

shown that the expansion of the density of states in terms of its moments involved only even moments. For the perfect monatomic or diatomic chain 14 moments gave reasonable results except near the spectra singularities. The moments are given by

$$u_{2n} = \frac{1}{N} \sum_{jk} \omega_j^{2n}(k) = \frac{1}{N} \mathrm{Tr}(D^N) = \int \omega^{2n} \nu(\omega) d\omega \qquad (1.16)$$

where tr is the trace
D is the dynamical matrix defined in Equation (1.7)
$\nu(\omega)$ is the density of states

Domb, et al.[17] reasoned that the disordered system should not possess the high frequency singularities and that the moment-trace method would be better for the disordered case than it was for the ordered chain. Their resulting spectra calculated from 20 momenta were relatively smooth with some bumps at the high frequency end which were attributed to clusters of light (impurity) atoms. However, the arguments and results of Domb, et al. are quite wrong. We show in the next section the spectrum of a disordered chain has a great deal of structure, more, not less, than the perfect chain. This in effect requires many moments to approximate a spectrum with no assurance that the higher moments are the smaller ones.

CHAPTER II

NUMERICAL CALCULATIONS FOR RANDOM BINARY CHAINS

Numerical Methods

To calculate the spectrum of a disordered chain requires some numerical effort. In one-dimension a single defect (or disordered atom) destroys the translational symmetry of the lattice. Plane waves will no longer diagonalize the eigenvalue Equation (1.5) and the solution to Equation (1.5) must be found directly.

Three types of boundary conditions are applicable to a chain of length, N. These are:

1. Fixed boundary conditions where $U_o=U_{N+1}=0$
2. Cyclic (Born and von Karman) boundary conditions where $U_1=U_{N+1}$
3. Free boundary conditons

Equation (1.5) can be rewritten as

$$m_i\omega^2 U_i = -\gamma_{i,i+1}(U_{i+1}-U_i)-\gamma_{i,i-1}(U_{i-1}-U) \qquad (2.1)$$

which for equal force constants reduces to

$$m_i\omega^2 U_i = -\gamma(U_{i+1}+U_{i-1}-2U_i) \tag{2.2}$$

subject to the boundary conditions listed above. In matrix form Equation (2.2) becomes

$$\underline{\underline{A}}\ \underline{U} = \omega^2 \underline{U} \tag{2.3}$$

when boundary conditions are applied, $\underline{\underline{A}}$ is specifically given by

1. $$A_{i,j} = \frac{2\gamma}{m_i}\delta_{i,j} - \frac{\gamma}{m_i}\delta_{i\pm1,j} \tag{2.4}$$

for fixed boundary conditions.

2. $$A_{i,j} = \frac{2\gamma}{m_i}\delta_{i,j} - \frac{\gamma}{m_i}\delta_{i\pm1,j} - \frac{\gamma}{m_i}\delta_{N,j}\delta_{i,1} - \frac{\gamma}{m_N}\delta_{N,i}\delta_{1,j} \tag{2.5}$$

for cyclic boundary conditions.

3. $$A_{i,j} = \left(\frac{2\gamma}{m_i} - \frac{\gamma}{m_i}(\delta_{i,1}+\delta_{i,N})\right)\delta_{i,j} - \frac{\gamma}{m_i}\delta_{i\pm1,j}$$

for free boundary conditions.

The matrix A is tridiagonal for free and fixed boundary conditions. The only difference in the matrix for the two is in the (1,1) and (N,N) diagonal elements given by $2\gamma/m_i$ for fixed boundary conditions and by γ/m_i for free boundary conditions. Clearly, one could easily mix the free and fixed boundary conditions. For cyclic boundary

conditions A is identical to the matrix for fixed boundary conditions except for the addition of non-zero (1,N) and (N,1) elements. The question of which boundary condition to impose on the problem is moot when one considers the following theorem proved by Ledermann:[22]

> If the elements of r rows and their corresponding columns of a Hermitian matrix are modified in any way whatever, as long as the matrix remains Hermitian, the number of eigenvalues in any interval cannot increase or decrease by more than 2r.

The three types of boundary conditions differ by only two elements from each other, and, therefore, no frequency interval may contain more than four additional eigenvalues or four fewer eigenvalues. As long as a frequency interval contains many eigenvalues compared to four, the frequency spectrum will be independent of boundary conditions. The eigenvectors, however, are another matter which we will discuss later. Therefore, for ease of numerical computation, we use fixed boundary conditions. The matrix A in Equation (2.4) can be made symmetric by the transformation

$$X_i = \sqrt{m_i}\, U_i \tag{2.6}$$

Then
$$\underline{\underline{A}}' \underline{X} = \omega^2 \underline{X} \tag{2.7}$$

where
$$A'_{i,j} = \frac{2\gamma}{m_i} \delta_{i,j} - \frac{\gamma}{\sqrt{m_i m_{i\pm1}}} \delta_{i\pm1,j} \tag{2.8}$$

The eigenvalues of $\underline{\underline{A}}$ and $\underline{\underline{A}}'$ are identical although the corresponding eigenvectors are different. $\underline{\underline{A}}'$ is now a

tridiagonal symmetric matrix. The Given's method for finding eigenvalues of a tridiagonal symmetric matrix can be employed.[42] Appendix A gives a description of the method and application to this problem. P. Dean[18] in 1959 first applied this technique to a disordered linear chain. Besides Dean and his coworkers,[19] Payton and Visscher[20] have performed similar numerical calculations for the spectra of disordered systems, including small two and three dimensional lattices. Also, Dean has performed these calculations on glass-like chains where the force constants vary in a probabilistic fashion. An excellent review article is Reference (21).

Numerical Spectra

The spectra of disordered chains presented in this section serve as an introduction to spectra with short range order. These spectra have been recalculated from Dean's work to conform to the rest of the spectra presented in the thesis. The spectra for the random chains are for a mass ratio of heavy to light mass of 2. The concentration of light mass will be called, C_d. To generate a chain of length, N, with a concentration C_d of light masses, we employ a random number generator which generates random numbers from zero to one. For each atom, the generator is sampled and if the number is less than C_d the atom is labeled a light mass (defect);

other wise, it is a heavy mass (host). A statistical analysis shows that 32% of the 100 unit chains generated for C_d =.5 will have C_d<.45 or >.55. By contrast, for N=1000, about 5% of the chains will have C_d<.49 or >.51. One of the problems with random chains is a determination of the length of chain necessary to insure a reasonably accurate spectrum. To examine this variability, we look at chains of 1000, 10000, 50000, and 100000 atoms. Whereas a spectrum for a 10000 unit chain requires less than thirty seconds on the UNIVAC 1108, the 100000 unit chain requires over five minutes of CPU. Figures (2.1) and (2.2) show spectra of two 1000 unit chains with concentrations of .43 and .48 light masses respectively. In the region $2 \leq \omega^2 \leq 4$, the two graphs are nearly identical with the only serious descrepancy occuring near $\omega^2=4$. The region .3 to 2, however, shows a large degree of variability. Figure (2.3) shows the fifty percent random 10000 unit chain with an actual concentration of C_d=.4956. The ω^2 region 2 to 4 is much the same as in the 1000 unit chains; however, there is a definite refinement in the spectrum in this region especially in the magnitudes of the maximums and minimums. The ω^2 region from .3 to 2 is markedly smoother around $D(\omega^2)$=.25 than the 1000 unit spectra. Figure (2.4) for the 50000 unit chain with C_d=.50093, is almost identical to the 10000 unit chain except for further smoothing in the .3 to 2 ω^2 region. Figure (2.5)

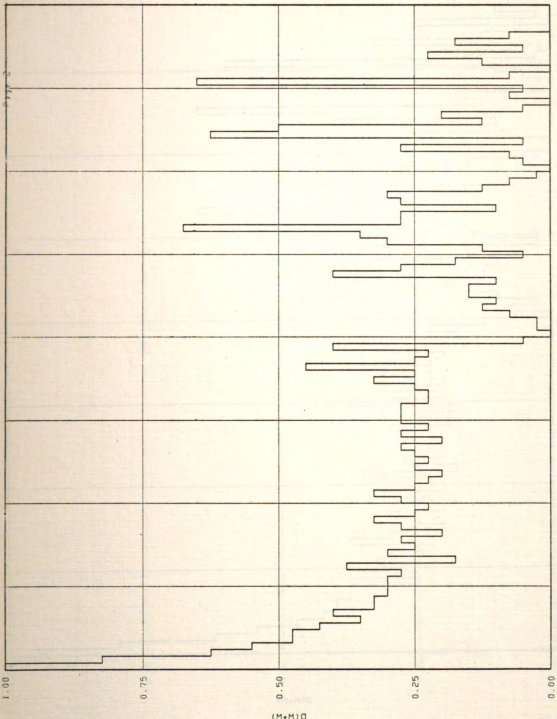

FIGURE 2.1.--Numerical density of states for a 50% random binary chain of length 1000 and mass ratio 2/1, Case 1.

FIGURE 2.2.--Numerical density of states for 50% random binary chain of length 1000 and mass ratio 2/1, Case 2.

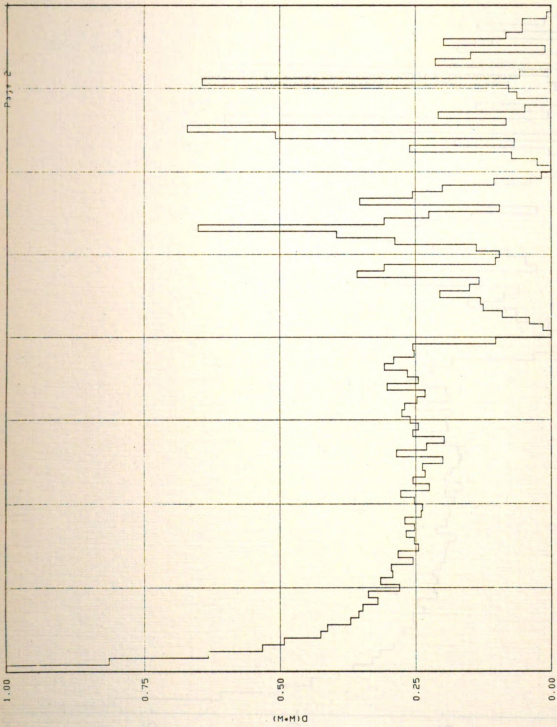

FIGURE 2.3.--Numerical density of states for a 50% random binary chain of length 10000 atoms and mass ratio 2/1.

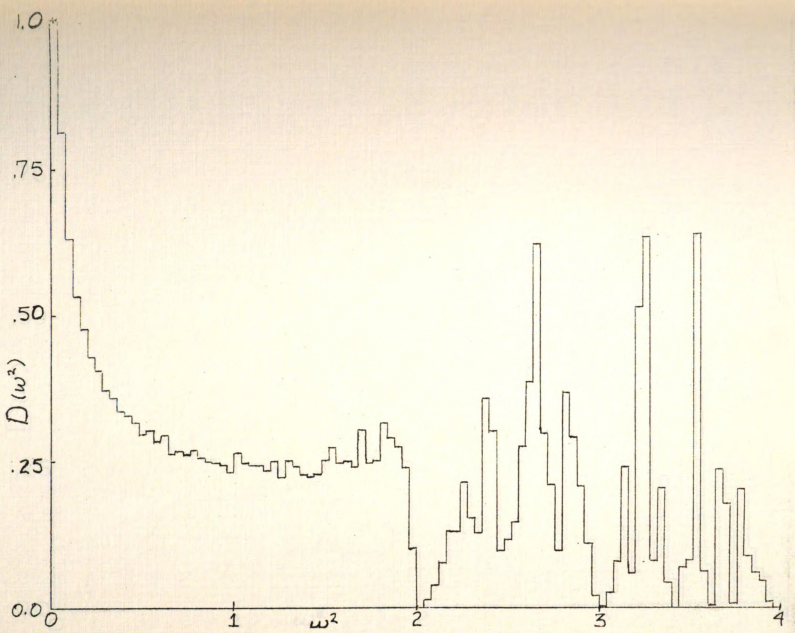

FIGURE 2.4.--Numerical density of states for a 50% random binary chain of length 50000 atoms and mass ratio 2/1.

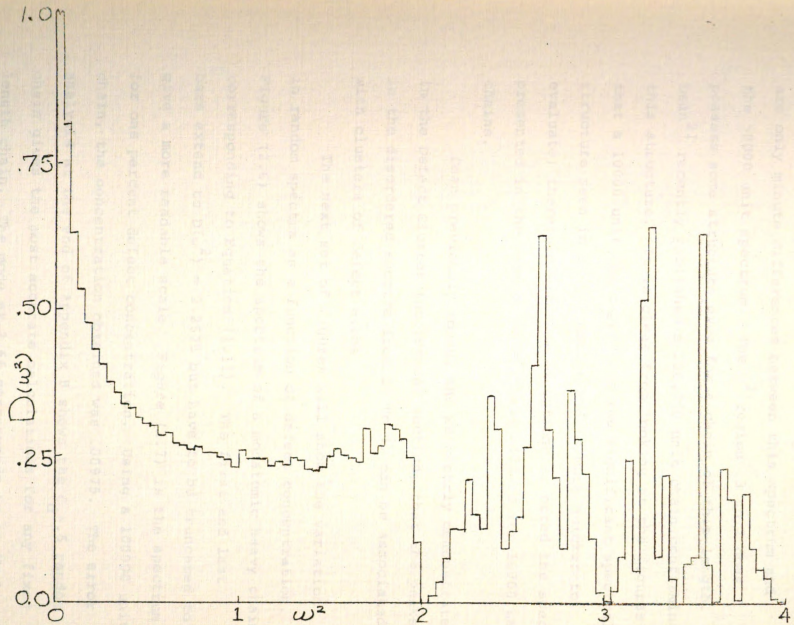

FIGURE 2.5.--Numerical density of states for a 50% random binary chain of length 100000 atoms and mass ratio 2/1.

shows the 100000 unit spectrum with C_d=.49809. There are only minute differences between this spectrum and the 50000 unit spectrum. The ω^2 region .3 to 2 does possess some structure even for a chain of this length. Dean[21] recently published a 250,000 unit chain confirming this structure. It is clear from looking at the figures that a 10000 unit chain provides the significant spectral structure seen in longer chains and is much quicker to evaluate; therefore with few exceptions as noted the spectra presented in the rest of this thesis will be for 10000 unit chains.

Dean previously found, and we clearly demonstrate in the Defect Cluster theoretical section, that the peaks in the disordered spectra from 2. to 4. can be associated with clusters of defect atoms.

The next set of figures will show the variation in random spectra as a function of defect concentration. Figure (2.6) shows the spectrum of a monatomic heavy chain corresponding to Equation (1.11). The first and last bars extend to $D(\omega^2)$ = 2.2575 but have to be truncated to give a more readable scale. Figure (2.7) is the spectrum for one percent defect concentration. Using a 100000 unit chain, the concentration obtained was .00975. The error analysis at the end of Appendix B shows the C_d=.5 random chain gives the most accurate calculations for any fixed length chain. The mode at 2.66 corresponds to an isolated

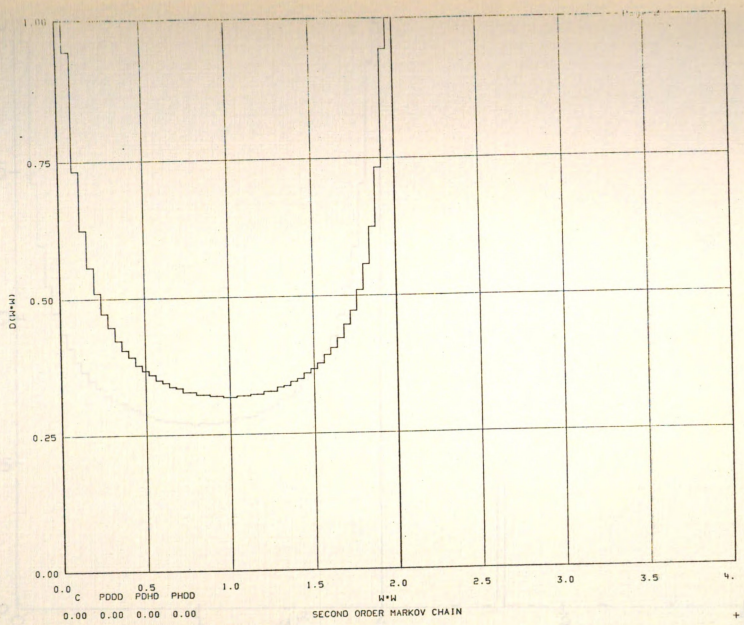

FIGURE 2.6.--Numerical density of states for a monatomic heavy chain of length 10000 atoms.

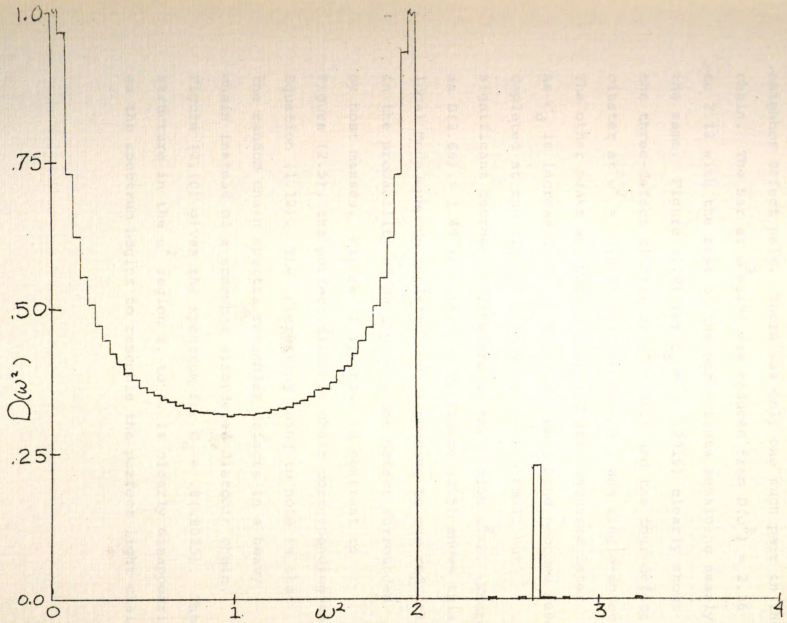

FIGURE 2.7.--Numerical density of states for a 1% random light mass binary chain of mass ratio 2/1 and 100,000 atoms.

defect whereas the mode at 3.22 corresponds to a nearest-neighbor defect pair. There was only one such pair in the chain. The bar at ω^2=1.98 was reduced from $D(\omega^2)$ = 2.26 to 2.12 with the rest of the bar heights remaining nearly the same. Figure (2.8) for C_d = .2(.2019) clearly shows the three-defect cluster at ω^2 = 3.54 and the four-defect cluster at ω^2 = .366 as well as the pair and single-defect. The other peaks are more subtle and are discussed later. As C_d is increased to 0.2 the heavy mass band becomes severely depleted at the high frequency end with a small but significant decrease everywhere in the region ω^2<2. Whereas D(2.66) = 1.45 in Figure (2.8), Figure (2.5) shows this local mode severely depleted, corresponding to the reduction in the probability of having only one defect surrounded by host masses. Figure (2.9) shows in contrast to Figure (2.5), the perfect diatomic chain corresponding to Equation (1.12). The interesting thing to note is that the random chain spectra resembles defects in a heavy chain instead of a somewhat disordered diatomic chain. Figure (2.10) gives the spectrum for C_d = .8(.8025). The structure in the ω^2 region 2. to 4. is clearly disappearing as the spectrum begins to resemble the perfect light chain.

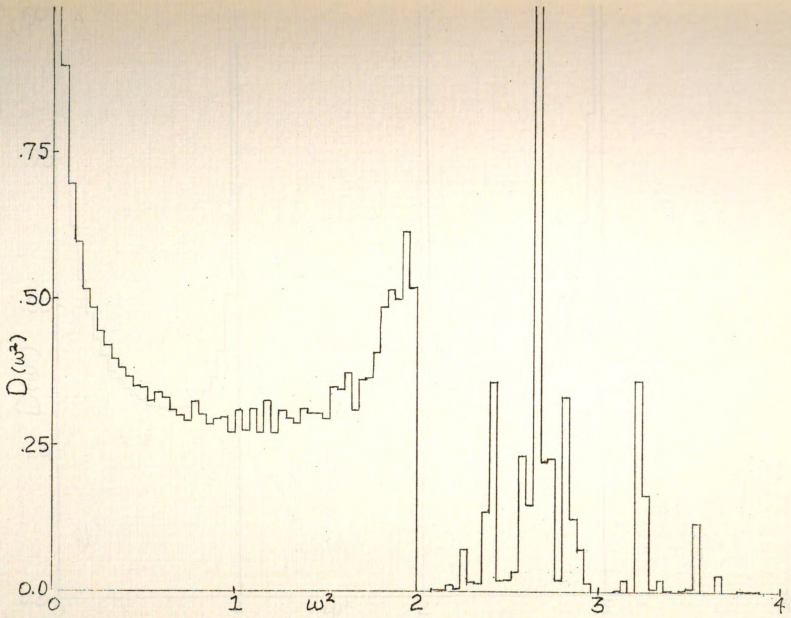

FIGURE 2.8.--Numerical density of states for a 20% random light mass chain of mass ratio 2/1 and 10000 atoms.

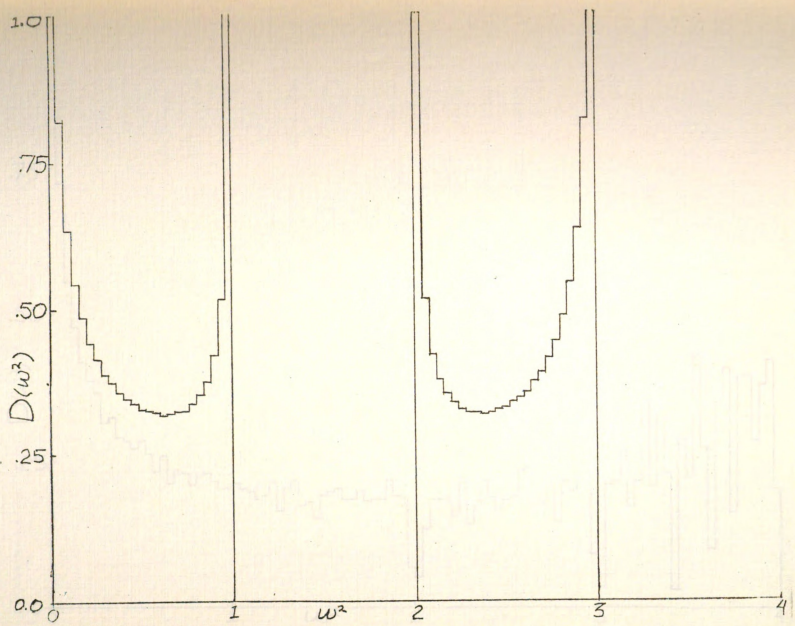

FIGURE 2.9.--Numerical density of states for a 50% ordered diatomic chain of mass ratio 2/1 and 10000 atoms.

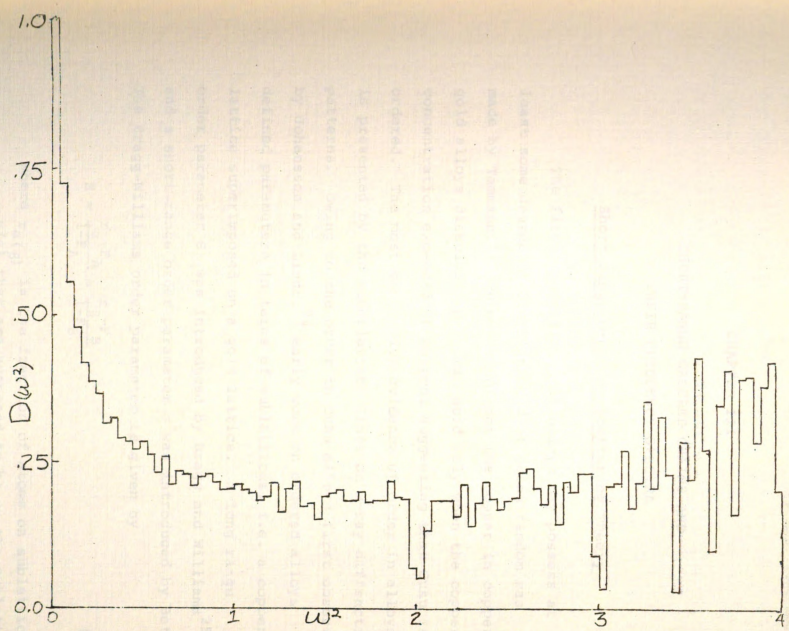

FIGURE 2.10.--Numerical density of states for a 80% random light mass chain of mass ratio 2/1 and 10000 atoms.

CHAPTER III

SHORT-RANGE ORDERED CHAINS AND THEIR FREQUENCY SPECTRA

Short Range Order in Scattering Theory

The first suggestion that alloys may possess at least some degree of order instead of being random was made by Tammann.[23] He observed that the copper in copper-gold alloys dissolved in nitric acid only when the copper concentration exceeded 50 percent suggesting that CuAu is ordered. The most conclusive evidence of order in alloys is presented by the superlattice lines on x-ray diffraction patterns. Owing to the order in CuAu alloys first observed by Johansson and Linde,[24] early work on ordered alloys defined parameters in terms of sublattices, i.e. a copper lattice superimposed on a gold lattice. A long range order parameter S was introduced by Bragg and Williams[25] and a short-range order parameter σ was introduced by Bethe.[26] The Bragg-Williams order parameter is given by

$$S = \frac{r_\alpha - F_A}{1 - F_A} = \frac{r_\beta - F_B}{1 - F_B} \tag{3.1}$$

where $r_{\alpha(\beta)}$ is the fraction of atoms on sublattice $\alpha(\beta)$ that are supposed to be on the sublattice $\alpha(\beta)$. $F_{A(B)}$ is the concentration of constituent A(B).

For a perfectly ordered system, $r_\alpha = r_\beta = 1$ and S=1, and for a disordered system (i.e. a system with no long range order) $r_\alpha = F_A$ and $r_\beta = F_B$ and S=0. The Bethe short-range order parameter is concerned only with the configuration of nearest neighbors.

$$\sigma = (q-q_r)/(q_m-q_r) \tag{3.2}$$

where q is the fraction of unlike pairs among nearest neighbors q_m is the fraction of unlike nearest neighbors for an ordered system (usually one) and q_r is the fraction of unlike nearest neighbors for a completely random system.

Therefore σ=1 represents a perfectly ordered system and σ=0 a random system. Only in the limit σ=1 does the short-range order parameter imply long-range order; generally, a system can have short-range order without long-range order. These order parameters represent the two extremes of the definition of order. The Bragg-Williams deals with the order present in the whole system whereas the Bethe parameter is concerned with only nearest neighbors. The concept of short range order must be generalized to understand the results of x-ray scattering experiments. Warren, Cowley[27] and Moss[28] introduced short-range order parameters in terms of conditional pair correlation functions for binary alloys as $\rho^{d,d}_{\ell_1,\ell_2}$, $\rho^{d,h}_{\ell_1,\ell_2}$, $\rho^{h,d}_{\ell_1,\ell_2}$ and $\rho^{h,h}_{\ell_1,\ell_2}$ and

$$\rho^{d,d}_{\ell_1,\ell_2} = C_d + (1-C_d)\alpha_{\ell_1,\ell_2} \tag{3.3}$$

where $\rho^{d,d}_{\ell_1,\ell_2}$ is the conditional pair correlation function between defects at sites ℓ_1 and ℓ_2, and α_{ℓ_1,ℓ_2} is the short-range order parameter.

Specifically, $\rho^{d,d}_{\ell_1,\ell_2}$ is the probability that if there is a defect at site ℓ_1, then there is a defect at site ℓ_2. From this definition we can deduce the following

$$\rho^{d,d}_{\ell_1,\ell_2} + \rho^{d,h}_{\ell_1,\ell_2} = 1 \tag{3.4}$$

$$\rho^{h,h}_{\ell_1,\ell_2} + \rho^{h,d}_{\ell_1,\ell_2} = 1 \tag{3.5}$$

since given that site ℓ_1 is occupied by a certain atom, ℓ_2 must be a host or defect for a binary system. For an isotropic system, the probability that site ℓ_1 is a host and ℓ_2 is defect must be equal to the probability that site ℓ_1 is a defect and site ℓ_2 is a host, i.e.

$$C_d \rho^{d,h}_{\ell_1,\ell_2} = C_h \rho^{h,d}_{\ell_1,\ell_2} \tag{3.6}$$

From Equation (3.3), we see α_{ℓ_1,ℓ_2} can assume any value between +1 and -1 with $\alpha_{\ell_1,\ell_2} = \delta_{\ell_1,\ell_2}$ being the random limit. For any case α_{ℓ_1,ℓ_1} is necessarily one.

Using these short-range order parameters, we show in Appendix C that for waves incident on a short-range ordered system the scattering intensity in the Born approximation is

$$I\alpha \sum_{n=-\infty}^{\infty} e^{ikna}[(f_h(1-C_d)+f_dC_d)^2+C_d(1-C_d)\alpha_n(f_d-f_h)^2] \tag{3.7}$$

where a is the lattice constant,
f_h is the structure factor for the host atom
f_d is the structure factor for the defect atom
k is the incident wave vector

Therefore, for structure factors independent of k,

$$I\alpha N \sum_m \delta(ka-2\pi m)[f_h(1-C_d)+f_dC_d]^2+C_d(1-C_d)\alpha(k)(f_d-f_h)^2 \tag{3.8}$$

where $$\alpha(k) = \sum_{n=-\infty}^{\infty} e^{ikan}\alpha_n \tag{3.9}$$

The first term of (3.8) gives the Bragg reflection from an average host-defect chain where all sites are randomly occupied by host or defects in proportion to their respective concentrations. The second term is a diffuse scattering.

There are several limiting cases in which the short-range order becomes long-range order.

Case 1: $\alpha_\ell = (-1)^\ell$; $C_d=.5$

In this case, the lattice is an ordered diatomic chain and

$$\alpha(k) = \sum_m[\delta[ka-(2m+1)\pi]] \tag{3.10}$$

The unit cell in real space is now twice as long as that for the monatomic case and Bragg peaks occur at both even and odd multiples of π/a.

Case 2: $\alpha_\ell = 1$

In this case, it is impossible to have any mixed chain, a possible interpretation of this case is to superimpose two perfect chains. The Bragg peaks occur at the superlattice reflection points with strength

$$I \alpha N \sum_m (C_d f_d^2 + (1-C_d) f_h^2) \delta(ka - 2\pi m) \qquad (3.11)$$

and there is no diffuse scattering.

The experimentalist measures $\alpha(k)$ using various energy x-rays and neutrons and inverts the results to find α_n.[29] In generating chains with short range order (SRO) we can find α_n and can consequently explore the implications of the order in terms of diffuse scattering.

Short Range Order Work

Using the long-range order parameters of Bragg and Williams with the Warren-Cowley short range order parameters, numerous contributions have been made to the theory of order-disorder transitions in alloys. A good summary of the work is given in Reference (30). The first attempt at introducing general short-range order into the theory of thermodynamic properties and frequency spectra was made in 1968 by Hartmann.[31] Using Green's function techniques, he was able to calculate a variety of physical properties in the low concentration of defects limit for three

dimensional crystals. These calculations were for arbitrary short-range order describable by pair correlations. Subsequently Taylor[32] was able to introduce the short-range parameters into his self consistent Green's function formalism (coherent potential approximation). Taylor's work will be discussed in more detail in the theory section (V). Taylor's formalism with short-range order was valid, however, only near the random limits.

The short-range order discussed above is in terms of pair correlation functions, which are in fact adequate for scattering theory in the Born approximation. However, for generating a binary chain and for exact calculations of physical quantities which can depend on scattering to higher order than the second in the defect perturbation, we need all orders of correlation functions. Also, the extension of pair correlation function formalism to n(>2) constituent chains is not readily apparent. Therefore, we consider the Markov process.

Markov Chain

To examine the eigenvalues and eigenvectors of a linear chain by numerical methods, a linear chain must be constructed. An ordered chain can be simply generated by placing unit cell clusters one after another. A random chain with n constitutents can be numerically generated as discussed in Chapter II. To generate a chain with

short-range order with the proper concentration of each constituent and the correct stochastic relationships between atoms, the theory of Markov processes is employed.[35,36]

Stochastic processes where the probability that a physical system will be in a given state at time t_2 may be deduced from a knowledge of its state at an earlier time t_1, and does not depend on the history of the system before time t_1 are called Markov processes. More formally, a discrete parameter stochastic process $[X(t), t=0,1,2 \ldots.]$ or a continuous parameter stochastic process $[X(t,), t\geq 0]$ is said to be a Markov process if for any set of n time points $t_1<t_2<t_3<\ldots.<t_n$ in the index set of the process, the conditional distribution of $X(t_n)$, for given values of $X(t_1), X(t_2), \ldots., X(t_{n-1})$ depends only on $X(t_{n-1})$ the most recent value; more precisely, for any real numbers $x_1, x_2, \ldots x_n$

$$\tilde{P}[X(t_n)\geq x_n \mid X(t_1)=x_1, \ldots, X(t_{n-1})=x_{n-1}] =$$

$$\tilde{P}[X(t_n)\geq x_n \mid X(t_{n-1})=x_{n-1}] \qquad (3.12)$$

This equation should be read as follows, the probability that the variable X at t_n is greater than or equal to the state x_n subject to the conditions that the variable X at t_1, has the value x_1, the variable X at t_2 has the value x_2, and so on up to the condition that X at t_{n-1} has the value x_{n-1} is equal to the probability that the variable

X at t_n is greater than or equal to the state x_n subject only to the condition that the variable X at t_{n-1} has the value x_{n-1}. The order among the states can be included in any self consistent arbitrary way.

Markov processes are classified according to the nature of the index set of the process (parameter) and the nature of the state space of the process. The index set of the process can be continuous or discrete. The index set is a special type of ordered set. When the parameter is time, an intuitive interpretation of a Markov process is a process where the future depends only on the present and not on the past. For the linear chain, the parameter is distance down the chain. This distance, however, must be directional in the sense of proceeding down the chain in only one direction. For a position along the chain ℓ_0, the position $\ell_0-\ell_1, \ell_1>0$ must be considered as a previously occurring state and $\ell_0+\ell_2, \ell_2>0$ as a future state. For atoms on lattice sites the index set is discrete. The state space of the linear chain is the set of the types of atoms in the chain. The state space is called discrete if it contains a finite or countable infinite number of states as does the linear chain. A state space which is not discrete is continuous. If the state space is discrete the Markov process is called a Markov chain.

Table 3.1 shows the four basic types of Markov processes. The one used to generate the linear atomic chain

is the discrete parameter Markov chain. Theoretical work is still very limited for the continuous state space Markov processes. A little more is known about continuous parameter Markov chains with the discrete parameter Markov chain being the best understood and most widely applied.

TABLE 3.1.--The classification of Markov processes.

		State Space	
		Discrete	Continuous
Parameter Space	Discrete	Discrete Parameter Markov Chain	Discrete Parameter Markov Process
	Continuous	Continuous Parameter Markov Chain	Continuous Parameter Markov Process

The remainder of our discussion will be concerned only with discrete parameter Markov chains.

Equation 3.12 can be rewritten for the discrete parameter Markov chain with lattice sites as the parameter as follows:

Definition: Let X_ℓ be a random variable where the value of X_ℓ represents the atom at position (lattice site) ℓ. The sequence $[X_\ell]$ is the linear chain. The sequence $[X_\ell]$ is a Markov chain, if the set of possible X_ℓ is discrete

and if for any integer $m>2$ and any set of m points $\ell_1<\ell_2<....<\ell_m$, the conditional distribution of X_{ℓ_m} for given values of $X_{\ell_1},...,X_{\ell_{m-1}}$ depends only on $X_{\ell_{m-1}}$, the closest atom; i.e. for any real numbers $x_1,x_2,...,x_m$,

$$\tilde{P}[X_{\ell_m}=x_m|X_{\ell_1}=x_1,...,X_{\ell_{m-1}}=x_{m-1}] = P[X_{\ell_m}=x_m|X_{\ell_{m-1}}=x_{m-1}] \quad (3.13)$$

A Markov chain is described by a transition probability function, $P_{j,k}(\ell_0,\ell_1)$, which represents the conditional probability that the state of the system will be at point ℓ_1 in the state k, given that at point $\ell_0(<\ell_1)$ the system is in state j. The Markov process is said to be homogeneous in space or to have stationary transition probabilities, if $P_{j,k}(\ell_0,\ell_1)$ depends on ℓ_1 and ℓ_0 only through the difference $(\ell_1-\ell_0)$. The transition probability function is also called the conditional probability mass function and is

$$P_{j,k}(\ell_0,\ell_1)=P[X_{\ell_1}=k|X_{\ell_0}=j] \text{ for } \ell_1>\ell_0 \quad (3.14)$$

In order to specify the probability law of a discrete parameter Markov chain, the probability mass function (not conditional)

$$P_j(\ell) = P[X_\ell=j] \quad (3.15)$$

must also be specified. The linear atomic chain should have homogeneous or stationary transition probabilities. For such a homogeneous chain it is physically realistic to expect the same stochastic relationships between atoms in different regions in the chain. For the homogeneous discrete parameter Markov chain, Equation (3.14) can be rewritten as

$$P_{j,k}(n)=\tilde{P}[X_{\ell+n}=k \mid X_{\ell}=j] \quad \text{for any integer} \quad \ell \geq 0 \qquad (3.16)$$

Equation (3.16) is called the n step transition probability function. In words, $P_{j,k}(n)$ is the conditional probability of making a transition to state k, n steps after being in state j. $P_{j,k}(1)$ is usually rewritten as $P_{j,k}$.

The transition probability function of a Markov chain $[X_n]$ satisfies the Chapman-Kolmogorov equation: for any lattice sites $\ell_3>\ell_2>\ell_1 \geq 0$ and states j and k

$$P_{j,k}(\ell_1,\ell_3) = \sum_i P_{j,i}(\ell_1,\ell_2)P_{i,k}(\ell_2,\ell_3) \qquad (3.17)$$

This is a necessary but not sufficient condition for a Markov chain.

The transition probabilities are best exhibited in the form of a matrix called the transition probability matrix

$$P(\ell_1,\ell_2) = [\{P_{i,j}(\ell_1,\ell_2)\}] \text{ with rows and columns i and j.} \tag{3.18}$$

The matrix elements also satisfy the following conditions

$$P_{i,j}(\ell_1,\ell_2) \geq 0 \text{ for all } i,j \tag{3.19}$$

and

$$\sum_k P_{j,k}(\ell_1,\ell_2) = 1 \text{ for all } j \tag{3.20}$$

The Chapman-Kolmogorov equation can be rewritten in matrix form as

$$P(\ell_1,\ell_3) = P(\ell_1,\ell_2)P(\ell_2,\ell_3) \tag{3.21}$$

From the Chapman-Kolmogorov equation some fundamental recursive relations can be derived for the discrete parameter Markov chain. For the homogeneous chain the transition probability matrix $P(\ell_1,\ell_2)$ depends only on the difference $n=(\ell_2-\ell_1)$ and can be rewritten as P(n). Equation (3.21) can be rewritten as

$$P(n) = P(m)P(n-m) \text{ where } m<n \tag{3.22}$$

P(1) is usually rewritten as P. Using Equation (3.22) recursively, we see

$$P(n) = P(n-1)P = P(n-2)PP = \ldots = P^n \tag{3.23}$$

Next, from the probability mass function defined in Equation (3.15), we can define the unconditional probability vector as the row vector

$$p(n) = [\{p_j(n)\}] \text{ with columns } j \tag{3.24}$$

Given an initial unconditional probability vector p(0), it follows that

$$p(n) = p(0)P(n) = p(0)P^n \tag{3.25}$$

As a consequence, the probability law of a homogeneous Markov chain $[X_n]$ is completely determined once one knows the one step probability transition matrix P and the unconditional probability vector p(0).

A Markov chain $[X_n]$ is said to be a finite Markov chain with k states if the number of possible values of the random variables $[X_n]$ is finite and equal to k. The transition probabilities $p_{j,k}$ are non-zero for only a finite number of values of j and k and the transition probability matrix P is then a k x k matrix.

An example of a discrete parameter finite homogeneous Markov chain would be a linear atomic chain consisting of two states a host state (atom) h and a defect state (atom) d. The unconditional probability vector would be

$$p(0) = [p_h, p_d] \tag{3.26}$$

and the transition probability matrix is

$$P = \begin{pmatrix} p_{h,h} & p_{h,d} \\ p_{d,h} & p_{d,d} \end{pmatrix} \tag{3.27}$$

Although we have not examined how we determine P as yet, it does have some interesting properties.

$$P(2) = P^2 = \begin{pmatrix} p_{h,h}^2 + p_{h,d}p_{d,h} & p_{h,d}(p_{h,h}+p_{d,d}) \\ p_{h,d}(p_{d,d}+p_{h,h}) & p_{d,d}^2 + p_{h,d}p_{d,h} \end{pmatrix} \tag{3.28}$$

and for $|p_{d,d}+p_{h,h}-1| < 1$, the n - step transition probability matrix is

$$P(n) = 1/(2-p_{h,h}-p_{d,d}) \begin{pmatrix} 1-p_{d,d} & 1-p_{h,h} \\ 1-p_{d,d} & 1-p_{h,h} \end{pmatrix} + \frac{(p_{h,h}+p_{d,d}-1)^n}{(2-p_{h,h}-p_{d,d})} \begin{pmatrix} 1-p_{h,h} & -(1-p_{h,h}) \\ -(1-p_{d,d}) & 1-p_{d,d} \end{pmatrix} \tag{3.29}$$

The proof of Equation (3.29) is given in Appendix B. The asymptotic expressions for the n - step transition probabilities are

$$\lim_{n\to\infty} p_{h,h}(n) = \lim_{n\to\infty} p_{d,h}(n) = \frac{1-p_{d,d}}{(2-p_{h,h}-p_{d,d})} \tag{3.30a}$$

$$\lim_{n\to\infty} p_{h,d}(n) = \lim_{n\to\infty} p_{d,d}(n) = \frac{1-p_{h,h}}{(2-p_{h,h}-p_{d,d})} \tag{3.30b}$$

To determine the transition probabilities, the evolution in parameter space (time or distance) of a discrete parameter homogeneous Markov chain $[X_n]$ must be studied. First, the states of a chain can be classified according to whether it is possible to go from a given state to another state.

Definition: A state k is said to be accessible from a state j ($j\to k$) if, for some integer $n\geq 1$, $p_{j,k}(n)>0$. Two states j and k are said to communicate ($j\leftrightarrow k$) if j is accessible from k and k is accessible from j.

For a fixed concentration linear chain all states must communicate; otherwise, some $p_{j,k}(n) = 0$ for all n implies that once the state j is entered state k can never be reentered modifying the concentration of the state k.

Given a state j of a Markov chain, its communicating class C(j) is defined to be the set of all k states in the chain which communicate with j, i.e.,

$$k \in C(j) \text{ if and only if } k\leftrightarrow j$$

For the linear atomic chain, we require all states of the chain to communicate with each other. Since the communicating class C contains all the states of the system, there are no states outside the set and C is defined as a closed set. More formally,

Definition: A non-empty set C of states is said to be closed if no state outside the set is accessible from any state inside the set.

Next, we can define the occupation number $N_k(n)$ of the state k in the first n transitions. More precisely, $N_k(n)$ is equal to the number of integers ν satisfying $1 \leq \nu \leq n$ and $X_\nu = k$. The total occupation time of k is

$$N_k(\infty) = \lim_{n \to \infty} N_k(n) \tag{3.31}$$

The occupation times can be represented as the sum of random variables. Define for any state k and n=1,2,....

$$\begin{aligned} Z_k(n) &= 1 \text{ if } X_n = k \\ &= 0 \text{ if } X_n \neq k \end{aligned} \tag{3.32}$$

Then, we can write

$$N_k(n) = \sum_{m=1}^{n} Z_k(m) \tag{3.33}$$

and

$$N_k(\infty) = \sum_{m=1}^{\infty} Z_k(m) \tag{3.34}$$

With these relationships we can define the following probabilities

$$f_{j,k} = P[N_k(\infty)>0 | X_0=j] \tag{3.35}$$

and

$$g_{j,k} = P[N_k(\infty)=\infty | X_0=j] \tag{3.36}$$

In words, $f_{j,k}$ is the conditional probability of ever visiting the state k given that the chain is initially in state j, and $g_{j,k}$ is the conditional probability of an infinite number of visits to the state k given the chain is at some initial time in state j. For the linear chain with fixed concentration of constituents, the requirement that every state communicates implies

$$f_{j,k} = 1 \tag{3.37}$$

and in an infinite chain every state occurs an infinite number of times to maintain fixed concentrations implying

$$g_{j,k} = 1 \tag{3.38}$$

Definition: A state is said to be recurrent if $f_{k,k}=1$ or a state k is recurrent if the probability is one that the Markov chain will return to state k.

Definition: A recurrent Markov chain is said to be irreducible if all pairs of states of the chain communicate ($f_{j,k}>0$ for all j,k).

Therefore, the linear atomic chain has a closed recurrent irreducible set of states. The chain must also have a fixed concentration of constituents as the length of the chain approaches infinity.

Definition: A Markov chain with state space C possesses a long run distribution if there exists a probability distribution $\{\pi_k, k\varepsilon C\}$, having the property that for every j and k in C

$$\lim_{n\to\infty} p_{j,k}(n) = \pi_k \tag{3.39}$$

summing over k

$$\sum_k \lim_{n\to\infty} p_{j,k}(n) = \lim_{n\to\infty} \sum_k p_{j,k}(n) = 1 = \sum_k \pi_k \tag{3.40}$$

which gives a useful relationship between the concentrations π_k. The interchange of the summation and limit in Equation (3.40) is not rigorous but Appendix B has a rigorous proof. No matter what the initial unconditional probability distribution $\{p_k(0), k\varepsilon C\}$, the unconditional probability $p_k(n)$ tends to π_k as n tends to infinity

$$\begin{aligned} \lim_{n\to\infty} p_k(n) &= \lim_{n\to\infty} \sum_j p_j(0) p_{j,k}(n) \\ &= \sum_j p_j(0) \lim_{n\to\infty} p_{j,k}(n) \\ &= \sum_j p_j(0) \pi_k = \pi_k \end{aligned} \tag{3.41}$$

Definition: A Markov chain with a state space C is said to have a stationary distribution if there exists a probability distribution $\{\pi_k, k\varepsilon C\}$ having the property that for every k in C

$$\pi_k = \sum_j \pi_j p_{j,k} \tag{3.42}$$

In order to state conditions under which the irreducible Markov chain possesses a long run distribution, we need to introduce the concept of the period of the state.

Definition: The period d(k) of a return state k of a Markov chain is defined to be the greatest common divisor of the set of integers n for which $p_{k,k}(n)>0$. A state is aperiodic if it has a period of 1.

For an irreducible Markov chain, if $p_{k,k}>0$ for any k in C, then the state is aperiodic. Also, if an integer n can be found such that $p_{j,k}(n)>0$ for all j and k in C, the chain is aperiodic. In fact, for the linear chain only ordered (periodic) chains are not aperiodic.

If a chain is irreducible, aperiodic, and recurrent it is called an ergodic chain. For our purposes we want a homogeneous chain, for which the stochastic relationships are the same throughout the entire length of the chain. Therefore we require a Markov chain which is ergodic. Such a chain has a unique long-run distribution.

Theorem 1: An ergodic Markov chain has a unique long-run distribution, $\{\pi_k, k\varepsilon C\}$ with $0<\pi_k<\infty$. The long-run distribution of an ergodic Markov chain is the unique solution of the system of Equation (3.42) satisfying Equation (3.40).

Theorem 1 is proved in Appendix B.

The converse of Theorem 1 is also true.

Converse of Theorem 1: If a Markov chain has a unique long run distribution $\{\pi_k, k\varepsilon C\}$ with $0<\pi_k<\infty$, then the chain is ergodic.

Proof: The converse is most easily proved by showing that any Markov chain which is not ergodic does not possess a unique long run distribution with $0<\pi_k<\infty$. A Markov chain is not ergodic if it is periodic and/or reducible and/or non-recurrent. The definition of periodic is the contrapositive of the definition of aperiodic.

Definition: If a chain is periodic, then an integer n cannot be found such that $P_{j,k}(n)>0$ for all j and k in C. The definition implies some $P_{j,k}(n)=0$ for any n and therefore $\lim_{n\to\infty} P_{j,k}(n)$ does not exist in the ordinary sense or is equal to zero. Therefore π_k is not unique or is equal to zero in violation of the conjecture.

A reducible Markov chain is defined by the contrapositive of the definition of an irreducible Markov chain.

Definition: If a chain is a reducible Markov chain, then not all pairs of states communicate. That is to say some $f_{j,k}=0$. This implies $P_{j,k}(n) = 0$ and therefore $\lim_{n\to\infty} P_{j,k}(n)= 0=\pi_k$ again in violation of the inequality $0<\pi<\infty$.

Finally, the contrapositive of a recurrent Markov chain, gives the definition of the non-recurrent Markov chain.

Definition: If a Markov chain state is non-recurrent, then the probability that the Markov chain will return to state k from a state k is not one ($f_{k,k}\neq 1$). This implies $f_{k,k}<1$. In Appendix B, we show the $f_{k,k}<1$ implies $g_{k,k}=0$ and $\sum_{n=0}^{\infty} P_{k,k}(n)<\infty$. Therefore; $\lim_{n\to\infty} P_{k,k}(n)=0=\pi_k$ in violation of the inequality $0<\pi_k<\infty$. This completes the proof of the converse. Therefore, the solution to Equations (3.42) satisfying Equation (3.40) will give a ergodic chain for all $\pi_k\neq 0$.

For the two component linear chain with concentrations c_h and c_d Equation (3.42) gives

$$c_h = c_h p_{h,h} + c_d p_{d,h} \tag{3.43}$$

$$c_d = c_h p_{h,d} + c_d p_{d,d} \tag{3.44}$$

Equation (3.40) gives

$$c_h+c_d = 1 \tag{3.45}$$

and Equation (3.20) gives

$$p_{h,h}+p_{h,d} = 1 \tag{3.46}$$

$$p_{d,d}+p_{d,h} = 1 \tag{3.47}$$

From this set of equations, it is obvious the combining of Equations (3.44), (3.45), (3.46), and (3.47) gives Equation (3.43) which is a redundant equation. Given c_d and $p_{d,d}$, the rest of the variables can be specified.

$$c_h = 1-c_d \tag{3.48}$$

$$p_{d,h} = 1-p_{d,d} \tag{3.49}$$

$$p_{h,d} = c_d(1-p_{d,d})/(1-c_d) \tag{3.50}$$

$$p_{h,h} = 1-p_{h,d} \tag{3.51}$$

The first atom in the chain is selected as in the random case. A uniformily distributed (0→1) random number is picked and compared with the concentration of defects c_d. If the number is less than c_d, the atom is a defect; otherwise, it is a host. After the first atom has been selected, a random number is picked and compared with either $p_{h,d}$ or $p_{d,d}$ depending on whether the previous atom was a host or a defect respectively. If the random number is less than this value the atom is defect, and otherwise it is a host. This procedure generates the correct Markov chain

with the proper concentration in the limit of long chains. A statistical analysis of these chains is included in Appendix B.

Another example is a three (state) constituent linear chain with concentrations c_1, c_2 and c_3 for atoms of types 1, 2 and 3. Equation (3.42) gives

$$c_1 = c_1p_{1,1}+c_2p_{2,1}+c_3p_{3,1} \tag{3.52}$$

$$c_2 = c_1p_{1,2}+c_2p_{2,2}+c_3p_{3,2} \tag{3.53}$$

$$c_3 = c_1p_{1,3}+c_2p_{2,3}+c_3p_{3,3} \tag{3.54}$$

Equation (3.40) becomes

$$c_1+c_2+c_3 = 1 \tag{3.55}$$

and Equation (3.20) gives

$$p_{1,1}+p_{1,2}+p_{1,3} = 1 \tag{3.56}$$

$$p_{2,1}+p_{2,2}+p_{2,3} = 1 \tag{3.57}$$

$$p_{3,1}+p_{3,2}+p_{2,3} = 1 \tag{3.58}$$

It is easily shown that one equation is redundant; therefore, eliminating Equation (3.54), six variables must be specified to construct an ergodic Markov chain. Picking c_1,c_2,$p_{1,1}$,$p_{1,2}$,$p_{2,1}$, and $p_{2,2}$ as specified, Equations (3.52) - (3.58) can be solved.

$$p_{1,3} = 1-p_{1,2}-p_{1,1} \tag{3.59}$$

$$p_{2,3} = 1-p_{2,1}-p_{2,2} \tag{3.60}$$

$$c_3 = 1-c_1-c_2 \tag{3.61}$$

$$p_{3,1} = [c_1(1-p_{1,1})-c_2p_{2,1}]/(1-c_1-c_2) \tag{3.62}$$

$$p_{3,2} = [c_2(1-p_{2,2})-c_1p_{1,2}]/(1-c_1-c_2) \tag{3.63}$$

$$p_{3,3} = 1-p_{3,1}-p_{3,2} \tag{3.64}$$

For the two and three state linear chains, there are constraints which limit the range of the input concentrations or the input probabilities to a range less than that between zero and one. For the two constituent chain when specifying arbitrary concentration for the defect c_d, the transition probability is constrained for $c_d<.5$.

$$0<p_{h,d}<1$$

$$0<[c_d(1-p_{d,d})]/(1-c_d)<1$$

$$0<1-p_{d,d}<(1-c_d)/c_d$$

$$(2-1/c_d)<p_{d,d}<1 \tag{3.65}$$

For the three constituent chain, the constraints are more complicated.

The restriction from the concentration of constituents is

$$0<c_3<1$$

which leads to

$$0<(c_1+c_2)<1 \tag{3.66}$$

The restrictions from the probabilities are: first,

$$0<p_{1,3}<1$$

which implies

$$0<(p_{1,1}+p_{1,2})<1 \tag{3.67}$$

Next,

$$0<p_{2,3}<1$$

which implies

$$0<(p_{2,1}+p_{2,2})<1 \tag{3.68}$$

The third restriction is

$$0<p_{1,3}<1$$

which gives

$$0<[c_1(1-p_{1,1})-c_2p_{2,1}]/(1-c_1-c_2)<1$$

$$p_{2,1}<c_1(1-p_{1,1})/c_2<[p_{2,1}+(1-c_1-c_2)/c_2] \tag{3.69}$$

The final restriction is

$$0<p_{2,3}<1$$

which gives

$$0<[c_2(1-p_{2,2})-c_1p_{1,2}]/(1-c_1-c_2)<1$$

$$p_{1,2}<[c_2(1-p_{2,2})/c_1]<[p_{1,2}+(1-c_1-c_2)/c_1] \qquad (3.70)$$

So far we have discussed strictly Markov chains. In constructing such a chain the choice for the state (occupancy) at site ℓ is affected only by the state at site $\ell-1$. We can generalize our method by bending somewhat the definition of the Markov chain. In the two state system for example an obvious extension would be to relate the atom at ℓ to the atoms at $\ell-1$ and $\ell-2$ instead of just the atom at $\ell-1$. In fact it is desireous to relate the atom at ℓ to the atoms at $\ell-1$, $\ell-2$, $\ell-3$,....,$\ell-n$. By analogy to the ergodic Markov chain we will define the following:

Def: the sequence $[X_\ell]$ is an n^{th} order Markov chain if each X_ℓ is discrete and for any integer $m>n+1$ and any set of m points $\ell_1<\ell_2<\ldots<\ell_m$, the conditional distribution of X_{ℓ_m} for given values of X_{ℓ_1}, X_{ℓ_2},...,$X_{\ell_{m-1}}$, depends only on $X_{\ell_{m-n}}$,...,$X_{\ell_{m-1}}$, the n closest atoms. For any real numbers $x_1,x_2,\ldots,x_m$

$$P[X_{\ell_m}=x_m | X_{\ell_1}=x_1, X_{\ell_2}=x_2, \ldots, X_{\ell_{m-1}}=x_{m-1}] = \tag{3.71}$$

$$P[X_{\ell_m}=x_m | X_{\ell_{m-n}}=x_{m-n}, X_{\ell_{m-n+1}}+x_{m-n+1}, \ldots, X_{\ell_{m-1}}=x_{m-1}]$$

The one step probability transition function would be

$$p_{i,j,\ldots,s;t}=P[X_\ell=t | X_{\ell-n}=i, X_{\ell-n+1}=j, \ldots X_{\ell-1}=s] \tag{3.72}$$

These transition probabilities satisfy the Chapman-Kolomogorov equation, but for n>1, the n^{th} order Markov chain as defined is not a Markov process. A transformation,[38] however, can be made to make it a Markov process. For an ergodic Markov chain with m constituents, an n^{th} order Markov chain will have m^n states with an m^n by m^n transition probability matrix with $m^n(m^n-m)$ identically zero transition matrix elements. The one step probability transition function is redefined as

$$p_{i,j,\ldots,s;t}=p_{i,j,\ldots,s;j,\ldots s,t}=$$

$$P[X_\ell=t, X_{\ell-1}=s, .., X_{\ell-n+1}=j | X_{\ell-n}=i, X_{\ell-n+1}=j, .., X_{\ell-1}=s] \tag{3.73}$$

For the two state linear chain, the second order Markov chain would consist of $2^2=4$ states; namely,

hh
hd
dh
dd (3.74)

with the transition matrix being 4 x 4 with 4(4-2) = 8 zero transition matrix elements.

$$\begin{aligned} p_{hh,dh} &= p_{hh,dd} = 0 \\ p_{hd,hd} &= p_{hd,hh} = 0 \\ p_{dh,dh} &= p_{dh,dd} = 0 \\ p_{dd,hd} &= p_{dd,hh} = 0 \end{aligned} \tag{3.75}$$

and 8 non-zero matrix elements

$$\begin{aligned} p_{dd,d} &= p_{dd,dd} \\ p_{dd,h} &= p_{dd,dh} \\ p_{dh,d} &= p_{dh,hd} \\ p_{dh,h} &= p_{dh,hh} \\ p_{hd,d} &= p_{hd,dd} \\ p_{hd,h} &= p_{hd,dh} \\ p_{hh,d} &= p_{hh,hd} \\ p_{hh,h} &= p_{hh,hh} \end{aligned} \tag{3.76}$$

Equation (3.40) then gives

$$c_{hh}+c_{hd}+c_{dh}+c_{dd} = 1 \tag{3.77}$$

which we need to relate to c_h and c_d. The relation is

$$c_h = c_{hh}+(c_{dh}+c_{hd})/2 \tag{3.78}$$

$$c_d = c_{dd}+(c_{dh}+c_{hd})/2 \tag{3.79}$$

so that

$$c_d+c_h = 1 \tag{3.80}$$

Equation (3.20) gives

$$p_{hh,hd}+p_{hh,hh}+p_{hh,dh}+p_{hh,dd} = 1 \tag{3.81}$$

$$p_{hd,hh}+p_{hd,hd}+p_{hd,dh}+p_{hd,dd} = 1 \tag{3.82}$$

$$p_{dh,hh}+p_{dh,hd}+p_{dh,dh}+p_{dh,dd} = 1 \tag{3.83}$$

$$p_{dd,hh}+p_{dd,hd}+p_{dd,dh}+p_{dd,dd} = 1 \tag{3.84}$$

which because of the zero elements reduce to

$$p_{hh,d}+p_{hh,h} = 1 \quad (p_{hh,hd}+p_{hh,hh} = 1) \tag{3.81'}$$

$$p_{hd,d}+p_{hd,h} = 1 \quad (p_{hd,dd}+p_{hd,dh} = 1) \tag{3.82'}$$

$$p_{dh,d}+p_{dh,h} = 1 \quad (p_{dh,hd}+p_{dh,hh} = 1) \tag{3.83'}$$

$$p_{dd,d}+p_{dd,h} = 1 \quad (p_{dd,dd}+p_{dd,dh} = 1) \tag{3.84'}$$

Equation (3.42) gives

$$c_{hh} = c_{hh}p_{hh,hh}+c_{hd}p_{hd,hh}+c_{dh}p_{dh,hh}+c_{dd}p_{dd,hh} \tag{3.85}$$

$$c_{hd} = c_{hh}p_{hh,hd}+c_{hd}p_{hd,hd}+c_{dh}p_{dh,hd}+c_{dd}p_{dd,hd} \tag{3.86}$$

$$c_{dh} = c_{hh}p_{hh,dh}+c_{hd}p_{hd,dh}+c_{dh}p_{dh,dh}+c_{dd}p_{dd,dh} \tag{3.87}$$

$$c_{dd} = c_{hh}p_{hh,dd}+c_{hd}p_{hd,dd}+c_{dh}p_{dh,dd}+c_{dd}p_{dd,dd} \quad (3.88)$$

These equations can also be simplified to

$$c_{hh} = c_{hh}p_{hh,h}+c_{dh}p_{dh,h} \quad (3.85')$$

$$c_{hd} = c_{hh}p_{hh,d}+c_{dh}p_{dh,d} \quad (3.86')$$

$$c_{dh} = c_{hd}p_{hd,h}+c_{dd}p_{dd,h} \quad (3.87')$$

$$c_{dd} = c_{hd}p_{hd,d}+c_{dd}p_{dd,d} \quad (3.88')$$

Using Equations (3.75) - (3.88), one equation is redundant. We can arbitrarily eliminate Equation (3.85'). From the remaining equations, we have ten equations with fourteen unknowns requiring us to specify <u>four</u> variables. If we take these four specifications to be c_d,$p_{dd,d}$,$p_{dh,d}$ and $p_{hd,d}$, the equations can be solved in terms of these variables.

$$c_h = 1-c_d \quad (3.89)$$

$$p_{dd,h} = 1-p_{dd,d} \quad (3.90)$$

$$p_{dh,h} = 1-p_{dh,d} \quad (3.91)$$

$$p_{hd,h} = 1-p_{hd,d} \quad (3.92)$$

from Equation (3.88') we have

$$c_{hd} = c_{dd}(1-p_{dd,d})/p_{hd,d} \quad (3.93)$$

from Equation (3.87') using Equations (3.93), (3.92), and (3.90)

$$c_{dh} = c_{dd}(1-p_{dd,d})(1-p_{hd,d})/p_{hd,d}+c_{dd}(1-p_{dd,d})$$

$$= c_{dd}(1-p_{dd,d})/p_{hd,d}$$

$$c_{dh} = c_{hd} \tag{3.94}$$

Using Equation (3.80) with (3.94), we get

$$c_{dh} = c_d - c_{dd} \tag{3.95}$$

Substituting Equation (3.95) into (3.93) gives

$$c_d - c_{dd} = c_{dd}(1-p_{dd,d})/p_{hd,d}$$

$$c_{dd} = c_d p_{hd,d}/(1+p_{hd,d}-p_{dd,d}) \tag{3.96}$$

Using Equation (3.96) in (3.95), gives

$$c_{dh} = c_{hd} = c_d(1-p_{dd,d})/(1+p_{hd,d}-p_{dd,d}) \tag{3.97}$$

Equation (3.81) gives

$$c_{hh} = 1-c_{dd}-2c_{dh}$$

$$c_{hh} = 1-c_d[p_{hd,d}+2(1-p_{dd,d})]/(1+p_{hd,d}-p_{dd,d}) \tag{3.98}$$

and from Equation (3.86'), we get

$$p_{hh,d} = c_{hd}(1-p_{dh,d})/c_{hh}$$

$$p_{hh,d} = \frac{c_d(1-p_{dd,d})(1-p_{dh,d})}{1+p_{hd,d}-p_{dd,d}-c_d[p_{hd,d}+2(1-p_{dd,d})]} \qquad (3.99)$$

Finally,

$$p_{hh,h} = 1-p_{hh,d} \qquad (3.100)$$

The procedure for generating the chain is identical to that for the first order Markov chain except the states are two atoms long. The first state is hh, hd, dh or dd depending on where the random number falls in the unit interval. The unit interval is divided into c_{hh}, c_{hd}, c_{dh} and c_{dd} respectively. From there on the probability the next atom will be a host or a defect depends on the preceding two atoms.

As in the case of the first order chain, the probabilities are constrained to the unit interval.

$$0 \leq p_{ij,jk} (= p_{ij,k}) \leq 1 \qquad (3.101)$$

Unlike the first order chain where $p_{i,j} = 1$ or 0 for a two state system gives an ordered chain, some $p_{ij,k}$ may equal zero or one and not produce an ordered chain. However, for a given c_d, $p_{dd,d}$, $p_{dh,d}$ and $p_{hd,d}$ are not always allowed any value from zero to one. Since $0 \leq p_{hh,d} \leq 1$, we have

$$0 \leq c_d(1-p_{dh,d})/[1-2c_d+(1-c_d)p_{hd,d}/(1-p_{dd,d})] \leq 1 \qquad (3.102)$$

One question we can easily answer is at what concentration if any does Equation (3.102) constrain the probabilities. Examining Equation (3.102) carefully for different values of c_d reveals the ≤ 1 is always the more constraining limit. Therefore, setting $p_{hh,d}$ equal to one we get

$$1 = c_d(1-p_{dh,d})/[1-2c_d+(1-c_d)p_{hd,d}/(1-p_{dd,d})] \quad (3.103)$$

$$p_{hd,d} = (1-p_{dd,d})c_d[3-1/c_d-p_{dh,d}]/(1-c_d) \quad (3.104)$$

since $p_{hd,d} \geq 0$

$$c_d \leq 1/3 \quad (3.105)$$

For $c_d \leq 1/3$ all $p_{dd,d}$, $p_{hd,d}$ and $p_{dh,d}$ from zero to one are allowed. Figures 3.1 to 3.7 show the allowable values for $p_{dd,d}$, $p_{hd,d}$ and $p_{dh,d}$ for c_d=.3,.4,.5,.6,.7,.8 and .9. Only the volume in front and above the surface is allowed for a ergodic chain. Though our choice of independent parameters is a convenient one it is arbitrary and therefore these figures, for the three parameters which we have chosen, may be somewhat misleading. One should not infer that the parameter space of the second order chain is more restricted for higher concentration. In fact the replacement of c_d by $1-c_d \equiv c_h$ and of all d subscripts by h subscripts leaves the figures still true.

A two state third order Markov chain and three state second order Markov chain are considered in Appendix B.

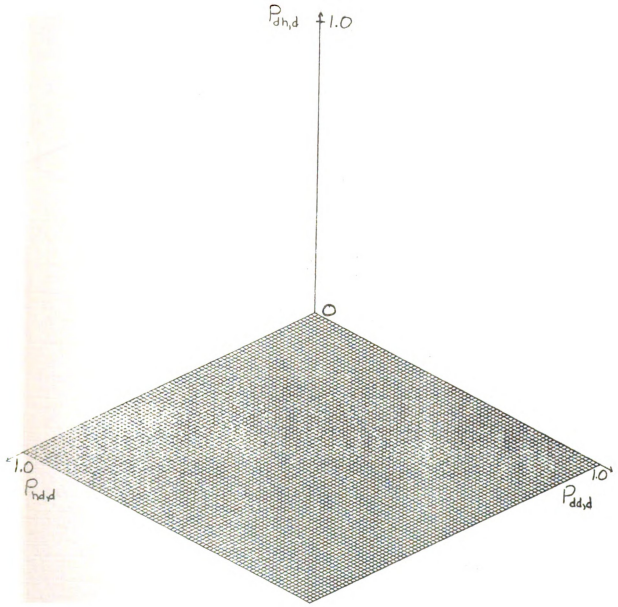

FIGURE 3.1.--Allowed values of $P_{dd,d}$, $P_{dh,d}$ and $P_{hd,d}$ for C_d=.3.

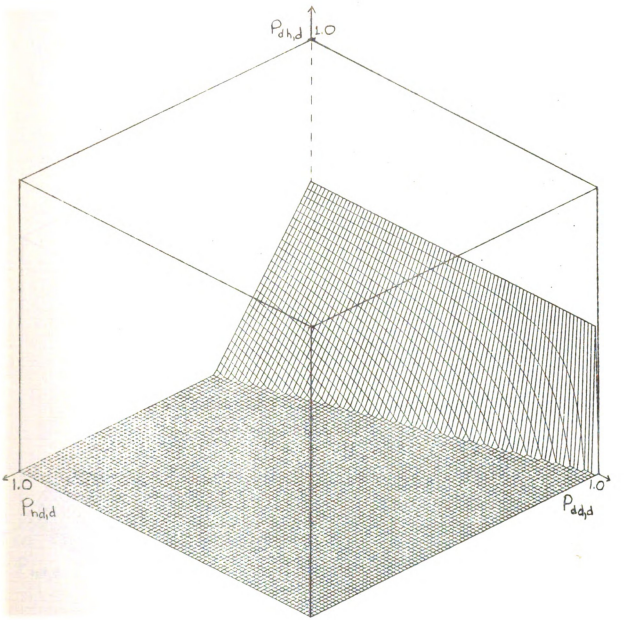

FIGURE 3.2.--Allowed values of $P_{dd,d}$, $P_{dh,d}$ and $P_{hd,d}$ for C_d=.4.

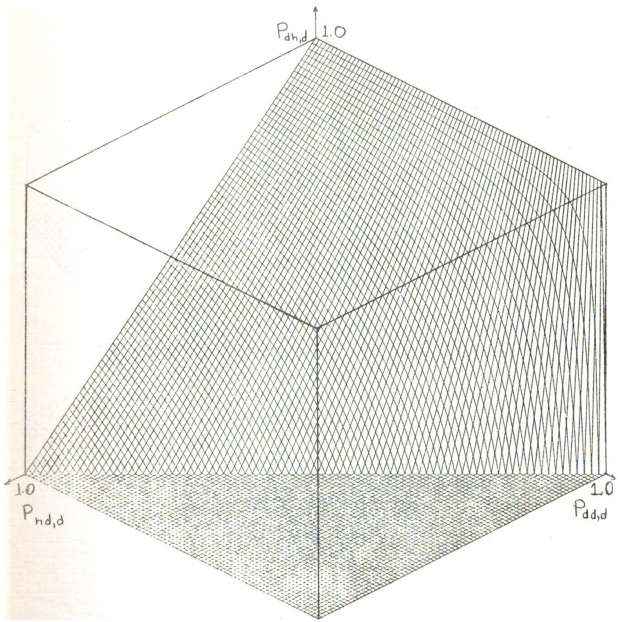

FIGURE 3.3.--Allowed values of $P_{dd,d}$, $P_{dh,d}$ and $P_{hd,d}$ for C_d=.5.

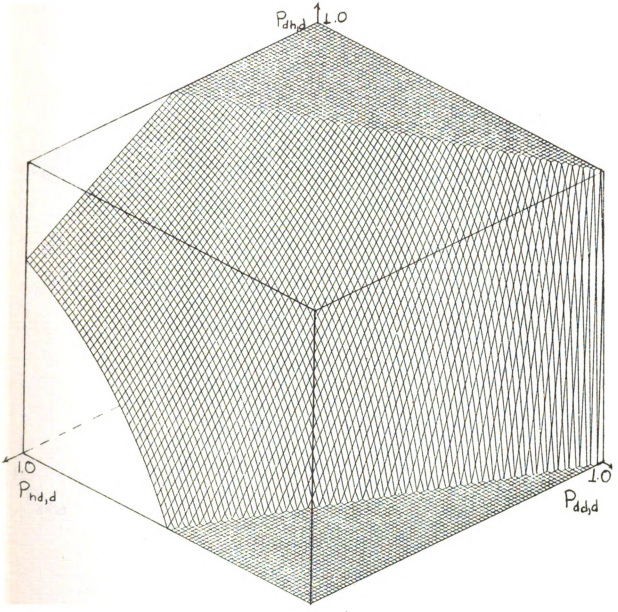

FIGURE 3.4.--Allowed values of $P_{dd,d}$, $P_{dh,d}$ and $P_{hd,d}$ for $C_d = .6$.

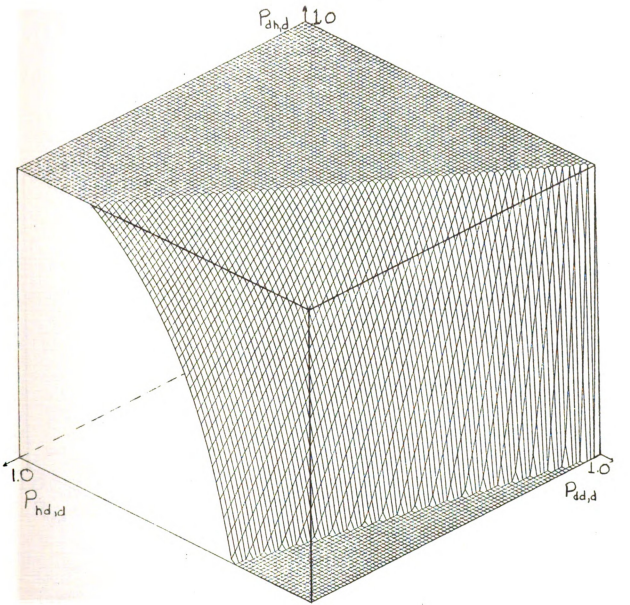

FIGURE 3.5.--Allowed values of $P_{dd,d}$, $P_{dh,d}$ and $P_{hd,d}$ for C_d=.7.

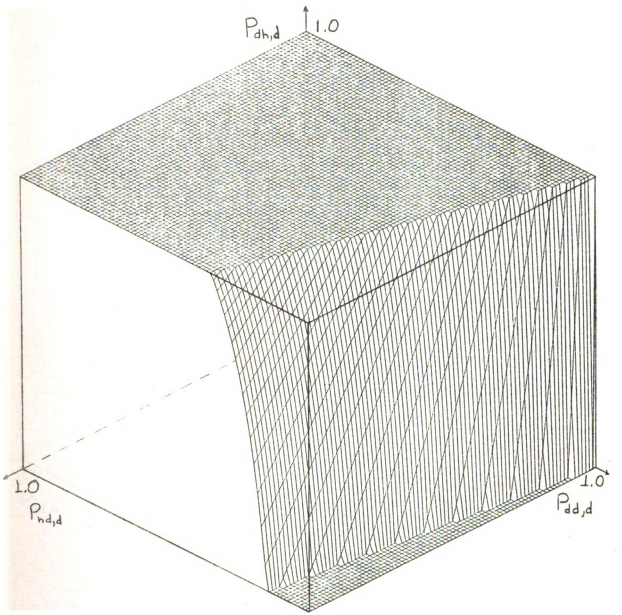

FIGURE 3.6.--Allowed values of $P_{dd,d}$, $P_{dh,d}$ and $P_{hd,d}$ for C_d=.8.

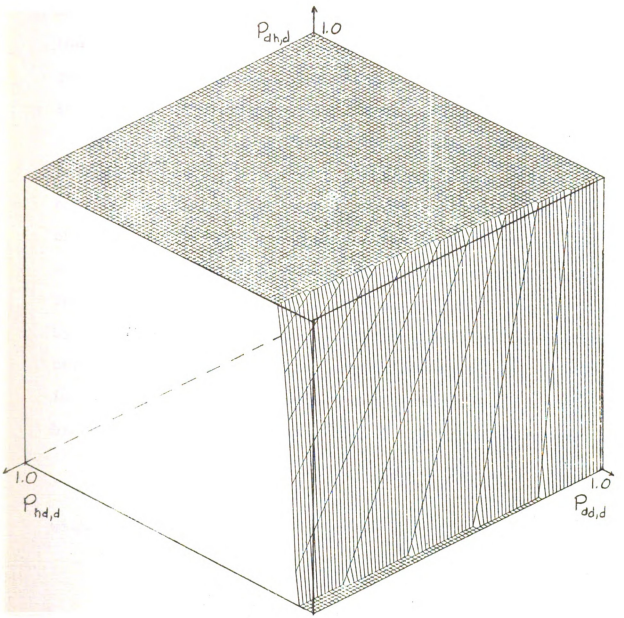

FIGURE 3.7.--Allowed values of $P_{dd,d}$, $P_{dh,d}$ and $P_{hd,d}$ for c_d=.9.

One of the major problems when generating a finite length linear atomic chain via the ergodic Markov chain theory is to generate a chain with the desired stochastic relationships between atoms. As the number of atoms in the chain becomes infinite the ergodic Markov chain theory guarantees the correct relationships, but when one looks at a 100 or 1000 unit chain the relationships can be quite different from those desired. The question we need to answer is: For a given length chain N and a given confidence level C what magnitude of error between the obtained and desired stochastic relationships can we tolerate before we discard the chain? A 99% confidence level says that 99% of the chains of length N, generated by a given transition probability matrix will fall within certain error limits. Since the actual value of $p_{d,d}(n)$ in the first order two constituent Markov chain is a binomial statistic, it has a mean number of occurrences

$$\mu = N\, p_{d,d}(n) \tag{3.106}$$

with a standard deviation of

$$\sigma^2 = N\, p_{d,d}(n)[1-p_{d,d}(n)] \tag{3.107}$$

For the binary random chain with $c_d=.5$, $p_{d,d}(n)=.5$ independent of n. First, for the 100 unit chain, the mean number of defects is $\mu=100(.5)=50$ with a standard deviation of $\sigma=[100(.5)(1-.5)]^{\frac{1}{2}}=5$ or 68% of the time the number of defects will range from 45 to 55 and 95% of the time the defects will be between 40 and 60 out of 100. In other words to a 95% confidence limit a random chain of length 100 could have 40 to 60 defect atoms and still be representative of a random chain. For the 100 unit chain Table 3.1 gives $p_{d,d}(n)$ for two computer generated chains.

TABLE 3.1.--Characteristics of two 100 unit Markov chains.

n	$c_d=.43$ $p_{d,d}(n)$	$c_d=.49$ $p_{d,d}(n)$
1	.357	.510
2	.452	.388
3	.463	.490
4	.450	.479
5	.385	.468
6	.385	.511
7	.461	.362
8	.333	.522
9	.513	.578
10	.289	.432

By a similar analysis, for N=10,000, the 68% confidence limits are 4950 to 5050 defect atoms out of 10,000 atoms. The concentration of defect atoms varies from .495 to .505 versus .45 to .55 for the 100 unit chain. Therefore, any calculations involving 100 unit chains should be averaged over many chains.

In Appendix C, we have related the Markov chain to the short-range order parameters. For the first order Markov chain, the pair correlation function is related to the conditional transition probability by

$$\rho^{i,j}_{\ell_1,\ell_2} = P_{i,j}(|\ell_1-\ell_2|) \tag{3.108}$$

The reason for the absolute value $|\ell_1-\ell_2|$ is that the Markov chain has direction; one can examine a chain in only one direction at a time. Since the Markov chain we generate is isotopic, it does not matter which direction we consider. This directionality is important if one considers the relationship of Markov probabilities to triplet correlation functions.

The short-range order parameter for the first order Markov chains is

$$\alpha_n = (\alpha_1)^n \text{ where } \alpha_1=(p_{dd,d}-c_d)/(1-c_d)$$

The Fourier transform of α_n can be computed in closed form

$$\alpha(k)=\sum_{n=-\infty}^{\infty} e^{ikna}\alpha_n=\sum_{n=-\infty}^{\infty} e^{ikna}(\alpha_1)^{(n)}$$

$$=1+2\sum_{n=1}^{0}\alpha_1^n\cos(nka)$$

$$=1+2\left[\frac{(1-\alpha_1\cos ka)}{1-2\alpha_1\cos ka+\alpha_1^2}-1\right] \quad (1.353.3)^{39}$$

$$\alpha(k)=\frac{1-\alpha_1^2}{1-2\alpha_1\cos ka+\alpha_1^2} \qquad (3.109)$$

$\alpha(k)$ is characterized by a single broad peak centered at $k=0$ or $k=\frac{\pi}{a}$ depending on whether $\alpha_1>0$ or $\alpha_1<0$ respectively. The relationship of the second order Markov conditional transition probabilities to the pair correlation function is not as simple as that for the first order chain; it is examined in Appendix C.

Frequency Spectra of Linear Chains With Short-Range Order

Before examining the spectra of chains with short-range order, we will mention other work using nearest neighbor short-range order. Payton[33] calculated a limited number of spectra using Dean's technique with short-range order for $C_d=.5$. Payton used nearest-neighbor pair correlation functions to generate his short-range order which for $C_d=.5$ are particularly simple, i.e.

$$\rho_{0,1}^{d,d}=\rho_{0,1}^{h,h}=\tfrac{1}{2}(1+\alpha_1) \qquad (3.110)$$

In general it is conceptually incorrect to generate a chain using pair correlation functions. However, for Payton's particular case of nearest neighbor correlations only, the logical fallacy does not result in an incorrect chain because the first order Markov transition probabilities are numerically identical to the nearest neighbor pair correlation functions. More recently, Papatriantafillou,[34] has introduced short-range order into the one dimensional electron problem. His order, although not stated in the paper, is a first order Markov chain. He does not generate frequency spectra, however. Neither, Payton or Papatriantafillou justified their method of generating short-range order or studied its implications in terms of correlation functions. We, on the other hand, have mathematically justified our method of generating short-range order and have examined the pair correlation functions for this order.

Matsuda and Teramoto[41] used first order Markov chain theory to calculate a formula for the integrated density of states of the harmonic mass defect linear chain to certain special frequencies. One point to note here is their use of Markov chain theory was in a much different context than presented in this thesis and was not easily reformulated into generation of linear chains. The special frequencies correspond to zeros in the density of states of random chain[40] and are given by

$$\omega^2(s,t) = \omega^2_{max} \cos^2(\frac{\pi s}{2t}) \tag{3.111}$$

where ω^2_{max} is the maximum allowable frequency of a perfect chain of light atoms (in our case $\omega^2_{max}=4.$) and s and t are integers prime to each other.

s and t are determined by the condition

$$\frac{m_h}{m_L} \geq 1+\cot(\pi/2t)\tan(s\pi/2t) \tag{3.112}$$

for a mass ratio of $\frac{m_h}{m_L}=2$, s must be equal to 1. In this case the Matsuda and Teramoto formula for integrated density of states is

$$N(\omega^2(s,t))=1-[c_d(1-p_{d,d})p^{t-2}_{d,d}/(1-p^t_{d,d})] \tag{3.113}$$

where N is the integrated density of states and $p_{d,d}$ is the Markov transition probability.

The justification for introduction of short-range order into the this formula is not clear. It seems to depend on the assumption that the special frequencies do not change with introduction of short-range order. Unfortunately numerical studies cannot adequately examine the special frequencies since we can use only finite length chains.

Table 3.3 gives some of the values of $t,\omega^2(s,t)$ and $N(\omega^2(s,t))$ for the 50 percent random chain.

TABLE 3.3.--Comparison of numerical spectra and Equation (3.113) for $c=.5, p_{d,d}=.5$.

t	$\omega^2(s,t)$	Eq. (3.113) $N[\omega^2(s,t)]$	Approximate Numerical
2	2.	.66667	.667
3	3.	.85714	.858
4	3.414	.93333	.934
5	3.618	.96774	.968
6	3.732	.98413	.984
7	3.802	.99213	.992

Looking at Figure (2.5) the first five zeros are visible. The agreement is excellent in this case.

First Order Markov Chain Spectra

First we will examine, the effect of short-range order generated by a first order Markov chain. Figures (3.8), (3.9), (3.10) and (3.11) are for $c_d=.2$ and $P_{d,d}=0.0$, 0.4, 0.6, 0.8 respectively. These can be compared to Figure (2.8) for the random case. For $P_{d,d}=0$, no defect atoms can be next to each other, therefore, we get an increase of the isolated defect peak to $D(\omega_L^2)=1.62$ vs 1.45 for the random case. The rest of the structure above $\omega^2=2.$ is due to defect pairs, triples which are not nearest neighbors. The host mass spectrum is considerably more depleted at the high energy end of the spectrum than in the random case. For $P_{dd}=.4$, .6, .8, the opposite is true, with the $\omega^2=2.66$ peak decreasing in magnitude.

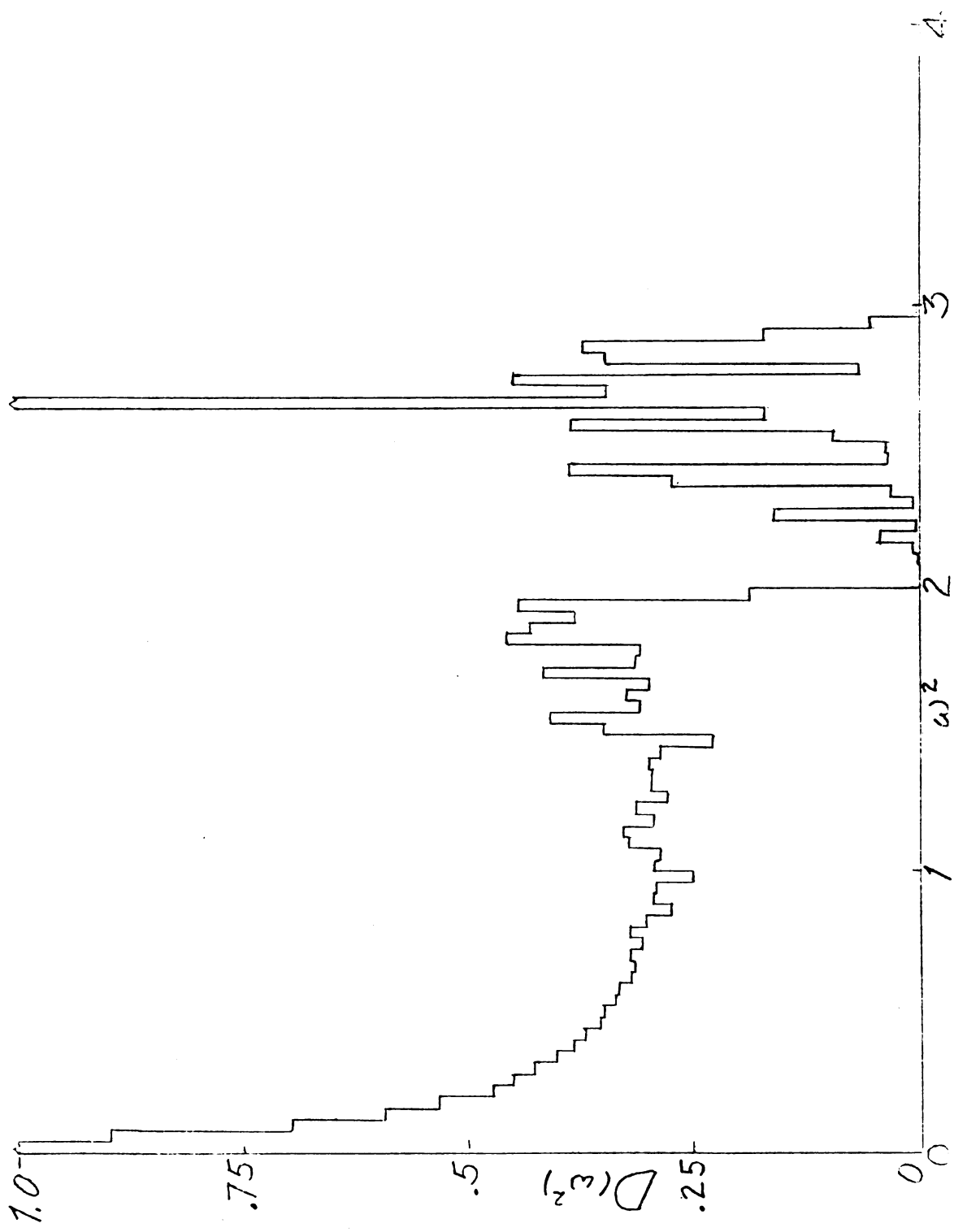

FIGURE 3.8.--Numerical density of states with C_2=.2, mass ratio 2/1 and $P_{d,d}$=0.0 for a 10000 unit chain.

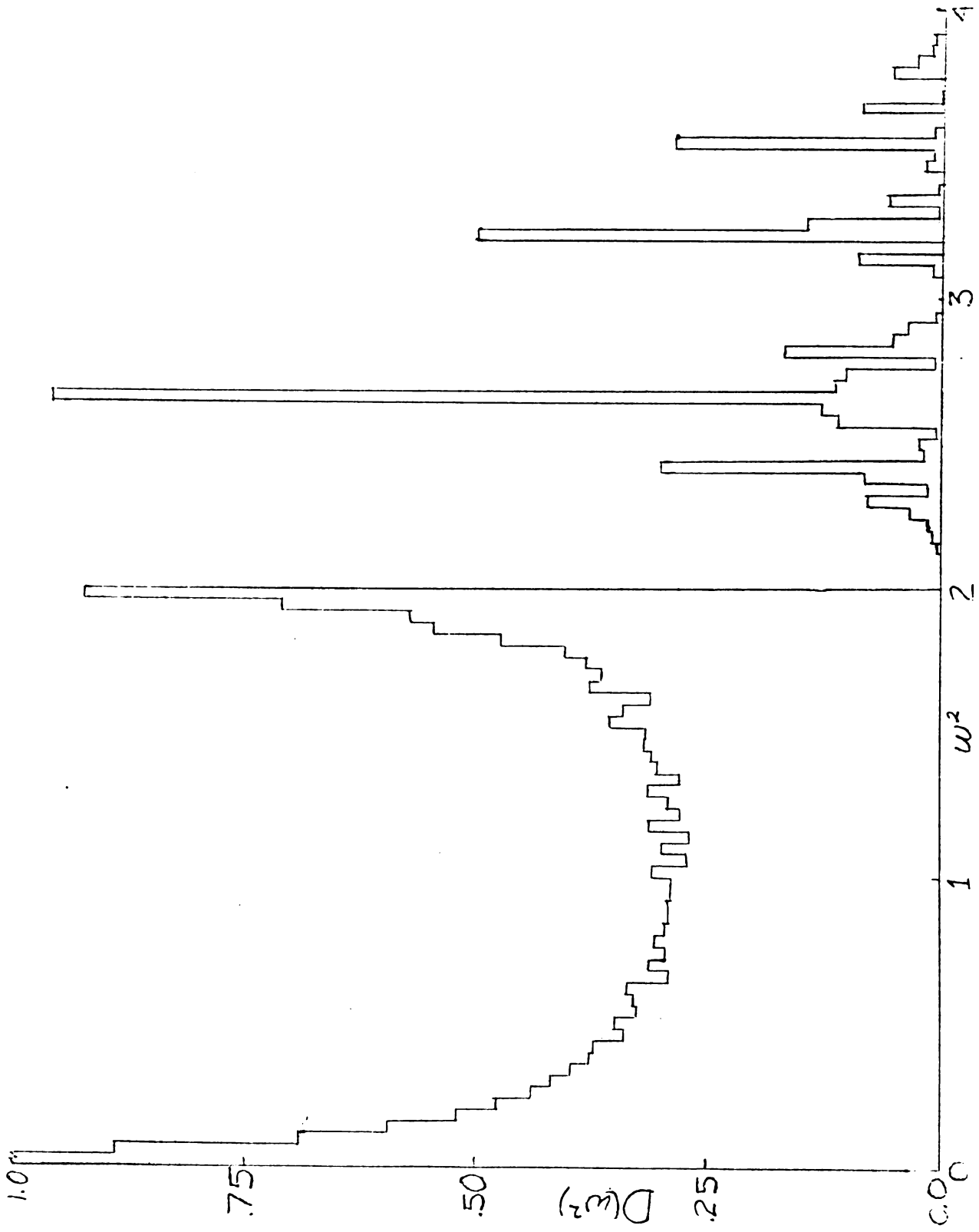

FIGURE 3.9.--Numerical density of states with C_d=.2, mass ratio 2/1 and $P_{d,d}$=.4 for a 10000 unit chain.

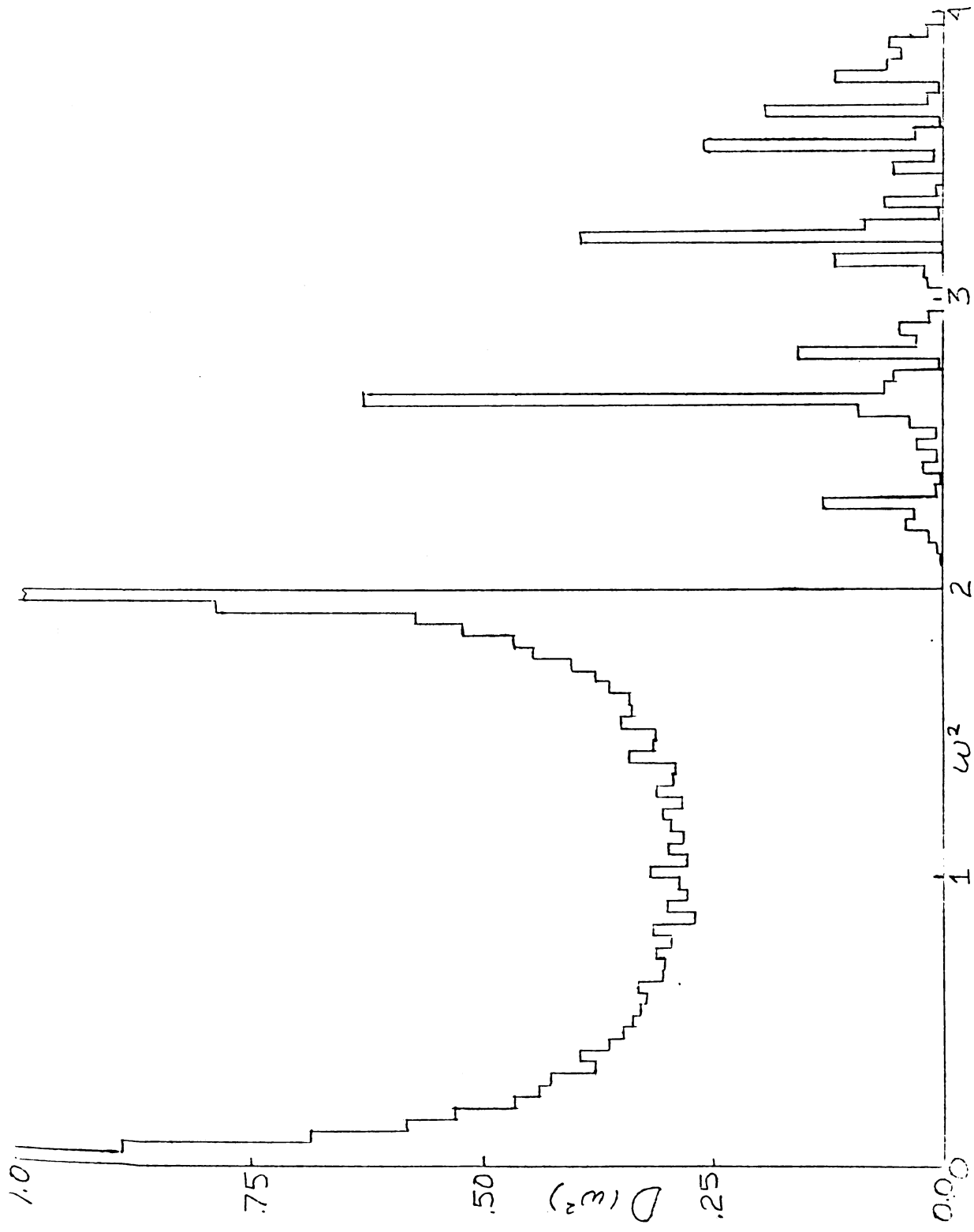

FIGURE 3.10.--Numerical density of states with C_d=.2, mass ratio 2/1 and $P_{d,d}$=.6 for a 10000 unit chain.

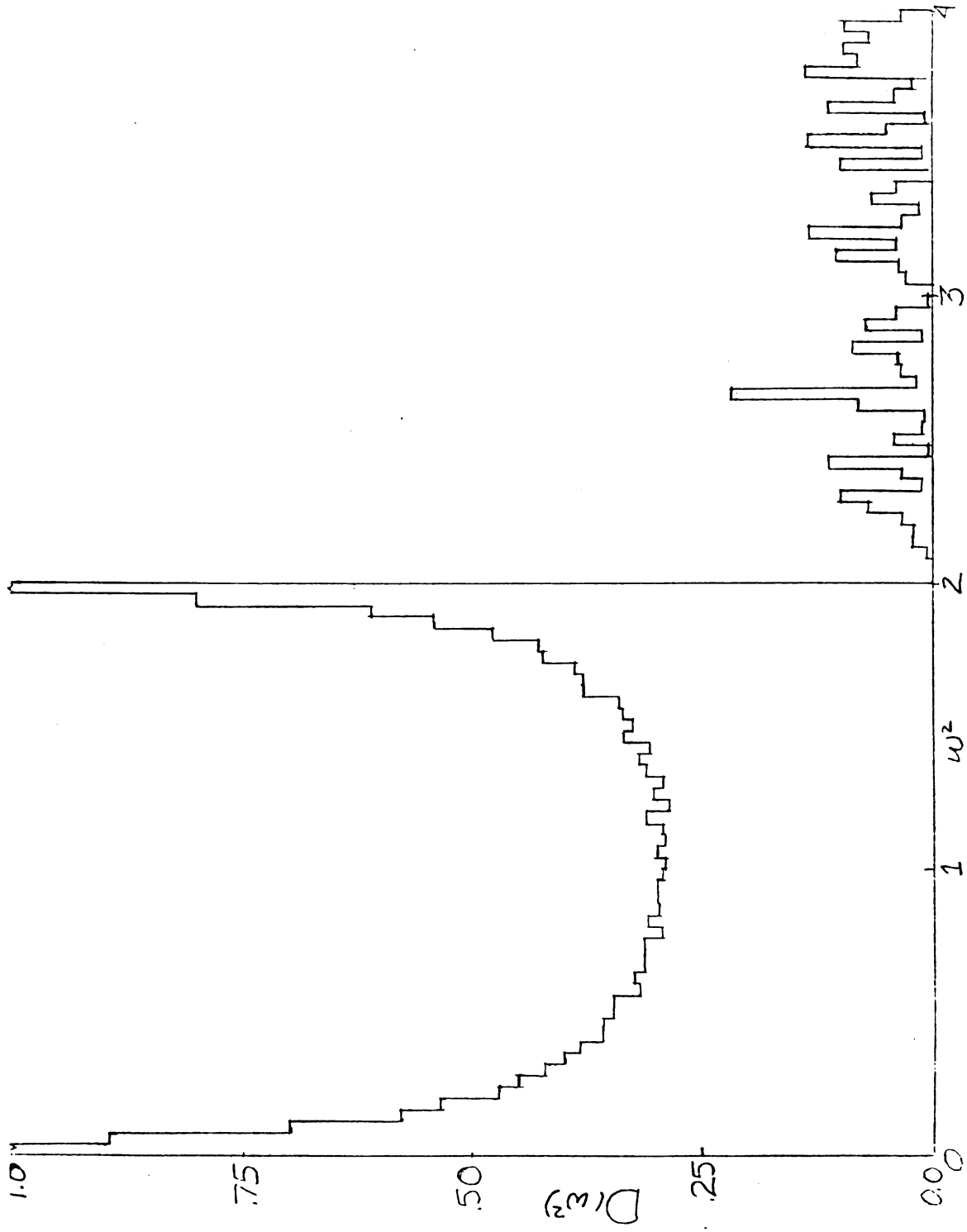

FIGURE 3.11.--Numerical density of states with C_d=.2, mass ratio 2/1 and $P_{d,d}$=.8 for a 10000 unit chain.

For $P_{d,d}=.8$ the impurity band spectrum is approximately evenly spread over the whole band. For this case the probability of long defect subchains and long host subchains is high. Figure (3.12) gives $\alpha(k)$ for these four chains. Table (3.4) compares the numerical integrated density of states to Equation (3.113).

TABLE 3.4.--Comparison of Equation (3.113) to numerical spectra for $c_d=.2$.

$P_{d,d}$	t	N(t)	Numerical
0.0	2	.8	.7966
	3	1.0	1.0
0.2	2	.8333	.8288
(random)	3	.9677	.9706
	4	.9936	.9936
0.4	2	.8571	.8538
	3	.9487	.9467
	4	.9803	.9792
	5	.9927	.9922
0.6	2	.8750	.8704
	3	.9388	.9371
	4	.9669	.9654
	5	.9813	.9796
	6	.9891	.9880
	7	.9936	.9929
0.8	2	.8889	.8963
	3	.9344	.9401
	4	.9566	.9601
	5	.9695	.9720
	6	.9778	.9785
	7	.9834	.9849

The agreement between the numerical results and Equation (3.113) is remarkably good considering that

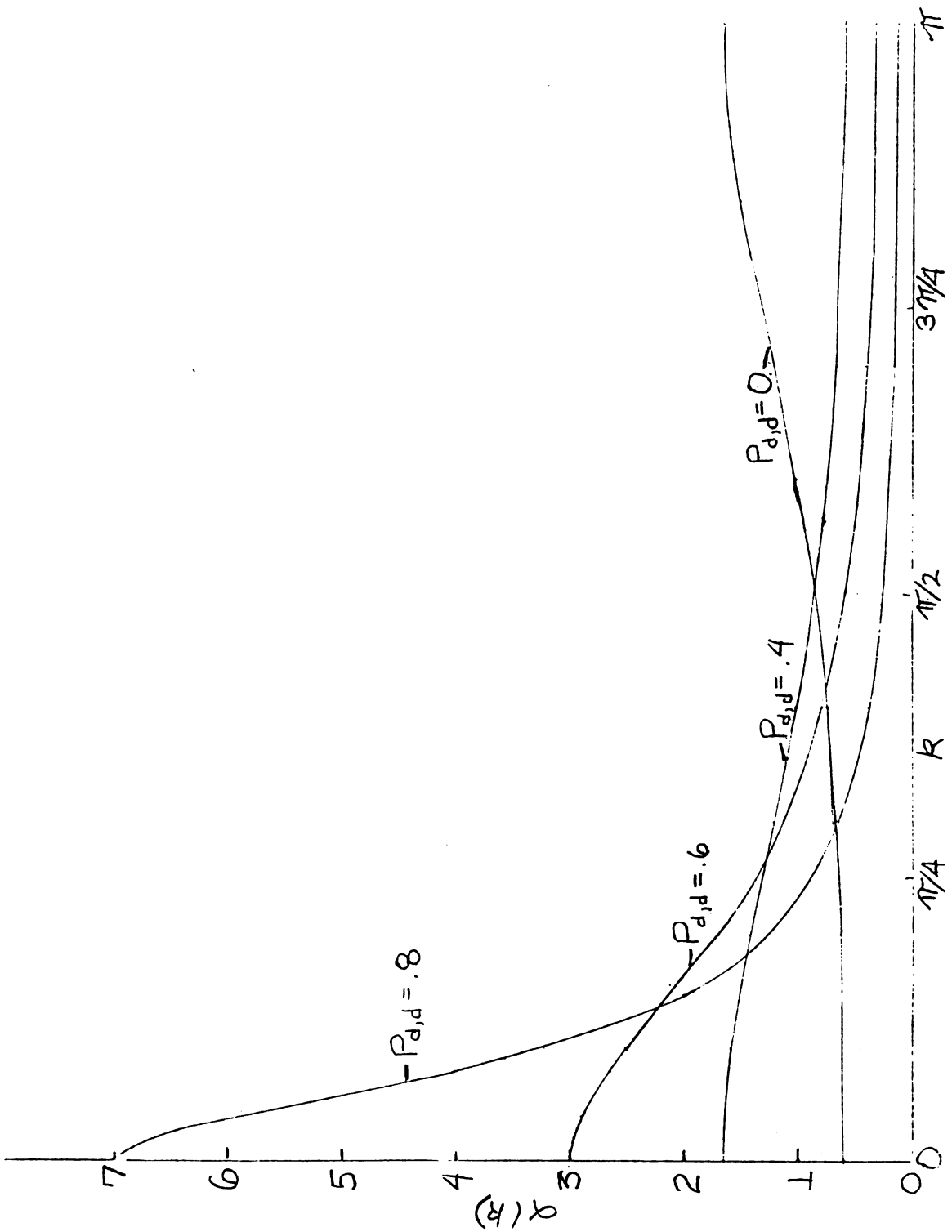

FIGURE 3.12.--Structure factor $\alpha(k)$ versus k for C_d=.2, $P_{d,d}$=0, .4, .6 and .8.

the concentration for $P_{d,d}$=0.8 came out to be .1852 instead of 0.2. Also, Equation (3.113) is exact only for infinite chains. The results in Table (3.4) tend to confirm the correctness of Equation (3.113) when short-range order is included.

Figures (3.13), (3.14), (3.15) and (3.16) are for c_d=.5 with $P_{d,d}$=.1, .25, .75 and .9 respectively. Figure (3.13) shows a slight deviation from the binary ordered chain in Figure (2.9) which would be obtained at c_d=.5, P_{dd}=0. The peaks between ω^2=1 and 2 come from 2 heavy mass clusters (ω^2=1.5) and 3 heavy mass clusters at ω^2=1.22. The peaks above ω^2=3 come from the light atom clusters. The band edge singularities at ω^2=1, and 2 disappear. For $P_{d,d}$=.25, Figure (3.14) shows that much of the ordered diatomic structure has been lost with the spectrum filling in the gap from ω^2=1 to 2. This can be compared to the c_d=.5 random case (Figure 2.5) where the spectrum looks like a depleted heavy mass spectrum with many modes in the forbidden region. Figures (3.15) and (3.16) show progressive clustering of light atoms which also gives clusters of heavy atoms. Clusters of heavy atoms produce the peak at the upper edge of the host band. For $P_{d,d}$=.75, the host band structure is reappearing and the impurity modes although highly structured are equally distributed between ω^2=2 and 4. For $P_{d,d}$=.9, the structure in the impurity

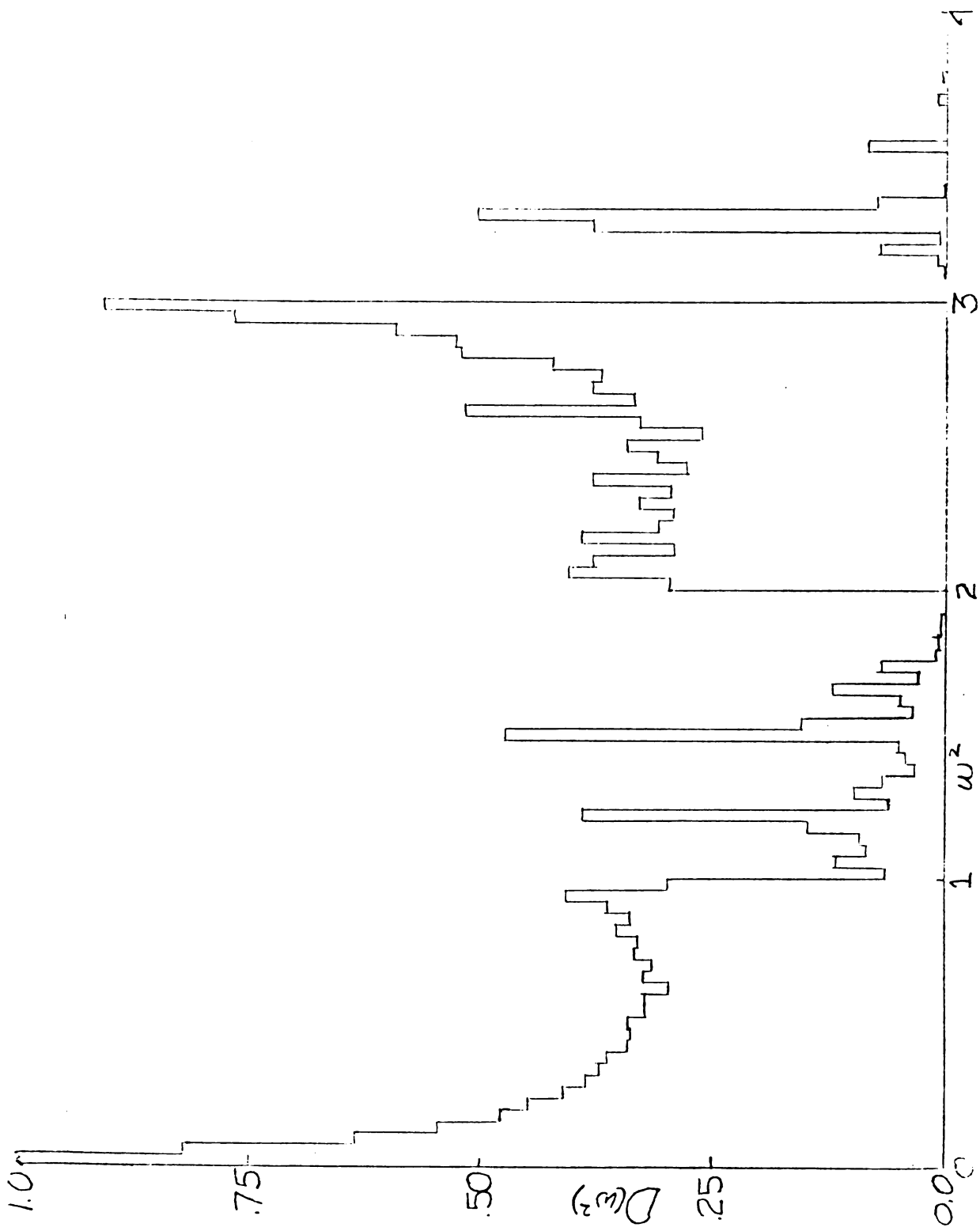

FIGURE 3.13.--Numerical density of states with C_d=.5, mass ratio 2/1, and $P_{d,d}$=.1 for a 10000 unit chain.

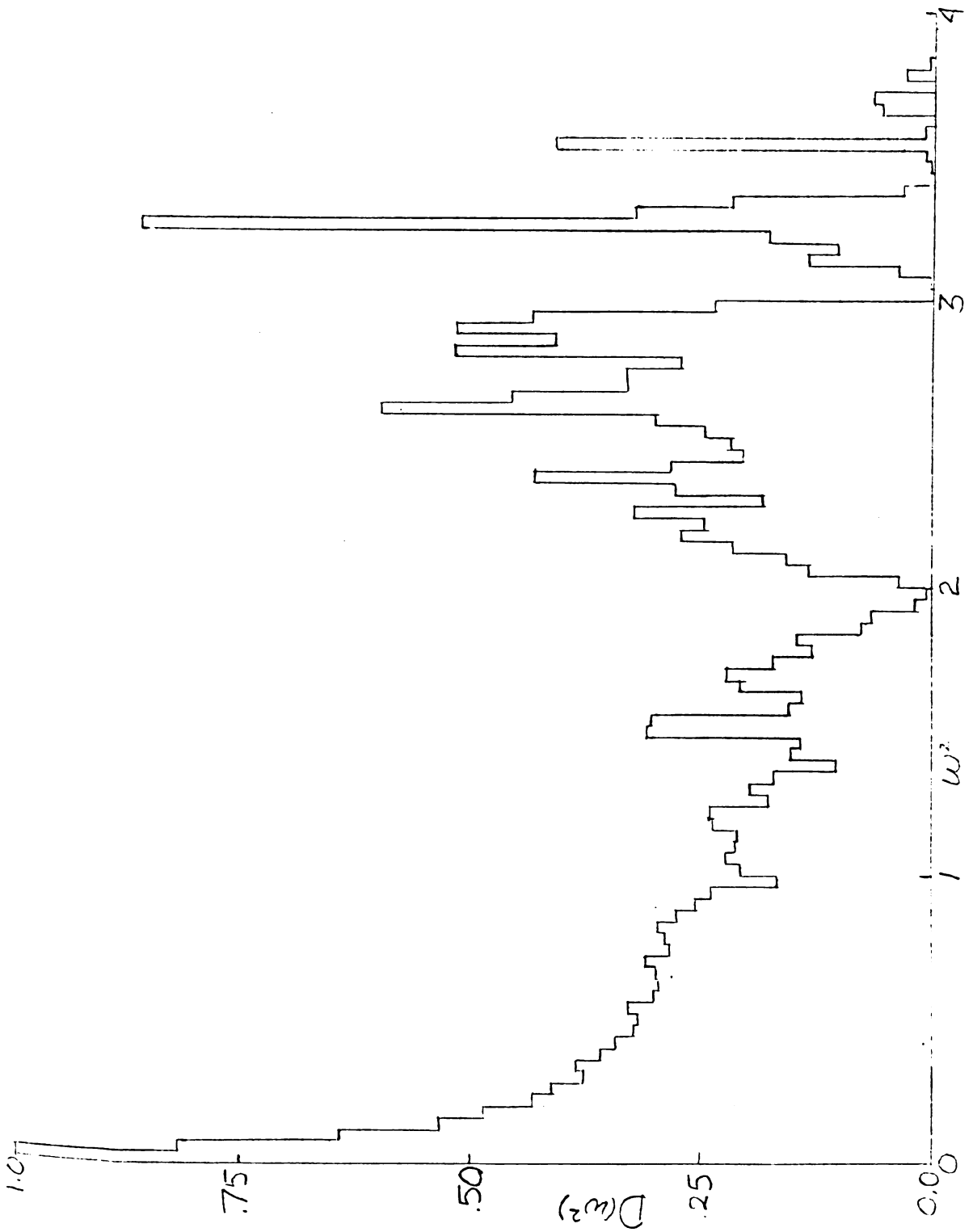

FIGURE 3.14.--Numerical density of states with C_d=.5, mass ratio 2/1, and $P_{d,d}$=.25 for a 10000 unit chain.

FIGURE 3.15.--Numerical density of states with C_d=.5, mass ratio 2/1 and $P_{d,d}$=.75 for a 10000 unit chain.

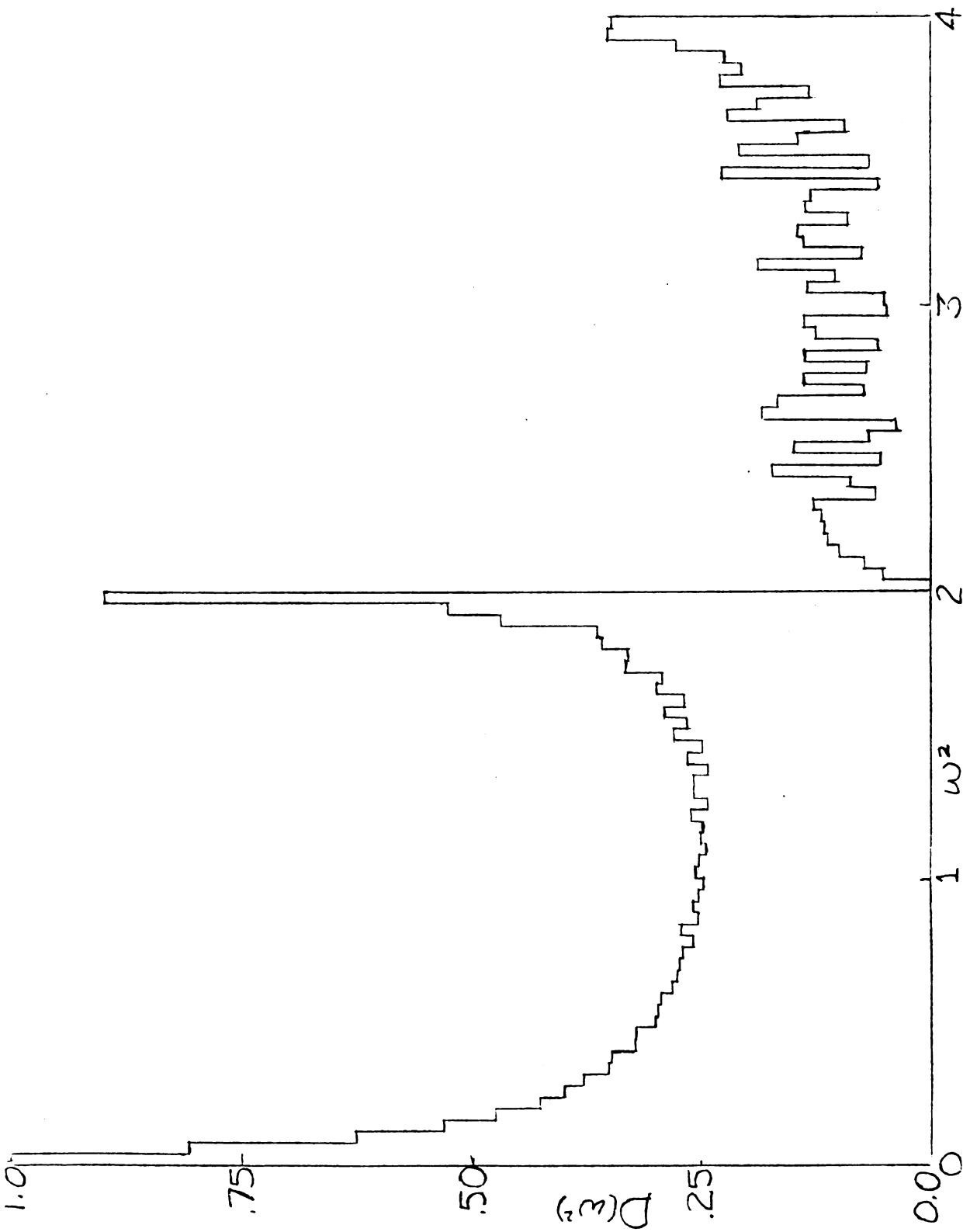

FIGURE 3.16.--Numerical density of states with C_d=.5, mass ratio 2/1 and $P_{d,d}$=.9 for a 10000 unit chain.

band is diminishing as the spectrum approaches the superposition of a light chain spectrum and a heavy chain spectrum with the integrated spectrum normalized to 1.0. Figure (3.17) shows the $\alpha(k)$'s for Figures (3.13)-(3.16). For c_d=.5, the $\alpha(k)$ corresponding to $p_{d,d}$=u is a mirror image of the $\alpha(k)$ corresponding to $p_{d,d}$=1.-u. The case $p_{d,d}$=0.1 approaches Case 1 and the case $p_{d,d}$=0.9 approaches Case 2 of Section II on x-ray scattering. Table (3.5) compares Equation (3.113) to the numerical integrated density of states at the special frequencies.

Second Order Markov Chains

Although numerous spectra were generated by second order Markov chain theory, we present only a few of the most interesting spectra herein. Figure (3.18) shows the only c_d=.2 spectra generated by second order Markov theory to be presented. Figure (3.18) is for $p_{dd,d}$=0. $p_{dh,d}$=.4 and $p_{hd,d}$=.8. Or, in words, the chain will not contain any defect clusters greater than two long ($p_{dd,d}$=0). In general, the defects will come in pairs ($p_{hd,d}$=.8) or separated by one host ($p_{dh,d}$=.4) with few isolated defects. The spectrum shows a large nearest-neighbor defect pair peak, ω=3.26 with only a small single defect peak ω=2.66. Figure (3.19) shows

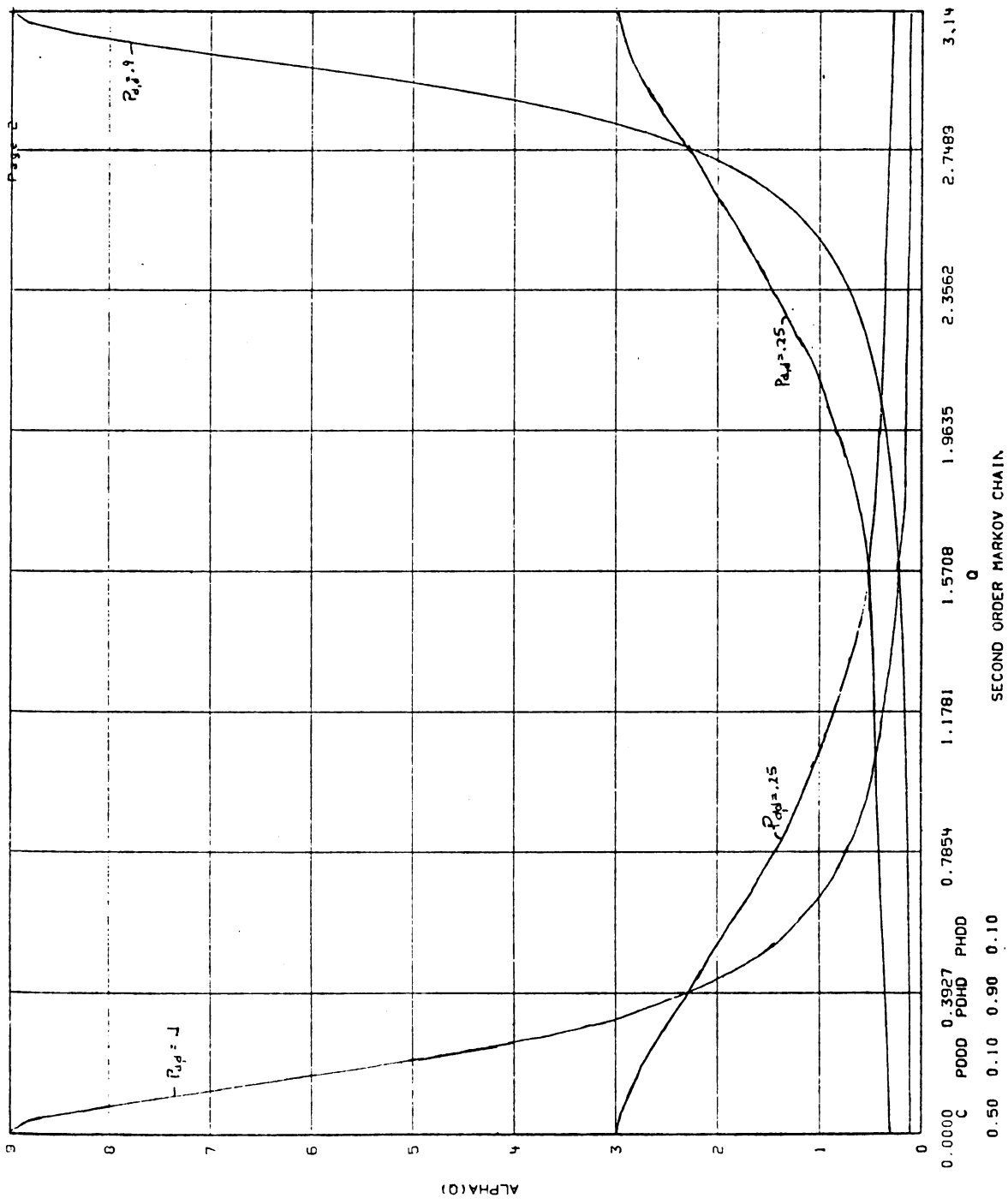

FIGURE 3.17.--Structure factor α(k) versus k for C_d=.5, $P_{d,d}$=.1, .25, .75 and .9.

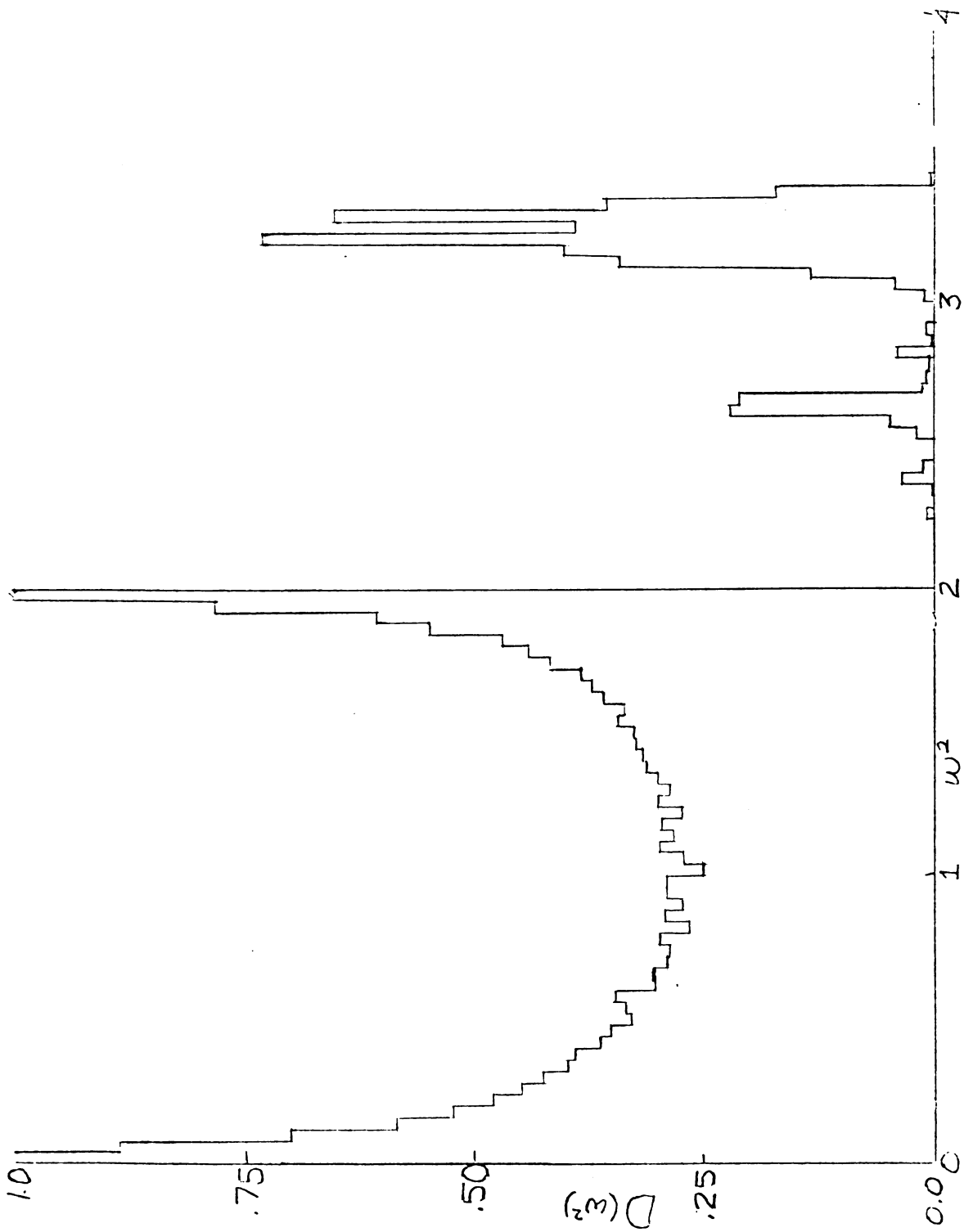

FIGURE 3.18.--Numerical density of states with C_d=.2, $P_{dd,d}$=0, $P_{dh,d}$=.4, $P_{hd,d}$=.8 and a mass ratio 2/1 for a 10000 unit chain.

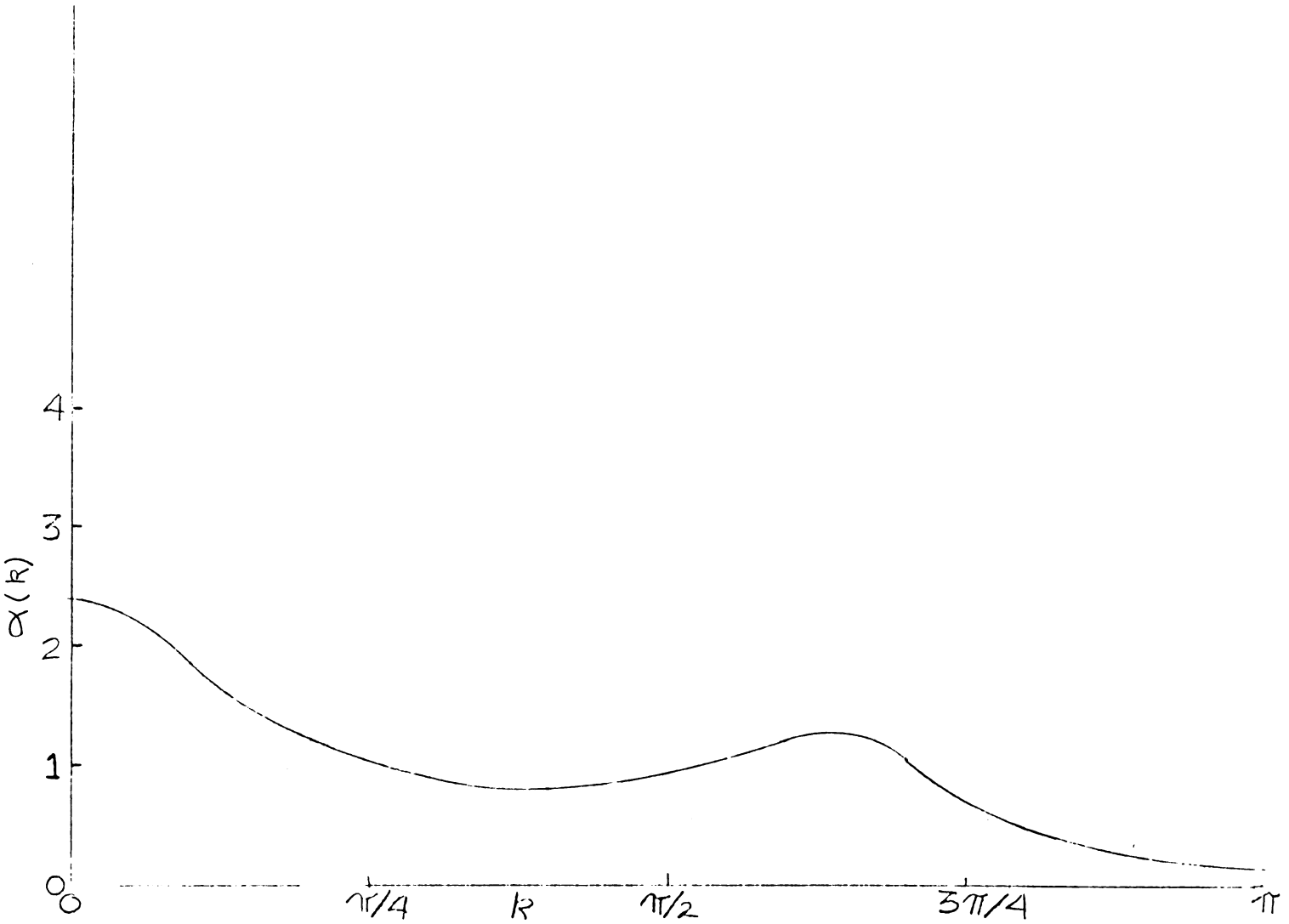

FIGURE 3.19.--Structure factor $\alpha(k)$ versus (k) for $C_d=.2$, $P_{dd,d}=0$, $P_{hd,d}=.8$ and $P_{dh,d}=.4$.

TABLE 3.5.--Comparison of Equation (3.113) to numerical spectra for c_d=.5.

$P_{d,d}$	t	N(t)	Numerical
0.1	2	.5455	.5466
	3	.9550	.9539
	4	.9955	.9960
0.25	2	.6000	.5970
	3	.9048	.9014
	4	.9765	.9767
	5	.9941	.9938
0.75	2	.7143	.7225
	3	.8378	.8433
	4	.8971	.9013
	5	.9309	.9330
	6	.9519	.9544
	7	.9658	.9670
0.9	2	.7368	.7363
	3	.8340	.8345
	4	.8822	.8818
	5	.9110	.9098
	6	.9300	.9298
	7	.9434	.9441

$\alpha(k)$ for this chain. It is quite different from that of the first order chain showing a local maximum between k=0 and π.

The line $P_{dd,d}=P_{hd,d}$;$P_{dh,d}=\frac{C_d(1-P_{dd})}{1-C_d}=P_{hh,d}$ in second order Markov space is equivalent to the first order Markov process. Figure (3.3) shows that for C_d=.5, this line is one of the diagonals in the unit cube. Two other diagonals for C_d=0.5 result in simple forms for $\alpha(k)$. These diagonals in Figure (3.3) are for C_d=.5:

$$P_{dd,d}=P_{dh,d};P_{hd,d}=P_{hh,d}=1-P_{dd,d} \tag{3.114}$$

and

$$P_{dd,d}=P_{hh,d};P_{dh,d}=P_{hd,d}=1-P_{dd,d} \tag{3.115}$$

Appendix B has a derivation of the short-range order parameters for each case.

$$\alpha(k) = \frac{1-\alpha_2^2}{1-2\alpha_2\cos(2ka)+\alpha_2^2} \tag{3.116}$$

where $\alpha_2 = (P_{dd,d}-C_d)/(1-C_d)=2P_{dd,d}-1$

corresponds to Equation (3.114) and

$$\alpha(k) = \frac{1-\alpha_3^2}{1-2\alpha_3\cos(3ka)+\alpha_3^2} \tag{3.117}$$

$$\text{where } \alpha_3=\frac{(C_d)}{1-C_d}\left(\frac{P_{dd,d}-C_d}{1-C_d}\right)^2=(2P_{dd,d}-1)^2 \tag{3.117a}$$

corresponds to Equation (3.115).

The period of Equation (3.116) is one-half the period of the short-range order function, $\alpha(k)$, for the first order Markov process; whereas the period of Equation (3.117) is only 1/3 of that for the first order Markov process. In addition from Equation (3.117a) we note that $P_{dd,d}$ can have two values for any α_3, therefore the identical short-range order function can result from two different $P_{dd,d}$. This ambiguity illustrates an important point which will be even more dramatically made at the end of this section. Whereas there is a one to one correspondance between chains which

can be generated by a first order Markov process and a set of short-range order parameters, namely the very simple set given by Equation (3.108), there is no such correspondance for the second-order Markov chain. In fact, quite different second order Markov chains may produce the same set of pair correlation functions. Therefore in order to study the statistical properties of a second-order Markov chain one needs triple (and perhaps higher) order correlation functions.

Figures (3.20) and (3.21) show vibrational spectra for second order Markov chains satisfying Equation (3.114) with $P_{dd,d}=.25$ and $P_{dd,d}=.75$, respectively.

With $P_{dd,d}=.25$, the spectrum is not radically different from the random case with only a reduction in the single defect mode (because $P_{hd,h}=.25$) and a corresponding increase in the nearest neighbor pair defect mode (because $P_{hd,d}=.75$). The spectrum for $P_{dd,d}=.75$ is, however, quite different. The band edge at $\omega^2=2$ is not visible. Since $P_{dh,d}=P_{hd,h}=0.75$ the chain has a structure rather like the binary ordered chain (with $P_{dh,d}=P_{hd,h}=1.0$) but because $P_{dd,d}=P_{hh,h}=0.75$ this structure includes some long clusters of similar atoms. The short-range order functions for these two chains differ by $\pi/2$ phase shift as shown in Figure (3.22) for $P_{dd,d}=.25$ and .75 respectively.

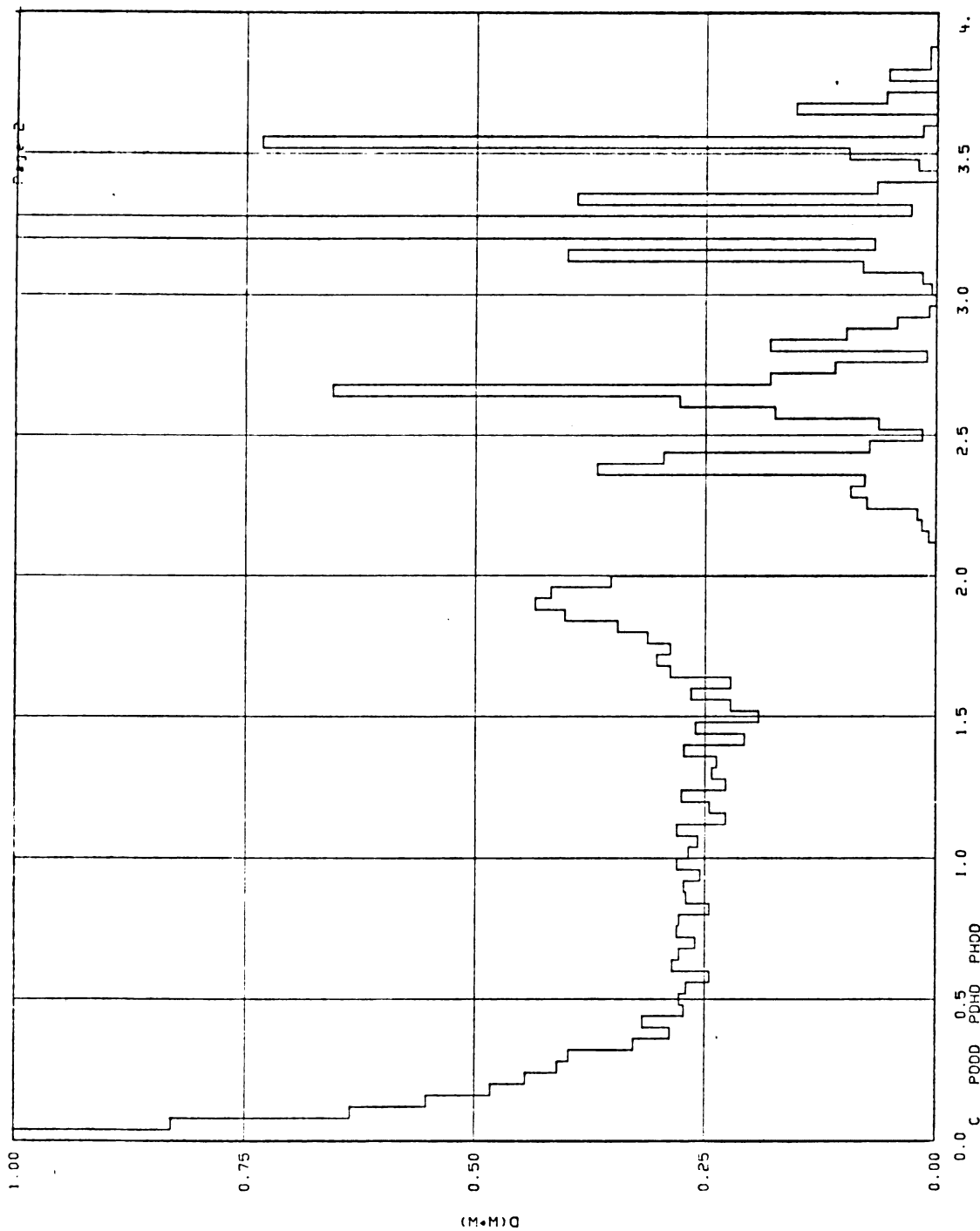

FIGURE 3.20.--Numerical density of states with C_d=.5, $P_{dd,d}$=$P_{dh,d}$=.25, $P_{hh,d}$=$P_{hd,d}$=.75 and mass ratio 2/1 for a 10000 unit chain.

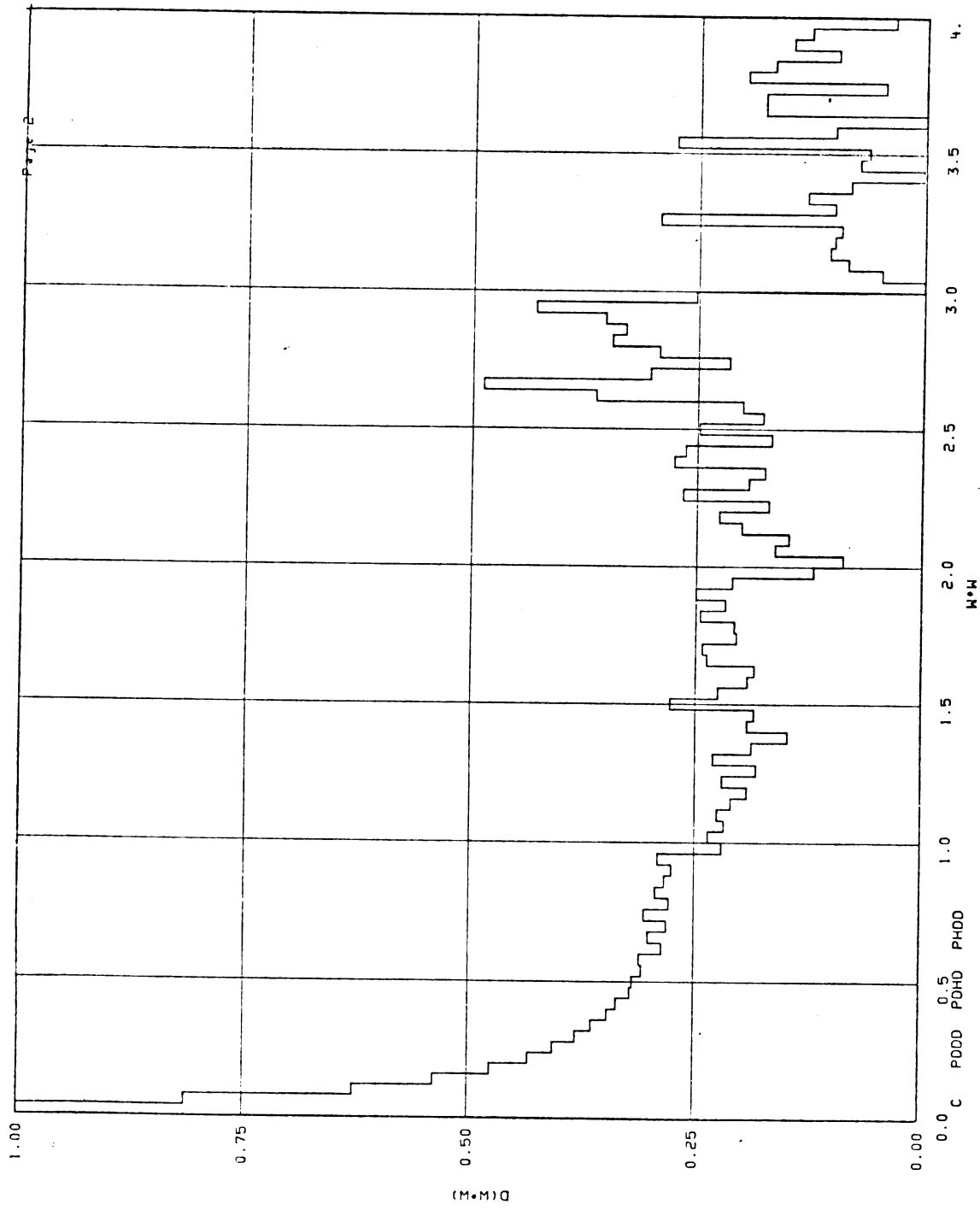

FIGURE 3.21.--Numerical density of states with C_d=.5, $P_{dd,d}$=$P_{dh,d}$=.75, $P_{hh,d}$=$P_{hd,d}$=.25 and mass ratio 2/1 for a 10000 unit chain.

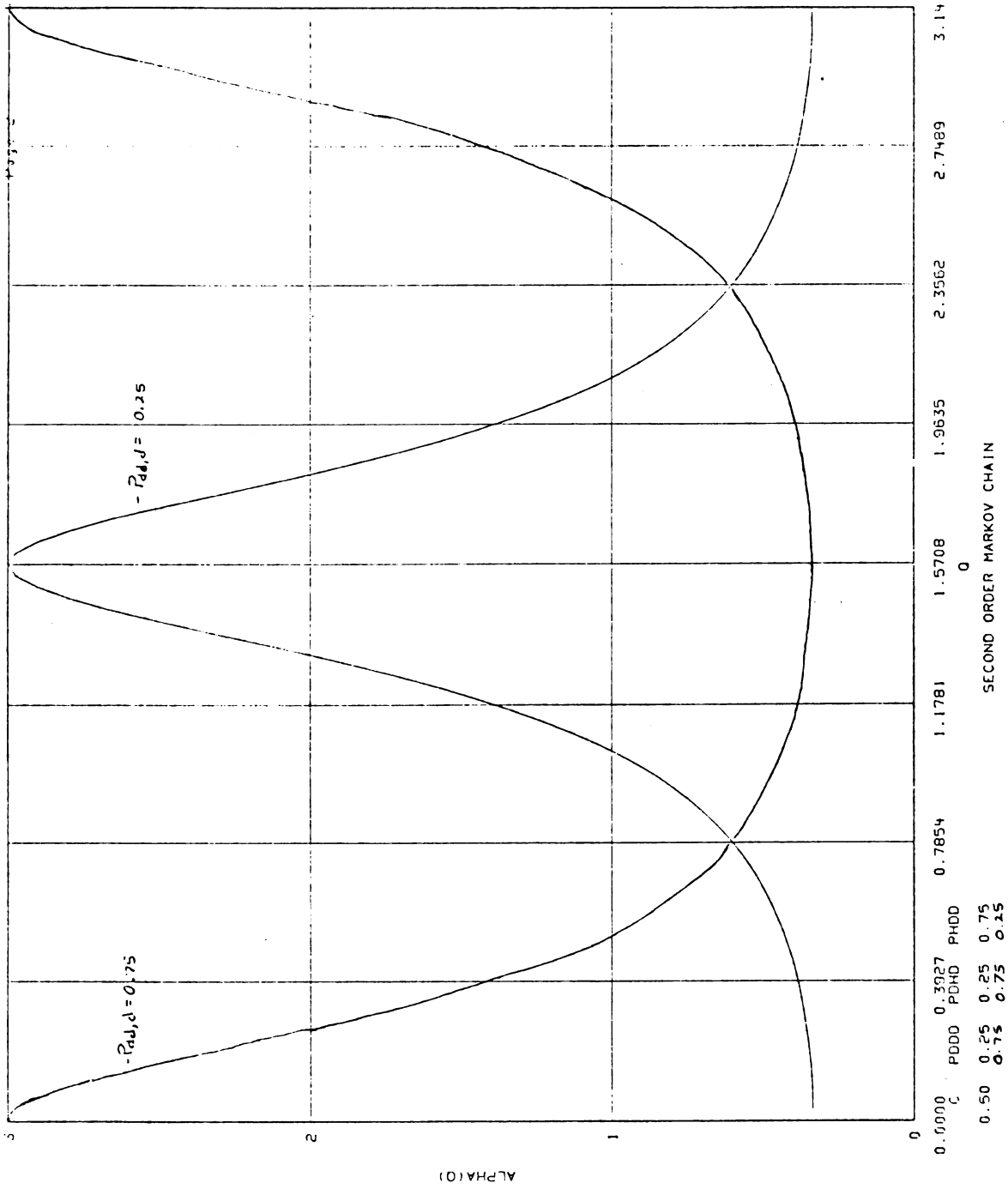

FIGURE 3.22.--Structure factor $\alpha(k)$ versus k for $C_d=.5$
$P_{dd,d}=P_{dh,d}=.25$, .75 and $P_{hh,d}=P_{hd,d}=.25$, .75.

Figures (3.23) and (3.24) show spectra for chains with short-range order satisfying Equation (3.115) with $P_{dd,d}=.25$ and $P_{dd,d}=.75$ respectively. The single curve in Figure (3.25) shows the short-range order function for both cases. Though the pair correlation functions are all identical, two spectra are never the less quite different! The probability of having defect clusters of size n surrounded by single host masses is given in Table 3.6.

TABLE 3.6.--Probability of cluster of light atoms of size n for Equation (3.115).

Cluster size h-nd-h	Probability of occurrance $C_d=.5, P_{dd,d}=P_{hh,d}=1-P_{nd,d}$			
n	random	$P_{dd,d}=.25$		$P_{dd,d}=.75$
1	.125	.0625	<	.1875
2	.0625	.140625	>	.015625
3	.03125	.035156	>	.011719
4	.015625	.008789	≡	.008789
5	.007812	.002197	<	.006592

Table 3.7 gives the probability of having n host-defect clusters for these two chains.

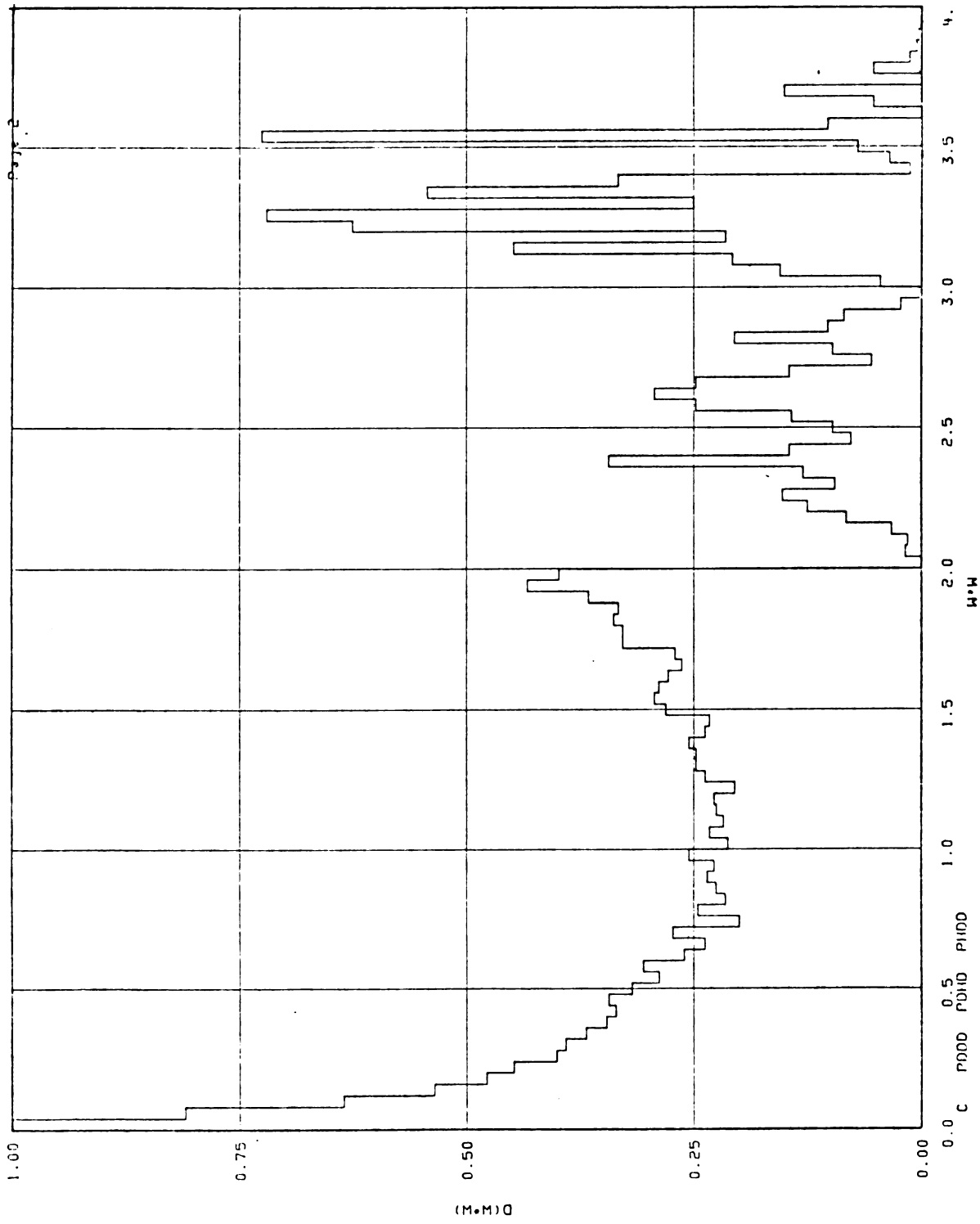

FIGURE 3.23.--Numerical density of states with C_d=.5, $P_{dd,d}=P_{hh,d}$=.25, $P_{dh,d}=P_{hd,d}$=.75 and mass ratio 2/1 for a 10000 unit chain.

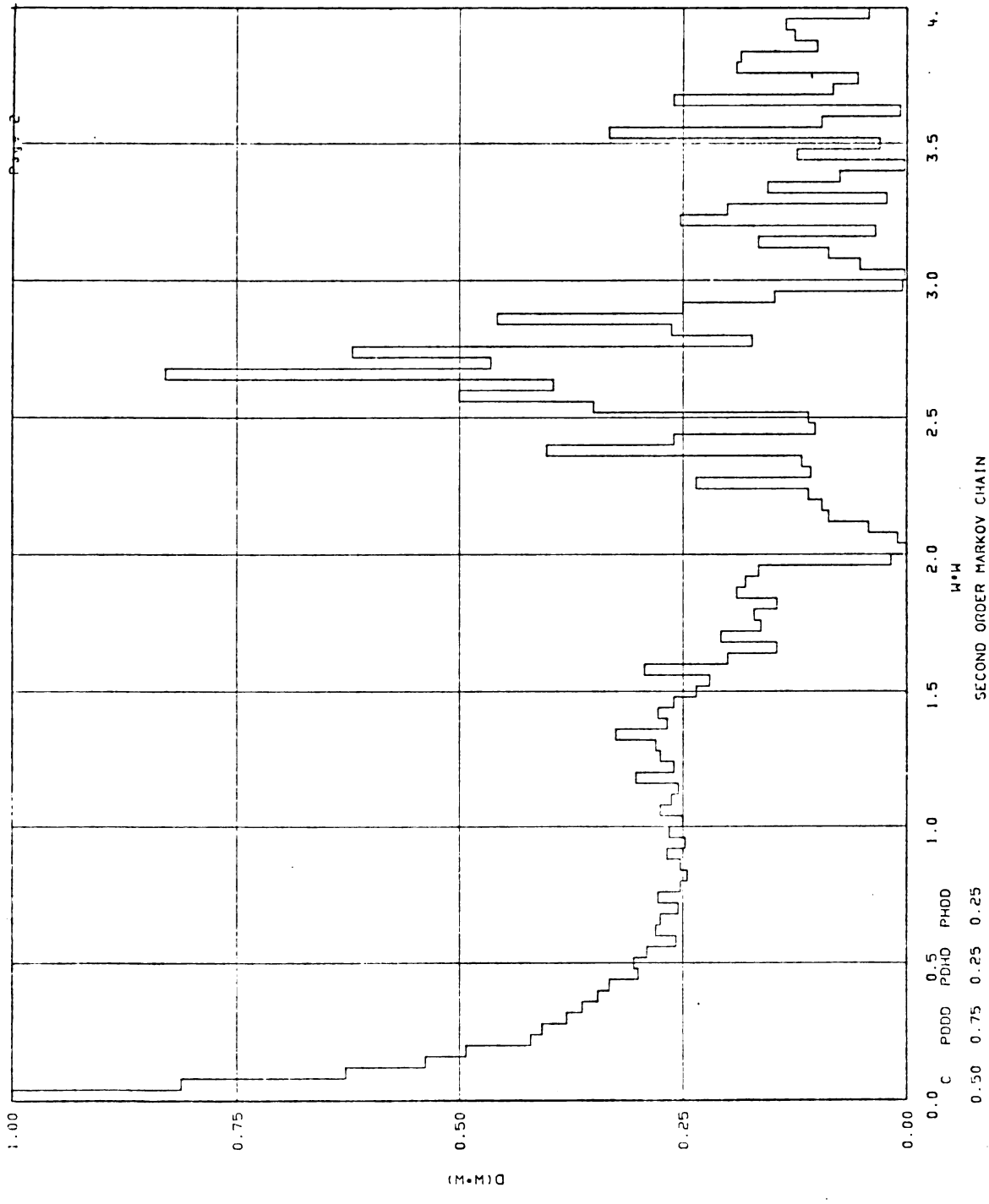

FIGURE 3.24.--Numerical density of states with C_d=.5, $P^2_{dd,d}$=$P_{hh,d}$=.75, $P^2_{dh,d}$=$P_{hd,d}$=.25 and mass ratio 2/1 for a 10000 unit chain.

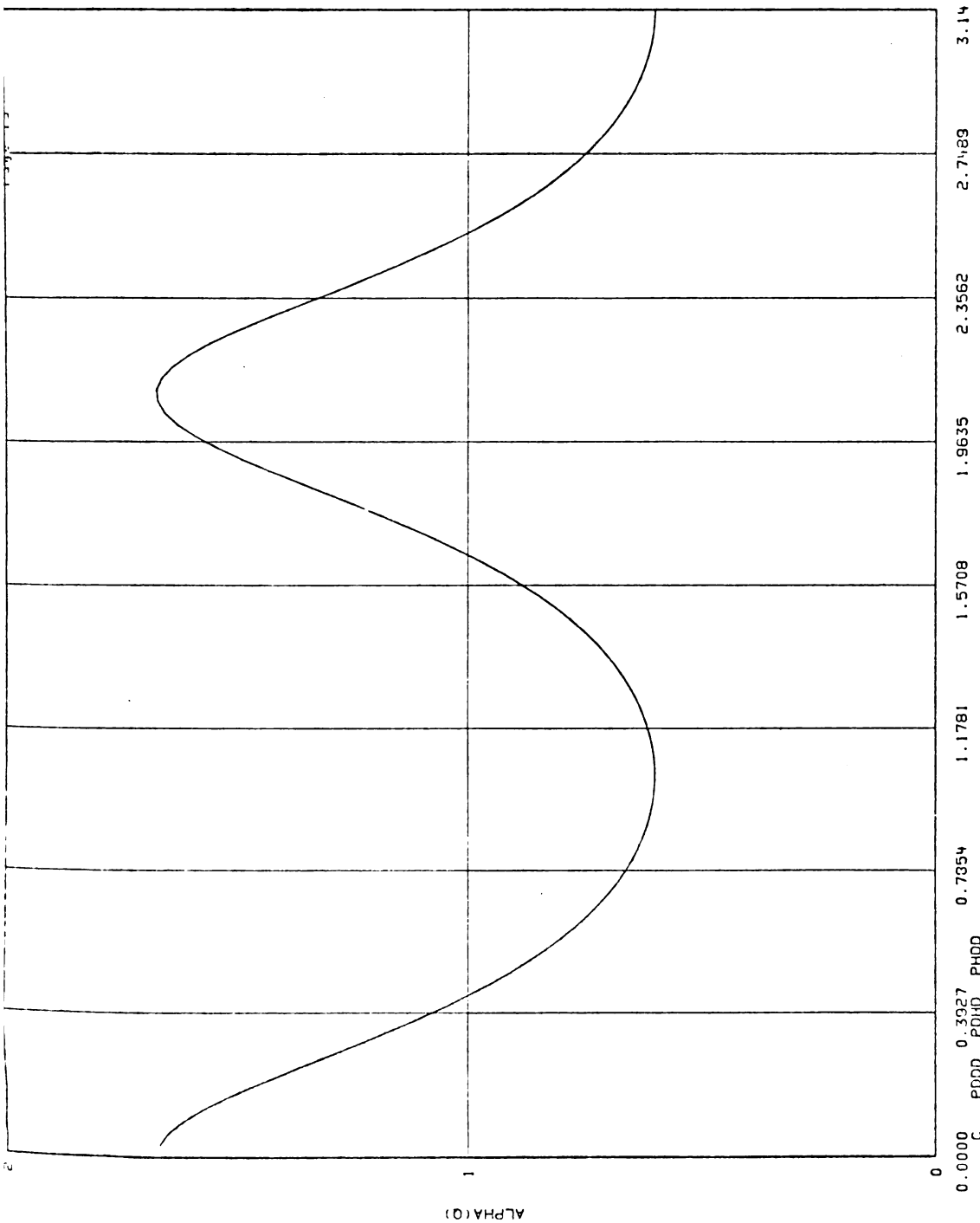

FIGURE 3.25.--Structure factor $\alpha(k)$ versus k for $C_d=.5$, $P_{hh,d}=P_{dd,d}=.25$, .75 and $P_{dh,d}=P_{hd,d}=.75$, .25.

TABLE 3.7.--Probability of having n-host defect clusters for Equation (3.115).

Cluster size n-(hd)	Probability $P_{dd,d}=.25$	Probability $P_{dd,d}=.75$	random
1	.25	.25	.25
2	.046875	.046875	.0625
3	.008789	.008789	.015625

From these two tables it is clear that the major difference between the two chains is that isolated defects are more probable for $P_{dd,d}=0.75$ and nearest neighbor defect pairs are considerably more probable for $P_{dd,d}=0.25$.

CHAPTER IV

LOCALIZATION OF EIGENSTATES OF DISORDERED CHAINS

There is considerable physical interest in whether eigenstates of disordered systems are localized or nonlocalized. In terms of thermodynamic quantities, thermal conductivity for phonons and electronic conductivity for electrons depend on the localization of the eigenstates of a system. The degree of localization of each eigenstate, also, gives information on the basic quantum mechanical mechanisms working in the system.

A precise general definition of a localized mode versus a nonlocalized mode is not available. However, an acceptable working definition is available. An eigenstate is localized if the eigenfunction is appreciable over some region of space and decays exponentially away from this region. In infinite systems, this is most likely as precise a definition as one needs. However, in finite systems, this definition, while catagorizing some of the eigenstates as localized, is insufficient to adequately describe the character of other modes.

For one dimensional systems with nearest neighbor interactions considerable localization work has been done. Mott and Twose[45] conjectured and Borland[46] proved that all one electron eigenstates of the disordered chain are localized. This proof is valid for eigenstates of arbitrarily large energy for an infinite chain with a finite fraction of disorder, and therefore applies to the exact solutions of a Schröedinger equation. Demonstration of localization in the lattice dynamics problem does not require such a dramatic result. The lattice dynamics problem is more akin to the Anderson model,[47] where the one-electron wave functions are expanded in functions which are eigenstates of a single atomic energy level (Tight binding model) or which correspond to a single band (Wannier picture). Dean[48] presented an analogous proof to Borland's theorem for the phonons in a disordered chain. Dean showed that all eigenfunctions of an infinite linear chain are localized. More recently, Economou and Cohen[49] presented a more general proof of the localization character of eigenstates of the Anderson Hamiltonian and of the lattice dynamics problem.

In the electron problem, the degree of randomness corresponds to the difference in energy levels and hopping terms between the two constituents in a binary chain. One might think that the mass ratio would be a similar measure of randomness in the phonon problem. It

is but only one of two measures in the phonon case, the other being the frequency of the eigenstate. As $\omega \to 0$ the modes must become delocalized. Hori[50] and coworkers have argued that Borland's definition of localization may be too loose for practical use, since according to it any one dimensional system with disorder (finite concentration of impurities) would have all eigenstates localized and no conductivity could occur in contradiction to physical intuition.

The problem with Borland and Dean's proofs involves the definition of infinite systems. In contrast for infinite systems with boundary conditions, P. Taylor[51] has argued that no eigenstate is strictly localized. His argument is based on the fact that changing the boundary conditions will change all eigenvalues and eigenvectors and a localized state would not be subject to "distant" boundary conditions. Hori has suggested that this definition of localization may be too strict.

Two note worthy attempts have been made in the one dimensional harmonic phonon problem to find eigenfrequencies in random systems beyond which all states are localized. Matsuda and Ishii[52] give an expression for the approximate number of vibrational modes in the finite mass-disordered system that are not "well localized". Using the assumption that the localization of eigenfunctions in "large" finite systems is equivalent to

the localization of eigenfunctions in infinite systems, the number of non-localized modes is

$$n = \frac{4}{\pi} \sqrt{N}\langle m\rangle / \sqrt{\langle (m-\langle m\rangle)^2\rangle} \qquad (4.1)$$

where N is the chain length
and $\langle m\rangle = C_d m_d + C_h m_h$ is the average mass of the chain. They admit that this formula is valid only to an order of magnitude since "well localized" is not a precisely defined quantity. Visscher,[53] using Matsuda and Ishii's ideas, performed some numerical studies on thermal energy transport in chains up to 1000 atoms. He arbitrarily defined the eigenfrequency above which all states are "localized" as the eigenfrequency above which the sum of the remaining eigenfrequencies gives a total contribution to the thermal conductivity of only 10%. Visscher obtains an emperical formula for the demarcation mode of

$$n_c = 5.5(N)^{\frac{1}{2}} \qquad (4.2)$$

for a two to one mass ratio random system. Both methods suffer in that a few modes of high frequency in nonrandom disordered systems could carry a significant amount of the thermal transport energy and be quite nonlocalized. These modes would not be of interest under Visscher's criteria and for finite system could violate Matsuda and Ishii's assumptions.

From the preceding discussion, it is apparent we need to catagorize the degree of localization as a function of frequency, mass ratio, and short-range order. Thouless[54] has given a number of localization criteria for the electron problem, some of which we can adopt to the phonon problem. The eigenfunctions of the electron exist continuously throughout space whereas the components of the eigenvector in lattice vibrations are defined only with respect to lattice points. Since Thouless considers an infinite system his criteria are binary in nature, either an electron is localized or it is delocalized. We propose that some of his criteria may be applied to the lattice dynamics of finite systems with the localization parameter taking on a continuum of values bounded by the localized and delocalized values for the infinite system.

Thouless feels the following criteria should give equivalent indications of localization. Using $\psi_\lambda(r)$ as the electron wave function and $U_\ell(\lambda)$ as the displacement of the ℓ^{th} atom for eigenfrequency λ, we have

1. Non-zero value of $\int|\psi_\lambda(r)|^4 d^3r$ which corresponds to

$$\alpha = \sum_\ell |U_\ell(\lambda)|^4 / \sum_\ell |U_\ell(\lambda)|^2 = \sum_\ell |U_\ell(\lambda)|^4 \qquad (4.3)$$

for a eigenvector normalized to one; α is an inverse localization length. For the perfect crystal with periodic boundary conditions $U_\ell(\lambda)= \frac{1}{\sqrt{N}} e^{ik_\lambda \ell a}$ and $\alpha = \frac{1}{N}$ where N is the number of atoms in the chains. A similar derivation for fixed boundary conditions is given in Appendix I. We can calculate the eigenvector of linear chains as given in Appendix D and easily apply this criteria.

2. Discrete (but dense) spectral density $\sum_\lambda |\psi_\lambda(r)|^2 \delta(E-\lambda)$ which corresponds to $\sum_\lambda |U_\ell(\lambda)|^2 \delta(\omega^2-\omega_\lambda^2) = J_\ell(\omega^2)$. For finite chains, the spectral density is necessarily discrete, therefore, the proper application of this criteria is difficult. Although we have looked at this criteria for finite chains, the interpretation of the results is inconclusive.

3. Non-infinite value of $\int |r-R_\lambda|^2 |\psi_\lambda(r)|^2 d^3r$ for some value of R_λ corresponding to $Q=\sum_\ell (\ell-L)^2 |U_\ell(\lambda)|^2$. This criterion only applies to the infinite system because it does not give a unique value of localization because of the ambiguity of R_λ.

4. Vanishing of d.c. conductivity (for a static lattice) and an A.C. conductivity of the order ω^2. This essentially corresponds to the work of Visscher and our comments on this work apply.

5. A change of boundary condition shifts energy levels by an amount of order $e^{-\sqrt{N}}$ rather than order N^{-1}. This method holds some promise in the phonon problem although we have not attempted to exploit it. To properly apply this criteria we would have to use cyclic boundary conditions so that the boundaries themselves do not influence the eigenvectors. Then, we could switch from periodic to antiperiodic boundary conditions and note the change in eigenvalues. Unfortunately, periodic boundary conditions make the dynamical matrix non-tridiagonal requiring more complicated methods than we have presented for finding the eigenvalues and eigenvectors.

Therefore, when we look at specific eigenstates of finite chains, we will use the criteria (4.3). We can interpret α, in terms of ideas developed by Bush[55] and expanded by Papatriantafillou.[34] They report that there are two quantities of interest when we talk of localization, especially in one dimension.

1. The length over which the eigenfunction is appreciable, $L_e(\lambda)$.

2. The exponential decay rate of the eigenfunction away from this region $L_E(\lambda)$ where $L_E(\lambda)$ is given by

$$U_\ell(\lambda) \alpha e^{-\frac{\ell}{L_E(\lambda)}} \tag{4.4}$$

The quantity $\alpha = \sum_{\ell} |U_{\ell}(\lambda)|^4$ is inversely proportional to $L_e(\lambda)$ since the sum over λ of $|U_{\ell}(\lambda)|^4$ will pick out only the $U_{\ell}(\lambda)$'s which are appreciable. Bush has given a Monte Carlo technique for calculating $L_E(\lambda)$ which we have adopted to the phonon problem. The procedure is much like that outlined in the first page of Appendix D for eigenvectors. First we assume we have a semi-infinite chain, i.e. a starting point but no end. Since Bush found, as expected, the value of $L_E(\lambda)$ is not subject to the initial boundary conditions, we can find successive displacements of atoms from equilibrium starting with fixed boundary conditions

$$U_{i+1} = (2 - \frac{m_i}{\gamma} \omega^2) U_i - U_{i-1} \tag{4.5}$$

where $U_0 = 0$ and $U_1 = 1$.

For the semi-infinite system as for infinite systems all values of ω^2 are eigenvalues except for a very limited number of values of ω^2 (special frequencies). Therefore, we can sample Equation (4.5) for a uniform distribution of ω^2. Given initial conditions for U_0 and U_1 we generate a chain using the appropriate Markov transition probabilities. As Dean proved the U_i's will always show an exponential increase as we proceed along the chain. We start sampling the chain after some U_i satisfies

$|U_i(\omega^2)|>e^4$. We then store the number of sites we must proceed before another U_j satisfies $|U_j(\omega^2)|>e^5$. We collect 30 data points for a given computer generated chain, i.e., U_i's vary from e^4 to e^{35}. The number of sites for an e increase in U_i is $L_E(\lambda)$. We then find the mean and probable error of $L_E(\omega^2)$. We repeat this Monte Carlo experiment for 20 chains for each ω^2 finding 20 means and probable errors. We finally combine the results using a weighted mean and probable error. Roberts and Makinson[56] have shown that even though the use of Equation (4.5) often will not generate the correct eigenvector given an accurate eigenvalue (see Appendix D), the exponential increase displayed in the successive U_i's has the same slope as that of the true eigenvector away from the region of where the eigenfunction is appreciable. Therefore, the Monte Carlo procedure should work and display small errors.

Papatriantafillou has in fact shown from probabilistic arguments that for infinite systems $L_E(\lambda)$ is sharply distributed (zero deviation about the mean) and $L_e(\lambda)$ has a finite distribution. We find that the probable error associated with an $L_E(\lambda)$ is usually less than 5% and the variability between chains is of the order of 10%.

We will first examine the exponential localization length, $L_E(\lambda)$ and , then, the length over which the eigenvector is appreciable. $\alpha = [L_e(\lambda)]^{-1}$. Since the computation of the eigenvalues and eigenvectors of a single 1000 unit chain requires nearly 45 minutes CPU on the UNIVAC 1108, and a complete sampling of the Monte Carlo exponent decay run usually requires ~2-3 minutes, we study $L_E(\lambda)$ in much greater detail than we can α which depends on the explicit eigenvectors. We will present the data as generated with no attempts made to smooth the data or to draw a smooth curve through it. It is clear that there is some actual structure in the data but we cannot at this time conclusively say whether some of the smaller variations in the data are due to the Monte Carlo technique or to actual structure. The circles around the data points give an indication of the probable error of $L_E(\lambda)$.

Figures (4.1) and (4.2) show $L_E(\omega^2)$ versus ω^2 for binary random chains with C_d=.5 and mass ratios of 1.5, 2, 3, 4, and 8 respectively. In every case, the maximum allowable frequency for these chains is normalized such that $\frac{\gamma}{m_L} = 1$, or $\omega^2_{max} = 4$. Therefore the perfect heavy chain spectrum would have a maximum allowable frequency of $\omega^2_m = \frac{8}{3}$, 2, $\frac{4}{3}$, 1 and $\frac{1}{2}$ for m_H = 1.5, 2, 3, 4, 8 respectively. A number of things are immediately apparent: (1) in all cases localization length tends

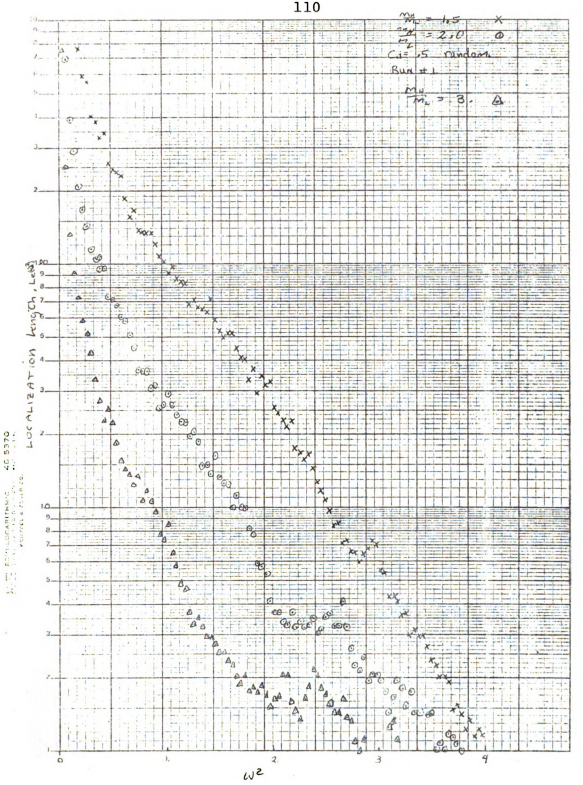

FIGURE 4.1.--Exponential localization length, $L_E(\omega^2)$, for C_d=.5 random and mass ratios of 1.5, 2.0, and 3.0.

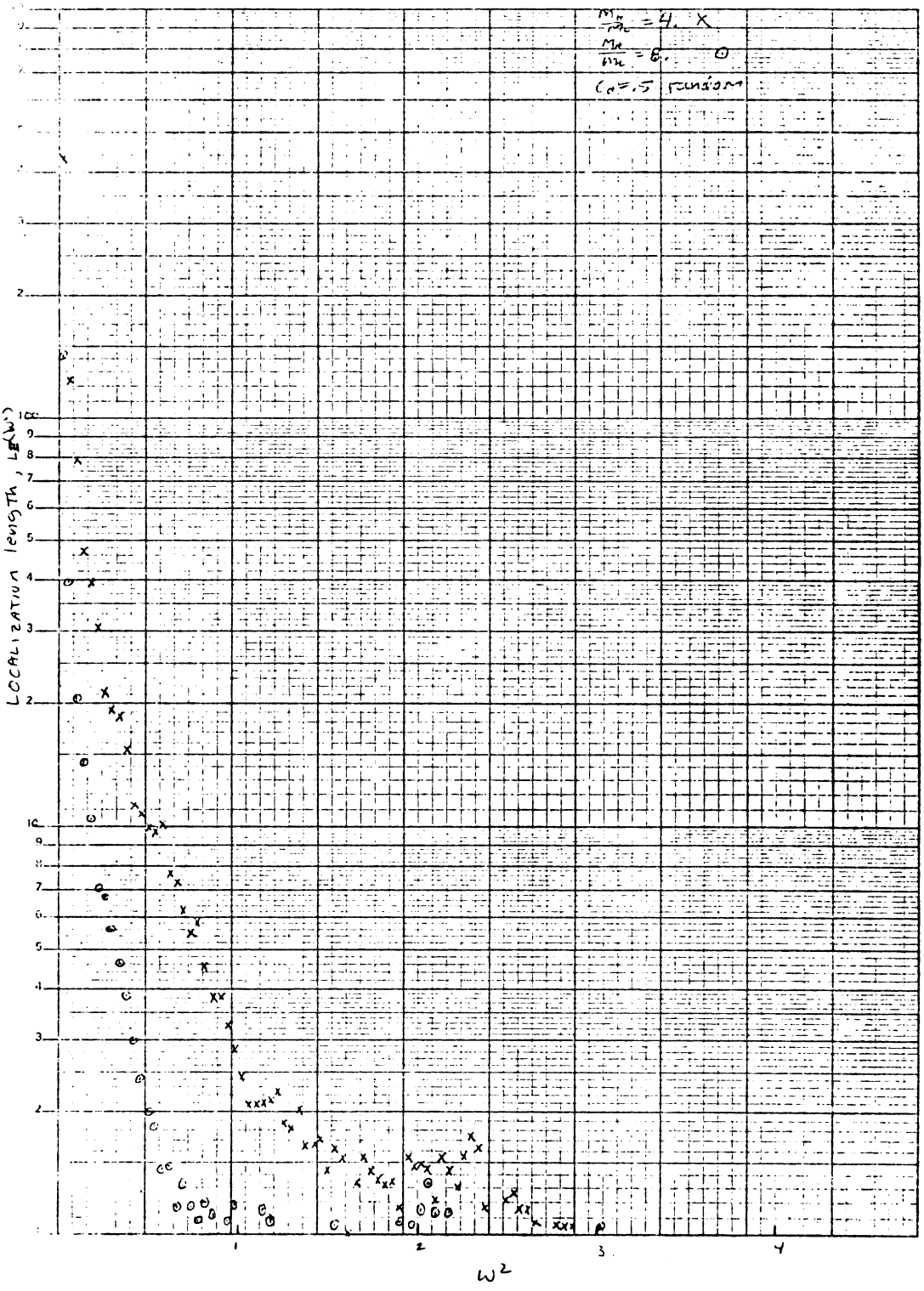

FIGURE 4.2.--Exponential localization length, $L_E(\omega^2)$ for C_d=.5 random and mass ratios of 4.0 and 8.0.

to infinity as $\omega^2 \to 0$; (2) the variability in the data is small from point to point following a definite functional trend; (3) the data show an almost uniform decrease in localization length with increasing frequency and (4) increasing mass ratio decreases localization length at a given ω^2. A few other trends are not as apparent: (1) the increase in mass ratio increases localization even within the host band. This can be seen by picking a point equivalent point in each host band, i.e. the band edge; (2) near the host band edge a marked drop in localization length is observed (and increase in the negative slope of the function $L_E(\omega^2)$ and (3) the localization length is not monotonically decreasing with increasing ω^2. If we repeat the given Monte Carlo run for any given value of the mass ratio, we see a definite persistence of peaking in the function $L_E(\omega^2)$. In Figure (4.1) the $\frac{M_H}{M_L} = 1.5$ curve shows a definite peak at $\omega^2=2.94$. The $\frac{m_h}{m_l} =2$ curve shows a peak at $\omega^2=2.66$ and possibly other peaks at $\omega^2=.98$ and a number of places above $\omega^2=3$. The $\frac{M_H}{m_L}=3$ curve has a peak a $\omega^2=2.38$ among others. In Figure (4.2) the $\frac{m_H}{m_L}=4$ curve gives a peak around $\omega^2=2.30$ and the $\frac{m_H}{m_L}=8$ curve gives a peak around $\omega^2=2.06$. A much finer grid and a much more detailed analysis of the data would almost surely reveal other structure. Even with the data we have presented, the

localization length increases although only slightly at the isolated light defect impurity frequency in each case. Equation (F.6) gives the local mode frequencies as $\omega^2=3$, $2\frac{2}{3}$, $2\frac{2}{5}$, $2\frac{2}{7}$ and $2\frac{2}{15}$ for mass ratios of 1.5, 2, 3, 4, and 8, respectively. We would expect similar peaks at all the local mode frequencies of isolated defect clusters in host mass chains. Again, we must emphasize that Figures (4.1) and (4.2) are for 50% random systems.

Figures (4.3), (4.4) and (4.5) are <u>random</u> chains with defects of mass $\frac{1}{2}$ m_H in concentrations of 0.1, 0.3, 0.5, 0.7 and 0.9, respectively. Figure (4.4) for $C_d=.5$ is an independent Monte Carlo run compared to the data in Figure (4.1) for $\frac{m_H}{m_L}=2$, and is included to show the variability from run to run. One can see that some structure in $L_E(\omega^2)$ is present and some of variability in the data is due to the Monte Carlo technique. Figures (4.3), (4.4) and (4.5) show some common features: (1) the localization length in the impurity band increases with increasing impurity concentration although not in a regular or uniform fashion; (2) there is a marked decrease in the change in localization length at the host band edge ($\omega^2=2$), varing from a change of an order of magnitude at $C_d=0.1$ to a change of less than 10% for $C_d=0.9$ and (3) localization length in the host band is smallest for $C_d=.5$ and increases as $C_d\to 0$ or $C_d\to 1$.

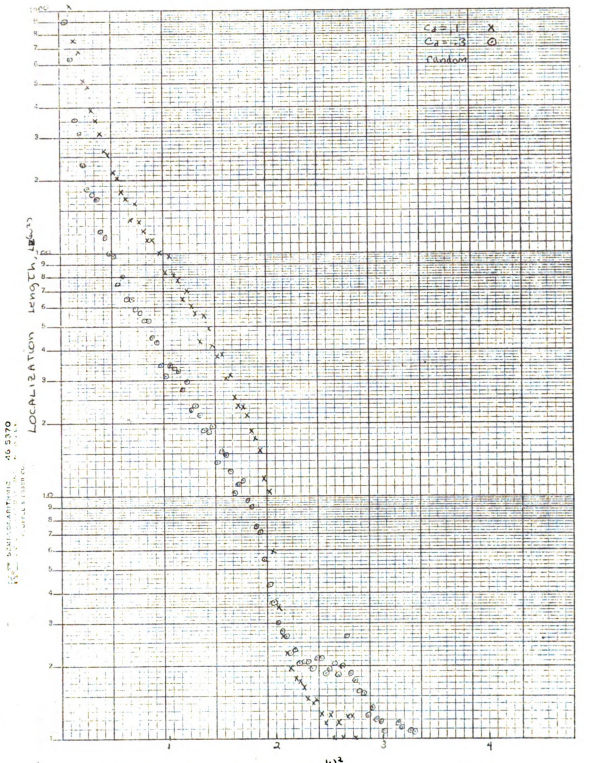

FIGURE 4.3.--Exponential localization length, $L_E(\omega^2)$ for mass ratio of 2 and C_d=.1 and .3 random.

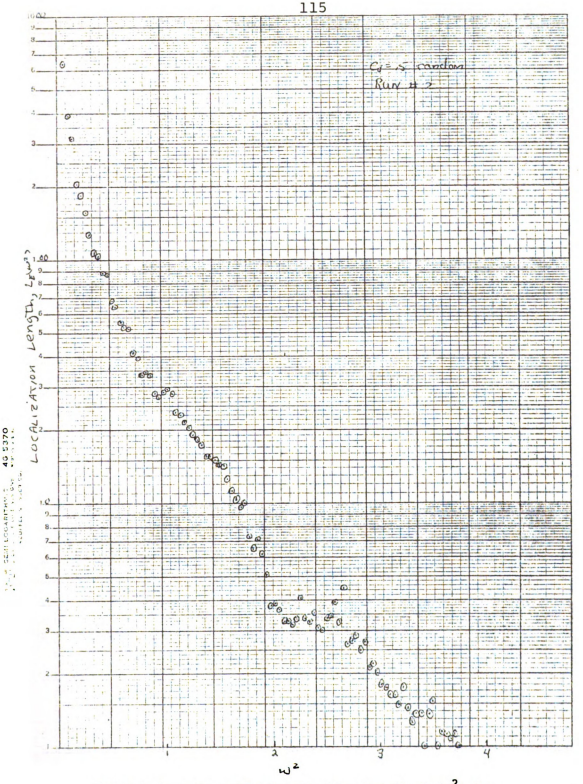

FIGURE 4.4.--Exponential localization length, $L_E(\omega^2)$ for mass ratio of 2 and C_d=.5 random.

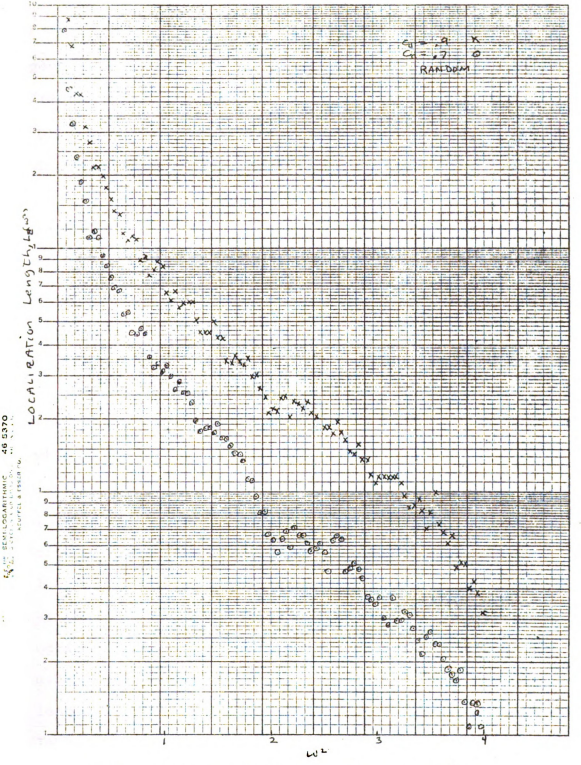

FIGURE 4.5.--Exponential localization length, $L_E(\omega^2)$ for mass ratio of 2 and C_d=.7 and .9 random.

As before Figures (4.3), (4.4) and (4.5) show a general decrease in localization length with increasing frequency. In all cases, the localization length is less than 100 atoms for $\omega^2 \geq 1$. In all cases the function $L_E(\omega^2)$ has definite structure, i.e., peaks.

Figures (4.6) and (4.7) are for $C_d=.5, M_H/M_L=2$, and first order Markov chain transition probabilities of $P_{d,d}=0.1$ and 0.3, and 0.7 and 0.9 respectively. Short-range order radically modifies the structure of the localization length as a function of frequency. These figures can be compared with the $C_d=.5$ random case given in Figures(4.1) and (4.4). We have previously presented the frequency spectra for $P_{d,d}=0.1$, 0.25, .5, 0.75 and 0.9 which provide insights into localization. Figure (4.6) with $P_{d,d}=0.1$ is close to the ordered binary chain $P_{d,d}=0$; therefore, we expect as shown in Figure (3.13) a degraded ordered binary frequency spectrum. The localization length is "large" in the $0 \leq \omega^2 \leq 1$ band, dropping sharply at the band edge. Also, the length increases in the optical band $2 \leq \omega^2 \leq 3$, with a maximum occurring near the middle of the band. A sharp peak in localization length at the local mode frequency ($\omega^2=2.66$) is observed. In the region of the ordered binary chain band gaps ($1<\omega^2<2$ and $\omega^2>3$), we see a marked decrease in $L_E(\omega^2)$. Figure (4.6) also shows a similar trend for $P_{d,d}=.3$ but the band gap decrease and in band increasing in localization length are not as pronounced. Figure (4.7) with

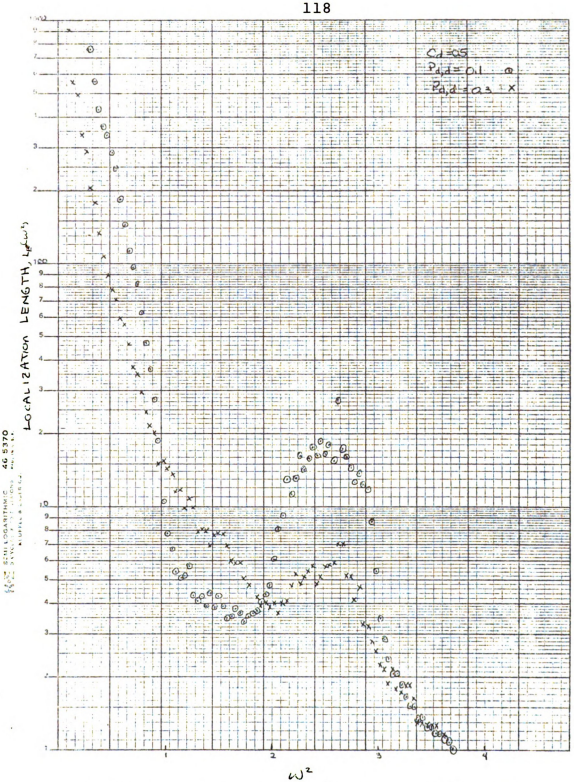

FIGURE 4.6.--Exponential localization length, $L_g(\omega^2)$ for mass ratio of 2, C_d=.5 and $P_{d,d}$=.1 and .3.

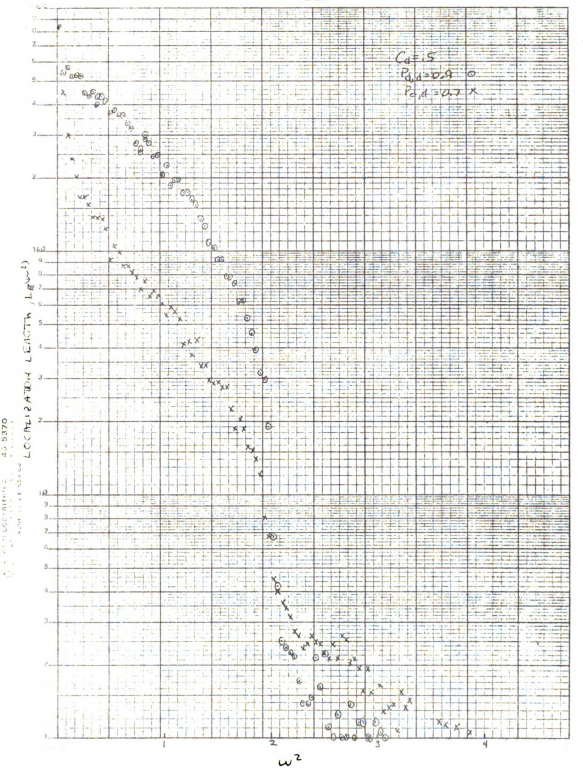

FIGURE 4.7.--Exponential localization length, $L_E(\omega^2)$ for mass ratio of 2. C_d=.5 and $P_{d,d}$=.7 and .9.

$P_{d,d}$=.9 can be compared with frequency spectrum Figure (3.16). For $P_{d,d}$=.9 we have large clusters of like masses, and the structure of the host band is recovered over the random case. The localization length in the host band is greatly enhanced with a marked decrease outside the host band. Comparing Figure (4.7) for $P_{d,d}$=.9 with Figure (4.3) for C_d=.1 we see that the short-range order makes the localization length in the host band for C_d=.5 greater than that of C_d=0.1 random an unexpected result. Near ω^2=0, this however is not the case. For $P_{d,d}$=0.9 and C_d=.5 it looks as if $L_E(\omega^2)$ approaches 600 atoms as ω^2 approaches zero and only the lowest ω^2 point indicates that actually $L_E(\omega^2)\to\infty$ as ω^2 goes to zero. Figure (4.7) with $P_{d,d}$=0.7, shows behavior similar to that for $P_{d,d}$=0.9, though the delocalization of the host band is less pronounced as expected.

We finish the analysis of the exponential localization length with a single second order Markov chain to show the effect which second nearest neighbor correlations can have on the localization length. Figure (4.8) is for C_d=0.5, M_H/M_L=2, and $P_{dd,d}$=$P_{dh,d}$=.1 and $P_{hd,d}$=$P_{hh,d}$=0.9. This is one of the special cases we discussed before. Figure (4.8) shows three definite humps in the localization length. This chain resembles an ordered binary chain of the form (AA-BB-AA-BB) ($P_{dd,d}$=$P_{dh,d}$=0 and $P_{hd,d}$=$P_{hh,d}$=1). The peaks in localization

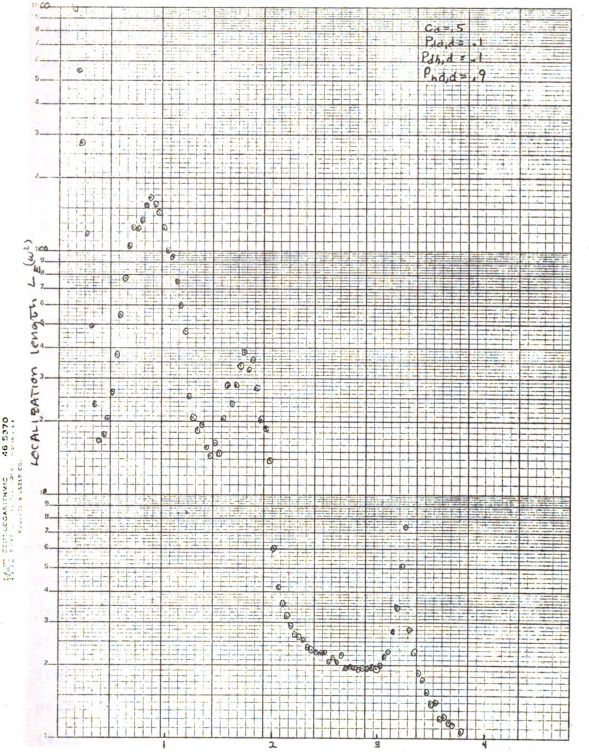

FIGURE 4.8.--Exponential localization length, $L_E(\omega^2)$ for mass ratio of 2, C_d=.5 and $P_{dd,d}$=$P_{dh,d}$=.1 and $P_{hd,d}$=.9.

length occur in the four bands (0→.313, .5→1.22, 1.5→2 and 3.19→3.28) (see Appendix G, Equation (G.12)), and the decrease in localization length occurs in the band gaps. There is a decrease in the maximum $L_E(\omega^2)$ in each successive band as ω^2 increases.

Next, we can study the length over which the eigenfunction is appreciable. Comparing the following results with the exponential localization length we will be able to make some interesting statements about the localization problem. In the remaining figures in this section we will be plotting, $\alpha=[L_e(\omega^2)]^{-1}$ versus ω^2 instead of $L_e(\omega^2)$, this makes direct comparison with $L_E(\omega^2)$ difficult although general trends are apparent.

Due to the large cost in generating eigenvectors of large chains (N>50), we will restrict the discussion to $C_d=0.5$, $m_H/m_L=2$ chains introducing short-range order via the first order Markov chain theory. Using fixed boundary conditions, Figures (4.9) and (4.11) show localization as a function of ω^2 for the perfect host chain and perfect diatomic chain with (N=100). (The lower curve in each figure). $\alpha=.01485$ for N=100 for the perfect host chain. The zone boundary values in Figure (4.11) are ($\alpha=.01485$, $\omega^2=0$), ($\alpha=.0297$ $\omega^2=1,2$), and ($\alpha=.0202$, $\omega^2=3$). These values are also found analytically in Appendix I.

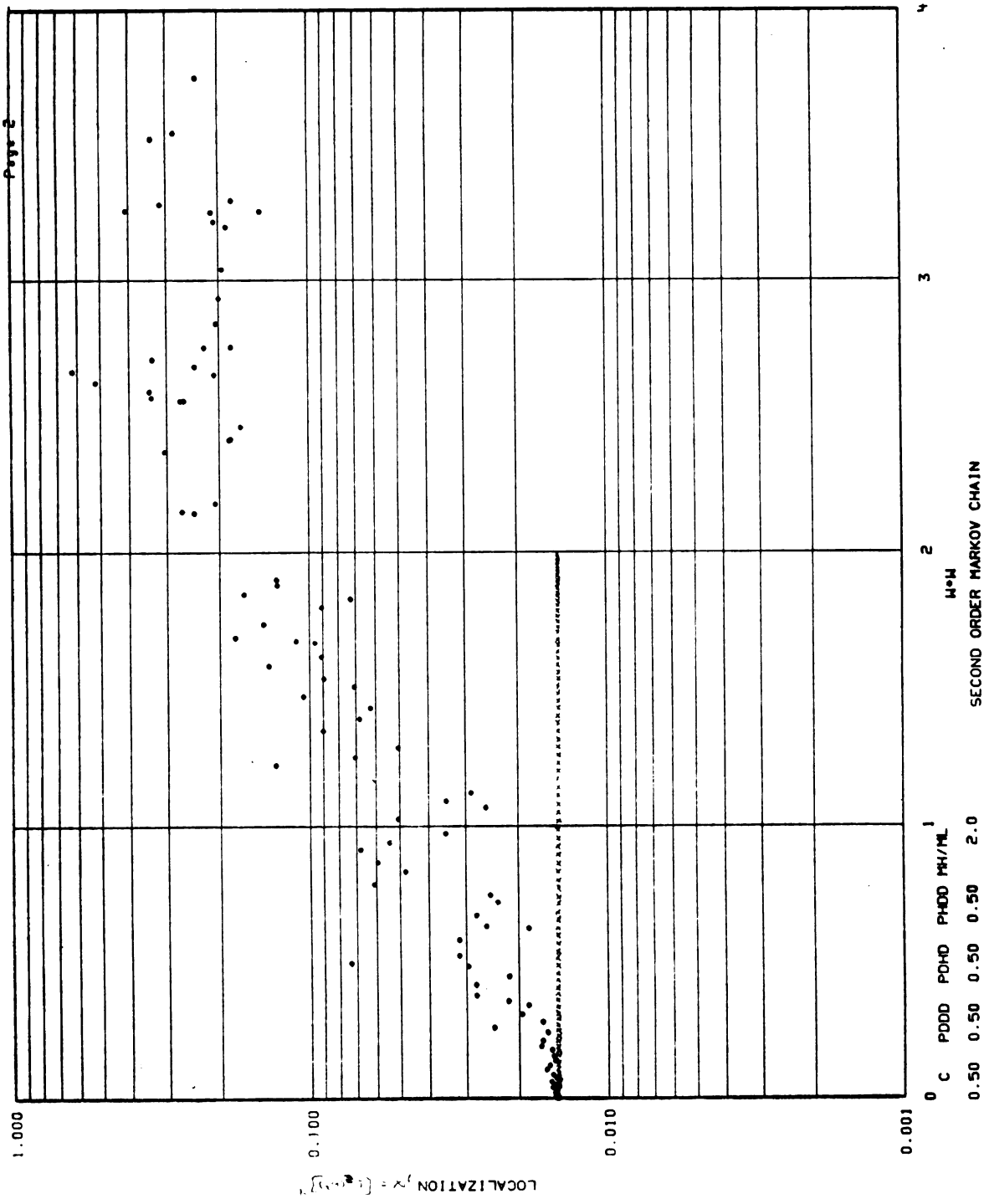

FIGURE 4.9.--Localization $\alpha=L_\theta^{-1}(\omega^2)$, for mass ratio of 2, C_d=.5 random and a 100 unit chain.

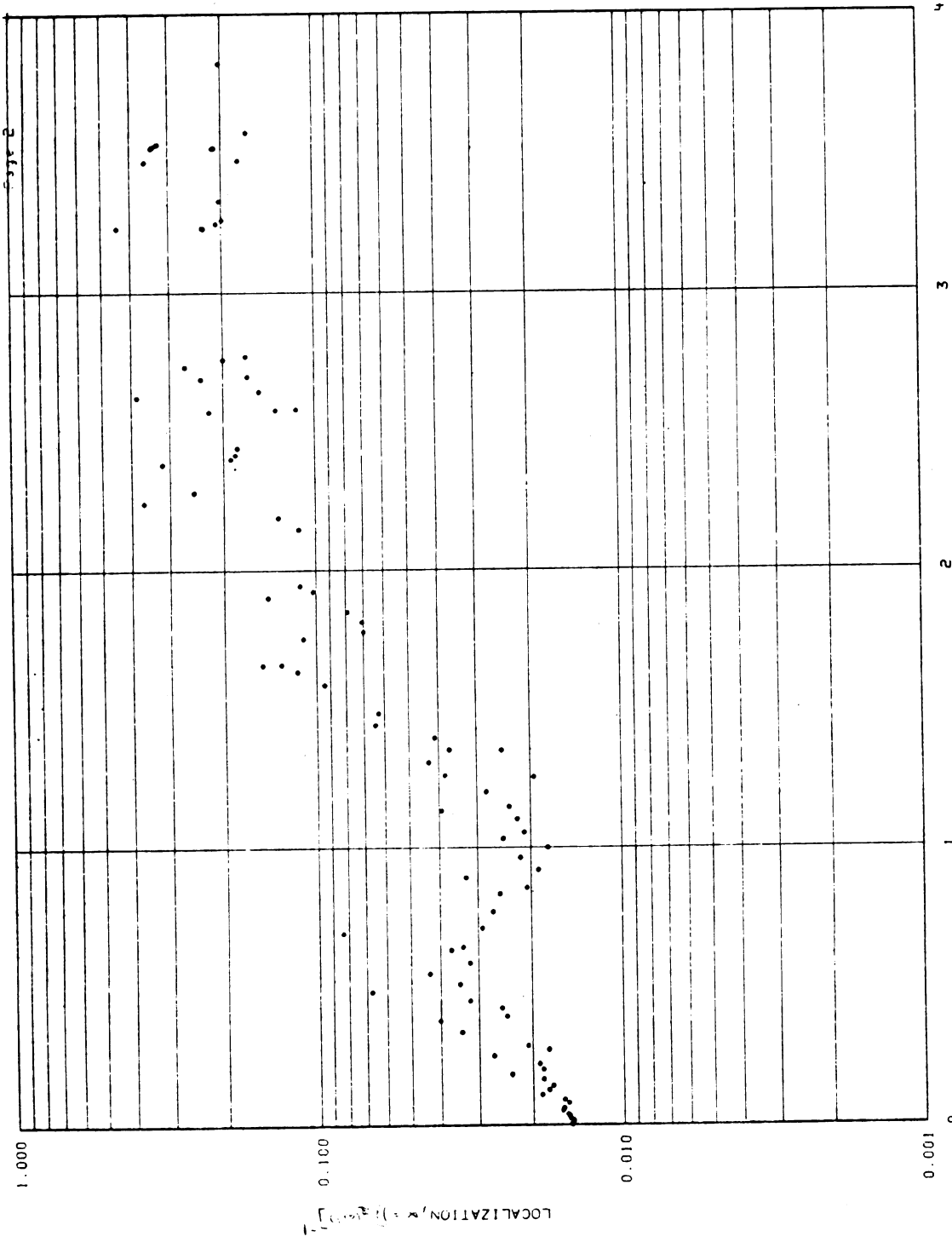

FIGURE 4.10.--Localization $\alpha=L_e^{-1}(\omega^2)$ for mass ratio of 2, C_d=.5 random and a 100 unit chain.

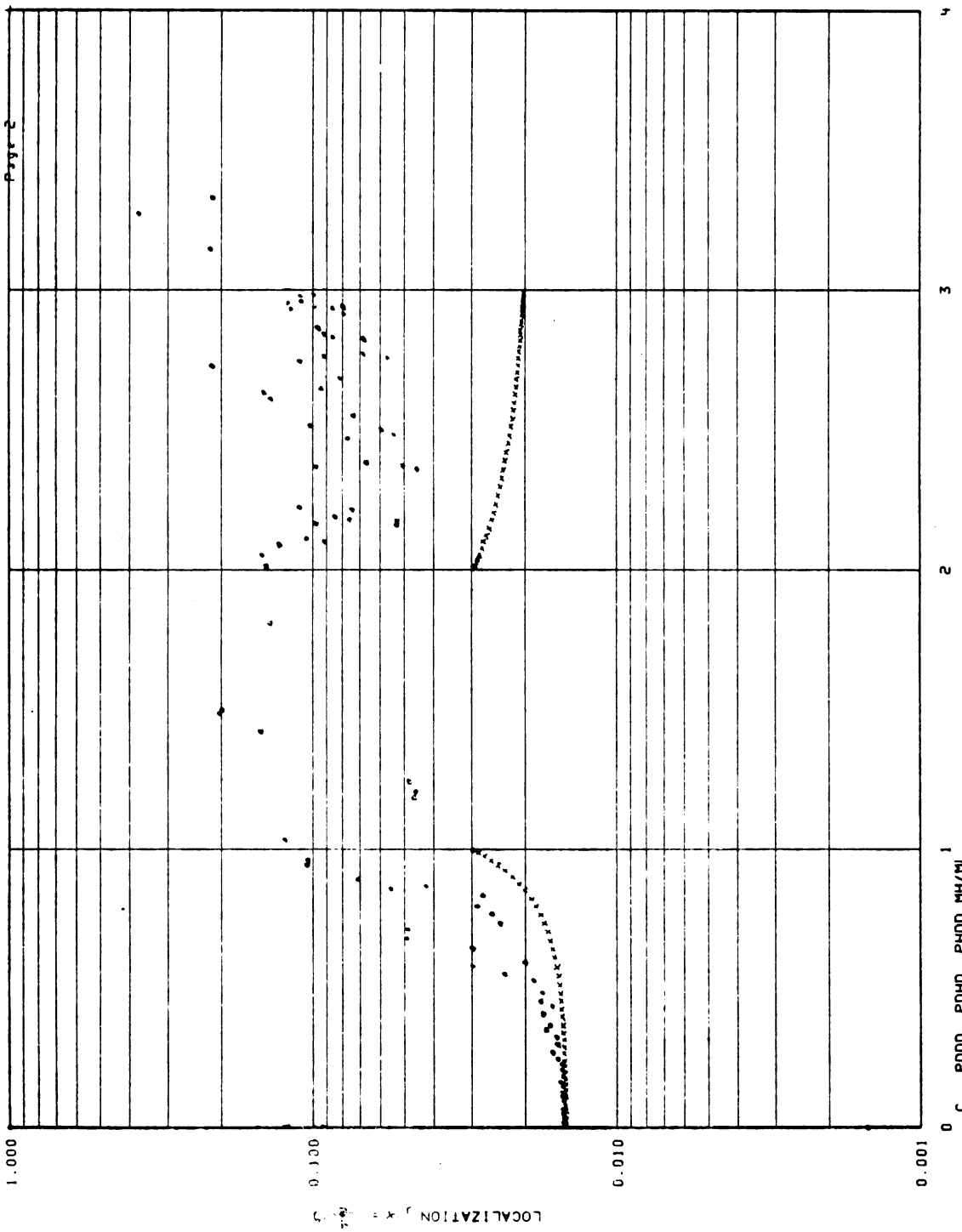

FIGURE 4.11.--Localization $\alpha=L_e^{-1}(\omega^2)$ for mass ratio of 2, C_d=.5, $P_{d,d}$=.1 and a 100 unit chain.

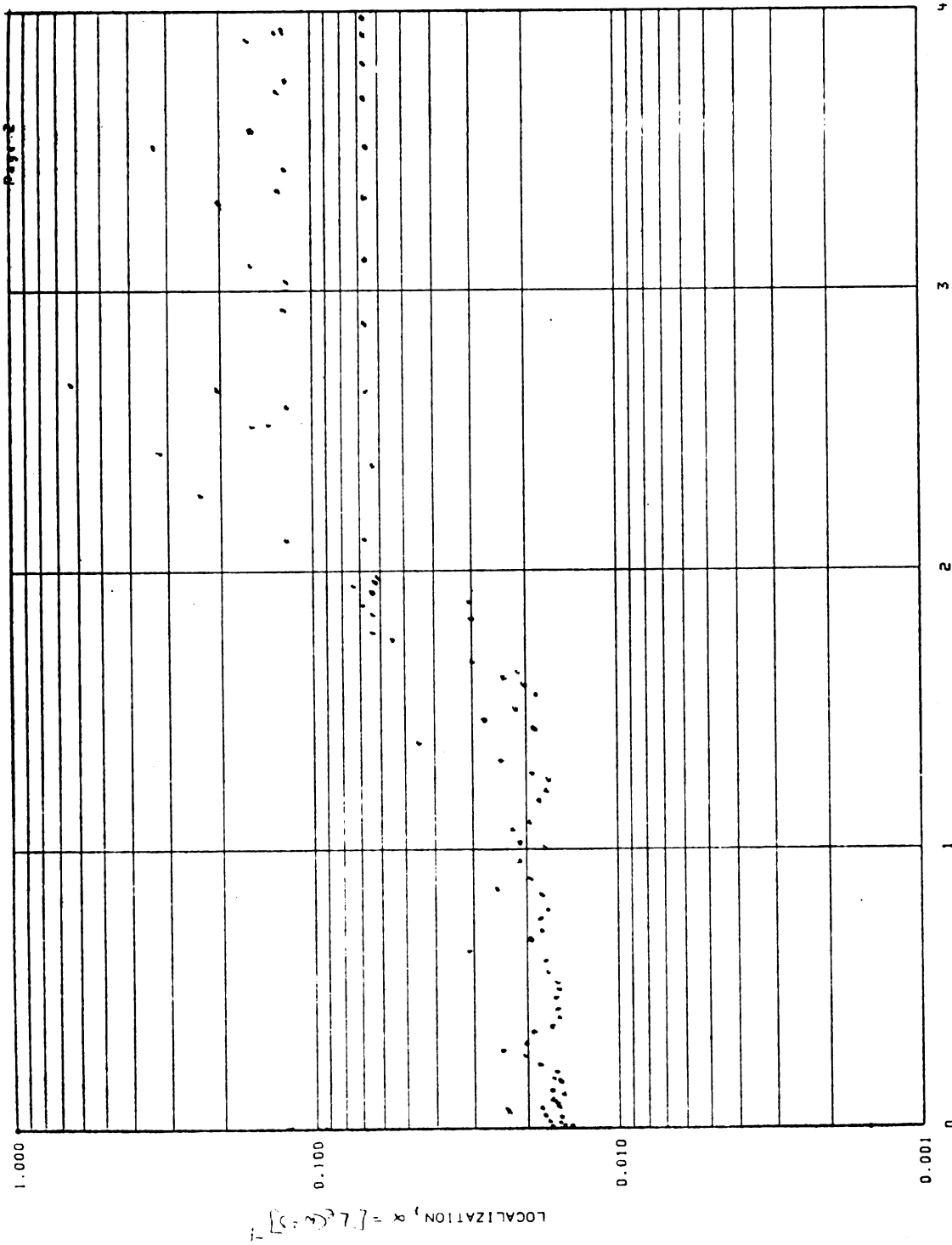

FIGURE 4.12.--Localization $\alpha=L_e^{-1}(\omega^2)$ for mass ratio of 2, C_d=.5 and $P_{d,d}$=.9 and a 100 unit chain.

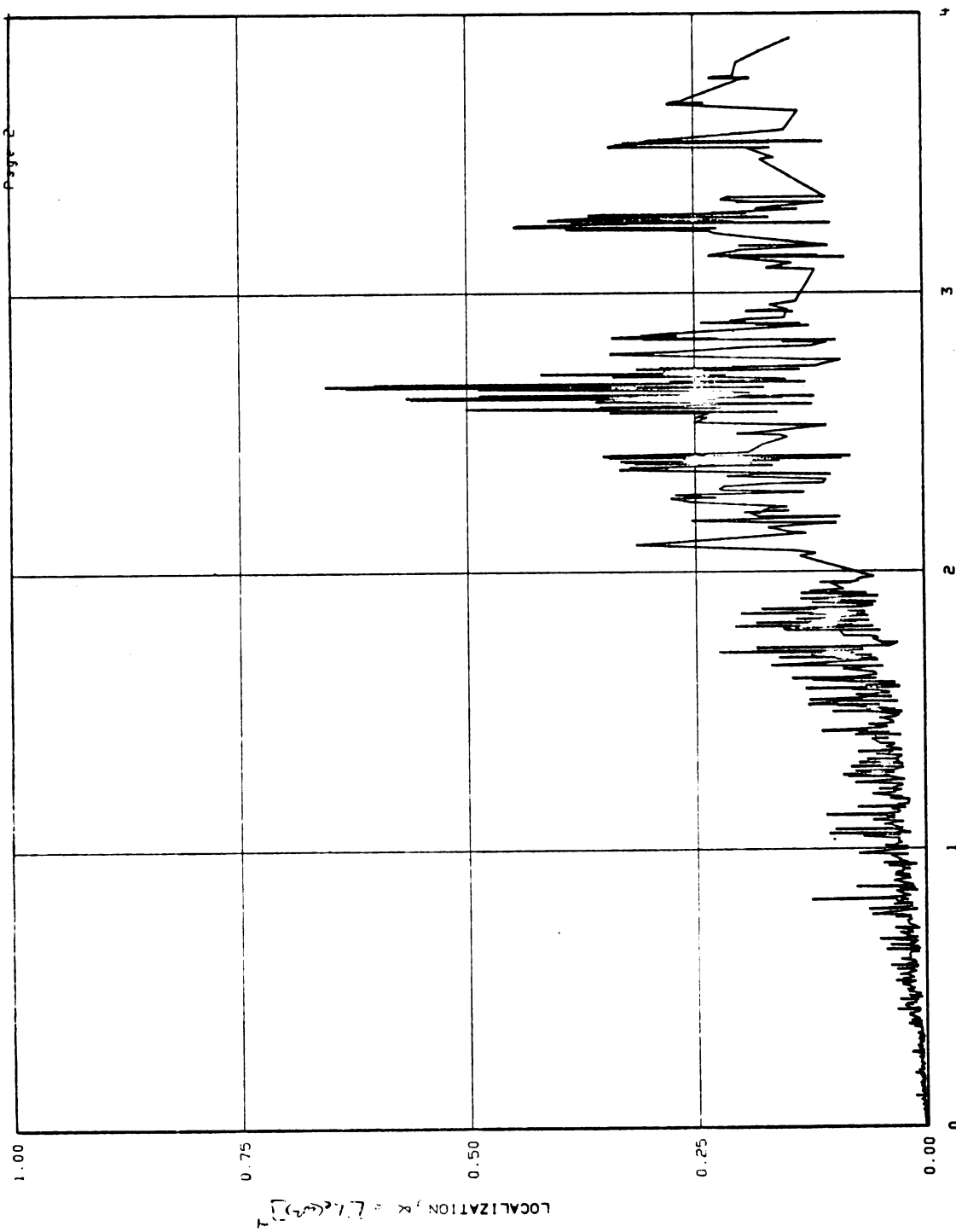

FIGURE 4.13.--Localization $\alpha=L^{-1}(\omega^2)$ for a mass ratio of 2, C_d=.5 random and a 1000 unit chain.

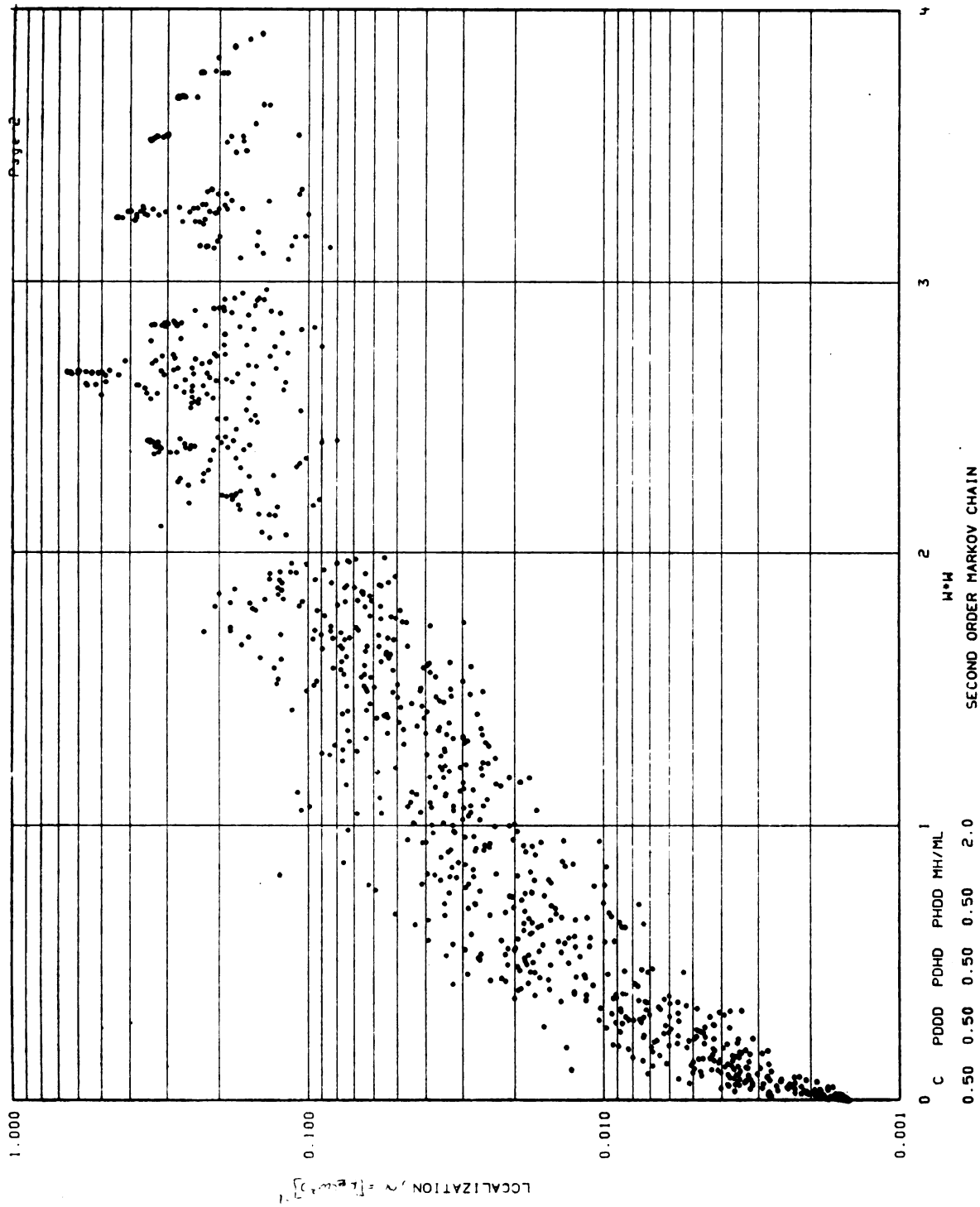

FIGURE 4.14.--Localization $\alpha=L_{\ell}^{-1}(\omega^2)$ for a mass ratio of 2, C_d=.5 random and a 1000 unit chain.

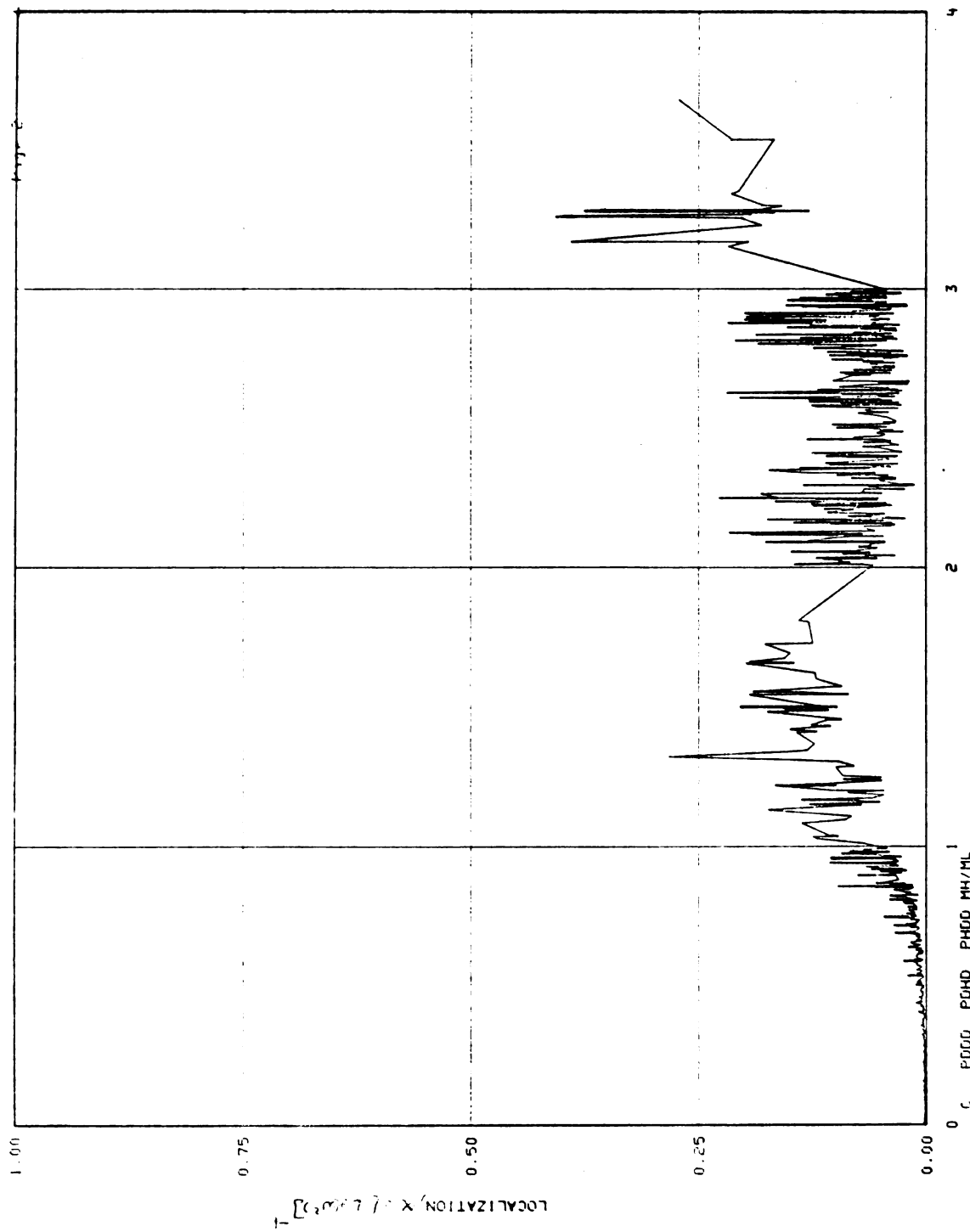

FIGURE 4.15.--Localization $\alpha=L_e^{-1}(\omega^2)$ for a mass ratio of 2, C_d=.5, $P_{d,d}$=.1 and a 1000 unit chain.

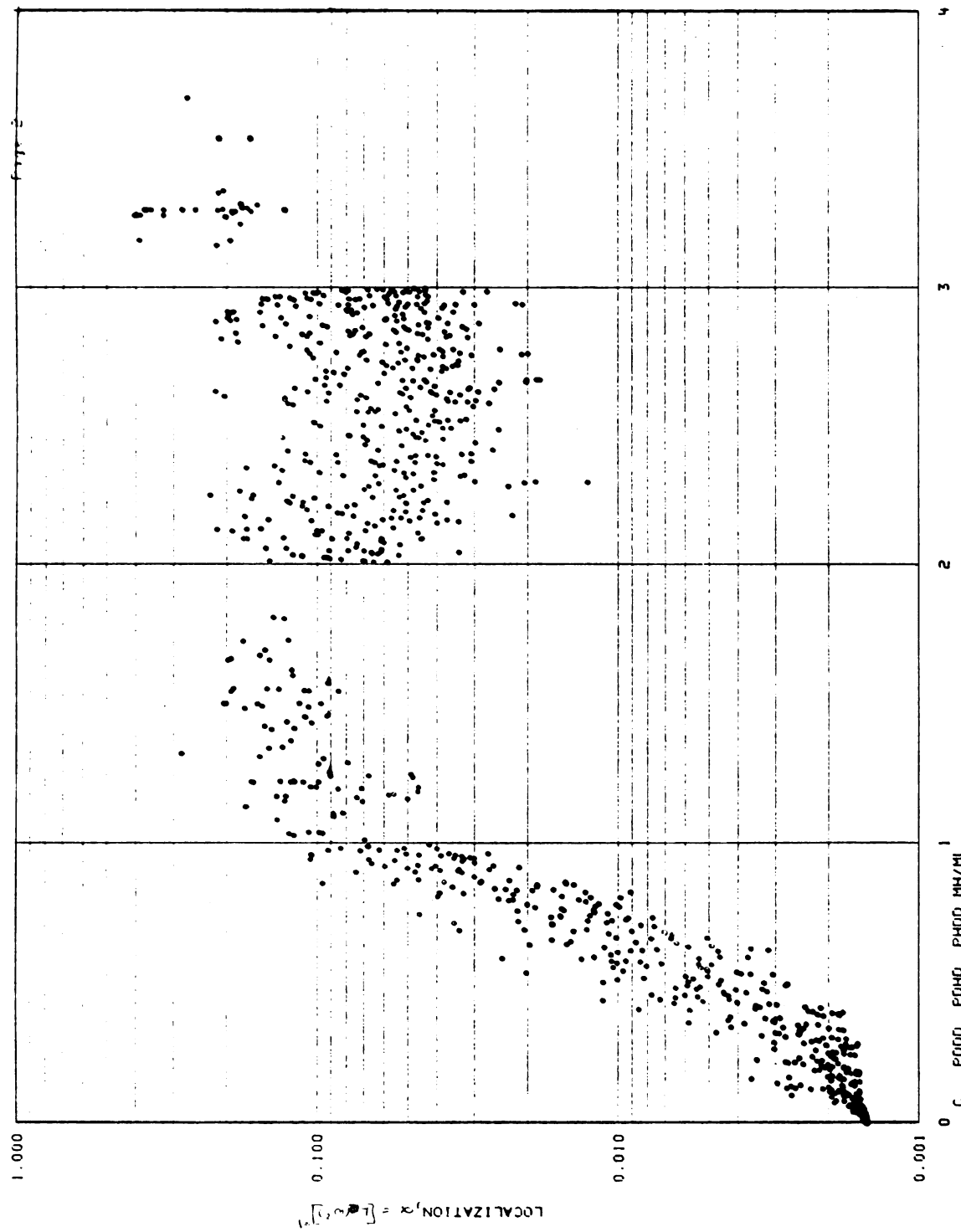

FIGURE 4.16.--Localization $\alpha=L^{-1}(\omega^2)$ for a mass ratio of 2, C_d=.5, $P_{d,d}$=.1 and a 1000 unit chain.

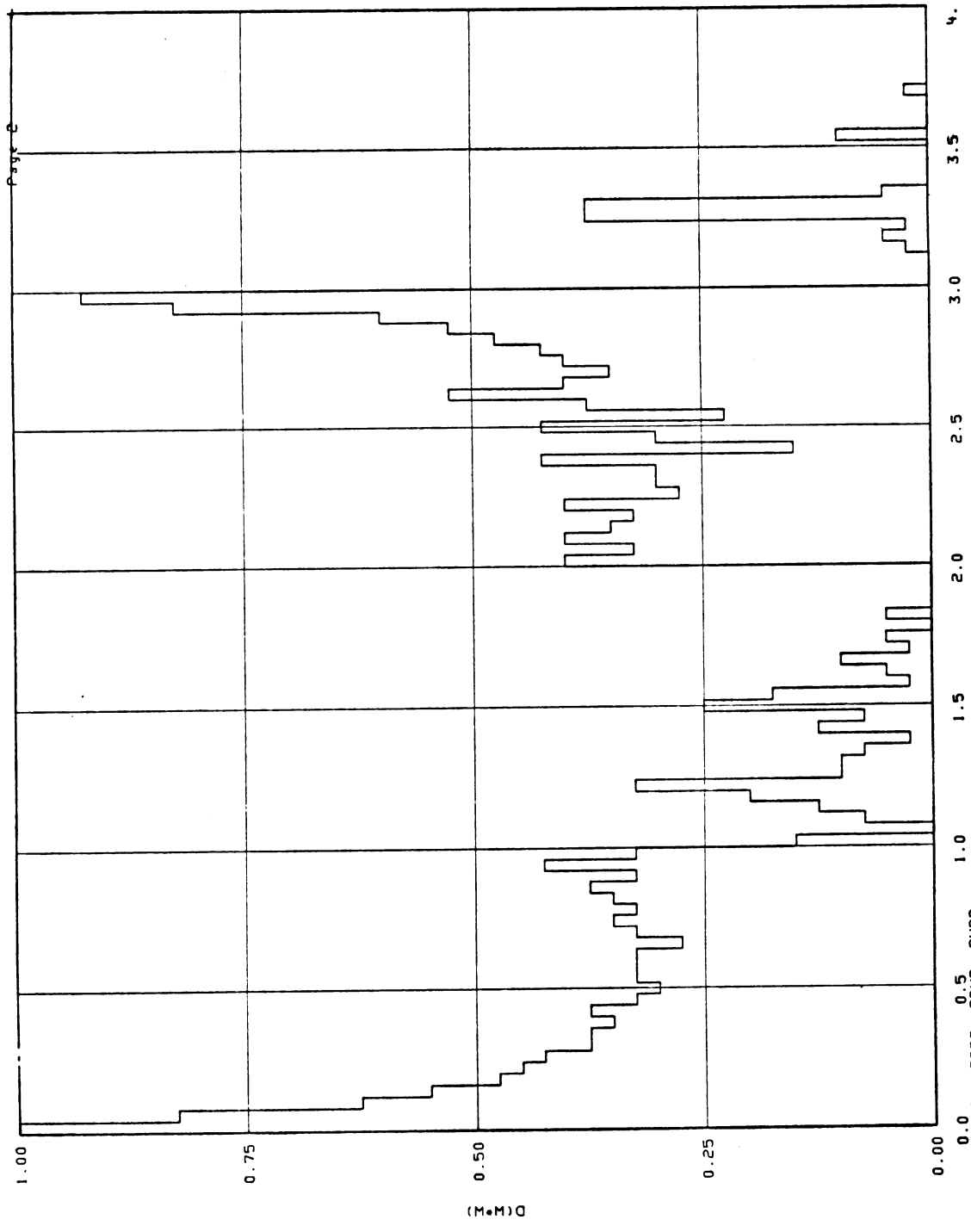

FIGURE 4.17.--Density of states for a 1000 unit chain with C_d=.5, $P_{d,d}$=.1 and a mass ratio of 2/1.

Figures (4.9) and (4.10) shows the localization plots for two different random C_d=0.5, N=100 chains. Since the chains are generated using a random number generator, one expects different stochastic relationships between atoms in the two chains. In Table (2.2) we gave a detailed analysis of these relationships with C_d=.43 corresponding to Figure (4.9). We can easily see that α does not follow a definite functional relationship with ω^2. The spread between individual points as well as differences in the two figures might seem to make the data inconclusive. This however is not the case. One problem is that a 100 unit chain does not contain a representative set of eigenmodes. The data are not therefore contradictory but complementary. We would need to run many 100 unit runs to get a decent data set. Looking at Figure (4.1) with m_H/m_L=2, we can expect that this collection of data would be quite good for $\omega^2 \geq 1.0$ where the exponential decay length is less than 30 atoms, and nearly exact for ω^2>2 where $L_E(\omega^2)$<5 atoms. The data below ω^2=0.5 is almost certainly affected by the chain length, which means that these data do not have the generality which we ascribe to the other data. The eigenvectors in this region are extended over the whole one hundred unit chain. Near the local mode α shows a great variability. Never the less one can distinguish

a peak in $\alpha[\alpha(\omega^2=2.666)=.633]$ or a dip in $\alpha^{-1}\equiv L_e(\omega^2)$ ($L_e(\omega^2=2.666)=1.58$) at the local mode frequency. A comparison between this plot and Figure 4.1 for $L_E(\omega^2)$ shows that whereas the local mode extends over a smaller number of atoms than do modes nearby it decays less rapidly with distance away from the region of appreciable strength, than do modes nearby. Therefore the two measures of localization vary in opposite directions as one approaches the local mode. However, as $\omega^2\to 0$ $L_e(\omega^2)\to N$ and $L_E(\omega)\to\infty$, or the two parameters follow each other. This comparison shows that although our two measures of localization actually measure different things the general trend of both parameters are the same. In Figures (4.9) and (4.10) the region of appreciable amplitude of the eigenfunction is less than 10 atoms for $\omega^2>2$ for the random system with an exponential decay length of less than 5 atoms. These modes are clearly localized even in chains of length 100 atoms.

Figure (4.11) is for $C_d=.5$ and $P_{d,d}=.1$ and N=100. Unfortunately for N=100 we get very few modes in the ordered binary chain gaps. Comparing this figure to Figure (4.6) we see that they follow the same general trend, i.e. as $L_E(\omega^2)$ increases $L_e(\omega^2)$ generally increases. For $\omega^2<0.9$ α can be limited by the chain length since $L_E(\omega^2)>50$ atoms. Figure (4.11) shows that α is near its minimum possible value for $\omega^2<.5$. The general increase

in $L_e(\omega^2)$ in the $2 \leq \omega^2 \leq 3$ band over the random case is clearly significant.

Figure (4.12) is for C_d=.5 N=100 and $P_{d,d}$=.9 or the case of clustering of atoms. Looking at $L_E(\omega^2)$ in Figure (4.7) we expect the results below ω^2=1.9 to be severly chain-length limited and not truly representative of the values of longer chains. With clustering of alike atoms, N=100 gives especially poor statistical relationships in the sense of seeing representative impurity clusters. Looking at the chain composition we can easily identify the modes in the $2 \leq \omega^2 \leq 4$ region that occur in this chain, all of which show rapid exponential decrease away from the region of appreciable displacements ($L_E(\omega^2)=0(1)$). The chain can be shown as follows:

$$|- 11m_L - 9m_H - 6m_L - 7m_H - 21m_L - 3m_H - 3m_L - 6m_H -$$

$$8m_L - 3m_H - 1m_L - 10m_H - 10m_L - 1m_H - 1m_L -|$$

for a C_d=.61. The isolated impurity at site 78 gives rise to the eigenfrequencies at ω^2=2.667 with α =.644. The isolated defect cluster of 3 atoms gives α=.33 and eigenfrequencies ω^2=3.52 and 2.414. The points for α=.20 comes from the 6 defect cluster; those at α=.16 arise from the 8 defect mode; α=.14 corresponds to the 10 defect cluster; α=.12 corresponds to the 11 defect cluster, and α=.066 corresponds to the 21 defect cluster.

Figures (4.13) and (4.14) show α versus ω^2 for a random 1000 unit chain plotted in two ways. Figure (4.13) gives the reader a feeling of the variability of α from point to point, although Figure (4.14) is the more useful. For N=1000, the minimum α is .00145 for the perfect monatomic chain. Figure (1.2) shows the frequency spectrum of this chain. Figure (4.1) indicates that some values of α could be chain-length limited for $\omega^2 \leq 0.4$ but other values may be valid. A negligibly small number of higher frequencies can be chain-length limited because they happen to have their appreciable displacements near one end of the chain. The data in Figures (4.9) and (4.10) for $\omega^2 > 1$, $C_d = .5$ random fall within the boundaries of the N=1000 unit chain spread supporting the use of the exponential localization as a test for the accuracy of $\alpha(\omega^2)$ for a given chain length. To get accurate values of α for the region $.02 \leq \omega^2 \leq .4$ would require approximately N=10,000. Since a dot in Figure (4.14) represents an eigenfrequency, the zeros in the frequency spectrum at $\omega^2 = 2, 3, 3.414$, and 3.618 are clearly visible. The clustering of points around defect cluster frequencies is also clearly seen. Also, by arguments given for the α versus ω^2 in Figure (4.12), we can explain the tendency to get lines with α constant in the impurity band. To give the reader a more fundamental understanding of the mechanisms involved we would

need to look at each eigenvector. Although this is obviously not possible herein we will look at a few of the eigenvectors of the next chain to be discussed.

Figures (4.15) and (4.16) give localization for C_d=.5 and $P_{d,d}$=0.1. Figure (4.17) gives the corresponding frequency spectrum for this chain. From Figure (4.16) the following can be said: (1) here, as in the random case, $L_e(\omega^2)=\alpha^{-1}$ has the same general structure as $L_E(\omega^2)$ but has a much greater spread about a mean; (2) the data in the band $2<\omega^2<3$ show a marked increase in $L_e(\omega^2)$. In fact some modes are longer than 100 atoms so that the N=100 chain, Figure (4.11), can never show completely the localization in this region; and (3) the values of α may be chain-length limited for $\omega^2<.5$ because of the long exponential decay given by Figure (4.6) below this frequency.

Figure (4.18) gives the n=100, n=250, n=353, and n=450 eigenvectors (n=1 labels the eigenvector of lowest energy) for the above chain, (N=1000, C_d=.5, $P_{d,d}$=.1). The figure shows that at ω^2=.06 (n=100) the eigenvector is completely delocalized over the whole chain. Therefore for this frequency we know $L_e(\omega^2)>>1000$. The mode n=250, ω^2=.36 is clearly also nonlocalized although structure is appearing in the eigenvector. The n=353 mode is one of the lowest energy modes that does not have amplitude

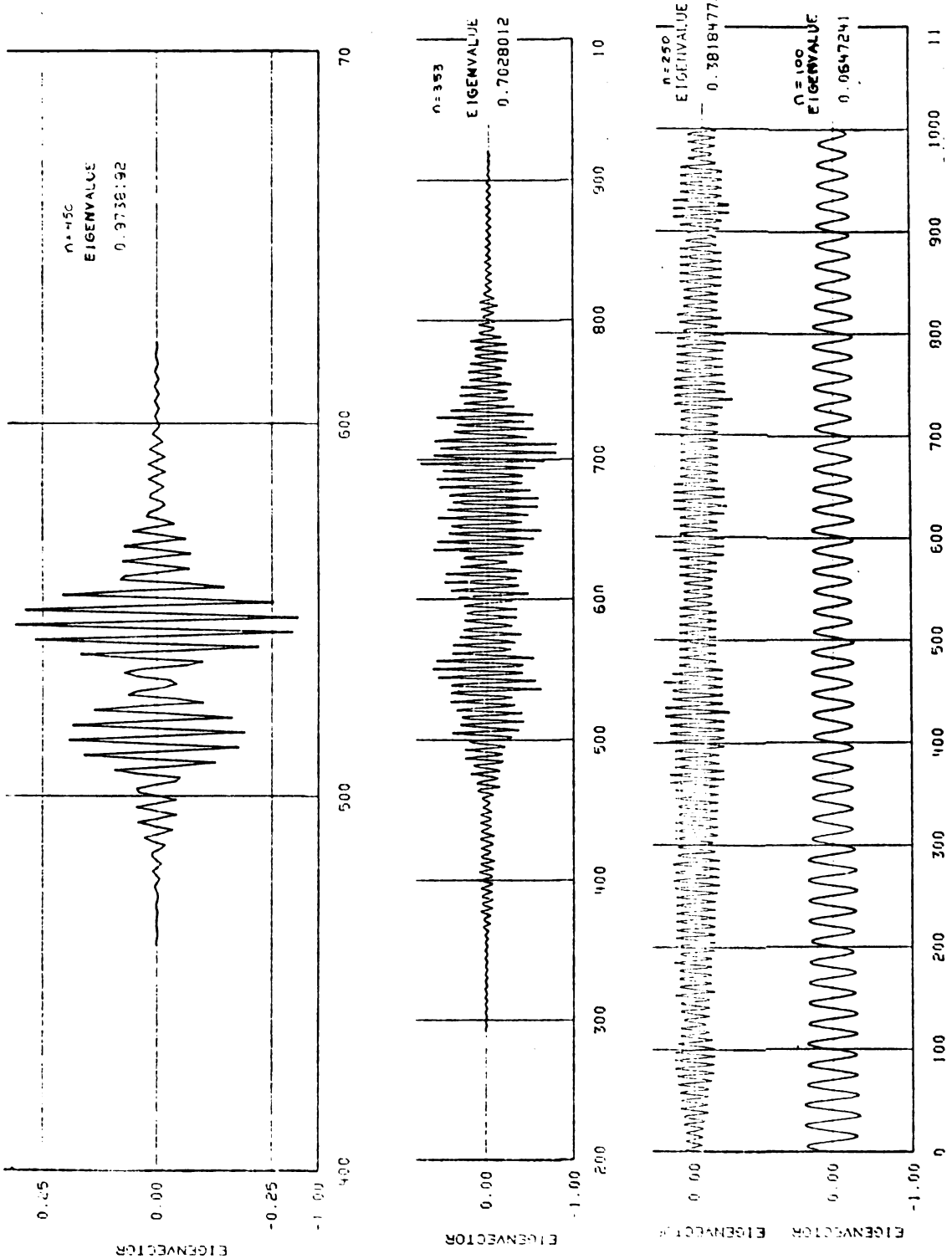

FIGURE 4.18.--Eigenvectors n=100, 250, 353, and 450 for a 1000 unit chain with C_d=.5, $P_{d,d}$=.1 and a 2/1 mass ratio.

at one boundary or the other, and it displays a clearly local character although extending well over 600 atoms. The n=450 mode is near the ordered binary chain band gap, the localization is quite distinct extending over about 100 atoms. The modes in the gap $1<\omega^2<2$, usually extend over 30 to 40 atoms. In the band $2<\omega^2<3$, the extent of appreciable magnitude of the eigenvector can often increase to over 100 atom as shown in Figure (4.19) for n=700 and n=775. The variation in the localization can be seen in Figures (4.19) and (4.20) for n=775 and n=776 respectively. Figure (4.20) also shows for n=950 as we get near the band edge $\omega^2=3$, the localization increases; $L_e(\omega^2)$ extends over ~20 atoms.

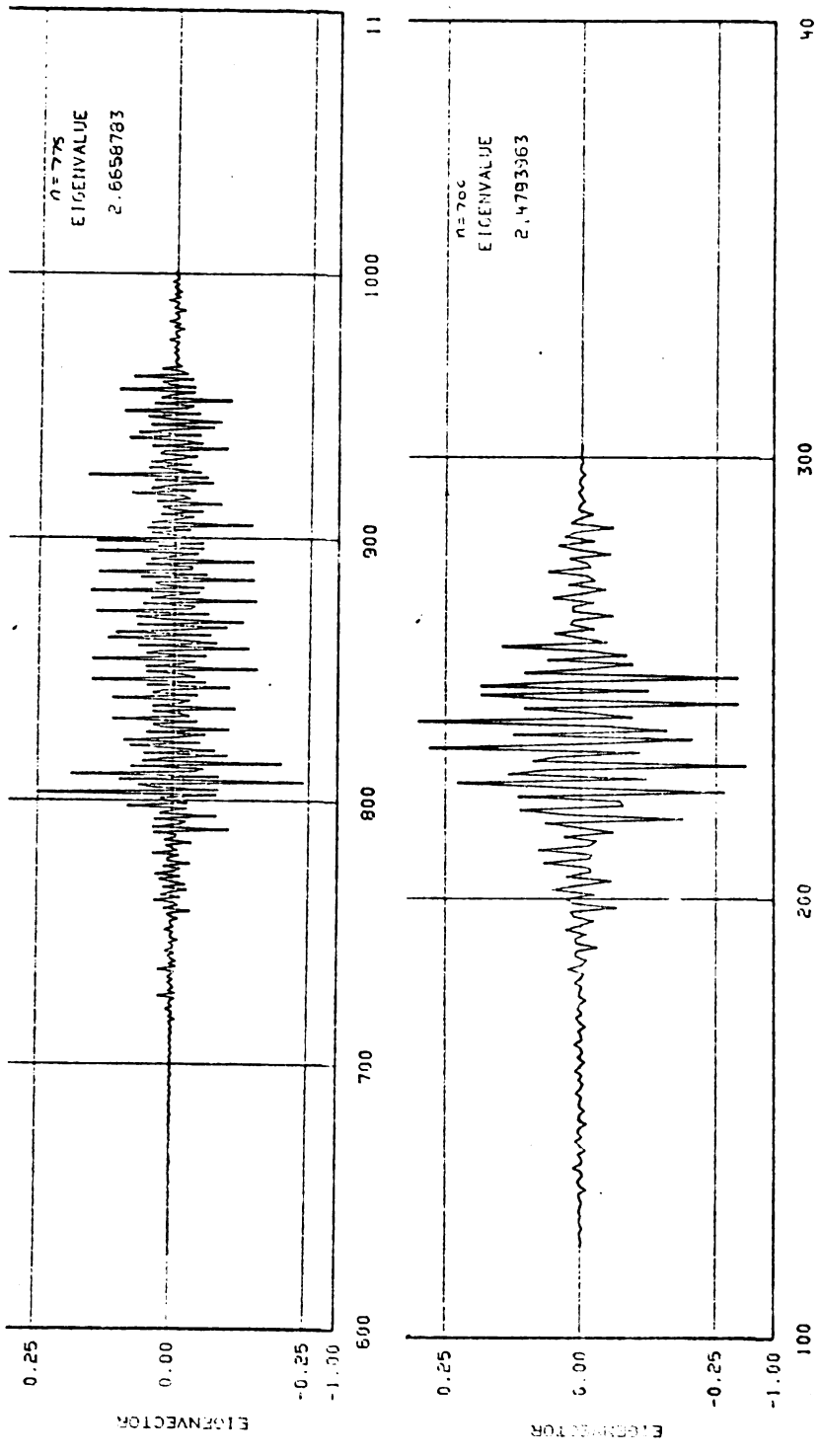

FIGURE 4.19.--Eigenvectors n=700 and 775 for a 1000 unit chain with C_d=.5, P_d,d=.1 and a 2/1 mass ratio.

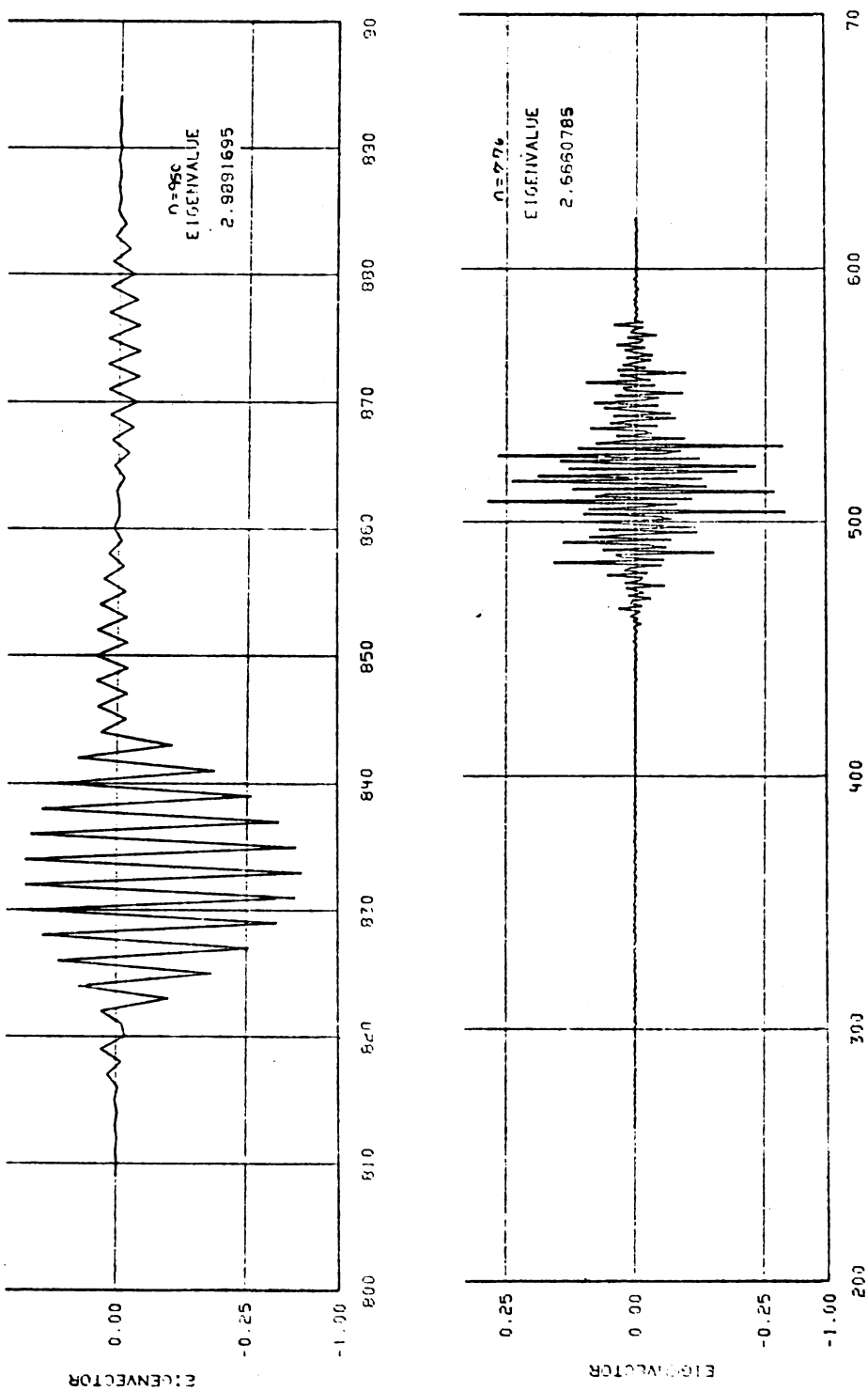

FIGURE 4.20.--Eigenvectors n=776 and 950 for a 1000 unit chain with C_d=.5, $P_{d,d}$=.1 and a 2/1 mass ratio.

CHAPTER V

THEORETICAL DEVELOPMENT

To explore the theory of vibrations of the linear chain, we will develop, in review, the quantum mechanics of the chain and the classical and quantum-mechanical Green's functions necessary for the theory. Given the classical Hamiltonian of the system (Equation (1.3), we can rewrite it in terms of the displacement and momentum operators ($U_\alpha(\ell,t)$ and $P_\alpha(\ell,t)$)

$$H(t) = \sum_{\ell\alpha} \frac{P^*_\alpha(\ell,t)P_\alpha(\ell,t)}{2m_\alpha(\ell)} + \tfrac{1}{2} \sum_{\substack{\alpha,\beta \\ \ell,\ell'}} U^*{}_\alpha(\ell,t)\,\phi_{\alpha\beta}(\ell,\ell')U_\beta(\ell',t) \tag{5.1}$$

where the quantization condition is

$$[P_\alpha(\ell,t);\ U_\beta(\ell',t)] = -i\hbar\delta_{\alpha,\beta}\delta_{\ell,\ell'} \tag{5.2}$$

$U_\alpha(\ell,t)$ and $P_\beta(\ell,t)$ are Heisenberg operators; Heisenberg's equation of motion for a general operator X(t) is

$$\dot{X}(t) = \frac{1}{i\hbar}[X(t),H(t)] \tag{5.3}$$

The time derivative of the displacement operator is

$$\dot{U}_\alpha(\ell,t) = \frac{P_\alpha(\ell,t)}{m_\alpha(\ell)} \tag{5.4}$$

and the second time derivative is

$$\ddot{U}_\alpha(\ell,t) = \frac{1}{i\hbar}\left[\frac{P_\alpha(\ell,t)}{m_\alpha(\ell)}, H\right]$$

$$= -\frac{1}{m_\alpha(\ell)} \sum_{\beta,\ell'} \phi_{\alpha\beta}(\ell,\ell') U_\beta(\ell',t) \tag{5.5}$$

This is identical in form to the classical equation of motion (1.4). The Fourier transform of Equation (5.5) gives Equation (1.5) in operator form.

For the perfect (periodic) chain $m_\alpha(\ell) = m_\alpha$, and we can expand the displacement operator in terms of a normal coordinate operator, $Q_j(k)$

$$U_\alpha(\ell) = \sum_{k,j} \frac{Q_j(k)}{\sqrt{Nm_\alpha}} \sigma_{\alpha j}(k)\, e^{ik\cdot R_\ell} \tag{5.6}$$

where $\sigma_{\alpha j}(k)$ is an expansion coefficient.

The expansion coefficients obey Equations (1.9) governing closure and completeness. Substituting Equation (5.6) into the Fourier transform of Equation (5.5) will again give Equation (1.8) for the eigenfrequencies.

Green's Function

Lifshitz[11] and Montroll and Potts[12] independently formulated the lattice dynamics problem in terms of the classical Green's function, defined to be the solution to the matrix equation.

$$(\omega^2 \underline{\underline{M}} - \underline{\underline{\phi}})\ \underline{\underline{g}} = \underline{\underline{I}} \tag{5.7}$$

where $\underline{\underline{M}}$ is the mass matrix
and $\underline{\underline{\phi}}$ is the potential matrix

In component form we have

$$\sum_{\gamma \ell''} [\omega^2 m_\alpha(\ell)\delta_{\alpha,\gamma}\ \delta_{\ell,\ell''} - \phi_{\alpha\gamma}(\ell,\ell'')]\, g_{\gamma\beta}(\ell'',\ell') = \delta_{\alpha\beta}\delta_{\ell\ell'} \tag{5.8}$$

where ϕ is defined in Equation (1.3).

The formal solution to Equation (5.7) is

$$\underline{\underline{g}} = (\omega^2 \underline{\underline{M}} - \underline{\underline{\phi}})^{-1} \tag{5.9}$$

In Appendices E, F and G, we make use of this solution to solve for specific elements of $\underline{\underline{g}}$ for some special systems. $\underline{\underline{g}}$ is therefore the inverse of the matrix A in Equation (1.5),

$$\underline{\underline{A}}\ \underline{U} = 0 \quad \text{where } \underline{\underline{A}} = (\omega^2 \underline{\underline{M}} - \underline{\underline{\phi}}) \tag{5.10}$$

First for the perfect periodic chain, $\underline{g}$ can be diagonalized by the normal coordinate transformation, i.e.

$$g_{\alpha\beta}(\ell,\ell') = \frac{1}{N} \sum_{\substack{j,j' \\ k,k'}} \frac{1}{\sqrt{m_\alpha m_\beta}} e^{-\vec{k}\cdot\vec{R}_\ell} \sigma^*_{j\alpha}(k) g_{jj'}(k,k') \; e^{i\vec{k}'\cdot\vec{R}_{\ell'}} \sigma_{j'\beta}(k') \tag{5.11}$$

From Equation (1.7) and (1.8) it is clear that the matrix transformation $T^{jk}_{\ell\alpha} \equiv \sigma^j_\alpha(k) e^{ik\cdot R_\ell}$ diagonalizes the periodic matrix $(\omega^2 M-\phi)$ in coordinate space (ℓ,α)

$$M^{-1} T^{jk}_{\ell\alpha} (\omega^2 M-\phi)^{\ell\alpha}_{\ell'\beta} T^{-1\,\ell'\beta}_{j'k'} = (\omega^2-\omega_j^2(k))\delta_{k,k'}\delta_{j,j'},$$

the same matrices also diagonalize the inverse of $(\omega^2 M-\phi)$ or

$$g_{jj'}(k,k') = g_j(k) = \frac{1}{\omega^2-\omega_j^2(k)} \delta_{k,k'}\delta_{j,j'} \tag{5.12}$$

Substituting back into Equation (5.11) we have

$$g_{\alpha\beta}(\ell,\ell') = \frac{1}{N} \sum_{j,k} \frac{\sigma^*_{j\alpha}(k)\, \sigma_{j\beta}(k) e^{ik(R_{\ell'}-R_\ell)}}{(\omega^2-\omega_j^2(k))\sqrt{m_\alpha m_\beta}} \tag{5.13}$$

where N is number of unit cells in the crystal.

In Appendix E, we use this equation to solve for the monatomic chain Green's function. The diagonal element of Equation (5.13) is

$$m_\alpha g_{\alpha\alpha}(\ell,\ell) = \frac{1}{N} \sum_{j,k} \frac{\sigma^*_{j\alpha}(k)\sigma_{j\alpha}(k)}{\omega^2-\omega_j^2(k)} \tag{5.14}$$

We can now find a relation between the Green's function and the density of states

$$\nu(\omega) = \frac{1}{N} \sum_{jk} \delta(\omega-\omega_j(k)) \tag{5.15}$$

where we normalized the density of states to one

$$\int_0^{\omega_m} \nu(\omega)\, d\omega=1 \tag{5.16}$$

Summing Equation (5.14) over α we have

$$\frac{1}{N} \sum_{\alpha\ell} m_\alpha g_{\alpha\alpha}(\ell,\ell) = \frac{1}{N} \sum_{jk} \frac{1}{\omega^2-\omega_j^2(k)}$$

which we can convert to an integral ($\omega \to \omega+i\varepsilon$)

$$\frac{1}{N} \sum_{jk} \frac{1}{\omega^2-\omega_j^2(k)} = sP\int_0^{\omega_m} \frac{\nu(\omega')\,d\omega'}{\omega^2-\omega'^2}$$

$$+ \frac{i\pi s}{2\omega} \sum_{jk} (\delta(\omega-\omega_j(k))+\delta(\omega+\omega_j(k)))$$

where

P is the principle part
and s is the number of atoms per unit basis

In terms of the density of states, this becomes

$$\sum_{\alpha} m_{\alpha} g_{\alpha\alpha}(\ell,\ell) = sP\int_{0}^{\omega_m} \frac{\nu(\omega')d\omega'}{\omega^2-\omega'^2} + \frac{\pi i s}{2\omega}(\nu(\omega)+\nu(-\omega))$$

$$= \text{real} + \text{imaginary}.$$

Since $\nu(-\omega) = 0$ for $\omega>0$ we have

$$\nu(\omega) = -\frac{2\omega}{s\pi} \text{ Im} \sum_{\alpha} m_{\alpha} g_{\alpha\alpha}(\ell,\ell) \tag{5.17}$$

where Im( ) is the imaginary part of ( ).

Also

$$\nu(\omega) = -\frac{2\omega}{sN\pi} \text{ Im} \sum_{\ell,\alpha} m_{\alpha} g_{\alpha\alpha}(\ell,\ell)$$

$$\nu(\omega) = -\frac{2\omega}{sN\pi} \text{ Im tr } (\underline{\underline{M}}\underline{\underline{g}}) \tag{5.18}$$

where tr( ) is the trace of the matrix ( )

and since $D(\omega^2) = \nu(\omega)/2\omega$

$$D(\omega^2) = -\frac{1}{Ns\pi} \text{ Im tr } (\underline{\underline{M}}\underline{\underline{g}}) \tag{5.19}$$

for a chain with N lattice points and s atoms per basis and $\omega^2 \to (\omega^2+i\varepsilon)$.

Although we have derived the density of states for the perfect lattice, Equation (5.19) is valid for the imperfect lattice where $Ns=N_T$ the total number of atoms. To show this, we look at the solution to the eigenvalue equation for the disordered system. For the imperfect crystal, we must start with Equation (1.4). We define $\Delta\phi_{\alpha\beta}(\ell,\ell')$ as the difference between the force

constant matrix of the disordered system and that of the perfect system ($\phi' - \phi^o$) (=0 for the mass defect problem) and m_α as the mass of site, α, of the perfect chain. We can define two quantities

$$\varepsilon_\alpha(\ell) = \frac{m_\alpha - m'_\alpha(\ell)}{m_\alpha} \tag{5.20}$$

and

$$C_{\alpha\beta}(\ell,\ell') = \Delta\phi_{\alpha\beta}(\ell,\ell') + \varepsilon_\alpha(\ell) m_\alpha \omega^2 \delta_{\alpha,\beta} \delta_{\ell,\ell'} \tag{5.21}$$

Then, we can rewrite Equation (1.4) in terms of the perfect lattice where

$$-\omega^2 \underline{\underline{M}}' + \underline{\underline{\phi}}' \equiv -\omega^2 \underline{\underline{M}}^o + \underline{\underline{\phi}}^o + \underline{\underline{C}} \cdot$$

We can expand the displacements in terms of the normal coordinates of the imperfect lattice

$$U_\alpha(\ell) = \sum_f X_\alpha(f,\ell) Q(f) \tag{5.22}$$

where $Q(f)$ are the normal coordinates and
$X_\alpha(f,\ell)$ are the expansion coefficients

and we get

$$\sum_{\beta\ell'} [-\omega^2(f) m_\alpha(\ell) \delta_{\alpha,\beta} \delta_{\ell,\ell'} + \phi^o_{\alpha\beta}(\ell,\ell') + C_{\alpha\beta}(\ell,\ell')] X_\beta(f,\ell') = 0 \tag{5.23}$$

for the eigenvalue equations. The Green's function for the system is formally

$$G = (\underline{\underline{M}}^{o}\omega^{2}-\underline{\underline{\phi}}^{o}-\underline{\underline{C}})^{-1} \tag{5.24}$$

Clearly, it is also diagonalized by the normal coordinate transformation of Equation (5.22). If we normalize the eigenvectors such that

$$\sum_{\alpha\ell} m_{\alpha}(\ell)\left|X_{\alpha}(f,\ell)\right|^{2} = 1 \tag{5.25}$$

we again can derive Equation (5.19). For a chain of length, N, we would in practice have to solve an Nx N matrix for the eigenvalues and eigenvectors.

We can also write the Green's function of the disordered lattice, G, in terms of the Green's function for the periodic lattice, $\underline{\underline{P}}\equiv\underline{\underline{g}}$. From Equation (5.24)

$$(\underline{\underline{M}}^{o}\omega^{2}-\underline{\underline{\phi}}^{o})\underline{\underline{G}}-\underline{\underline{C}}\,\underline{\underline{G}}=\underline{\underline{I}}$$

Since $P^{-1} = \underline{\underline{M}}^{o}\omega^{2}-\underline{\underline{\phi}}^{o}$, we have

$$\underline{\underline{P}}^{-1}\underline{\underline{G}} - \underline{\underline{C}}\,\underline{\underline{G}}=I$$

which gives

$$\underline{\underline{G}} = \underline{\underline{P}} + \underline{\underline{P}}\,\underline{\underline{C}}\,\underline{\underline{G}} \tag{5.26a}$$

$$\underline{\underline{G}} = \underline{\underline{P}} + \underline{\underline{G}}\,\underline{\underline{C}}\,\underline{\underline{P}} \tag{5.26b}$$

These two equations are often called the Dyson equations.

The classical Green's function is a generating function which allows us to solve complicated interaction problems by solving much simplier force free equations. However, the classical Green's function has no quantum mechanical foundation. Following the work of Elliott and Taylor,[57] we restructure the problem in terms of the Zubarev[58] double-time single-particle Green's functions. These functions are generalizations of correlation functions and, therefore, have a definite physical interpretation. We use the retarded and advanced Green's functions

$$G^r(t,t') = -\frac{2\pi i}{\hbar}\,\theta(t-t')\langle[A(t),B(t')]\rangle \tag{5.27a}$$

$$G^a(t,t') = \frac{2\pi i}{\hbar}\,\theta(t'-t)\langle[A(t),B(t')]\rangle \tag{5.27b}$$

where A(t) and B(t) are two operators in the Heisenberg representation

$$A(t) = e^{iHt/\hbar}A\,e^{-iHt/\hbar} \tag{5.28}$$

$\theta(t-t')$ is the unit step function

$$\theta(t) = \begin{matrix} 1 & t>0 \\ 0 & t<0 \end{matrix} \tag{5.29}$$

The commutator is defined as

$$[A(t),B(t')] = A(t)B(t')-\eta\,B(t')A(t) \tag{5.30}$$

where η = 1 for bosons
-1 for fermions

The phonon problem is a boson problem, therefore, $\eta = 1$.

Also, the average is

$$\langle \ldots \rangle = \frac{tr(\rho \ldots)}{tr\ (\rho)} \tag{5.31}$$

where $\rho = e^{-H/\tau}$. $(\tau \equiv kT)$

H is the Grand canonical Hamiltonian and is related to the canonical Hamiltonian by

$$H = H - \mu N \tag{5.32}$$

where μ is the chemical potential and
N is the number of particles

Using $tr(AB) = tr(BA)$, and Equation (5.28) we can show

$$G(t,t') = G(t-t') \tag{5.33}$$

Next, we define the correlation functions

$$F_{AB}(t,t') = \langle A(t)\ B(t') \rangle \tag{5.34a}$$

$$F_{BA}(t,t') = \langle B(t')A(t) \rangle \tag{5.34b}$$

The correlation functions also depend on the time variables through their differences, and one related by

$$F_{BA}(t + \tfrac{i\hbar}{\tau}) = F_{AB}(t) \tag{5.35}$$

The relation between the Green's function and correlation function can be shown to be

$$F_{BA}(t) = i\hbar \lim_{\varepsilon \to +0} \int \frac{(G(\omega+i\varepsilon)-G(\omega-i\varepsilon))e^{i\omega t}}{e^{\frac{\hbar\omega}{\tau}} - \eta} d\omega \qquad (5.36)$$

The correlation functions of interest in the phonon problem include those of the operators $U_\alpha(\ell,t)$, $P_\alpha(\ell,t)$, $a_j^+(k)$, $a_j(k)$. We will look at the displacement-displacement correlation function

$$F_{AB}(t) = \langle U_\alpha(\ell,0)\ U_\beta(\ell',t)\rangle \qquad (5.37)$$

For $\alpha=\beta$, $\ell=\ell'$ and $t=0$, F gives the mean square displacement used to calculate the Debye-Waller factor in scattering theory and in the Mössbauer effect, and to calculate the frequency spectrum. The mean squared momentum correlation function is used for calculating the doppler energy shift in the Mössbauer effect which is velocity dependent whereas the probability of emission is dependent on the mean squared displacement. The creation-destruction operator correlation functions are used in phonon scattering calculations of lifetimes of modes and transport processes. The displacement operator Green's function is

$$G^r_{\alpha\beta}(\ell,\ell',t,t') = \frac{-2\pi i}{\hbar}\,\theta(t-t')\langle[U_\alpha(\ell,t),U_\beta(\ell',t')]\rangle \qquad (5.38)$$

First, we want to find the equations of motion of this quantity. Taking the first time derivative with respect to t, we have

$$\dot{G}^r_{\alpha\beta}(\ell,\ell',t,t') = \frac{-2\pi i}{\hbar}\delta(t-t')\langle[U_\alpha(\ell,t),U_\beta(\ell',t)]\rangle^{0} + \frac{-2\pi i}{\hbar}\theta(t-t')\langle[\dot{U}_\alpha(\ell,t),U_\beta(\ell',t')]\rangle$$

where $\dot{U}_\alpha(\ell,t) = P_\alpha(\ell,t)/m_\alpha(\ell)$. Taking the second time derivative, we have

$$\ddot{G}^r_{\alpha\beta}(\ell,\ell',t,t') = \frac{-2\pi i}{\hbar}\frac{\delta(t-t')}{m_\alpha(\ell)}\langle[P_\alpha(\ell,t),U_\beta(\ell',t)]\rangle - \frac{2\pi i}{\hbar m_\alpha(\ell)}\theta(t-t')\langle[\ddot{U}_\alpha(\ell,t),U_\beta(\ell',t')]\rangle$$

Using Equations (5.2) and (5.5), we have

$$\ddot{G}^r_{\alpha\beta}(\ell,\ell',t,t') = \frac{-2\pi}{m_\alpha(\ell)}\delta(t-t')\delta_{\alpha,\beta}\delta_{\ell,\ell'} + \frac{2\pi i}{\hbar}\frac{\theta(t-t')}{m_\alpha(\ell)}\sum_{\ell''}\phi_{\alpha\gamma}(\ell,\ell'')\langle[U_\gamma(\ell'',t),U_\beta(\ell',t')]\rangle$$

$$\ddot{G}^r_{\alpha\beta}(\ell,\ell',t,t') = \frac{-2\pi}{m_\alpha(\ell)}\delta(t-t') - \frac{1}{m_\alpha(\ell)}\sum_{\gamma\ell''}\phi_{\alpha\gamma}(\ell,\ell'')G^r_{\gamma\beta}(\ell'',\ell';t,t')$$

Taking the Fourier transform we have

$$\sum_{\gamma\ell''}(\omega^2 m_\alpha(\ell)\delta_{\alpha,\gamma}\delta_{\ell,\ell''} - \phi_{\alpha\gamma}(\ell,\ell''))G^r_{\gamma\beta}(\ell'',\ell';\omega) = \delta_{\alpha,\beta}\delta_{\ell,\ell'} \quad (5.39)$$

This is identical to Equation (5.8) showing that the Zubarev double-time Green's function and the classical Green's function satisfy the same equations with the corresponding quantum operators replacing the classical variables.

With the theoretical background we can now look at various theoretical approaches to the density of states.

Defect Clusters

Our first model for the density of states for the phonon spectra of disordered chains will concern itself only with the light impurity-band modes. Dean[18] associated the structure in the impurity band ($2<\omega^2<4$ for $\frac{m_H}{m_L} = 2$ and $\frac{\gamma}{m_L} = 1$) with isolated clusters for random chains. We will attempt to reconstruct the impurity band density of states by configuration averaging all the impurity modes in an n site defect cluster embedded in a host chain. For example, for a 6 site cluster one possible configuration would be one defect and 5 hosts (h-h-h-d-h-h), etc.). For the random system, the probability of occurrance of their configuration is $6\ C_d(1-C_d)^5$. This configuration gives rise to only one impurity mode as we shortly show. For this mode we have weight $6\ C_d(1-C_d)^5$. Using the monatomic chain Green's function derived in Appendix E, we use the Green's

function techniques to enumerate all the impurity modes arising in defect cluster to size 3 in Appendix F. We, also, have generated the impurity mode frequencies for defect clusters up to size 6, by embedding the clusters in a 1000 unit host chain, then finding the eigenvalues and eigenvectors for $\omega^2>2$ by the methods previously described. Table 5.1 lists the eigenfrequencies in the impurity band of all possible clusters of size less than or equal to 6, where the defect mass is half the host atom mass.

Once we have the relative weights of each eigenfrequency, we can form a bar graph like those in Sections II and III. To get the correct density of states in the impurity band we can normalize this bar graph to correspond to the Matsuda-Teramoto formula, Equation (3.113). First, for sake of comparison with the numerical plots we normalize the bar graph instead so that the peak at $\omega^2=2.66$ is equal to that of the corresponding numerical calculation. This normalization gives a cumulative density of state well under that given by Equation (3.113). Figures (5.1), (5.2) and 5.3) are the density of states plots in the region $2<\omega^2<4$ for 4, 5, and 6 site embedded cluster approximations for $C_d=.5$ random systems. The corresponding numerical density of states is superimposed. The four site cluster displayes 6 of the peaks of the numerical density of states structure. The 5 site

TABLE 5.1.--Impurity mode frequencies of defect clusters embedded in a host chain, $m_h/m_d=2$.

Cluster size	Cluster type	eigenmodes in region $2 \leq \omega^2 \leq 4$
1	d	2.6667
2	dd	3.23607
3	ddd	2.4142,3.5214
	dhd	2.4142,2.8393
4	dddd	3.675,2.839
	dhdd	2.623,3.258
	dhhd	2.592,2.727
5	ddddd	2.306,3.132,3.7659
	ddhdd	3.132,3.332
	dhddd	2.293,2.707,3.528
	dhhdd	2.6618,3.237
	dhdhd	2.274,2.643,2.906
	dhhhd	2.643,2.6876
6	dddddd	2.636,3.332,3.8236
	ddhddd	2.3929,3.224,3.536
	ddddhd	2.573,2.8995,3.678
	ddhhdd	3.212,3.2591
	dddhhd	2.3928,2.6724,3.5217
	dhddhd	2.552,2.6876,3.278
	dhdhdd	2.3921,2.815,3.25995
	ddhhhd	2.6661,3.23614
	dhdhhd	2.3920,2.6622,2.847
	dhhhhd	2.659,2.6738

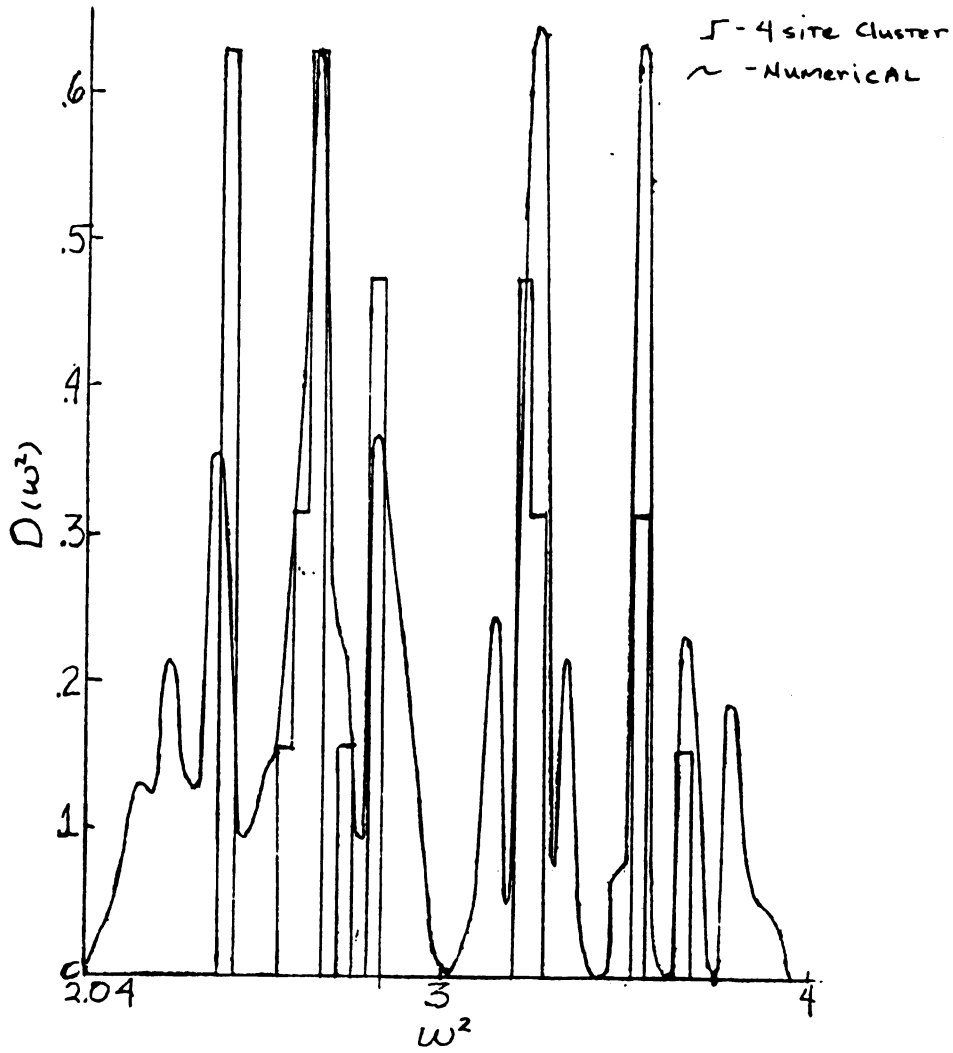

FIGURE 5.1.--Density of states for C_A=.5 random generated by a 4 site embedded cluster.

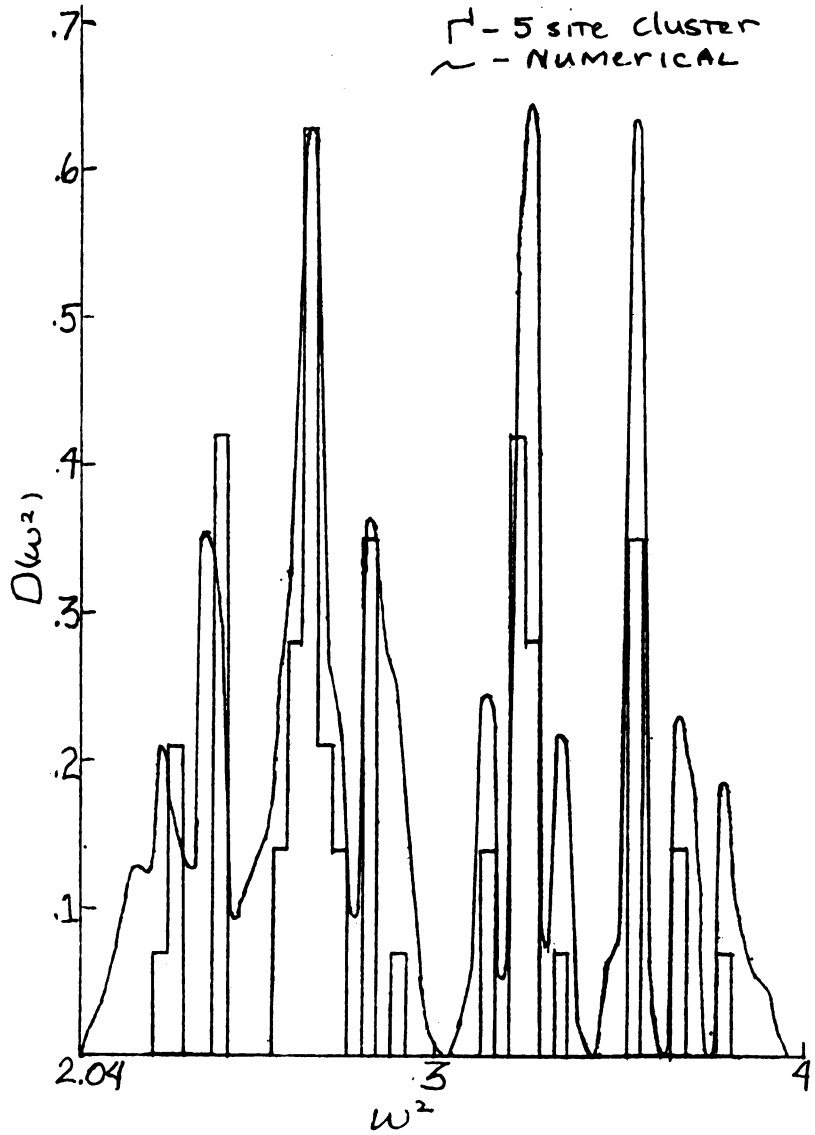

FIGURE 5.2.--Density of states for C_A=.5 random generated by a 5 site embedded cluster.

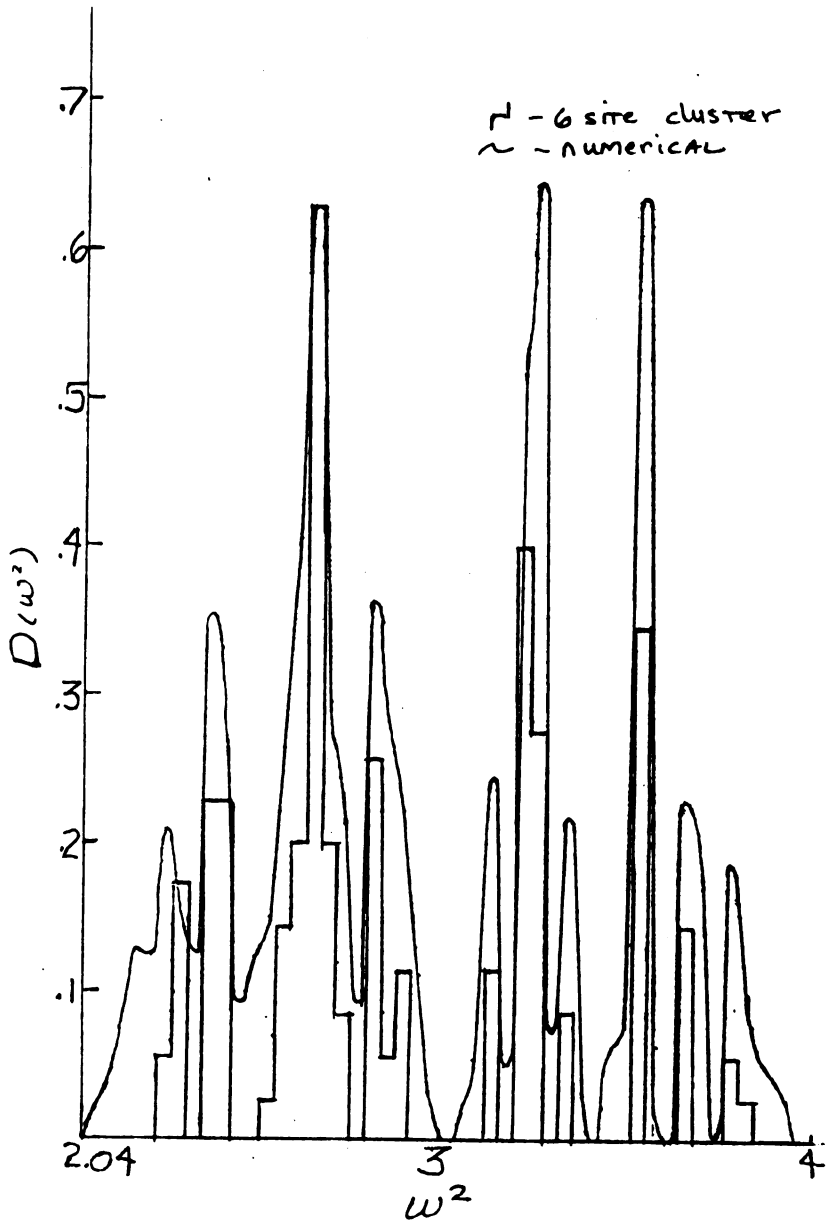

FIGURE 5.3.--Density of states for C_A=.5 random generated by a 6 site embedded cluster.

cluster displays 10 of these peaks. The 6 site cluster gives no major new information as to the defect cluster modes responsible for the peaks. The 6 site cluster does, however, weight the peaks much more realistically than does either the 4 or 5 site cluster. It also gives a clue to the reason for the non-zero density of states between the 1, 2 and 3 site cluster modes. This peak broadening is due to an effective cluster-cluster energy splitting (dd-h-h-dd). A ten site cluster would give even a better frequency spectrum. As one might expect, as we go to lower concentrations of defects this approach works even better since the defect clusters will be more isolated from each other by host masses and the probability of many defect strings is greatly diminished. Figure (5.4) gives the 6 site embedded cluster spectrum for C_d=.2 random along with the corresponding numerical plot. The agreement is remarkably good. In each case presented above, we will look at the integrated density of states of the 6 site cluster "properly" normalized compared to the numerical results. Figure (5.5) is for C_d=.5 and Figure (5.6) is for C_d=.2. The numerical results for C_d=.2 random are for a 10,000 unit chain and give an integrated density of states in the impurity band of .1712 versus .1667 theoretically. If we adjust for this error, we can see that except for a

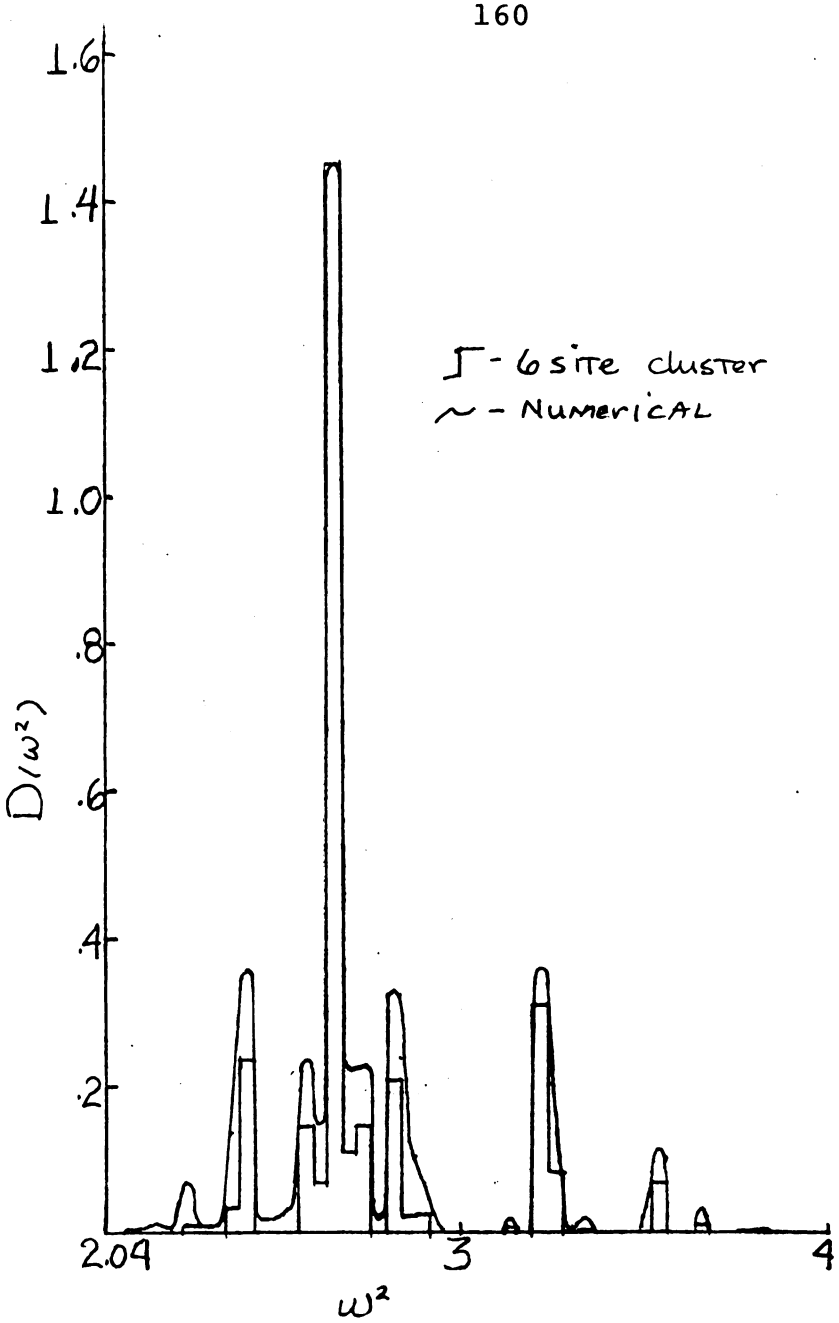

FIGURE 5.4.--Density of states for C_A=.2 random generated by a 6 site embedded cluster.

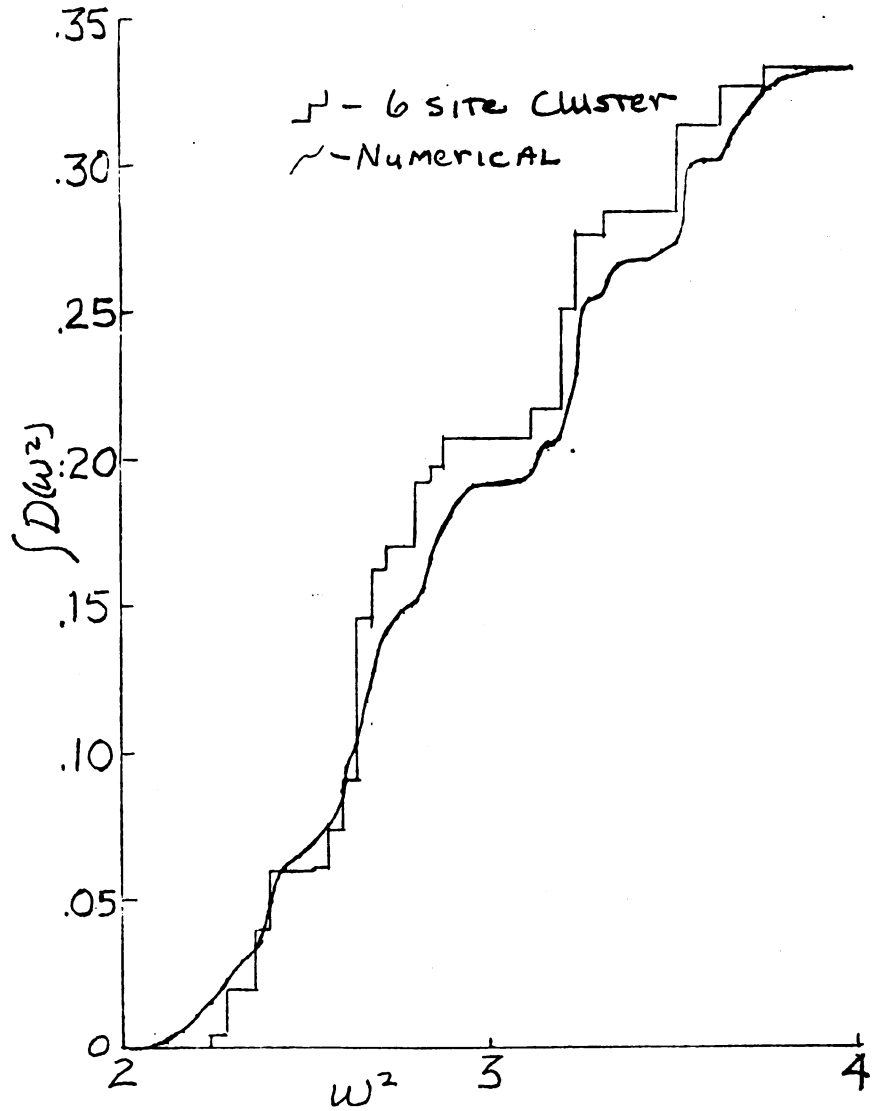

FIGURE 5.5.--Integrated density of states for C_d=.5 random generated by a 6 site embedded cluster.

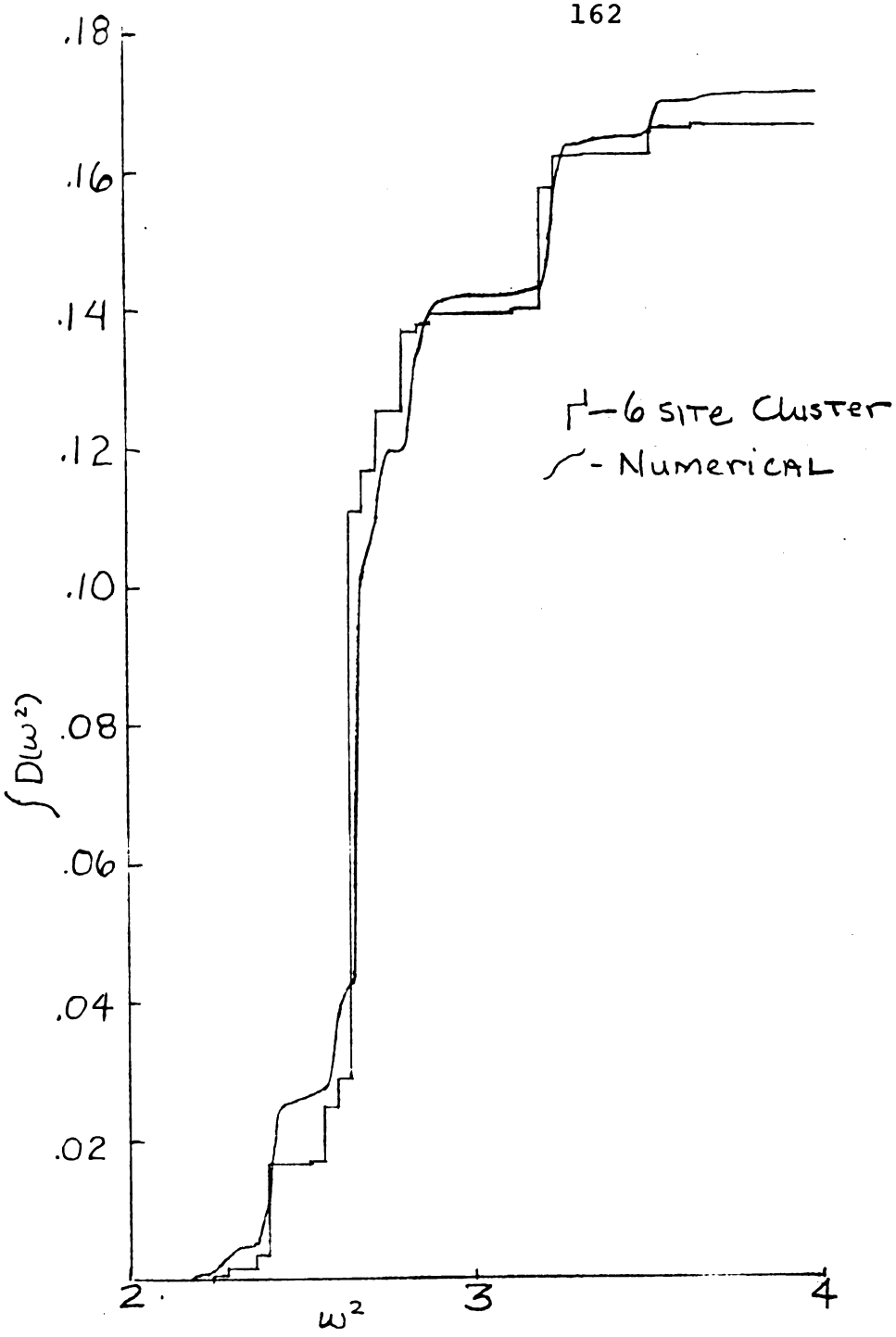

FIGURE 5.6.--Integrated density of states for C_d=.2 random generated by a 6 site embedded cluster.

region $2.66<\omega^2<2.80$ the fit is almost perfect. The $C_d=.5$ plot shows serious discrepancies throughout the region. This is one indication of larger clusters than we considered being important. Any short-range order only makes this problem more serious. The correlation between the correctness of this model and the localization length is apparent. If the localization lengths $L_e(\omega^2)$ and $L_E(\omega^2)$ are short (~1-5 atoms) in the impurity region, the model works well.

Not only does this model fail at high defect concentrations, it also gives no information on the density of states in the host band ($0\leq\omega^2\leq 2$) and on how it is depleted to form the impurity band. Therefore, we look at another simple model.

n Site Periodically Extended Model

Butler and Kohn[59] first suggested reconstructing the electronic density of states by taking clusters as we did in the last section and periodically continuing a given cluster throughout the system. Then they configuration averaged the density of states over all possible clusters. We, in a similar manner, take the possible spectra resulting from a periodic chain with an n site basis, and obtain an "average" spectrum by properly weighting each individual n site periodic spectrum. The weighted average is based on the probability

of obtaining the given sequence of atoms that make up the basis. Essentially, the average is performed as if the basis were in fact a cluster in the medium. This procedure has some definite advantages over the embedded cluster approach. These are: (1) we obtain the total frequency spectrum not just the impurity band; (2) the errors are not as concentration and short-range order dependent as in the embedded cluster; (3) the frequency spectrum is normalized to one as constructed without the introduction of some ad-hoc renormalization criteria. It however also has some bad features. These are: (1) the averaged n site periodic system does not display the theoretical zeros in the density of states often tending to infinity instead of zero at the theoretical zeros; (2) the host band ($0<\omega^2<2$ for $\frac{m_H}{m_L}=2$; $\frac{m_L}{\gamma}=1$) has many infinite singularities in it. This is a very undesirable feature since theoretically most of the singularities should not occur and numerically most of them do not show up.

In Appendix G, we derived the theoretical density of states of these n site periodic systems for the binary chain with n=1,2,3,4 and 6. In Table 5.2 we list a complete set of bases which give all the unique frequency spectra for 4 and 6 site periodic systems. We note some of the 4 and 6 site bases are not primitive bases but are composed of multiple 1,2, and 3 site periodic bases.

TABLE 5.2.--The bases for all possible 4 and 6 site periodic chains.

Basis Size		Complete Basis Set
4	(1)	hhhh
	(1)	dddd
	(2)	hdhd
	(4)	hhdd
	(4)	dddh
	(4)	hhhd
6	(1)	hhhhhh
	(1)	dddddd
	(2)	hdhdhd
	(3)	hhdhhd
	(3)	ddhddh
	(6)	hhhhdd
	(6)	ddddhh
	(6)	hdhhhd
	(6)	dhdddh
	(6)	dddhhh
	(6)	hdhhdd
	(6)	dddddh
	(6)	hhhhhd

The four site periodic system has only 6 unique bases out of $2^4=16$ and the six site periodic system has only 13 unique basis out of $2^6=64$ possibilities.

By using the analytic expressions for density of states given in Appendix G we can generate the average density of states to any desired accuracy. We have, however, found difficulties in getting a reasonable integrated density of states with the numerous singularities in each spectrum (about 12 singularities per 6 site configuration). We have in fact 104 unique singularities in an average 6 site density of states spectrum. Therefore, we average the numerical spectra generated by 10,000 atom chains with an n site basis, instead of the analytical expressions to avoid the infinite singularity difficulties in the analytic expressions. Figure (5.7) shows the $C_d=.5$ random spectrum produced by an averaged 4 site cluster. Comparing with the superimposed numerical results we conclude that the 4 site periodic system gives a quite poor reproduction of the frequency spectrum. Figure (5.8) for $C_d=.5$ random produced by an averaged 6 site periodic system looks much more like the experiment. The structure in the region $0<\omega^2<2$, however, does not appear in the numerical results. The density of states is in good agreement with numerical results in the region $2<\omega^2<4$. The density of states in the impurity band is

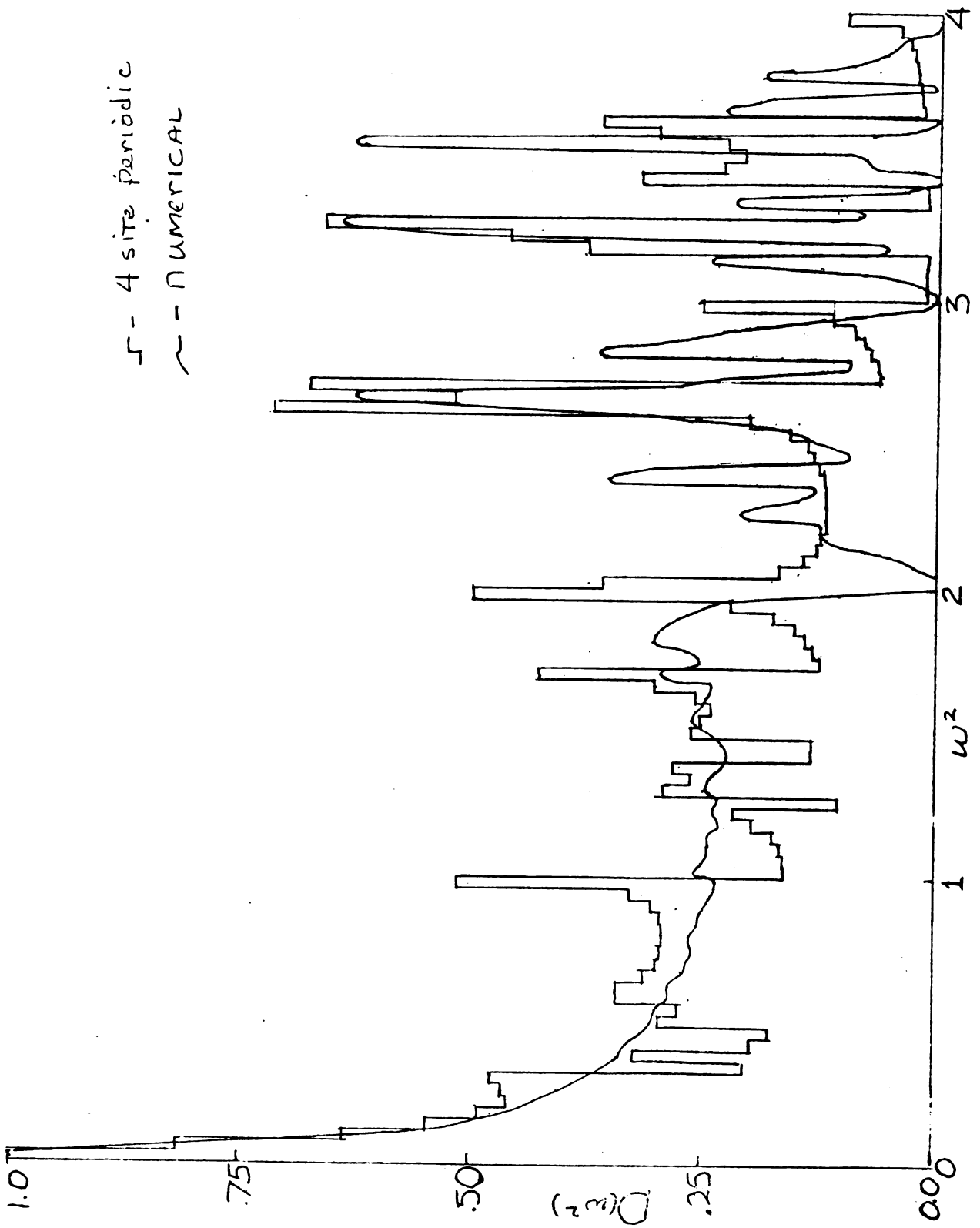

FIGURE 5.7.--Density of states for C_A=.5 random generated by a 4 site periodically extended cluster.

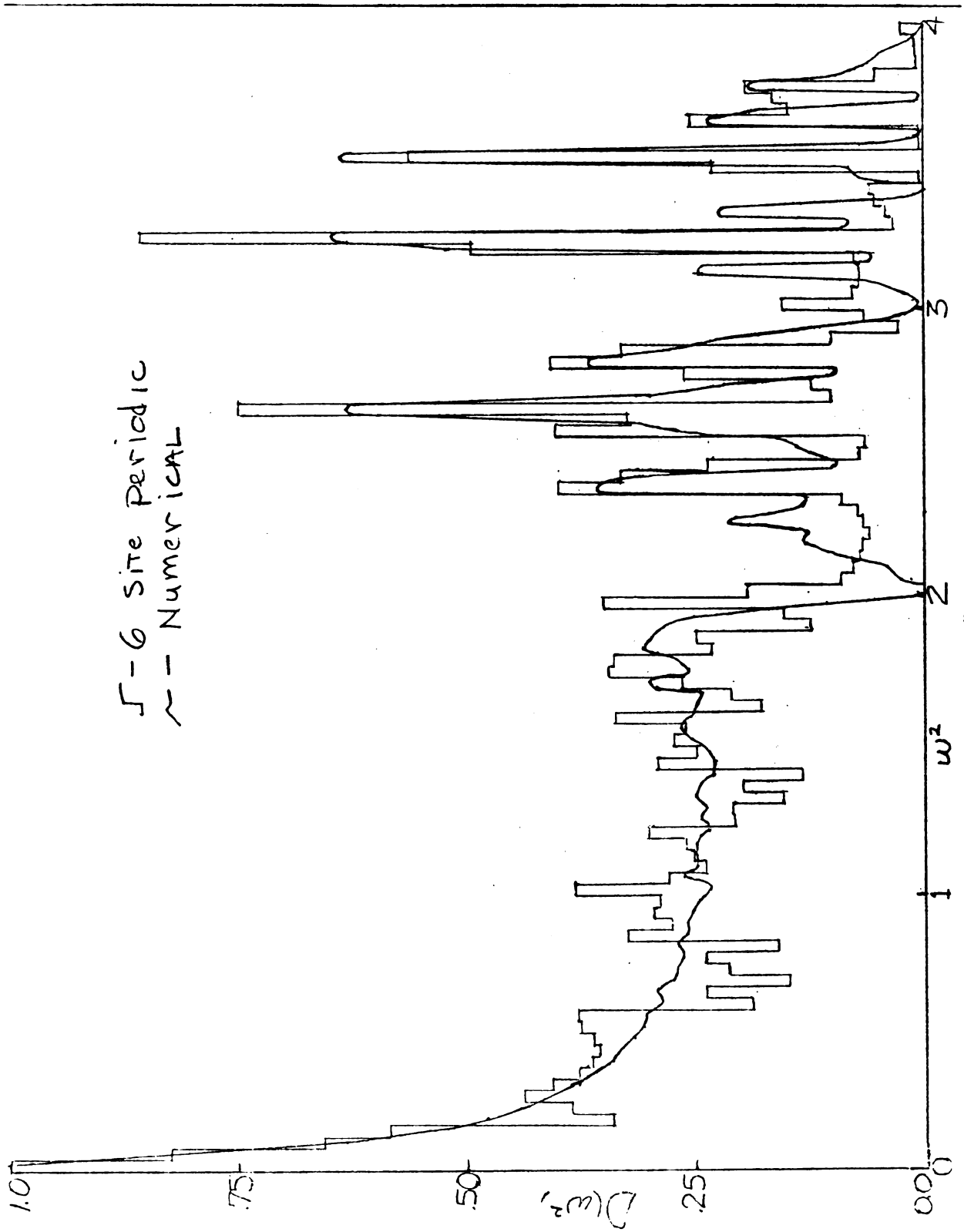

FIGURE 5.8.--Density of states for C_A=.5 random generated by a 6 site periodically extended cluster.

in fact overall in much better agreement with experiment than is the embedded cluster density of states. We see very good agreement in the structure of the density of states except at ω^2=3.14 and 3.34 where the 6 site periodic system does not reproduce the expected peaks which the embedded cluster approach did. Figure (5.9) is the six site periodic averaged spectrum for C_d=.2 random. The host band structure is much more vivid than in the C_d=.5 random case. This is just opposite to the experimental behavior where the in-band structure for C_d=.2 is less than that in the C_d=.5 random spectrum. The calculational reason for the increased structure in the periodic cluster calculation is clear. Of the possible 6 site periodic clusters, the clusters containing 0 or 1 defects are given much more weight than the bases containing 5 or 6 defects. For C_d=.5, all clusters have equal weight. In the impurity band, the embedded clusters spectrum is of equal accuracy if not superior to the averaged periodic structure.

Figure (5.10) for C_d=.5, $P_{d,d}$=0.1 was generated by the 6 site periodic system. Comparing this figure with the superimposed numerical results we see that the 6 site periodic system gives the general overall structure quite reasonably. However, the actual detail is quite poor. The in-band structure ($0<\omega^2<1$, $2<\omega^2<3$) is, for the most part, not present in the numerical results and

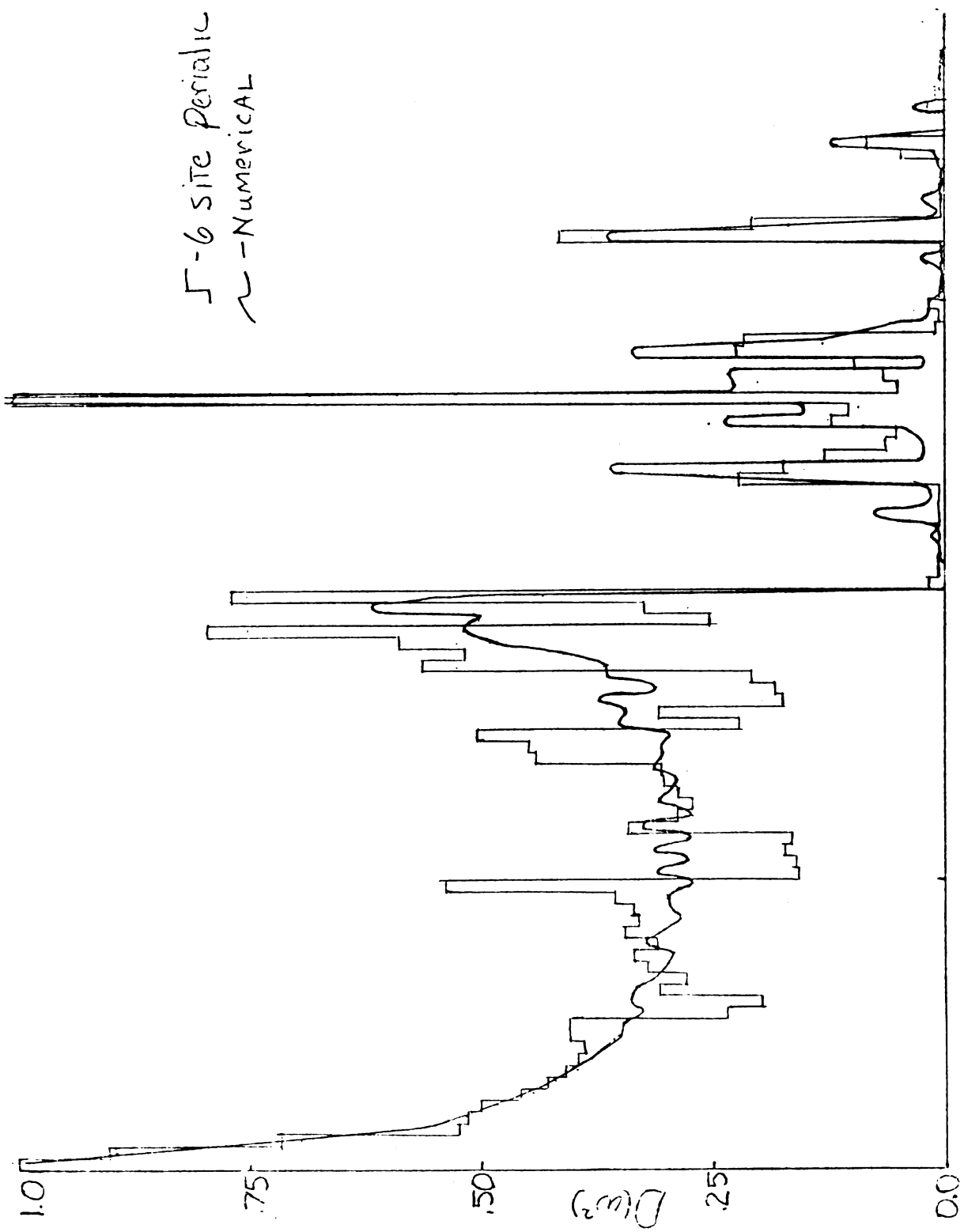

FIGURE 5.9.--Density of states for C_d=.2 random generated by a 6 site periodically extended cluster.

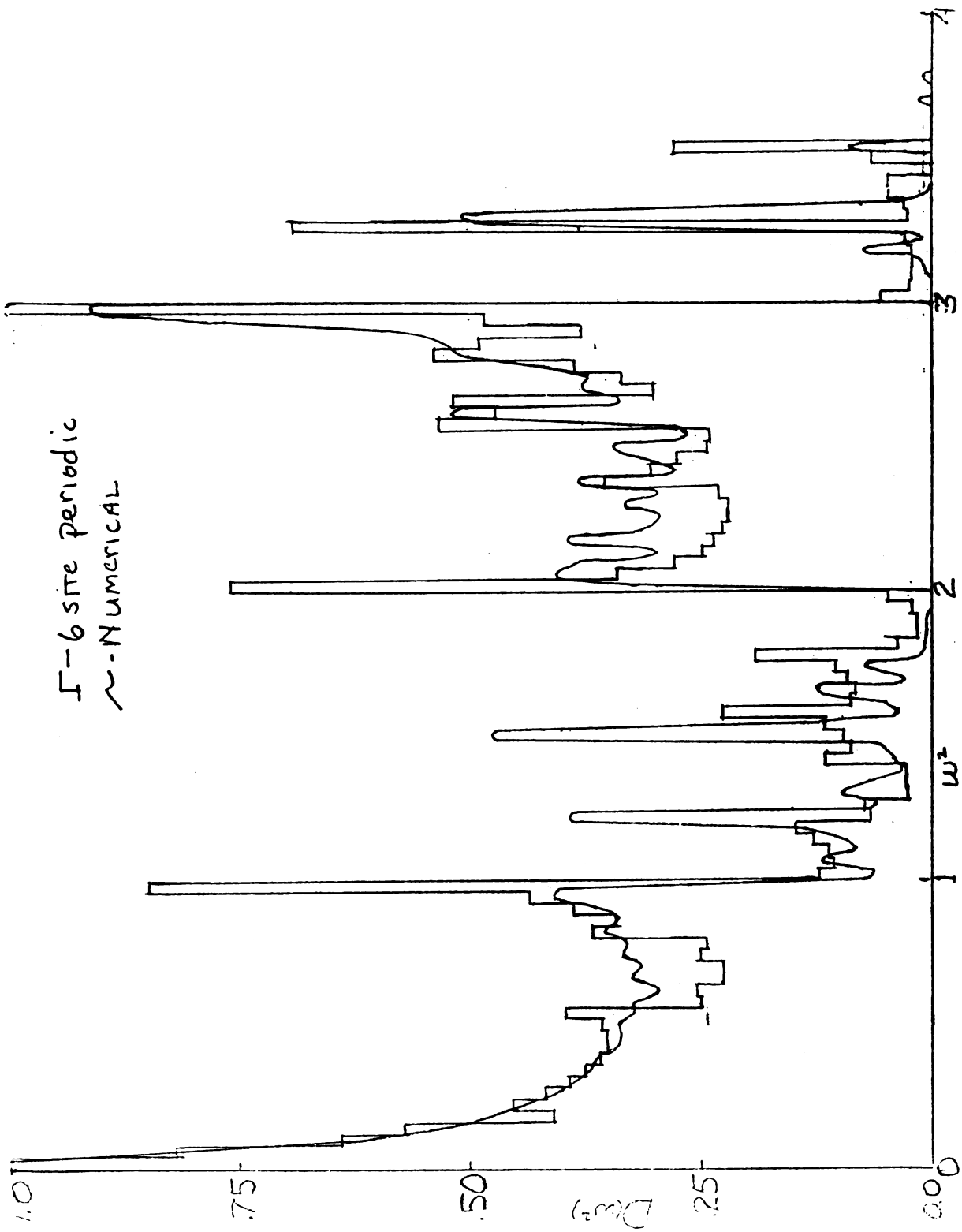

FIGURE 5.10.--Density of states for C_d=.5, P_{dd}=.1 generated by a 6 site periodically extended cluster.

the peaks in the rest of the density of states do not carry the proper weights.

Figures (5.11), (5.12) and (5.13) show the integrated density of states for C_d=.2 random, C_d=.5 random and C_d=.5, $P_{d,d}$=.1, respectively. The 6 site periodic system even with the spurious structure in the host band region does a remarkable job of recreating the integrated density of states. The errors are less for the random systems but the relative error is in no case over 5%. We would expect a 10 site periodic cluster to do even better.

Using the basic concepts developed in these two simple theories for the density of states, we can now look at a more complicated theory which will eliminate the deficiencies of these theories.

Self-Consistent Cluster Theory

With clusters imbedded in a host chain we found that the basic impurity modes could be described, but we had no handle on the host band structure. From the periodically extended cluster model, we were able to reasonably reconstruct the whole density of states. The periodicity introduced in this model had the effect of producing regions of finite spectral density versus isolated peaks in the embedded cluster approach. The difficulty with the periodically extended cluster method is that in each configuration a given cluster only

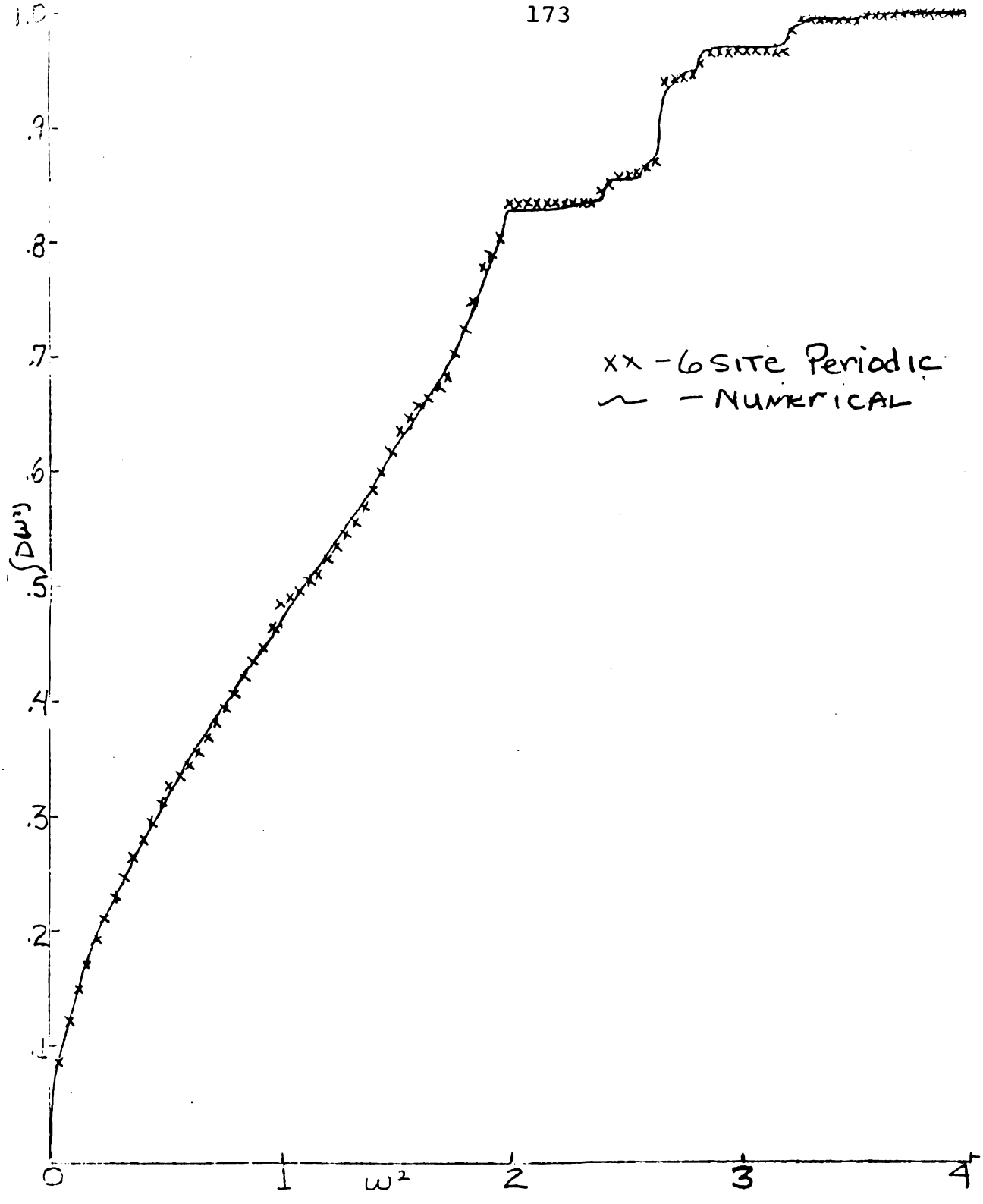

FIGURE 5.11.--Integrated density of states for C_d=.3 random generated by a 6 site periodically extended cluster.

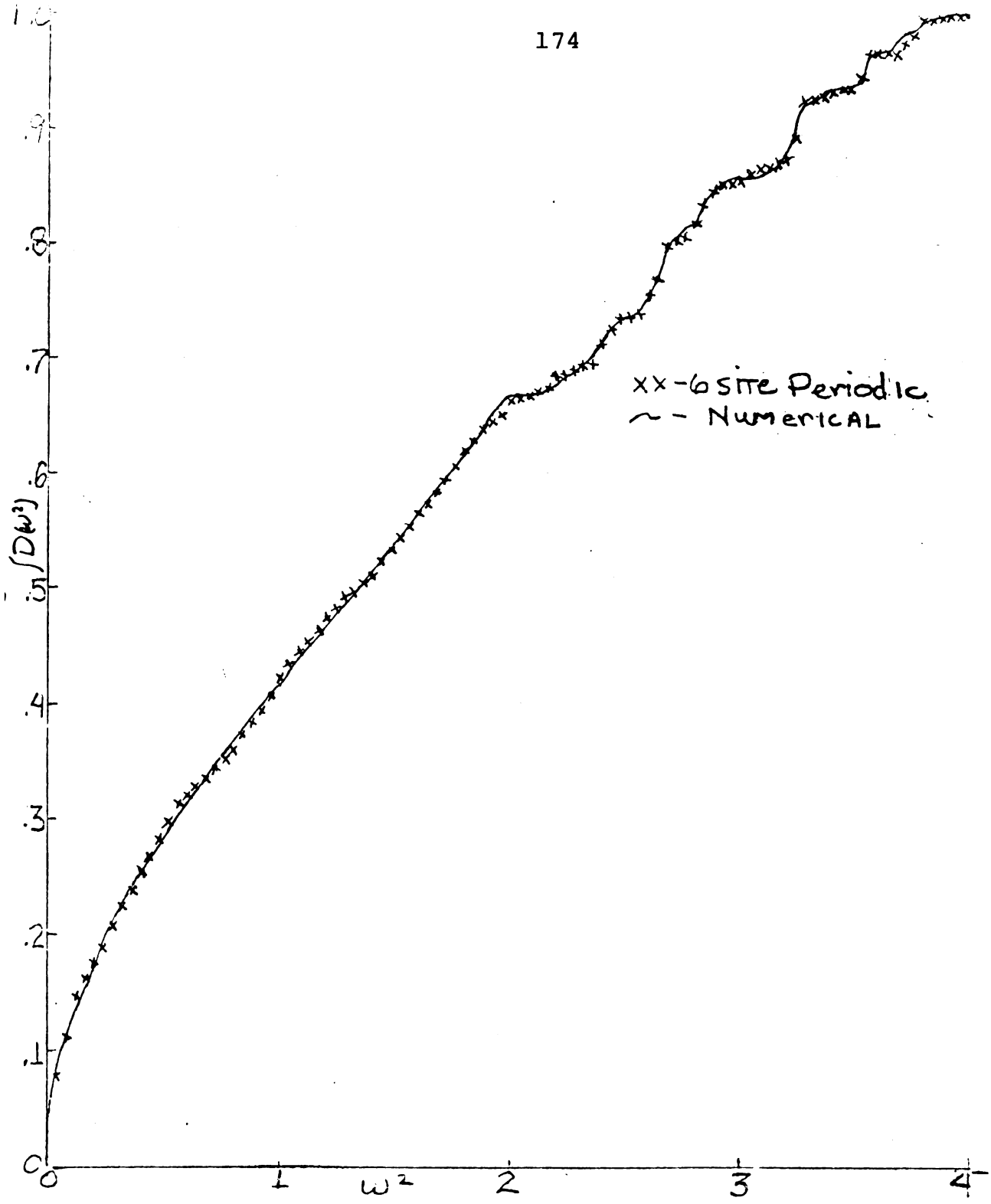

FIGURE 5.12.--Integrated density of states for C_d=.5 random generated by a 6 site periodically extended cluster.

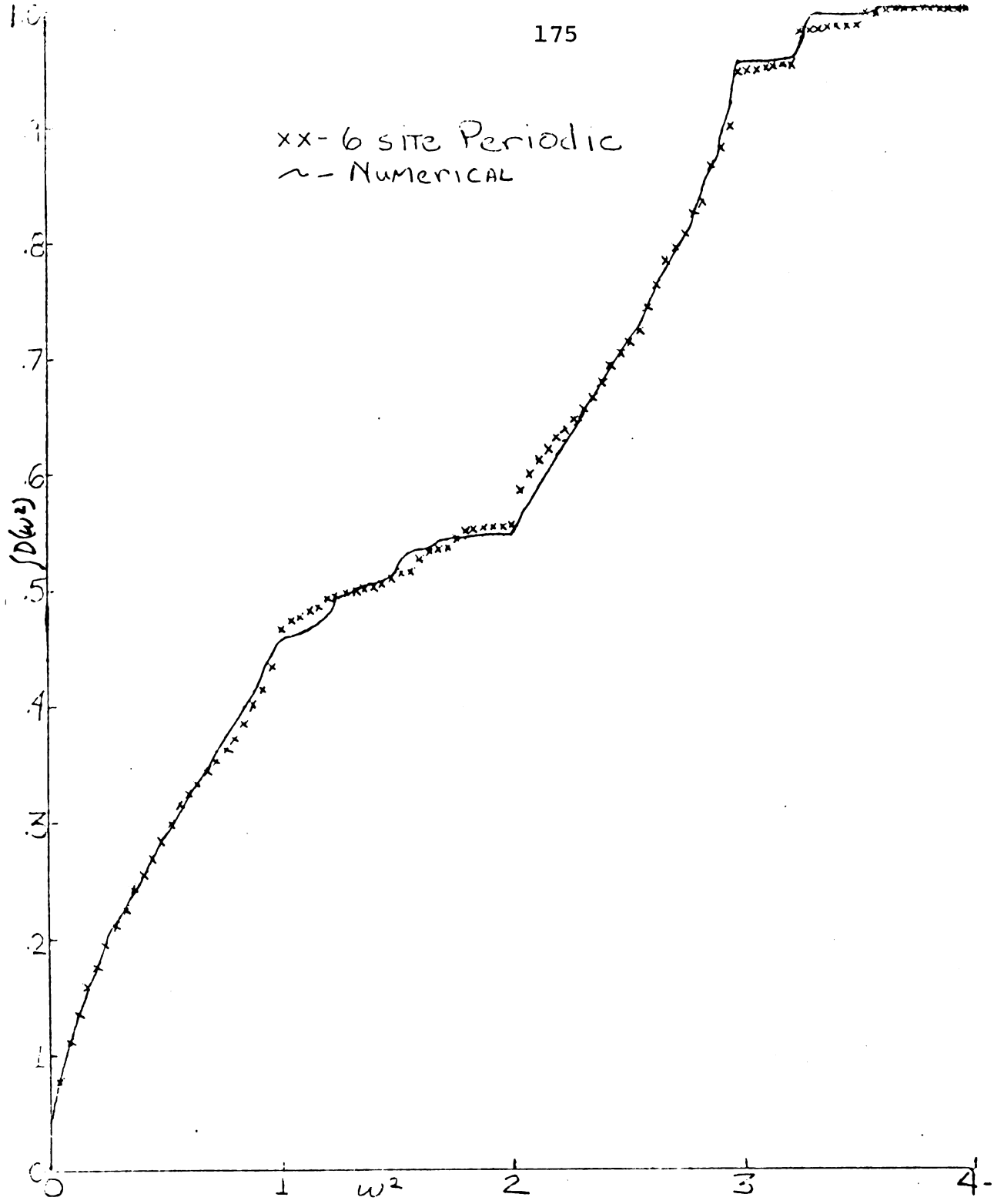

FIGURE 5.13.--Integrated density of states for C_d=.5, $P_{d,d}$=.1 generated by a 6 site periodically extended cluster.

interacts with identical clusters, clearly an unphysical assumption. An ideal cluster approach would allow a given cluster to interact with all other possible clusters throughout the entire chain. In practice however, such a calculation is impossible and therefore we now consider a theory in which the cluster interacts with an effective medium of identical average clusters. By including, in an average way, the interactions among different types of clusters we remove the unphysical singularities of the periodically extended cluster method, while retaining the short-range correlations among atomic vibrations, which is the virtue of the above cluster methods. Clearly there must be some optimum way to chose the effective medium; in the work which follows we shall show how the effective medium can be chosen in a self-consistent way. First we shall review some of the history of self-consistent effective medium approaches to scattering theory. Then we shall introduce the so called single-site Coherent Potential Approximation (CPA) and finally we shall consider the cluster CPA and apply it to our problem.

Lax[60] examined the many body problem in terms of multiple scattering theory. Lax used the method of self consistent fields. This method assumes that a wave is emitted by each scatterer of an amount and directionality determined by the field incident on the scatterer. The

incident field is the effective field which includes the effects of all other scatterers. In other words, the effective field is composed of the waves emitted by all other scatterers. Although a self consistent solution is often difficult to obtain, the solution will contain all orders of scattering. Ten years later in 1961, Langer,[61] recognizing that a phonon in a disordered system can be treated as a wave scattered at lattice sites, attempted to calculate the density of states of a one-dimensional harmonic random chain with no force constant changes. In the scattering wave formalism, the Green's function has the interpretation of the phonon propagator. Langer reasoned that in a random system any site is as likely to be occupied by a host or defect as any other site and that for the density of states or other quantities directly calculable from the propagator a configuration averaged phonon propagator is needed instead of the propagator for one possible configuration of atoms. The averaged crystal will possess the same symmetry as the monatomic chain where we have placed a self consistent mass on each lattice site. Langer reiterated the Dyson equation (5.40a) in a k space representation where the perfect chain Green's function is site diagonal. He, then, took the configuration average of each term of the series. By diagramatic arguments he extracted from each term all single particle scattering. He was able to

solve the self consistent problem where only single particle or two particle multiple scattering occurred. In each case, the singularity at the top of the host band was reduced from a square root singularity to a fourth root singularity. The density of states was not an analytically continuous function as one would expect.

Davies and Langer[61] were able to write a self consistent equation to all orders in scattering, simply by replacing certain unperturbed propagators in their expansion for the self energy with the final propagator for which they were solving. The physical reasoning for this replacement however was unclear. Davies and Langer were not able to solve their equation for all concentrations of defects. They, however, found a solution for small C_d. The solution had the bad feature that as concentration C_d increased, one can obtain a finite density of states in regions forbidden even to the light mass chain, a completely unphysical result.

Taylor[63] and Soven[64], on a suggestion from Lax, reformulated the self-consistent scattering problem for the phonon and electron problems, respectively. We will present the basic theoretical structure of the theory in text with the specific details of Taylor's single site self-consistent method left to Appendix H.

First, we define a number of different Green's functions.

(1) $\underline{\underline{P}} = (\underline{\underline{M}}\omega^2 - \underline{\underline{\phi}})^{-1}$, the Green's function of the perfect monatomic chain.

(2) $\underline{\underline{G}} = (\underline{\underline{M}}\omega^2 - \underline{\underline{\phi}} - \underline{\underline{C}})^{-1}$, the Green's function for a specific configuration of a disordered chain.

(3) $\langle \underline{\underline{G}} \rangle \equiv \bar{\underline{\underline{G}}} = (\underline{\underline{M}}\omega^2 - \underline{\underline{\phi}} - \underline{\underline{\Sigma}})^{-1}$, the configuration averaged Green's function for the disordered lattice. (We use both a bar and <> to indicate configuration averages.) $\bar{G}$ has the symmetry of the perfect lattice. Σ is often called the self energy although for the phonon problem it is really a self consistent mass.

(4) $\underline{\underline{R}} = (\underline{\underline{M}}\omega^2 - \underline{\underline{\phi}} - \underline{\underline{\sigma}})^{-1}$ a reference Green's function displaying the periodicity of the perfect chain.

We define the scattering matrix, $\underline{\underline{T}}$ by

$$\underline{\underline{G}} = \underline{\underline{R}} + \underline{\underline{R}}\,\underline{\underline{T}}\,\underline{\underline{R}} \tag{5.40}$$

Using the definitions of G and R we have

$$\underline{\underline{R}}^{-1} + \underline{\underline{\sigma}} = \underline{\underline{M}}\omega^2 - \underline{\underline{\phi}} = \underline{\underline{G}}^{-1} + \underline{\underline{C}}$$

$$\text{or} \quad \underline{\underline{G}} = \underline{\underline{R}} + \underline{\underline{R}}(\underline{\underline{C}} - \underline{\underline{\sigma}})\underline{\underline{G}} \tag{5.41}$$

Substituting Equation (5.40) in (5.41), we get

$$(\underline{\underline{C}} - \underline{\underline{\sigma}}) = \underline{\underline{T}}(\underline{\underline{1}} + \underline{\underline{R}}\,\underline{\underline{T}})^{-1} \tag{5.42}$$

For the mass defect problem $\underline{\underline{C}}$ is site diagonal and so is $\underline{\underline{g}}$ by definition. We expand T and $\underline{\underline{C}}-\underline{\underline{g}}$ in terms of a site representation

$$\underline{\underline{T}} = \sum_{\ell} \underline{\underline{T}}_{\ell} \tag{5.43}$$

$$\underline{\underline{C}}-\underline{\underline{g}} \equiv \sum_{\ell} \underline{\underline{V}}_{\ell} \tag{5.44}$$

It is important to understand Equations (5.43) and (5.44). Where as $\underline{\underline{T}}$ and and $(\underline{\underline{C}}-\underline{\underline{g}})$ are diagonal matrices with all diagonal elements non-zero, the matrices $\underline{\underline{T}}_{\ell}$ and $\underline{\underline{V}}_{\ell}$ are zero except at diagonal site ℓ. For example,

$$\underline{\underline{T}}_{\ell} = \begin{pmatrix} 0 & & & & & \\ & 0 & & & & \\ & & 0 & & 0 & \\ & & & \boxed{T_{\ell}} & & \\ & & & 0 & & \\ & & 0 & & & 0 \end{pmatrix} \tag{5.45}$$

whereas

$$\underline{\underline{T}} = \begin{pmatrix} T_1 & & & & & \\ & \ddots & & & & \\ & & 0 & & & \\ & & & T_{\ell} & & \\ & & & & T_{\ell+1} & \\ & & & 0 & & \\ & & & & & \ddots \\ & & & & & & T_N \end{pmatrix} \tag{5.46}$$

Substituting Equations (5.43) and (5.44) into (5.42) we get

$$\sum_{\ell} \underline{\underline{V}}_{\ell} = \sum_{\ell} \underline{\underline{T}}_{\ell} \left(\underline{\underline{1}}+\underline{\underline{R}}\sum_{\ell'}\underline{\underline{T}}_{\ell'}\right)^{-1}$$

Equating terms in ℓ, we get

$$\underline{\underline{T}}_{\ell} = \underline{\underline{V}}_{\ell} \left(\underline{\underline{1}}+\underline{\underline{R}}\sum_{\ell'}\underline{\underline{T}}_{\ell'}\right) \tag{5.47}$$

Removing the term $\ell'=\ell$ from the summation and solving for T_{ℓ} , we get

$$\underline{\underline{T}}_{\ell} = \left(\underline{\underline{1}}-\underline{\underline{V}}_{\ell}\underline{\underline{R}}\right)^{-1}\underline{\underline{V}}_{\ell}\left(\underline{\underline{1}}+\underline{\underline{R}}\sum_{\ell'\neq\ell}\underline{\underline{T}}_{\ell'}\right) \tag{5.48}$$

We now define the single site scattering matrix

$$\underline{\underline{t}}_{\ell} = \left(\underline{\underline{1}}-\underline{\underline{V}}_{\ell}\underline{\underline{R}}\right)^{-1} \underline{\underline{V}}_{\ell} \tag{5.49}$$

Even though $\underline{\underline{R}}$ has all elements possibly non zero, $\underline{\underline{t}}_{\ell}$ has only one matrix element, that at (ℓ,ℓ). Substituting (5.49) into (5.48) we get

$$\underline{\underline{T}}_{\ell} = \underline{\underline{t}}_{\ell} \left(\underline{\underline{1}}+\underline{\underline{R}}\sum_{\ell'\neq\ell}\underline{\underline{T}}_{\ell'}\right) \tag{5.50}$$

Finally, taking the configuration average we get

$$\langle\underline{\underline{T}}_{\ell}\rangle = \langle\underline{\underline{t}}_{\ell}\left(\underline{\underline{1}}+\underline{\underline{R}}\sum_{\ell'\neq\ell}\underline{\underline{T}}_{\ell'}\right)\rangle \tag{5.51}$$

The theory is exact to this point. The configuration average of the RHS of Equation (5.51) requires the solution of the full NxN matrix for a chain of length, N.

The single site approximation decouples the configuration average into

$$\langle \underline{\underline{T}}_\ell \rangle = \langle \underline{\underline{t}}_\ell \rangle (1+\underline{\underline{R}}_\ell \sum_{\ell' \neq \ell} \langle \underline{\underline{T}}_{\ell'} \rangle) \tag{5.52}$$

where we have in effect made an error of

$$\langle \underline{\underline{t}}_\ell \underline{\underline{R}}_\ell \sum_{\ell' \neq \ell} (\underline{\underline{T}}_{\ell'} - \langle \underline{\underline{T}}_{\ell'} \rangle) \rangle . \tag{5.53}$$

The first Equation (5.52) describes the average effective wave seen by the ℓ^{th} ion while the second Equation (5.53) describes fluctuations in the effective wave.[65] Neglecting the terms in (5.53) means that we neglect all correlations between scattering on different sites and consequently cannot see the effects of short range order between sites.

If we add the $\ell'=\ell$ term back into the RHS of Equation (5.52) we get

$$\langle \underline{\underline{T}}_\ell \rangle = \langle \underline{\underline{t}}_\ell \rangle \ (\underline{\underline{1}}+\underline{\underline{R}}\langle \underline{\underline{T}} \rangle) - \langle \underline{\underline{t}}_\ell \rangle \underline{\underline{R}} \langle \underline{\underline{T}}_\ell \rangle$$

$$\langle \underline{\underline{T}}_\ell \rangle = (\underline{\underline{1}}+\langle \underline{\underline{t}}_\ell \rangle \underline{\underline{R}})^{-1} \langle \underline{\underline{t}}_\ell \rangle (\underline{\underline{1}}+\underline{\underline{R}}\langle T \rangle) \tag{5.54}$$

Since from Equation (5.43),

$$\langle \underline{\underline{T}} \rangle = \sum_\ell \langle \underline{\underline{T}}_\ell \rangle , \tag{5.55}$$

we can sum Equation (5.54) over ℓ getting

$$\langle \underline{\underline{T}} \rangle = \sum_\ell (\underline{\underline{1}}+\langle \underline{\underline{t}}_\ell \rangle \underline{\underline{R}})^{-1} \langle \underline{\underline{t}}_\ell \rangle (\underline{\underline{1}}+\underline{\underline{R}}\langle \underline{\underline{T}} \rangle) \tag{5.56}$$

Using the definitions of the reference Green's function and the configuration averaged Green's function, we have

$$\underline{\underline{R}}^{-1} + \underline{\underline{\sigma}} = \bar{\underline{\underline{G}}}^{-1} + \underline{\underline{\Sigma}}$$

$$\text{or} \quad \bar{\underline{\underline{G}}} = \underline{\underline{R}} + \underline{\underline{R}}(\underline{\underline{\Sigma}} - \underline{\underline{\sigma}})\bar{\underline{\underline{G}}} \tag{5.57}$$

Configuration averaging Equation (5.58), we get

$$\langle \underline{\underline{G}} \rangle = \bar{\underline{\underline{G}}} = \underline{\underline{R}} + \underline{\underline{R}} \langle \underline{\underline{T}} \rangle \underline{\underline{R}} \tag{5.58}$$

Substituting Equation (5.58) into (5.57) yields

$$(\underline{\underline{\Sigma}} - \underline{\underline{\sigma}}) = \langle \underline{\underline{T}} \rangle (\underline{\underline{1}} + \underline{\underline{R}} \langle \underline{\underline{T}} \rangle)^{-1} \tag{5.59}$$

Using Equation (5.56), this reduces to

$$\underline{\underline{\Sigma}} - \underline{\underline{\sigma}} = \sum_{\ell} (1 + \langle \underline{\underline{t}}_{\ell} \rangle \underline{\underline{R}})^{-1} \langle \underline{\underline{t}}_{\ell} \rangle \tag{5.60}$$

In site representation, we have

$$\underline{\underline{\Sigma}}_{\ell} = \underline{\underline{\sigma}}_{\ell} + (1 + \langle \underline{\underline{t}}_{\ell} \rangle \underline{\underline{R}})^{-1} \langle \underline{\underline{t}}_{\ell} \rangle \tag{5.61}$$

The single site approximation has resulted in a scattering expression in terms of the single site t matrices t_{ℓ}. It includes in an approximate way all scatterings apart from that at site ℓ. Self-consistency is achieved by asserting that on the average the remaining scattering, by t_{ℓ}, be zero. Therefore $\bar{t}_{\ell}=0$.

For this case, we see by Equation (5.56) that $\langle \underline{\underline{T}} \rangle = 0$ and $\bar{\underline{\underline{G}}} = \underline{\underline{R}}$ and $\underline{\underline{\Sigma}} = \underline{\underline{g}}$. This approximation is also called the coherent potential approximation (CPA). Setting the configuration average Green's function equal to the reference Green's function requires a self consistent solution to the configuration average of Equation (5.49), where $\underline{\underline{R}} = (\underline{\underline{P}}^{-1} - \underline{\underline{g}})^{-1}$. We show this calculation in Appendix H. For this single site CPA we can also obtain CPA self-consistency by reiteration. The procedure is as follows.

(1) initially take $\underline{\underline{g}} = 0$

(2) calculate $\underline{\underline{R}} = (\underline{\underline{P}}^{-1} - \underline{\underline{g}})^{-1}$

(3) calculate $\langle \underline{\underline{t}}_\ell \rangle$ using Equation (5.49)

(4) calculate $\underline{\underline{\Sigma}}$ from Equation (5.61)

(5) set $\underline{\underline{g}} = \underline{\underline{\Sigma}}$ and start over at step (2).

We reiterate until $\langle \underline{\underline{t}}_\ell \rangle$ becomes as small as desired.

The only real complication in the procedure is finding $\underline{\underline{R}}$, which is non-trivial because $\underline{\underline{P}}^{-1}$ is finite over the entire matrix. We use the method of matrix inversion described in Appendix E. The explicit calculation is done in Appendix H.

In the corresponding electron problem the configuration averaged density of states is simply given by the imaginary part of the trace of the configuration averaged Green's function. In the phonon case, the configuration averaged density of states is given by

$$\bar{D}(\omega^2) = \frac{1}{sN\pi} \text{ Im Tr } (\overline{\underline{\underline{MG}}}) \tag{5.62}$$

where we used Equation (5.19).

Therefore we will have to get an expression for the configuration average of $\underline{\underline{MG}}$. First we have, in site representation,

$$\langle \underline{\underline{MG}} \rangle = \overline{\underline{\underline{MG}}} = \sum_{\delta,\ell} x^{\delta} \underline{\underline{M}}_{\ell}^{\delta} \underline{\underline{G}}_{\ell}^{\delta} \tag{5.63}$$

where x^{δ} is the concentration of constituent δ, of mass M_{ℓ}^{δ} and G_{ℓ}^{δ} is the conditionally configuration averaged Green's function when we require that there be an atom of type δ on site ℓ.

The Green's function for the disordered system satisfies the Dyson equation

$$\underline{\underline{G}} = \underline{\underline{P}} + \underline{\underline{P}}\underline{\underline{C}}\underline{\underline{G}}$$

which we configuration average to yield

$$\bar{\underline{\underline{G}}} = \underline{\underline{P}} + \underline{\underline{P}}\overline{\underline{\underline{C}}\underline{\underline{G}}} = \underline{\underline{P}} + \underline{\underline{P}} \sum_{\delta,\ell} x^{\delta} \underline{\underline{C}}_{\ell}^{\delta} \underline{\underline{G}}_{\ell}^{\delta} \tag{5.64}$$

where $\underline{\underline{C}}_{\ell}^{\delta} = (\underline{\underline{M}} - \underline{\underline{M}}^{\delta})\omega^2$

Therefore

$$\bar{\underline{\underline{G}}} = \underline{\underline{P}} + \underline{\underline{P}}\ \underline{\underline{M}}\ \omega^2 \sum_{\delta,\ell} x^{\delta} \underline{\underline{G}}_{\ell}^{\delta} - \underline{\underline{P}}\omega^2 \sum_{\delta,\ell} x^{\delta} \underline{\underline{M}}_{\ell}^{\delta} \underline{\underline{G}}_{\ell}^{\delta}$$

Since $\sum_{\delta,\ell} x^{\delta} \underline{\underline{G}}_{\ell}^{\delta} = \bar{\underline{\underline{G}}}$, we can solve for $\overline{\underline{\underline{MG}}}$ in Equation (5.63) getting

$$\sum_{\delta \ell} x^{\delta} \underline{\underline{M}}_{\ell}^{\delta} \underline{\underline{G}}_{\ell}^{\delta} = \underline{\underline{M}}\bar{\underline{\underline{G}}} - (\underline{\underline{P}}^{-1}\bar{\underline{\underline{G}}} + \underline{\underline{I}})\omega^{-2}$$

since $\bar{\underline{\underline{G}}} = (\underline{\underline{P}}^{-1} - \underline{\underline{\Sigma}})^{-1}$, $\underline{\underline{P}}^{-1}\bar{\underline{\underline{G}}} - \underline{\underline{I}} = \underline{\underline{\Sigma}}\bar{\underline{\underline{G}}}$

and

$$\overline{\underline{\underline{MG}}} = (\underline{\underline{M}} - \underline{\underline{\Sigma}}/\omega^2)\bar{\underline{\underline{G}}} \tag{5.65}$$

where $\underline{\underline{M}}$ is the mass matrix of the perfect chain and $\underline{\underline{\Sigma}}=\underline{\underline{g}}$. For the single site self consistent theory, the site representation of most of these quantities are scalars. The reason we have kept the full matrix notation will become apparent in the next few pages. From Equation (5.65) we see in the phonon case, the parameter $\Sigma/\omega^2=\sigma/\omega^2$ plays the part of a frequency dependent complex effective mass i.e.

$$\overline{\underline{\underline{MG}}} = \tilde{\underline{\underline{M}}}\,\bar{\underline{\underline{G}}} \text{ where } \tilde{\underline{\underline{M}}} = (\underline{\underline{M}} - \underline{\underline{\Sigma}}/\omega^2)$$

By using the single site approximation we are neglecting all correlations between scatterings on different sites no matter how close together those different sites may be. All scatterings are either multiple scattering from a single site or else they are scatterings from an effective medium. Such an approximation might be alright if all modes were so localized that there was no overlap between them, but as we have seen from the plots of localization of the eigenstates, there is appreciable overlap of the modes even at rather high frequencies. The

advantage of a cluster calculation is that local correlations between scatterings from different but close sites can be exactly included.

An obvious generalization of the single site approximation is to consider each site in the above formalism as a cluster. The site representation becomes a cluster representation. Again we neglect correlations in multiple scattering between clusters. We can however introduce short-range order in the cluster and treat all scattering in the cluster correctly. In most general form, the self consistent parameter $\underline{\underline{g}}$ becomes block diagonal with each block the size of a cluster.

$$\underline{\underline{g}} = \begin{pmatrix} \boxed{\sigma_{I}} & & & & & \\ & \boxed{\sigma_{II}} & & & & \\ & & \boxed{\sigma_{III}} & & & \\ & & & \boxed{\sigma_{IV}} & & \\ & & & & \boxed{\sigma_{V}} & \\ & & & & & \ddots \end{pmatrix} \tag{5.66}$$

where cluster σ's (Roman numerals ℓ) are

$$\sigma_{\ell} = \begin{pmatrix} \sigma_1 & \sigma_2 & \sigma_3 \\ \sigma_4 & \sigma_5 & \sigma_6 \\ \sigma_7 & \sigma_8 & \sigma_9 \end{pmatrix} \tag{5.67}$$

for a three site cluster.

Butler[67] has noted that by symmetry $\sigma_1=\sigma_9$, $\sigma_4=\sigma_8=\sigma_2=\sigma_6$ and $\sigma_3=\sigma_7$; there are only 5 independent parameters instead of 9. The reference Green's function R has the same periodicity as the self energy σ. A characteristic block ℓ of R can be found by using the methods of Appendix E for the inversion of an infinite tridiagonal matrix. Introducing the symbol

$$\beta = m\omega^2-2\gamma \tag{5.68}$$

we have

$$R_\ell \equiv (P^{-1}-\sigma)^{-1}_\ell = \begin{pmatrix} \beta-A-\sigma_1 & \gamma-\sigma_2 & -\sigma_3 \\ \gamma-\sigma_2 & \beta-\sigma_5 & \gamma-\sigma_2 \\ -\sigma_3 & \gamma-\sigma_2 & \beta-B-\sigma_1 \end{pmatrix}^{-1} \tag{5.69}$$

where A and B are the boundary diagonal elements of matrices as follows

$$A/\gamma^2 = \begin{pmatrix} \beta-A-\sigma_1 & \gamma-\sigma_2 & -\sigma_3 \\ \gamma-\sigma_2 & \beta-\sigma_5 & \gamma-\sigma_2 \\ -\sigma_3 & \gamma-\sigma_2 & \beta-\sigma_1 \end{pmatrix}^{-1}_{3,3} \tag{5.70}$$

$$B/\gamma^2 = \begin{pmatrix} \beta-\sigma_1 & \gamma-\sigma_2 & -\sigma_3 \\ \gamma-\sigma_2 & \beta-\sigma_5 & -\sigma_2 \\ -\sigma_3 & \gamma-\sigma_2 & \beta-\sigma_1-B \end{pmatrix}^{-1}_{1,1} \tag{5.71}$$

from which we see A=B.

Now generally Equation (5.69) may be rewritten

$$\underline{\underline{R}}^{-1} = \underline{\underline{P}}^{-1} - \sum_{\ell} \underline{\underline{g}}_{\ell}. \tag{5.72}$$

As before, $\underline{\underline{g}}_{\ell}$ takes on the interpretation of a matrix as big as the entire system but with all elements, apart from those in the cluster ℓ, equal to zero whenever $\underline{\underline{g}}_{\ell}$ appears as a term in an equation for matrices with the dimension of the whole system. The Green's function describing a system with a cluster of configuration δ embedded in an average medium with the periodicity of the cluster has the following form within the space of that cluster, ℓ.

$$(G_{\ell}^{\delta})^{-1} = (R_{\ell})^{-1} - (C_{\ell}^{\delta} - \sigma_{\ell}) \tag{5.73}$$

Performing the same algebra as above for inversion we find

$$(G_{\ell}^{\delta})^{-1} = \begin{pmatrix} \beta_1 - A & \gamma & 0 \\ \gamma & \beta_2 & \gamma \\ 0 & \gamma & \beta_3 - A \end{pmatrix}. \tag{5.74}$$

$$\text{where } \beta_i \equiv m_i \omega^2 - 2\gamma \equiv m(1-\varepsilon_i)\omega^2 - 2\gamma \tag{5.75}$$

The coherent potential self-consistency now takes the form

$$\underline{\underline{\bar{G}}} = \underline{\underline{R}} \tag{5.76}$$

or, because the set of configurations over which we average gives $\bar{G}$ the translational periodicity of R,

$$\overline{\underline{\underline{G}}_{\ell}^{\delta}} = \sum_{\delta} x^{\delta} \underline{\underline{G}}_{\ell}^{\delta} = \underline{\underline{R}}_{\ell}. \tag{5.77}$$

We can show that this equation for the self consistency can be obtained by setting the average cluster t matrix to zero.

Proof: $$0 = \langle \underline{\underline{t}}_{\ell} \rangle = \sum_{\delta} x^{\delta} [\underline{\underline{1}} - (\underline{\underline{C}}_{\ell}^{\delta} - \underline{\underline{\sigma}}_{\ell}) \underline{\underline{R}}_{\ell}]^{-1} (\underline{\underline{C}}_{\ell}^{\delta} - \underline{\underline{\sigma}}_{\ell}) \tag{5.78}$$

$$0 = \sum_{\delta} x^{\delta} \{\underline{\underline{1}} - [\underline{\underline{R}}_{\ell}^{-1} - (\underline{\underline{G}}_{\ell}^{\delta})^{-1}] \underline{\underline{R}}_{\ell}\}^{-1} [\underline{\underline{R}}_{\ell}^{-1} - (\underline{\underline{G}}_{\ell}^{\delta})^{-1}] \tag{5.79}$$

or, multiplying by $\underline{\underline{R}}_{\ell}$ on right and left

$$\sum_{\delta} x^{\delta} [\underline{\underline{G}}_{\ell}^{\delta} - \underline{\underline{R}}_{\ell}] \tag{5.80}$$

or, since $$\sum_{\delta} x^{\delta} = 1, \tag{5.81}$$

$$\underline{\underline{R}}_{\ell} = \underline{\underline{\bar{G}}}_{\ell} \qquad \text{Q.E.D.}$$

which is the same as Equation (5.77).

A possible self-consistent procedure now becomes clear. One must numerically set the configuration average of the inverse of the matrix in Equation (5.74) equal to the matrix for R_{ℓ} in Equation (5.69).

We have attempted to use the reiterative solution of the CPA given above for the three site cluster. However, we have never achieved convergence beyond $\omega^2=1.52$. As long as the off-diagonal elements of $\underline{\underline{\sigma}}$ remain small, convergence is rapid; however as the values of σ_3 and σ_2 become as large as σ_1 and σ_5, the number of steps to

convergence increases. In fact as we approach $\omega^2=1.50$ rapid changes begin to occur in the off diagonal elements of σ.

Because this method of solution failed we use the ideas recently developed by Butler[68] for a cluster treatment of the electron problem. In fact, Equations (5.69) through (5.74) are in Butler's form and make the following argument perspicuous.

Because matrix A is a function only of the external medium it is independent of configuration. Therefore once we have determined A we have essentially determined $\bar{G}$ or R. The statement $\bar{G}_\ell=R_\ell$ is, of course, the statement that corresponding matrix elements are equal. Therefore if we can find an equation including A for one of the elements of this matrix equality and if we can solve that equation for A then we have found the desired configuration averaged Green's function. We have such an equation in the equality of the boundary elements, say the (1,1) elements.

From Equation (5.69) we find

$$R_\ell(11,\omega^2) = [\beta-\sigma_1-\underline{U}\underline{\underline{Y}}\underline{U}^T]^{-1} \tag{5.82}$$

where, for the 3-site cluster

$$\underline{U} = (\gamma-\sigma_2, -\sigma_3);\ U^T \text{ is the transpose of U} \tag{5.83}$$

and

$$\underline{\underline{Y}} = \begin{pmatrix} \beta-\sigma_5 & \gamma-\sigma_2 \\ \gamma-\sigma_2 & \beta-\sigma_1-A \end{pmatrix} \tag{5.84}$$

Similarly from Equation (5.70)

$$A = \gamma^2[\beta-\sigma_1-\underline{U}\underline{\underline{Y}}\underline{U}^T]^{-1} \tag{5.85}$$

Inserting Equation (5.85) into Equation (5.82) we find an equation for R(1,1) involving A only.

$$R_\ell(1,1,\omega^2) = A[\gamma^2-A^2]^{-1} \tag{5.86}$$

Next we can write the (1,1) element of $\overline{G_\ell^\delta}$ as a continued fraction, and finally set

$$\sum_{\beta_1\beta_2\beta_3} P(\beta_1,\beta_2,\beta_3)G_\ell(11,\beta_1\beta_2\beta_3,\omega^2) = R_\ell(11,\omega^2) \tag{5.87}$$

where the probability P of various configurations may include short-range order within the cluster, and β_i may take on two values.

$$\beta_i = \begin{cases} m_d\omega^2-2\gamma=m(1-\varepsilon)\omega^2-2\gamma \\ m_h\omega^2-2\gamma=m\omega^2-2\gamma=\beta \end{cases} \tag{5.88}$$

we obtain

$$\frac{A}{\gamma^2-A^2} = \sum_{\beta_i} P(\beta_1\beta_2\beta_3)\{\beta_1-A-\gamma^2[\beta_2-\gamma^2(\beta_3-A)^{-1}]^{-1}\}^{-1} \tag{5.89}$$

for our final self-consistent equation. The result may be easily extended to clusters larger than the 3x3 which we have used here for illustrating; on the right hand side

of Equation (5.89) one simply extends the continued fraction to as many sites as desired.

Before discussing the numerical solution of Equation (5.89) we will make one more point. The cluster CPA which we have solved above is akin to the periodically extended cluster method discussed previously. The difference, of course, is that in the cluster CPA a given cluster can interact, though in an average way, with all other possible clusters, whereas the periodically extended model includes only configurations in which a given cluster can interact with other identical clusters. This point raises the question of whether there is a CPA analogy to the embedded cluster method. Indeed such an analogy motivated Butler's recent work on the cluster problem. We show below the CPA analogy to the embedded cluster method and then, following Butler, we show that if one makes the so-called Self-Consistent Boundary Site (SCBS) approximation one obtains the same result for $\bar{G}_{\ell}^{\delta}$ as we obtained above in the cluster CPA, namely Equation (5.89).

For this analogy we embed a n(=3)xn cluster with a particular configuration δ, with probability $P(\beta_1\beta_2\ldots\beta_n)$, in an average chain. The average chain has the periodicity of the host lattice with atoms of average self-consistent complex mass $m(1-\bar{\varepsilon})$. Using the symbol

$$\bar{\beta} \equiv m(1-\bar{\varepsilon})\omega^2 - 2\gamma \tag{5.90}$$

and as before in Equation (5.75)

$$\beta_i \equiv m_i\omega^2 - 2\gamma$$

The inverse Green's function for a 3-site system is

$$(G^{\delta})^{-1} = \begin{pmatrix} \ddots & & & & & & \\ \gamma & \bar{\beta} & \gamma & & & & \\ & \gamma & \bar{\beta} & \gamma & & & \\ & & \gamma & \boxed{\begin{matrix} \beta_1 & \gamma & 0 \\ \gamma & \beta_2 & \gamma \\ 0 & \gamma & \beta_3 \end{matrix}} & & & \\ & & & \gamma & \bar{\beta} & \gamma & \\ & & & & \gamma & \bar{\beta} & \gamma \\ & & & & & & \ddots \end{pmatrix} \tag{5.91}$$

Within the cluster ℓ then

$$G_{\ell}^{\delta} = \begin{pmatrix} \beta_1 - A' & \gamma & 0 \\ \gamma & \beta_2 & \gamma \\ 0 & \gamma & \beta_3 - A' \end{pmatrix}^{-1} \tag{5.92}$$

$$\text{where } A'/\gamma^2 = (\bar{\beta} - A')^{-1} \tag{5.93}$$

We determine the self consistent mass $\bar{\varepsilon}$ as Butler did by requiring the configuration averaged boundary element of the Green's function (here $\overline{G_{11}}$) to be equal to the

diagonal element of the reference Green's function, which is

$$R_{11} = (P^{-1}-\sigma)^{-1} = (\bar{\beta}-2A')^{-1} \tag{5.94}$$

where the constant A' on taking the inverse is the same as in Equation (5.93). From Equations (5.92) and (5.94) we have

$$R_{11} = A'(\gamma^2-A'^2)^{-1}. \tag{5.95}$$

Writing G^{δ}_{11} in continued fractions the self consistency condition is

$$\frac{A'}{(\gamma^2-A'^2)} = \sum_{\beta_1\beta_2\beta_3} P(\beta_1\beta_2\beta_3)\{\beta_1-A'-\gamma^2[\beta_2-\gamma^2(\beta_3-A')^{-1}]^{-1}\}^{-1} \tag{5.96}$$

The important point is that because $\bar{G}_{11}$ for the embedded cluster analogy is the same function of its argument (A') as is $\bar{G}_{11}$ for the cluster CPA, the self consistency equations for A' and for A in the two methods (5.89) and (5.96) are the same. Therefore the two methods are identical!

We now return to a solution of the cluster CPA. We can reiterate Equation (5.87) or the n site equivalent to the correct solution. We have found in practice that we always get convergence to the correct solution by initially picking A to be the value of the perfect

monatomic heavy chain plus a small imaginary part.

$$A = \frac{\beta - \sqrt{\beta^2 - 4\gamma^2}}{2} \tag{5.97}$$

We used the Newton-Raphson method[69] to speed the convergence of the reiteration to A. The procedure takes 3 to 6 reiterations in general to give A to .01% error. For the 3-site cluster, for example, we have the error F on any reiteration

$$F(A) = A/(\gamma^2 - A^2) - \sum_{\delta} x^{\delta} \{\beta_1 - A - \gamma^2 [\beta_2 - \gamma^2 (\beta_3 - A)^{-1}]^{-1}\}^{-1} \tag{5.98}$$

and $F'(A) = dF/dA$

$$= \frac{A^2+\gamma^2}{(\gamma^2 - A^2)^2} - \sum_{\delta} x^{\delta} \{\beta_1 - A - \gamma^2 [\beta_2 - \gamma^2 (\beta_3 - A)^{-1}]^{-1}\}^{-2}$$

$$x\{1 + \gamma^4 [\beta_2 - \gamma^2 (\beta_3 - A)^{-1}]^{-2} [\beta_3 - A]^{-2}\} \tag{5.99}$$

Therefore the value of A chosen for the (J+1)-th iteration is

$$A_{J+1} = A_J - F(A_J)/F'(A_J) \tag{5.100}$$

There is one difficulty to overcome in calculating the density of states for the phonon problem which does not arise in the electron problem where the density is the trace of the configuration averaged Green's function.

For the phonon problem

$$D(\omega^2) = -\frac{1}{N\pi} \text{ tr Im } \overline{MG} = -\frac{1}{n\pi} \text{ Im tr } \overline{M_\ell G_\ell} \tag{5.101}$$

where the last expression is that for an n site cluster. In fact we calculated several candidates for the density of states. In order of increasing agreement with experimental spectra we tried

$$1. \quad D(\omega^2) = -\frac{1}{\pi} \text{Im tr } m(1-\bar{\epsilon})R_{11} \tag{5.102}$$

an expression involving only the effective medium in the embedded cluster analogy. We solved for $\bar{\epsilon}$ by using Equation (5.93) in the form

$$(1-\bar{\epsilon})m\omega^2 = A+2\gamma+\gamma^2/A \tag{5.103}$$

The result for $D(\omega^2)$ was a series of broad flat peaks rather similar to the results of the single site CPA as one might have expected.

$$2. \quad D(\omega^2) = -\frac{1}{\pi} \text{Im} \sum_{\delta} x^{\delta} m_1^{\delta} G_{11}^{\delta} \tag{5.104}$$

a configuration average of the boundary site expression. Because the configuration average of the boundary site Green's function is R_{11} this result for the density of states closely resembles the result (1).

3. We calculated the full cluster trace indicated by Equation (5.101)

$$\begin{aligned} D(\omega^2) &= -\frac{1}{\pi n} \text{Im tr} \sum_{\delta} x^{\delta} M^{\delta} G^{\delta} \\ &= -\frac{1}{\pi n} \text{Im} \sum_{i} \sum_{\delta} x^{\delta} m_i^{\delta} G_{ii}^{\delta}(\omega^2) \end{aligned} \tag{5.105}$$

This spectrum showed some of the peaks of the experimental spectrum but the peaks are rather broad and do not have their centers at the right frequencies. Actually our test of this expression was only for the 3-site cluster. This method has the advantage that as the number of sites in the cluster gets larger the method is guaranteed to improve, a statement which cannot be made for our final and best expression for D.

$$4.\quad D(\omega^2) = -\frac{1}{\pi}\,\mathrm{Im}\sum_{\delta} x^{\delta} m^{\delta}_{cc} G^{\delta}_{cc} \tag{5.106}$$

where cc indicates central site. For the 3-site cluster, for example

$$D(\omega^2) = -\frac{1}{\pi}\,\mathrm{Im}\sum_{\delta} x^{\delta} m(1-\varepsilon_2)\{\beta_2-\gamma^2[\beta_1-A]^{-1}-\gamma^2[\beta_3-A]^{-1}\}^{-1} \tag{5.107}$$

We now show computations of the density of states using the central site expression (5.106).

Figure (5.14) shows the density of states for C_d=.1 random for the 1, 3 and 7 site self-consistent clusters. All three cluster sizes reproduce the host band structure reasonably well. The seven site cluster is able to display some of the fine structure in this region. In the impurity band, the improvement with increasing cluster size is remarkable. The seven site cluster reproduces the total density of states with great precision. The superimposed 10,000 unit numerical chain probably shows some small spurious structure in the host band due to its short length.

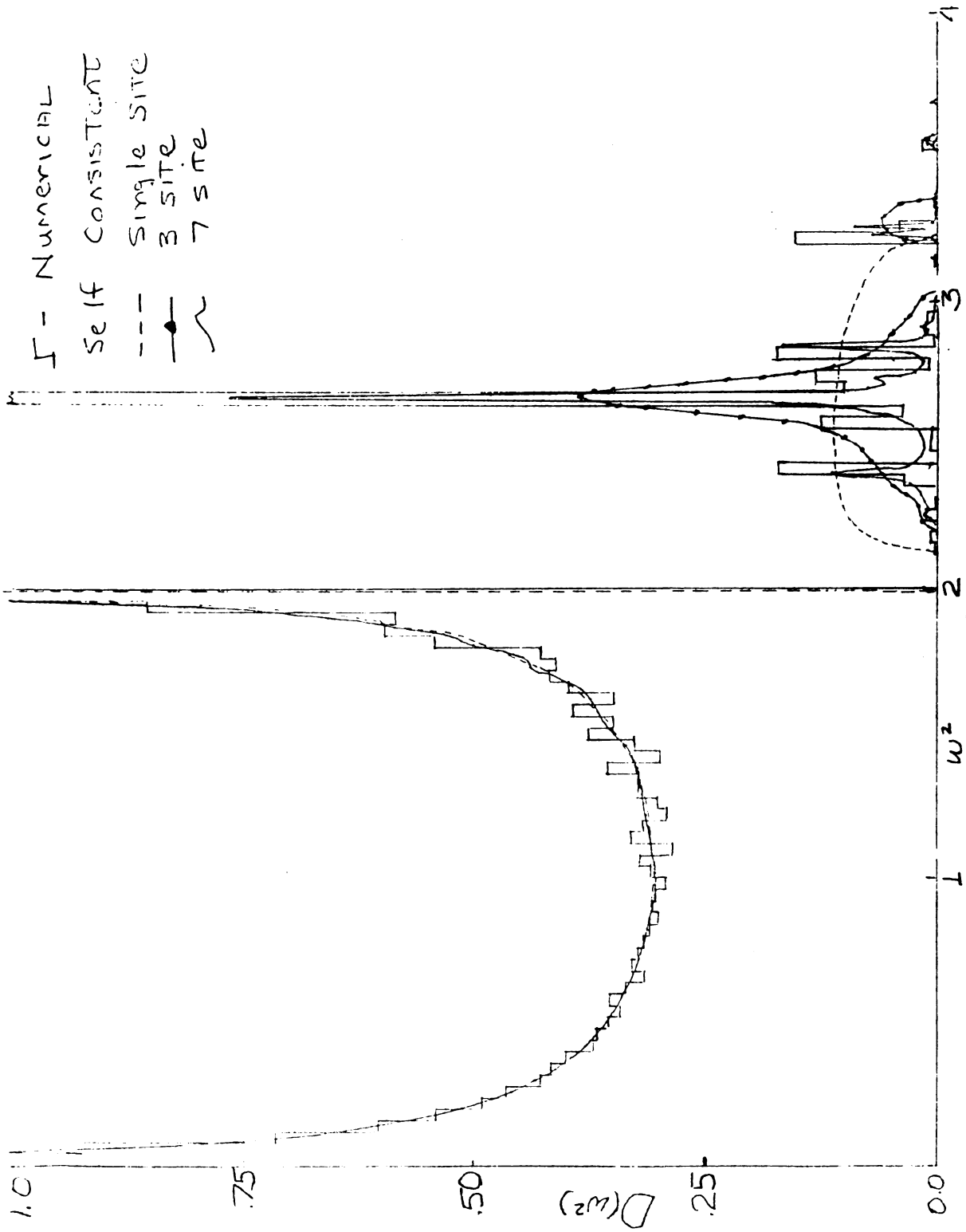

FIGURE 5.14.--Density of states for C_d=.1 random generated by self consistent 1, 3 and 7 site clusters.

Figure (5.15) shows the density of states for C_d=.5 random for the 1, 3 and 7 site self-consistent clusters. The single site CPA completely fails to reproduce any structure. With the three site cluster, we pick up some of the major structure. The seven site cluster again does a remarkable job recreating both host and impurity band structure.

Figure (5.16) shows the single and 7 site self-consistent cluster for C_d=.9. The superimposed numerical plot is for 10,000 atoms which probably includes some small spurious structure. The seven site cluster progressively shows more structure with increasing ω^2.

Figures (5.17) and (5.18) are for C_d=.5, $P_{d,d}$=.1 and .9 respectively. For these two cases with very high degrees of order, the seven site self-consistent cluster does not give as good a frequency spectrum as in the random cases. Both figures however, display all the correct peaks in the frequency spectrum. They also seem to display structure apparently absent from the experimental spectra. We say apparently because the experimental grid is Δ=.04 whereas the cluster grid is .01333. The spectra show that a cluster size of seven is not large enough to adequately reproduce the respective spectra with high degrees of short-range order.

As a final comparison of the 7 site self consistent cluster with experimental results we compare the

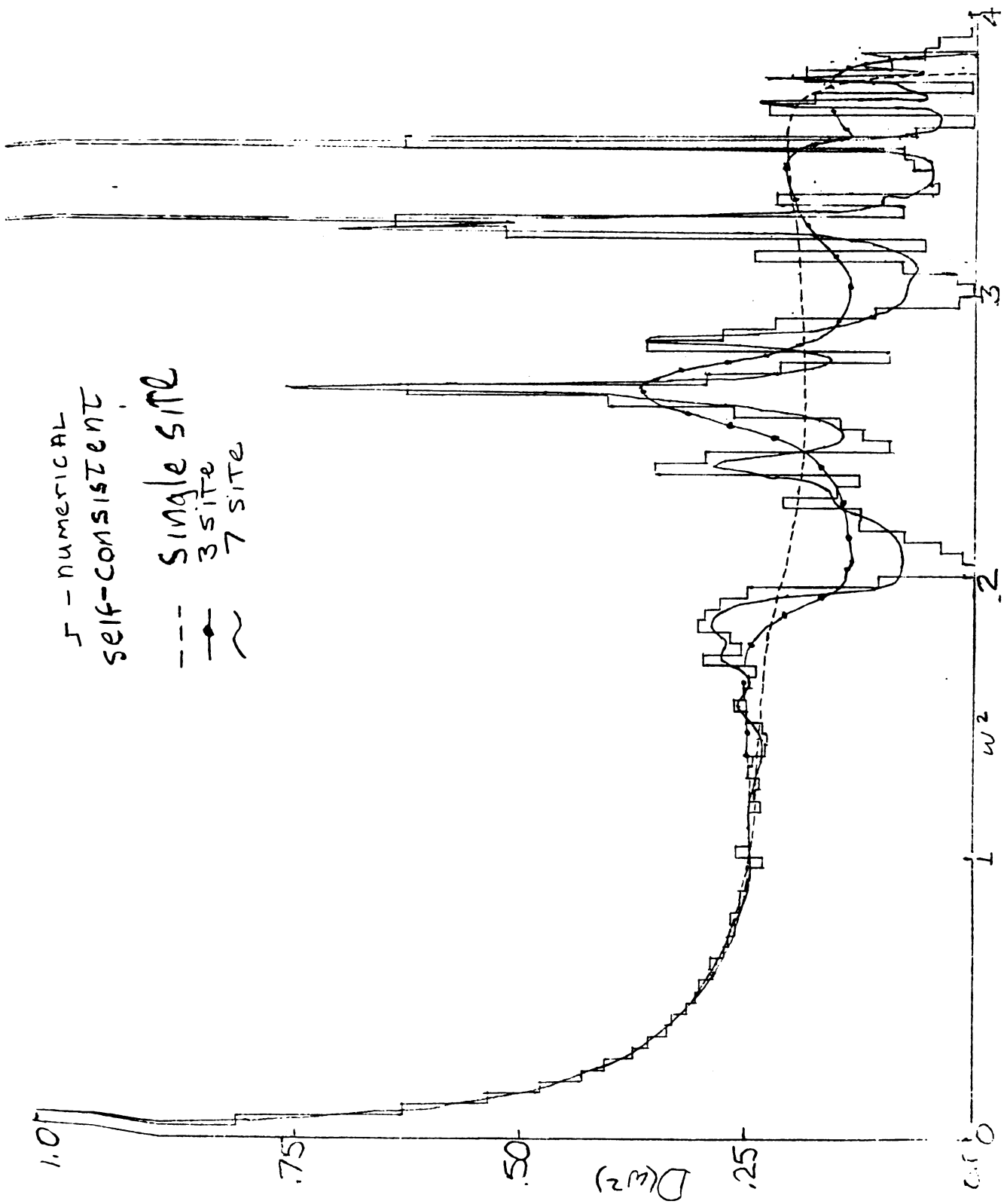

FIGURE 5.15.--Density of states for C_d=.5 random generated by self consistent 1, 3 and 7 site clusters.

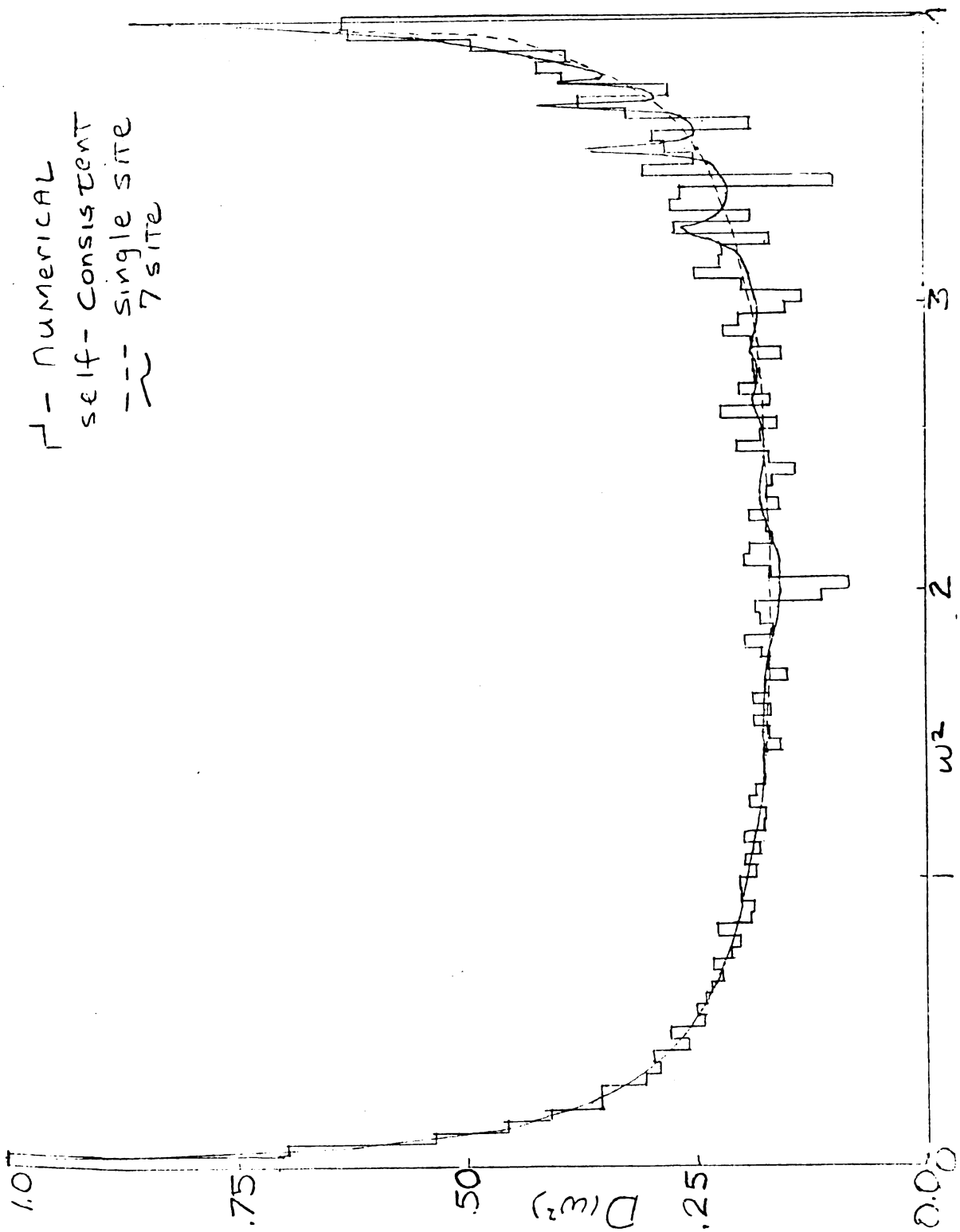

FIGURE 5.16.--Density of states for C_d=.9 random generated by self consistent 1, and 7 site clusters.

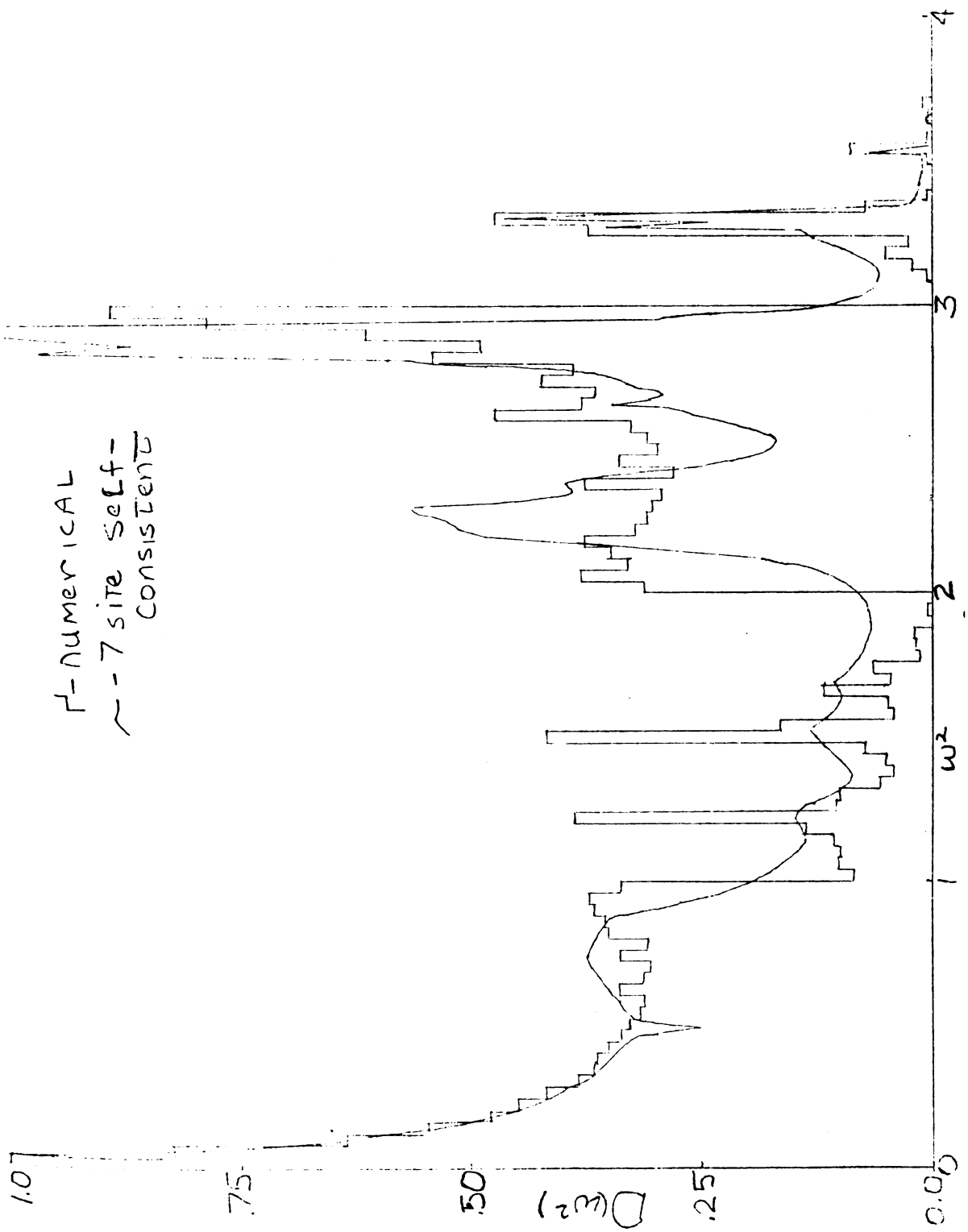

FIGURE 5.17.--Density of states for C_d=.5, $P_{d,d}$=.1 generated by a 7 site self consistent cluster.

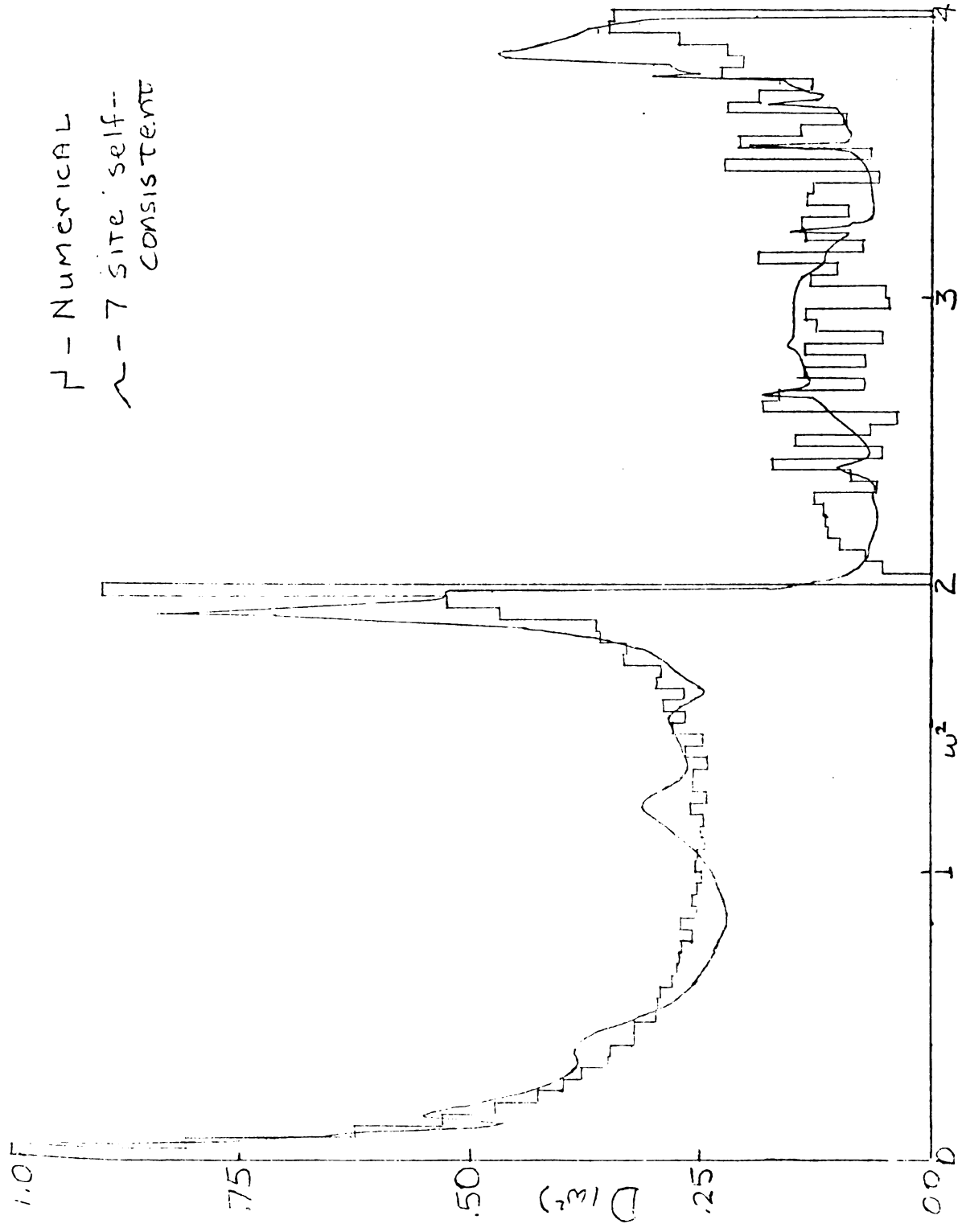

FIGURE 5.18.--Density of states for C_d=.5, $P_{d,d}$=.9, generated by a 7 site self consistent cluster.

integrated density of states for C_d=.5, random and $P_{d,d}$=.1. Figure (5.19) gives the comparison between the experimental and analytic cluster results for C_d=.5 random. From this figure we see that at each sharp peak in the spectrum we lose some contribution to the density of state for the seven-site self-consistent cluster. The total integrated density of states is .975 instead of one. When we compensate for this, the curves of the numerical and 7 site cluster integrated density of states coincidence until ω^2>1.9, whereupon the deviations between the two are about 1% at most. Figure (5.20) shows the comparitive integrated density of states for C_d=.5 $P_{d,d}$=.1. Although significant deviations between the two curves are evident, the maximum relative errors are of the order of 5-6%.

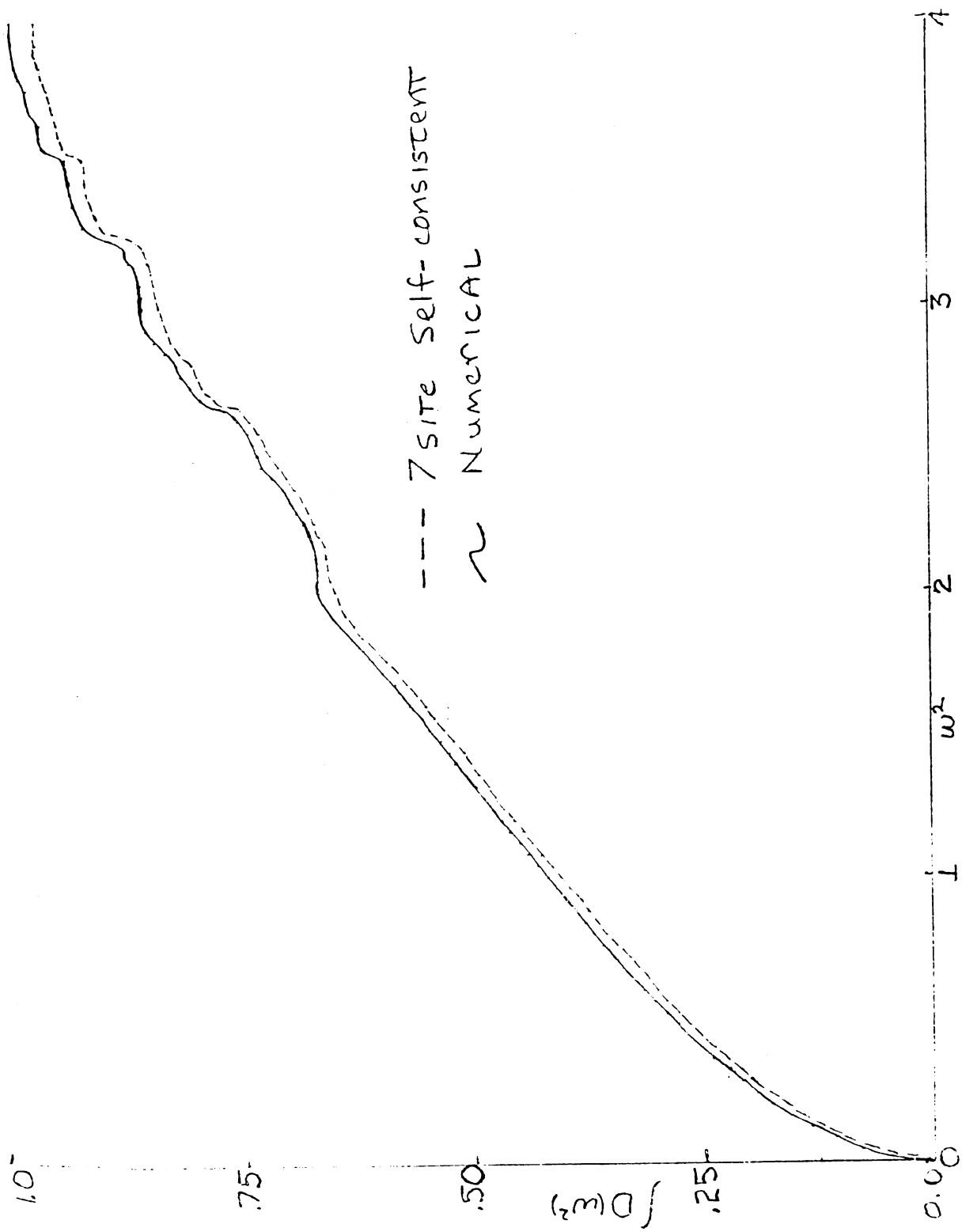

FIGURE 5.19.--Integrated density of states for C_d=.5 random generated by a 7 site self consistent cluster.

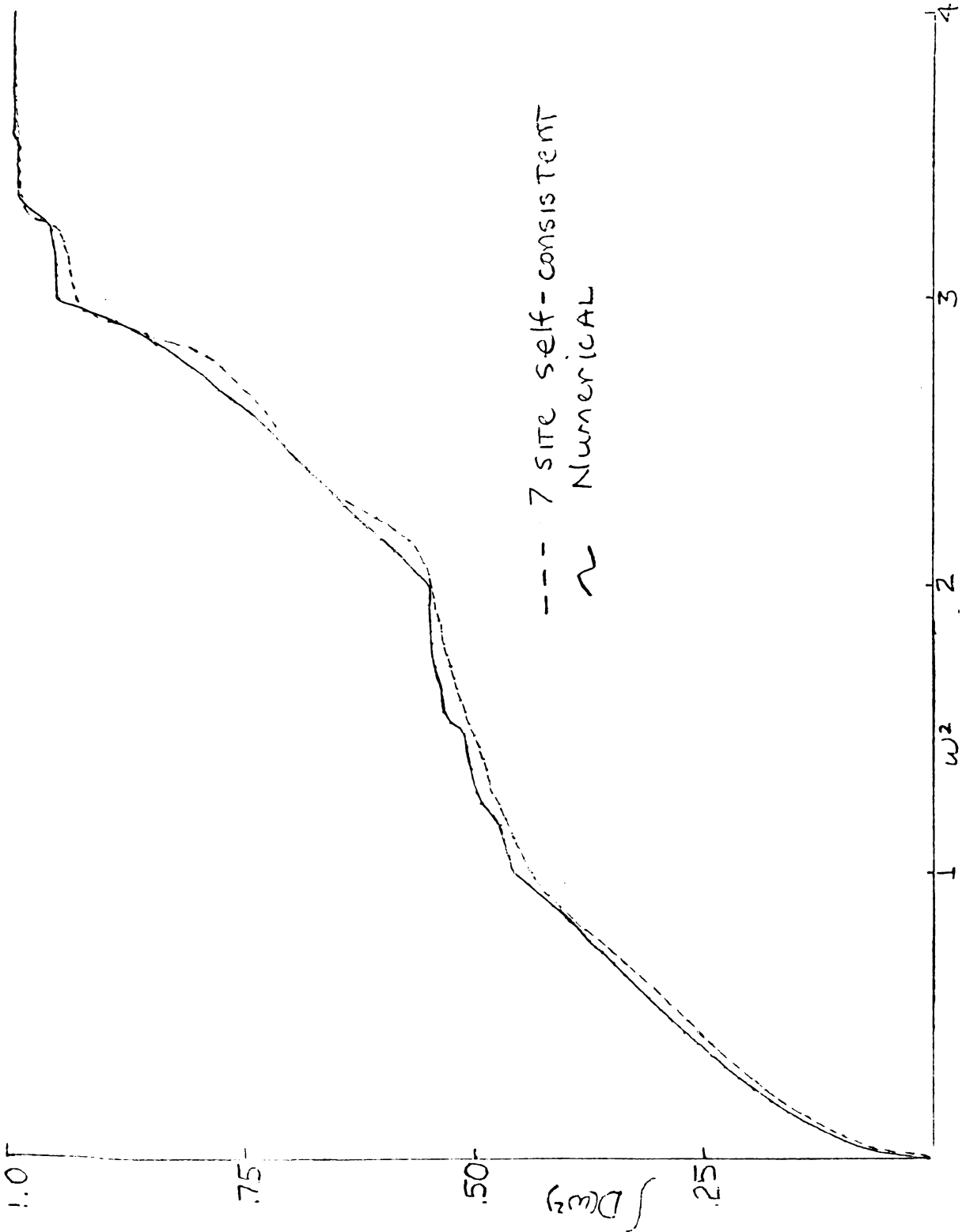

FIGURE 5.20.--Integrated density of states for C_d=.5, $P_{d,d}$=.1 generated by a 7 site self consistent cluster.

CHAPTER VI

CONCLUSIONS

In the preceding chapters, we have examined the vibrations of disordered binary chains in the harmonic approximation with all force constants equal. First, we numerically examined the phonon density of states of binary chains with short-range order generated by ergodic Markov theory. The theory was used to introduce nearest-neighbor and next-nearest-neighbor correlations. When these spectra were compared to the spectra of random binary chains with the same concentrations of constituents, we found marked differences between them.

For the first order Markov chain we found that the pair correlation functions were particularly simple and that all higher order correlation functions can be expressed in terms of the pair correlation functions. The second order Markov chain theory does not give as simple pair correlation functions and higher order correlation functions cannot be expressed in terms of the pair correlation functions. With the second order Markov chain, we demonstrated that a pair of quite different frequency spectra can be obtained from chains with identical pair correlation functions.

In addition to numerically examining the frequency spectra (eigenvalues) we also numerically examined the eigenvectors of the chains. We were able to characterize both the extent of appreciable amplitude of the eigenvectors and the exponential decay rate away from this region of appreciable amplitude. We found that both localization parameters displayed the same general functional relationship versus ω^2; however, they were found to have quite different functional trends at certain points. Short-range order was found to radically change localization values and their functional relationship to ω^2.

Theoretically, we constructed the phonon frequency spectrum in three ways. First, we embedded impurity clusters of size n in a host chain. We found the impurity modes arising from each possible cluster configuration. We were then able to reconstruct the impurity band spectrum by properly weighting all possible n-site configurations. This reconstruction conclusively demonstrated the origins of the peaks and peak broadening in the impurity band. It did not give any information on the host band region of the frequency spectrum. The embedded cluster theory was found to be highly dependent on defect concentration, working much more satisfactorily below $C_d=0.5$ than above this value.

The second approach for reconstructing the phonon density of states involved periodically extending the n-site cluster throughout the chain. We then obtained both analytically and numerically the spectrum of each possible periodic chain with an n-site basis. The density of states was reconstructed by averaging over all possible spectra. Unlike the embedded cluster calculation, this method reconstructed the whole frequency spectrum. For a six-site periodic system, the impurity band was reasonably accurate independent of concentration and short-range order. The host band region, although generally correctly reproduced, possessed many discontinuities which are not physically realistic.

The third method for reconstructing the frequency spectrum was a self-consistent Green's function method. An n-site cluster was embedded in a self-consistent host medium. The self-consistency was determined by requiring the phonon scattering from the configuration average of all clusters to be zero. We were able to simplify greatly the problem by using the self-consistent boundary site theory developed by Butler for the one-dimensional electron problem. We were able to prove that Butler's approach gives zero scattering from the configuration averaged cluster. For the seven-site self-consistent cluster we obtained excellent agreement with the numerically generated density of states for all concentrations in

random systems. When high degrees of short-range order were introduced, general agreement was obtained. By correlating the cluster size, localization lengths, and goodness of frequency spectrum, we were able to predict the approximate size of the cluster required to give agreement with numerical results.

REFERENCES

REFERENCES

1. P. Debye, Ann. Physik. 39,789(1912).
2. M. Born and T. von Karman, Z. Physik 13,297(1912).
3. J. Baden-Powell, View of the Undulatory Theory as Applied to the Dispersion of Light, London, 1841.
4. W. R. Hamilton, Mathematical Papers, Cambridge University Press, London and New York, 1940.
5. W. Thomson, Lord Kelvin, Popular Lectures and Addresses, 2nd ed., Macmillan, London 1891.
6. W. Thomson, Lord Kelvin, Baltimore Lectures on Molecular Dynamics and the Wave Theory of Light, Clay, London, 1904.
7. Lord Rayleigh, Theory of Sound, Vol. I, Dover, New York, 1945.
8. R. L. Bjork, Phys. Rev. 105,456(1957).
9. A. A. Maradudin, E. W. Montroll, G. H. Weiss, and I. P. Ipatova, Theory of Lattice Dynamics in the Harmonic Approximation, second edition, Academic Press, New York and London, 1971.
10. A. Einstein, Ann. Physik 22,180(1907).
11. I. M. Lifshitz, J. Physics, USSR 7,215(1943); USSR 7,249(1943); USSR 8,89(1944).

12. E. W. Montroll and R. B. Potts, Phys. Rev. 100,525(1955); Phys. Rev. 102,72(1956).

13. F. J. Dyson, Phys. Rev. 92,1331(1953).

14. H. Schmidt, Phys. Rev. 105,425(1957).

15. R. L. Agacy, Proc. Phys. Soc. 83,591(1964).

16. A. A. Maradudin, P. Mazur, E. W. Montroll, G. H. Weiss, Rev. Mod. Phys. 30,175(1958).

17. C. Domb, A. A. Maradudin, E. W. Montroll, G. H. Weiss, Phys. Rev. 115,18(1959); Phys. Rev. 115,24(1959).

18. P. Dean, Proc. Phys. Soc. 73,413(1959); Proc. Roy. Soc. A254,507(1960); Proc. Roy. Soc. A260,263(1961); Proc. Phys. Soc. 84,727(1964).

19. P. Dean, M. D. Bacon, Proc. Phys. Soc. 81,642(1963); Proc. Roy. Soc. A283,64(1965); P. Dean, J. L. Martin, M. D. Bacon, Proc. Phys. Soc. 80,174(1962).

20. D. Payton, W. M. Visscher, Phys. Rev. 154,802(1967); Phys. Rev. 156,1032(1967); Phys. Rev. 175,1201(1968).

21. P. Dean, Rev. Mod. Phys. 44,127(1972).

22. W. Ledermann, Proc. Roy. Soc. 182A,362(1944).

23. G. Tammann, Z. Anorg Chem. 107,1(1919).

24. C. H. Johansson, J. O. Linde, Ann. Physik. 78,439(1925).

25. W. L. Bragg, E. J. Williams, Proc. Roy. Soc. A145,699 (1934); Proc. Roy Soc. A151,540(1935).

26. H. Bethe, Proc. Roy. Soc. A150,552(1935).

27. J. M. Cowley, Phys. Rev. 77,669(1950); 120,1648(1960); 138,A1384(1965).

28. S. C. Moss, P. C. Clapp, Phys. Rev. 142,418(1966).

29. S. C. Moss, Journal of Applied Phys. 35,3547(1964).

30. T. Muto, Y. Takagi, Solid State Physics, Vol. 1, ed. F. Seitz, D. Turnbill, Academic Press, Inc., New York, 1955.

31. W. M. Hartmann, Phys. Rev. 172,677(1968).

32. D. W. Taylor, Private communication to W. M. Hartmann, 1967.

33. D. N. Payton, III, Los Alamos Report No. 3510 (Thesis), Dynamics of Disordered Harmonic Lattices (1966).

34. C. T. Papatriantafillou, Preprint.

35. E. Parzen, Stochastic Processes, Holden-Day, Inc., 1964. This was the primary reference for this work.

36. J. G. Kemeny, J. L. Snell, Finite Markov Chains, D. Van Nostrand Co., Inc., Princeton, New Jersey, 1969.

37. A. T. Bharucha-Reid, Elements of the Theory of Markov Processes and Their Applications, McGraw Hill Book Co., New York, 1960.

38. P. Billingsley, Statistical Methods in Markov Chains, Address presented on August 23, 1960 at Stanford meetings of the Institute of Mathematical Statistics.

39. I. S. Gradshteyn, I. M. Ryshik, Table of Integrals Series and Products, Academic Press, New York and London, 1965.

40. J. Hori, Prog. Theor. Phys. 31,940(1964).

41. H. Matsuda, E. Teramoto, Prog. Theor. Physics 34,314(1965).

42. J. H. Wilkinson, The Algebraic Eigenvalue Problem, Clarendon Press, Oxford, 1965.

43. H. B. Rosenstock, R. E. McGill, Jour. Math. Phys. 3,200(1962).

44. R. H. Dicke, J. P. Wittke, Introduction to Quantum Mechanics, Addison-Wesley Publishing Co., Inc., Reading, Mass. (1961).

45. N. F. Mott and W. D. Twose, Adv. in Phys. 10,107 (1961).

46. R. E. Borland, Proc. Roy. Soc. (London) A274,529(1963).

47. P. W. Anderson, Phys. Rev. 109,1492(1958).

48. P. Dean, Proc. Phys. Soc. (London) 84,727(1964). Also, reprinted in Lieb-Mattis, Mathematical Physics in One Dimension, Academic Press, New York and London, 1966.

49. E. N. Economou, M. H. Cohen, Phys. Rev. B4,396(1971).

50. J. Hori, Spectra Properties of Disordered Chains and Lattices, Pergamon Press, New York, 1958. Hori and co-authors have an extensive list of publications in Japanese journals, references are given in this text.

51. P. L. Taylor, Physics Letters 18,13(1965).

52. H. Matsuda and K. Ishii, Supp. Prog. Theor. Phys. 45,56(1970). This supplement is on the theory of lattice dynamics. Also, Matsuda and coworkers have extensive publications in this field, a good bibliography is given in the Hori reference.

53. W. Visscher, Prog. Theor. Physics 46,729(1971).

54. D. J. Thouless, Journ. of Non-Crys. Solids 8-10, 461(1972).

55. R. L. Bush, Phys. Rev. B6,1182(1972).

56. A. P. Roberts, R. E. Makinson, Proc. Phys. Soc. 79, 630(1962).

57. R. J. Elliott and D. W. Taylor, Proc. Phys. Soc. 83, 189(1964).

58. D. N. Zubarev, Sov. Phys. USPEKHI , 3,320(1960).

59. W. H. Butler, W. Kohn, Jour. of Research of Nat. Bur. of Standards 74A,443(1970).

60. M. Lax, Rev. Mod. Phys. 23,287(1951).

61. J. S. Langer, J. Math. Phys. 2,584(1961).

62. R. W. Davies and J. S. Langer, Phys. Rev. 131,163(1963).

63. D. W. Taylor, Phys. Rev. 156,1017(1967).

64. P. Soven, Phys. Rev. 156,809(1967).

65. L. Schwartz, F. Browers, A. V. Vedyayev and H. Ehrenreich, Phys. Rev. B4,3383(1971).

66. W. H. Butler, Preprint.

67. D. D. McCrachen, W. S. Dorn, Numerical Methods and Fortran Programming, John Wiley and Sons, New York, 1964.

APPENDICES

APPENDIX A

NUMERICAL COMPUTATION OF EIGENVALUES OF CHAINS

To calculate the density of states (spectrum) of a linear chain of length N, we need to be able to calculate the eigenvalues of the eigenvalue Equation (2.3) in text. Rewriting Equation (2.3) as

$$(\underline{\underline{B}}-\underline{\underline{I}}\omega^2)\underline{X} = 0 \tag{A.1}$$

where

$$b_{ij} = \frac{2\gamma}{m_i}\,\delta_{i,j} \quad \frac{-\gamma}{\sqrt{m_i\, m_{i\pm1}}}\,\delta_{i,j\pm1}$$

$\underline{\underline{B}}$ is clearly a symmetric tridiagonal matrix. Now, we denote the principal minor of order r of $(\underline{\underline{B}}-\underline{\underline{I}}\omega^2)$ by $P_r(\omega^2)$. Letting $P_0(\omega^2)=1$, we can write a recursion relationship between these principal minors.

$$P_1(\omega^2) = \frac{2\gamma}{m_1} - \omega^2 \tag{A.2}$$

$$P_i(\omega^2) = (\frac{2\gamma}{m_i} -\omega^2)P_{i-1}(\omega^2) - (\frac{\gamma^2}{m_i m_{i-1}})P_{i-2}(\omega^2) \tag{A.3}$$

$$2 \leq i \leq N$$

The zeros of $P_r(\omega^2)$ are the eigenvalues of the leading principal submatrix of order r of $\underline{\underline{B}}$. We denote this submatrix by $\underline{\underline{B}}_r$. Since $\underline{\underline{B}}$ and $\underline{\underline{B}}_r$ are Hermitian their eigenvalues are all real. Now, we will show that eigenvalues of $\underline{\underline{B}}_r$ are separated in the strict sense from the

eigenvalues of $\underline{\underline{B}}_{r+1}$. The proof is by contradiction. Assume u as a zero of $P_r(u)$ and $P_{r-1}(u)$; then, using Equation (A.3), we have u is also a zero of $P_{r-2}(u)$ since $(\omega^2/m_i m_{i-1}) \neq 0$. Continuing this argument, we have u is a zero of $P_0(u)$ which is a contradiction of the definition of $P_0(u)$.

Because of the strict separation of zeros of the $\underline{\underline{B}}_r$'s, Given's was able to devise one of the most effective ways of determining the eigenvalues of a symmetric tridiagonal N by N matrix. The chain with periodic boundary conditions is not tridiagonal requiring a transformation to reduce it to tridiagonal form, whereas the chain with fixed boundary conditions is already tridiagonal.

> Theorem: Let the quantities $P_0(\omega^2)$, $P_1(\omega^2)$.... $P_N(\omega^2)$ be the principal minors of a symmetric tridiagonal matrix, evaluated for some value of ω^2; then $S(\omega^2)$, the number of agreements in sign of consecutive members of this sequence, is the number of eigenvalues of $\underline{\underline{B}}$ which are strictly greater than ω^2.

To apply this theorem we must find a way to determine a sign if $P_r(\omega^2)$ is exactly zero. If $P_r(\omega^2)=0$, then $P_r(\omega^2)$ is taken to have the opposite sign of $P_{r-1}(\omega^2)$.

The proof of the eigenvalue theorem is by induction. Assume that the number of agreements in sign $S_r(u)$, in the sequence $P_0(u), P_1(u) \ldots P_r(u)$ is the number of eigenvalues of $\underline{\underline{B}}_r$ which are greater than u. If we denote the eigenvalues of $\underline{\underline{B}}_r$ by $x_1, x_2 \ldots x_r$, then

$$x_1 > x_2 > x_3 > \ldots > x_s > u \geq x_{s+1} > x_{s+2} > \ldots > x_r \tag{A.4}$$

Next, the eigenvalues of $\underline{\underline{B}}_{r+1}$, we denote by $y_r, y_2 \ldots y_r$. Since the eigenvalues of $\underline{\underline{B}}_r$ and $\underline{\underline{B}}_{r+1}$ are separate in the strict sense, we have

$$y_1 > x_1 > y_2 > x_2 > \ldots > y_3 > x_s > y_{s+1} > x_{s+1} > \ldots y_r > x_r > y_{r+1}. \tag{A.5}$$

$\underline{\underline{B}}_{r+1}$, therefore, has s or s+1 eigenvalues greater than u. In terms of these eigenvalues the principle minors can easily be evaluated.

$$P_r(u) = \prod_{i=1}^{r} (x_i - u) \tag{A.6}$$

and

$$P_{r+1}(u) = \prod_{i=1}^{r+1} (y_i - u) \tag{A.7}$$

If no $x_j = u$ and no $y_j = u$, there are two cases to consider. If $y_{s+1} > u$, then $P_r(u)$ and $P_{r+1}(u)$ have the same sign and $S_{r+1}(u) = S_r(u) + 1$. If $y_{s+1} < u$, then $P_r(u)$ and $P_{r+1}(u)$ have opposite signs and $S_r(u) = S_{r+1}(u)$. Using the definition of sign of $P_r(u)$ when $x_s = u$ and $P_{r+1}(u)$ when

$y_{s+1}=u$ completes the proof. A sequence of principal minors, $P_0(\omega^2)$, $P_1(\omega^2)\ldots P_N(\omega^2)$ satisfying the above theorem is said to possess the Sturm sequence property.

For the linear chain, Rosenstock and McGill[43] have shown that the atomic displacements from equilibrium, $U_1, U_2, U_3 \ldots U_N$ form a Sturm sequence with initial conditions $U_0=0$ and $U_1=1$ where Equation (2.2) is rewritten as

$$U_{i+1} = (2 - \frac{m_i}{\gamma}\omega^2)U_i - U_{i-1} \qquad (A.8)$$

Since the Sturm sequence generated by Equation (A.8) requires either approximately one half the computer storage or one half the computing time of Equation (A.3), we have used Equation (A.8) for most of the spectra presented.

To determine the range of permissible eigenvalues of the matrix $\underline{\underline{B}}$ in Equation (A.1), we use the fact that the absolute value of all the eigenvalues of $\underline{\underline{B}}$ must be less than or equal to the infinite norm of $\underline{\underline{B}}$,[42] or

$$|\omega^2| \leq ||B||_\infty \qquad (A.9)$$

$$\text{where } ||B||_\infty = \operatorname{Max}_i \sum_{j=1}^{N} |b_{ij}|$$

For the linear chain

$$||B||_\infty = |-\frac{\gamma}{m_L}| + \frac{2\gamma}{m_L} + |-\frac{\gamma}{m_L}| = \frac{4\gamma}{m_L} \qquad (A.10)$$

where m_L is the lightest mass in the chain. For computational convenience we take $\frac{M_L}{\gamma}=1$; therefore, $|\omega^2|\leq 4$ sets bounds on the frequency spectra. We, also, know that physically ω must be real or $\omega^2\geq 0$. Therefore, the spectra of all chains must be in the interval $0\leq\omega^2\leq 4$. If we divide the interval into 100 equal parts each .04 wide, a reasonable histogram frequency spectrum is produced.

To calculate the eigenvector of a chain given in Appendix D, we will need to know individual eigenvalues to a considerable degree of precision. Any eigenvalue can be determined to any degree of precision by the method of bisection. First, we know that all eigenvalues must lie between 0.0 and 4.0. If we take $a_0=0$, and $b_0=4.$, then for the s step in the bisection we have

$$C_s = \tfrac{1}{2}(a_{s-1}+b_{s-1}) \tag{A.11}$$

where C_s is the midpoint of the interval (a_{s-1},b_{s-1}). Next, we compute the Sturm sequence with $\omega^2=C_s$ and determine $S(C_s)$. Suppose we are looking for ω_k^2, then if $S(C_s)\geq K$, then we take $a_s=C_s$ and $b_s=b_{s-1}$, and if $S(C_s)<K$, we take $a_s=a_{s-1}$ and $b_s=C_s$. By this method we can locate an eigenvalue ω_k^2 in p steps to be in an interval (a_p,b_p) of width $(b_0-a_0)/2^p = 4/2^p = 2^{2-p}$.

For implimentation of this procedure on a digital computer, the precision to which the computation is carried is important because of computer rounding errors. The

error in the bisection described above is $\frac{1}{2}(4/2^p)$ or 2^{1-p}. In addition, Wilkinson[42] has shown the computer error is $18.08/2^t$ where t is the binary precision to which the computation is carried. One significant fact is that the error is independent of the chain length. The total error is, therefore,

$$E_T = (18.08)2^{-t} + 2^{1-p} \qquad (A.12)$$

where p is the number of steps in the reiteration and t is the conputational binary precision.

For example, for computations on the UNIVAC 1108 single precision computations (27 binary bits) give a minimum error of 1.35×10^{-7} and double precision computations (60 binary bits) give a minimum error of 1.57×10^{-17}. To obtain errors of less than 10^{-8}, ($\sim 2^{-27}$) we must use double precision computations requiring $2^{-27} \geq 2^{1-p}$ or $p \geq 28$.

For each computation of the Sturm sequence there are of the order of 2N multiplications and subtractions. For each eigenvalue there are 2Np computations. To find all the eigenvalues requires $2N^2p$ computations by the method of bisection versus N^3 for most other methods. For N>2p, the method of bisection is favored.

The method of bisection must be carefully examined for the case of eigenvalues near zero and close eigenvalues. For eigenvalues near zero, the accuracy of the eigenvalue computed by bisection may be small. For example,

if $\omega_r^2 \simeq 10^{-4}$, single precision computation with errors of at least 1.35×10^{-7} will give less than three digit accuracy for ω_r^2. In double precision with p=28, the error is $\sim 10^{-8}$ or ω_r^2 is good to about four digit accuracy. For close eigenvalues, more than one eigenvalue may lie in the interval (a_p, b_p) of error. The eigenvector computations give indications of this trouble and are discussed in Appendix D.

APPENDIX B

MARKOV THEORY SUPPLEMENT

PROOF OF ERGODIC MARKOV CHAIN THEOREM

Theorem 1: An irreducible aperiodic recurrent Markov chain possesses a unique long run distribution. The long run distribution $\{\pi_k, k\epsilon C\}$ of an irreducible aperiodic recurrent Markov chain is the unique solution of

$$\pi_k = \sum_j \pi_j P_{j,k} \tag{B.1}$$

satisfying

$$\sum_k \pi_k = 1. \tag{B.2}$$

Recall that $P_{j,k}(n)$ is the n step transition probability to go from state j to k and $P_{j,k}=P_{j,k}(1)$.

To prove this theorem, a number of new quantities and additional theorems will have to be introduced. By analogy to Equation 3.35 for the conditional probability, $f_{j,k}$, of even visiting the state k, given the chain was in state j, we define the conditional probability $f_{j,k}(n)$ of the first passage from j to k occurring in exactly n steps.

$$f_{j,k}(n) = P[V_k(n) \,|\, X_o=j] \tag{B.3}$$

where for any state k and integer n=1,2,... we define chain segment, or set, V

$$V_k(n) = [X_n=k, X_m\neq k \text{ for } m=1,2,3...n-1]$$

Theorem 2: For any states j and k,

$$f_{j,k} = \sum_{n=1}^{\infty} f_{j,k}(n) \qquad (B.4)$$

Proof: Define

$V_k = [X_n = k \text{ for some } n > 0]$, then

V_k is the union of the sequence of disjoint sets

$$\{V_k(n), n=1,2,\ldots\}$$

$$f_{j,k} = P[V_k | X_o = j] = \sum_{n=1}^{\infty} P[V_k(n) | X_o = j] = \sum_{n=0}^{\infty} f_{j,k}(n)$$

Q.E.D.

The n-step transition probabilities $P_{j,k}(n)$ and the first passage probabilities $f_{j,k}(n)$ can now be related.

Theorem 3: For any states j and k and integer $n \geq 1$,

$$P_{j,k}(n) = \sum_{m=1}^{n} f_{j,k}(m) P_{k,k}(n-m) \qquad (B.5)$$

where we must logically have

$$P_{j,k}(0) = \delta_{j,k} \quad \text{(the Kronnecker delta)}$$

Proof:

$$P[X_n = k | X_o = j] = \sum_{m=1}^{n} P[X_n = k, X_m = k, X_q \neq k \text{ for } q = 1,2,\ldots m-1 | X_o = j]$$

$$= \sum_{m=1}^{n} P[X_n = k | X_m = k] P[X_m = k, X_q \neq k \text{ for } q = 1,2,\ldots m-1 | X_o = j]$$

$$P_{j,k}(n) = \sum_{m=1}^{n} P_{k,k}(n-m)\ f_{j,k}(m) \qquad \text{Q.E.D.}$$

In the step before the last one we multiplied the conditional probability that if m is in state k then n is state k by the probability that m is the first passage to state k to obtain the probability that both occur. Such a multiplication of probabilities is correct only if the probabilities are independent, which is not true for arbitrary chains but is true for Markov chains. Next, we can relate the conditional probability of ever visiting a state $f_{j,k}$ to the conditional probability of visiting the state an infinite number of times, $g_{j,k}$.

Theorem 4: For any states j and k

$$g_{k,k} = \lim_{n\to\infty} (f_{k,k})^n \tag{B.6}$$

and

$$g_{j,k} = f_{j,k}\ g_{k,k} \tag{B.7}$$

Proof of B.7: From Equation 3.36

$$g_{j,k} = P[N_k(\infty)=\infty \mid X_o=j]$$

$$= \sum_{n=1}^{\infty} P[N_k(\infty) - N_k(n)=\infty,\ X_n=k,\ X_q\neq k \text{ for}$$

$$q=1,2,\ldots n-1 \mid X_o=j]$$

$$= \sum_{n=1}^{\infty} P[N_k(\infty)-N_k(n)=\infty \mid X_n=k] \; x$$

$$P[X_n=k,\ X_q\neq k \text{ for } q=1,2,\ldots n-1 \mid X_o=j]$$

$$= \sum_{n=1}^{\infty} g_{k,k}\, f_{j,k}(n) = g_{k,k} \sum_{n=1}^{\infty} f_{j,k}(n)$$

by Theorem 2

$$g_{j,k} = g_{k,k}\, f_{j,k} \qquad \text{Q.E.D.}$$

Proof of (B.6):

For $n \geq 1$ look at

$$P[N_k(\infty) \geq n \mid X_o=k] =$$

$$= \sum_{m=1}^{\infty} P[N_k(\infty)-N_k(m) \geq n-1,\ X_m=k,\ X_q\neq k,\ \text{for } q=1,2,\ldots m-1 \mid X_o=k]$$

$$= \sum_{m=1}^{\infty} P[N_k(\infty)-N_k(m) \geq n-1 \mid X_m=k] \; x$$

$$P[X_m=k,\ X_q\neq k \text{ for } q=1,2,\ldots m-1 \mid X_o=k]$$

$$= \sum_{m=1}^{\infty} P[N_k(\infty) \geq n-1 \mid X_o=k]\, f_{k,k}(m)$$

$$= P[N_k(\infty) \geq n-1 \mid X_o=k]\, f_{k,k}$$

repeating this procedure n times

$$P[N_k(\infty) \geq n \mid X_o=k] = f_{k,k}^{n} \quad n \geq 1$$

therefore

$$P[N_k(\infty)=\infty \mid X_o=k] = \lim_{n\to\infty} P[N_k(\infty) \geq n \mid X_o=k]$$

$$= \lim_{n\to\infty} f_{k,k}^{n} \qquad \text{Q.E.D.}$$

From Theorem 4, since $0 \leq f_{kk} \leq 1$,

$$g_{k,k}=1 \text{ or } 0 \tag{B.8}$$

and

$$g_{k,k}=1 \text{ if and only if } f_{k,k}=1 \tag{B.9}$$

$$g_{k,k}=1 \text{ if and only if } f_{k,k}<1 \tag{B.10}$$

Theorem 5: For any state k,

$$f_{k,k}<1 \text{ if and only if } \sum_{n=1}^{\infty} P_{k,k}(n)<\infty \tag{B.11}$$

and

$$f_{k,k}=1 \text{ if and only if } \sum_{n=1}^{\infty} P_{k,k}(n)=\infty \tag{B.12}$$

Proof: To prove theorem 5, we need to perform a transformation on the transition probability and the conditional probability of first passage

$$P_{j,k}(Z) = \sum_{n=0}^{\infty} Z^n P_{j,k}(n)=\delta_{jk} + \sum_{n=1}^{\infty} Z^n P_{j,k}(n) \tag{B.13}$$

$$f_{j,k}(Z) = \sum_{n=1}^{\infty} Z^n f_{j,k}(n) \tag{B.14}$$

for $|Z|<1$

Next, take Equation B.5, multiply by Z^n and sum over n from one to infinity; we get

$$\sum_{n=1}^{\infty} Z^n P_{j,k}(n) = \sum_{n=1}^{\infty} Z^n \sum_{m=1}^{n} f_{j,k}(m) P_{k,k}(n-m)$$

interchanging the sumation on the RHS

$$P_{j,k}(Z)-\delta_{j,k} = \sum_{m=1}^{\infty} Z^m f_{j,k}(m) \sum_{n=m}^{\infty} Z^{n-m} P_{k,k}(n-m)$$

$$P_{j,k}(Z)-\delta_{jk} = f_{j,k}(Z)\ P_{k,k}(Z) \qquad \text{(B.15)}$$

From this

$$P_{k,k}(Z)-1 = f_{k,k}(Z)\ P_{k,k}(Z)$$

$$\text{or } f_{k,k}(Z) = 1 - \frac{1}{P_{k,k}(Z)} \qquad \text{(B.16)}$$

Next since $f_{k,k} = \sum_{n=1}^{\infty} f_{k,k}(n)$ (B.17)

$$\text{and } \lim_{Z\to 1^-} f_{k,k}(Z) = \sum_{n=1}^{\infty} f_{k,k}(n) \qquad \text{(B.18)}$$

$$\lim_{Z\to 1^-} P_{k,k}(Z) = \sum_{n=0}^{\infty} P_{k,k}(n) \qquad \text{(B.19)}$$

where 1^- is approaching one from less than one we have

$f_{k,k}<1$ iff $\sum_{n=1}^{\infty} f_{k,k}(n)<1$ from Equation B.17

$\sum_{n=1}^{\infty} f_{k,k}(n)<1$ iff $\lim_{Z\to 1^-} f_{k,k}(Z)<1$ from Equation B.18

$\lim_{Z\to 1^-} f_{k,k}(Z)<1$ iff $\lim_{Z\to 1^-} P_{k,k}(Z)<\infty$ from Equation B.16

$\lim_{Z\to 1^-} P_{k,k}(Z)<\infty$ iff $\sum_{n=0}^{\infty} P_{k,k}(n)<\infty$ from Equation B.19

similiarly

$$f_{k,k}=1 \text{ iff } \sum_{n=1}^{\infty} f_{k,k}(n)=1 \text{ iff } \lim_{Z\to 1^-} f_{k,k}(Z)=1$$

$$\text{iff } \lim_{Z\to 1^-} P_{k,k}(Z)=\infty \text{ iff } \sum_{n=0}^{\infty} P_{k,k}(n)=\infty \qquad \text{Q.E.D.}$$

Next, we define the expected first passage length

$$m_{k,k} = \sum_{n=1}^{\infty} n\, f_{k,k}(n) \tag{B.20}$$

Theorem 6: Let k be a state such that

$$f_{k,k}=1 \text{ and } m_{k,k}<\infty, \text{ then } \lim_{n\to\infty} \frac{1}{n} \sum_{m=1}^{\infty} P_{k,k}(m) = \frac{1}{m_{k,k}} \tag{B.21}$$

and for any state j

$$\lim_{n\to\infty} \frac{1}{n} \sum_{m=1}^{\infty} P_{j,k}(m) = f_{j,k} \frac{1}{m_{k,k}} \tag{B.22}$$

Proof: Assume that

$$\lim_{Z\to 1^-} ((1-Z)\, A(Z))=L \text{ exists where} \tag{B.23}$$

$$A(Z) = \sum_{n=0}^{\infty} a_n Z^n \tag{B.24}$$

Expand A(Z) in a Laurent series about Z=1

$$A(Z) = \frac{L}{1-Z} + \sum_{n=0}^{\infty} b_n (Z-1)^n$$

$$= L\left(\sum_{m=0}^{\infty} Z^m\right) + \sum_{n=0}^{\infty} b_n \sum_{m=0}^{n} \binom{n}{m} Z^m (-1)^{n-m}$$

interchanging summations in the second term on the RHS

$$A(Z) = L\left(\sum_{m=0}^{\infty} Z^m\right) + \sum_{m=0}^{\infty} Z^m \sum_{n=m}^{\infty} \binom{n}{m} (-1)^{n-m} b_n$$

$$= \sum_{m=0}^{\infty} Z^m \left(L+ \sum_{n=m}^{\infty} \binom{n}{m} (-1)^{n-m} b_n\right)$$

Therefore, equating powers of Z to Equation B.24

$$a_n = L+ \sum_{n=m}^{\infty} \binom{n}{m} (-1)^{n-m} b_n$$

Now, look at

$$\lim_{N\to\infty} \frac{1}{N} \sum_{m=0}^{N} a_m = L + \lim_{N\to\infty} \frac{1}{N} \sum_{m=0}^{N=\infty} \sum_{n=m}^{\infty} \binom{n}{m} (-1)^{n-m} b_n$$

$$= L + \lim_{N\to\infty} \frac{1}{N} \sum_{n=0}^{\infty} b_n \left[\sum_{m=0}^{n} \binom{n}{m} (-1)^{n-m} = (1-1)^n = \delta_{n0} \right]$$

$$= L + \lim_{N\to\infty} \frac{bo}{N} = L$$

Therefore to show $\lim_{n\to\infty} \frac{1}{n} \sum_{m=1}^{n} P_{kk}(m) = \frac{1}{m_{k,k}}$

we need to show that

$$\lim_{Z\to 1^-} ((1-Z)\ P_{k,k}(Z)) = \frac{1}{m_{k,k}}$$

or equivalently

$$\lim_{Z\to 1^-} \frac{1}{(1-Z)(P_{k,k}(Z))} = m_{k,k}$$

using Equation B.16 , we get

$$\lim_{Z\to 1^-} \left(\frac{1-f_{k,k}(Z)}{1-Z} \right) = m_{k,k}$$

$$f_{k,k}(Z) = \sum_{n=1}^{\infty} f_{k,k}(n)\ Z^n = \sum_{n=1}^{\infty} f_{k,k}(n)\ ((Z-1)+1)^n$$

$$= \sum_{n=1}^{\infty} f_{k,k}(n) \sum_{m=0}^{\infty} \binom{n}{m} (Z-1)^m$$

$$= \sum_{n=1}^{\infty} f_{k,k}(n) + \sum_{n=1}^{\infty} f_{k,k}(n) \sum_{m=1}^{n} \binom{n}{m} (Z-1)^m$$

$$= f_{k,k} + \sum_{n=1}^{\infty} f_{k,k}(n) \sum_{m=1}^{n} \binom{n}{m} (Z-1)^m$$

Since $f_{k,k}=1$ is given

$$\frac{1-f_{k,k}(Z)}{1-Z} = \sum_{n=1}^{\infty} f_{k,k}(n) \sum_{m=1}^{n} \binom{n}{m} (Z-1)^{m-1}$$

Therefore, $\lim_{Z\to 1^-} \left(\frac{1-f_{kk}(Z)}{1-Z}\right) = \sum_{n=1}^{\infty} n\, f_{k,k}(n) = m_{k,k}$

Finally for $\lim_{n\to\infty} \frac{1}{n} \sum_{m=1}^{n} P_{j,k}(m)$ we can look at

$$\lim_{Z\to 1^-} ((1-Z)\, P_{j,k}(Z))$$

using Equation B.15 we have

$$\lim_{Z\to 1^-} [(1-Z)\, f_{j,k}(Z)\, P_{k,k}(Z)] =$$

$$\lim_{Z\to 1^-} f_{j,k}(Z)\, \frac{(1-Z)}{1-f_{k,k}(Z)} = f_{j,k}\, \frac{1}{m_{k,k}} \qquad \text{Q.E.D.}$$

For an irreducible recurrent Markov chain

$f_{j,k}=1$ for all j and k, implies

$$\lim_{n\to\infty} \frac{1}{n} \sum_{m=1}^{n} P_{j,k}(m) = \lim_{n\to\infty} \frac{1}{n} \sum_{m=1}^{n} P_{k,k}(m) = \frac{1}{m_{k,k}} \qquad (B.25)$$

The sum is independent of the starting state. This implies the limit exists in the ordinary sense so that

$$\lim_{n\to\infty} P_{k,k}(n) = \frac{1}{m_{k,k}} = \lim_{n\to\infty} P_{j,k}(n) = \pi_k \qquad (B.26)$$

where Equation 3.39 is employed. This shows the ergodic chain possesses a unique long run distribution. Now, we can complete the proof of Theorem 1.

First, we define

$$P^*_{j,k}(n) = \frac{1}{n} \sum_{m=1}^{n} P_{j,k}(m) \tag{B.27}$$

clearly,

$$\pi_k = \lim_{n\to\infty} P^*_{j,k}(n)$$

Summing over k, we get

$$\sum_k \pi_k = \sum_k \lim_n P^*_{j,k}(n) \leq \lim_{n\to\infty} \sum_k P^*_{j,k}(n) = 1$$

$$\text{or} \quad \sum_k \pi_k \leq 1 \tag{B.28}$$

Next, using the Chapman-Kolmogorov equation, we have

$$P_{j,k}(n+1) = \sum_i P_{j,i}(n)\, P_{i,k} \tag{B.29}$$

Then,

$$P^*_{j,k}(n+1) = \frac{1}{n+1} \sum_{m=1}^{n+1} P_{j,k}(m)$$

$$(n+1)P^*_{j,k}(n+1) = \sum_{m=1}^{n+1} P_{j,k}(m) = P_{j,k} + \sum_{m=2}^{n+1} P_{j,k}(m)$$

$$= P_{j,k} + \sum_{m=1}^{n} P_{j,k}(m+1)$$

Substituting Equation B.29 into the above

$$(n+1)P^*_{j,k}(n+1) - P_{j,k} = \sum_{m=1}^{n} \sum_i P_{j,i}(m) P_{i,k}$$

Dividing by n and interchanging the summations of the RHS, we get

$$(1+\frac{1}{n})P^*_{j,k}(n+1) - \frac{1}{n}P_{j,k} = \sum_i \left(\frac{1}{n}\sum_{m=1}^{n} P_{j,i}(m)\right)P_{i,k}$$

$$= \sum_i P^*_{j,i}(m)P_{i,k}$$

Taking the limit as $n\to\infty$, we get

$$\lim_{n\to\infty}\left[(1+\frac{1}{n})P^*_{j,k}(n+1) - \frac{1}{n}P_{j,k}\right] = \pi_k =$$

$$\lim_{n\to\infty}\sum_i P^*_{ji}(n)P_{i,k} \geq \sum_i (\lim_{n\to\infty} P^*_{j,i}(n))P_{ik}$$

$$= \sum_i \pi_i P_{i,k}$$

or
$$\pi_k \geq \sum_i \pi_i P_{i,k} \qquad (B.30)$$

Now, we sum over k

$$\sum_k \pi_k \geq \sum_k \sum_i \pi_k P_{i,k} = \sum_i \pi_i \sum_i P_{i,k} = \sum_i \pi_i$$

Therefore, the equality is proved and

$$\pi_k = \sum_i \pi_i P_{i,k} \qquad (B.31)$$

and the inequality in Equation B.28 is actually an equality giving

$$\sum_k \pi_k = 1 \qquad (B.32)$$

Q.E.D.

Finally, the following definition is often employed

Definition: A recurrent state i is called positive if $m_{k,k}<\infty$ or null if $m_{k,k}=\infty$. A recurrent state which is neither null nor periodic is called ergodic.

Third Order Two Constituent Markov Chain

For a two state, third order Markov chain, the transition probability matrix is 2^3 by 2^3 or has 64 elements of which only $2^{3+1}=16$ are nonzero. These elements are:

$$
\begin{aligned}
P_{ddd,d} &= P_{ddd,ddd} \\
P_{ddd,h} &= P_{ddd,ddh} \\
P_{ddh,d} &= P_{ddh,dhd} \\
P_{ddh,h} &= P_{ddh,dhh} \\
P_{dhd,d} &= P_{dhd,hdd} \\
P_{dhd,h} &= P_{dhd,hdh} \\
P_{dhh,d} &= P_{dhh,hhd} \\
P_{dhh,h} &= P_{dhh,hhh} \\
P_{hdd,d} &= P_{hdd,ddd} \\
P_{hdd,h} &= P_{hdd,ddh} \\
P_{hdh,d} &= P_{hdh,dhd} \\
P_{hdh,h} &= P_{hdh,dhh} \\
P_{hhd,d} &= P_{hhd,hdd} \\
P_{hhd,h} &= P_{hhd,hdh} \\
P_{hhh,d} &= P_{hhh,hhd} \\
P_{hhh,h} &= P_{hhh,hhh}
\end{aligned}
\qquad \text{(B.33)}
$$

Using the reduced notation and eliminating identically zero elements, Equation 3.42 gives

$$C_{ddd}P_{ddd,d} + C_{hdd}P_{hdd,d} = C_{ddd} \quad (B.34)$$

$$C_{ddh}P_{ddh,d} + C_{hdh}P_{hdh,d} = C_{dhd} \quad (B.35)$$

$$C_{ddd}P_{ddd,h} + C_{hdd}P_{hdd,h} = C_{ddh} \quad (B.36)$$

$$C_{hhd}P_{hhd,d} + C_{dhd}P_{dhd,d} = C_{hdd} \quad (B.37)$$

$$C_{dhh}P_{dhh,d} + C_{hhh}P_{hhh,d} = C_{hhd} \quad (B.38)$$

$$C_{dhd}P_{dhd,h} + C_{hhd}P_{hhd,h} = C_{hdh} \quad (B.39)$$

$$C_{ddh}P_{ddh,h} + C_{hdh}P_{hdh,h} = C_{dhh} \quad (B.40)$$

$$C_{hhh}P_{hhh,h} + C_{dhh}P_{dhh,h} = C_{hhh} \quad (B.41)$$

Equation 3.20 becomes

$$\begin{aligned} P_{ddd,d} + P_{ddd,h} &= 1 \\ P_{ddh,d} + P_{ddh,h} &= 1 \\ P_{dhd,d} + P_{dhd,h} &= 1 \\ P_{hdd,d} + P_{hdd,h} &= 1 \\ P_{dhh,d} + P_{dhh,h} &= 1 \\ P_{hhd,d} + P_{hhd,h} &= 1 \\ P_{hdh,d} + P_{hdh,h} &= 1 \\ P_{hhh,d} + P_{hhh,h} &= 1 \end{aligned} \quad (B.42)$$

Finally, Equation 3.40 gives

$$C_{ddd} + C_{dhd} + C_{ddh} + C_{dhh} + C_{hdh} + C_{hhd} + C_{hdd} + C_{hhh} = 1 \quad (B.43)$$

One of the above equations is redundant. We can arbitrarily eliminate Equation B.41. Also, we must relate the cluster

concentrations to the host and defect concentrations. This relationship is

$$C_d = C_{ddd} + \frac{2}{3}(C_{hdd}+C_{dhd}+C_{ddh}) + \frac{1}{3}(C_{hhd}+C_{hdh}+C_{dhh}) \quad (B.44)$$

and $$C_h + C_d = 1. \quad (B.45)$$

Therefore, we have 16 equations with 24 unknowns requiring the specification of 8 variables. If we specify $C_d, P_{ddd,d}, P_{ddh,d}, P_{dhd,d}, P_{hdd,d}, P_{dhh,d}, P_{hhd,d}$ and $P_{hdh,d}$, we get

$$C_{hdd} = C_{ddd}(1-P_{ddd,d})/P_{hdd,d} \quad (B.46)$$

$$C_{ddh} = C_{hdd} \quad (B.47)$$

$$C_{dhd} = C_{ddd}\left(\frac{1-P_{ddd,d}}{P_{hdd,d}}\right)\left(\frac{P_{hhd,d}P_{hdh,d}-P_{hdh,d}-P_{ddh,d}P_{hhd,d}}{P_{hhd,d}P_{hdh,d}-P_{dhd,d}P_{hdh,d}-P_{hhd,d}}\right) \quad (B.48)$$

$$C_{hhd} = (C_{ddh}-C_{dhd}P_{dhd,d})/P_{hhd,d} \quad (B.49)$$

$$C_{hdh} = (C_{dhd}-C_{ddh}P_{ddh,d})/P_{hdh,d} \quad (B.50)$$

$$C_{hhd} = C_{dhh} \quad (B.51)$$

$$C_{hhh} = 1-(C_{ddd}+C_{dhd}+2C_{dhh}+2C_{ddh}+C_{hdh}) \quad (B.52)$$

where

$$C_{ddd} = \frac{C_d}{\left(1+\frac{1-P_{ddd,d}}{P_{hdd,d}}\right)\left(\frac{2P_{hhd,d}P_{hdh,d}-2P_{dhd,d}P_{hdh,d}-P_{hhd,d}(1+P_{ddh,d})+P_{dhd,d}P_{ddh,d}}{P_{hdh,d}(P_{hhd,d}-P_{dhd,d})-P_{hhd,d}}\right)^{-1}} \tag{B.53}$$

and

$$P_{hhh,d} = C_{hhd}(1-P_{dhh,d})/C_{hhh} \tag{B.54}$$

The specification of all eight inputs in a coherent fashion is clearly difficult. The constraints on these inputs are not clearly visible requiring trial and error specification. The complications involved in the third order Markov chain will inherently limit its application.

Second Order, Three Constituent Markov Chain

We will briefly examine the three constituent second order Markov chain because it can be applied to generating "salt" like chains. For the 3 state, second order chain the transition probability matrix has $3^2 \cdot 3^2 = 81$ elements of which $3^{2+1} = 27$ are nonzero.

Equation 3.20 in text when we eliminate the zero matrix elements becomes

$$P_{11,1}+P_{11,2}+P_{11,3} = 1$$

$$P_{12,1}+P_{12,2}+P_{12,3} = 1$$

$$P_{13,1}+P_{13,1}+P_{13,3} = 1$$

$$P_{21,1}+P_{21,2}+P_{21,3} = 1 \qquad \text{(B.55)}$$

$$P_{22,1}+P_{22,2}+P_{22,3} = 1$$

$$P_{23,1}+P_{23,2}+P_{23,3} = 1$$

$$P_{31,1}+P_{31,2}+P_{31,3} = 1$$

$$P_{32,1}+P_{32,2}+P_{32,3} = 1$$

$$P_{33,1}+P_{33,2}+P_{33,3} = 1$$

where we have constituents 1, 2, and 3 and, for example, $P_{33,1} \equiv P_{33,31}$.

Equation 3.42 in text becomes

$$C_{11}P_{11,1}+C_{21}P_{21,1}+C_{31}P_{31,1} = C_{11} \qquad \text{(B.56)}$$

$$C_{12}P_{12,1}+C_{22}P_{22,1}+C_{32}P_{32,1} = C_{21} \qquad \text{(B.57)}$$

$$C_{13}P_{13,1}+C_{23}P_{23,1}+C_{33}P_{33,1} = C_{31} \qquad \text{(B.58)}$$

$$C_{11}P_{11,2}+C_{21}P_{21,2}+C_{31}P_{31,2} = C_{12} \qquad \text{(B.59)}$$

$$C_{12}P_{12,2}+C_{22}P_{22,2}+C_{32}P_{32,2} = C_{22} \qquad \text{(B.60)}$$

$$C_{13}P_{13,2}+C_{23}P_{23,2}+C_{33}P_{33,2} = C_{32} \qquad \text{(B.61)}$$

$$C_{11}P_{11,3}+C_{21}P_{21,3}+C_{31}P_{31,3} = C_{13} \qquad \text{(B.62)}$$

$$C_{12}P_{12,3}+C_{22}P_{22,3}+C_{32}P_{32,3} = C_{23} \qquad \text{(B.63)}$$

$$C_{13}P_{13,3}+C_{23}P_{23,3}+C_{33}P_{33,3} = C_{33} \qquad \text{(B.64)}$$

Finally Equation 3.40 in text gives

$$C_{11}+C_{12}+C_{13}+C_{21}+C_{22}+C_{23}+C_{31}+C_{32}+C_{33} = 1 \qquad (B.65)$$

These cluster concentrations can be related to the individual concentration of constituents by

$$C_1 = C_{11} + \frac{1}{2}(C_{12}+C_{21}+C_{31}+C_{13}) \qquad (B.66)$$

$$C_2 = C_{22} + \frac{1}{2}(C_{12}+C_{21}+C_{32}+C_{23}) \qquad (B.67)$$

and

$$C_1+C_2+C_3 = 1 \qquad (B.68)$$

Here once again one equation can be shown to be redundant leaving 21 equations with 39 unknowns or 18 specifications being required. In itself 18 specifications makes the use of the three constituent second order Markov chain almost impossible.

However, with the solution of the 2 state, first and second order Markov chains, we can make the following hypothesis: A n constituent, t^{th} order Markov chain will require $(n-1)(n^t)$ specifications.

Next, we will look at the three state, second order chain where adjacent alike constituents (11,22,33) are disallowed. Therefore, we have

$$C_{11} = C_{22} = C_{33} = 0 \qquad (B.69)$$

$$P_{12,2} = P_{13,3} = P_{21,1} = P_{23,3} = P_{32,2} = P_{31,1}=0 \quad (B.70)$$

We now rewrite Equations B.55 - B.68 as

$$C_1+C_2+C_3 = 1 \quad (B.71)$$

$$C_1=C_{12}+C_{13} \quad (B.72)$$

$$C_2=C_{12}+C_{32} \quad (B.73)$$

$$C_3=C_{13}+C_{23} \quad (B.74)$$

$$C_{12}+C_{32}=C_{23}+C_{21} \quad (B.75)$$

$$C_{13}+C_{23}=C_{31}+C_{32} \quad (B.76)$$

$$P_{12,1}+P_{12,3}=1 \quad (B.77)$$

$$P_{13,1}+P_{13,2}=1 \quad (B.78)$$

$$P_{21,2}+P_{21,3}=1 \quad (B.79)$$

$$P_{23,1}+P_{23,2}=1 \quad (B.80)$$

$$P_{31,2}+P_{31,3}=1 \quad (B.81)$$

$$P_{32,1}+P_{32,3}=1 \quad (B.82)$$

$$C_{12}P_{12,1}+C_{32}P_{32,1}=C_{21} \quad (B.83)$$

$$C_{13}P_{13,1}+C_{23}P_{23,1}=C_{31} \quad (B.84)$$

$$C_{21}P_{21,2}+C_{31}P_{31,2}=C_{12} \quad (B.85)$$

This equation set includes 15 equations with 21 unknowns requiring only 6 specifications. We take the first four specifications as

C_1, C_2, $P_{12,1}$, and $P_{32,1}$

The solution of $C_3, P_{12,3}$ and $P_{32,3}$ are trival. In addition, we get

$$C_{21}=\frac{2P_{12,1}(C_1+C_2)-P_{12,1}+P_{32,1}-P_{32,1}(2C_1+C_2)}{1-P_{32,1}+P_{12,1}} \qquad (B.86)$$

Using B.86 we can easily solve for C_{23}, C_{13}, C_{12}, C_{32}, and C_{31} in that order. Since all the concentrations have been found with these four specifications Equations B.84 and B.85 give

$$P_{13,1} \alpha P_{23,1} \qquad (B.87)$$

$$P_{21,2} \alpha P_{31,2} \qquad (B.88)$$

Apriori, we would not have expected this dependence among probabilities. For the last two specifications we can take $P_{13,1}$ and $P_{21,2}$ completely specifying the problem.

For the special case of an 1 2_{1-X} 3_X salt in which the substitutions are made on only one sublattice of an otherwise perfect chain we must have $C_1=0.5$ and $C_{11}=C_{22}=C_{33}=C_{23}=C_{32}=0$. We then have $X=2C_3$ and,

$$C_2+C_3=0.5$$
$$P_{21,2}+P_{21,3}=1$$
$$P_{31,2}+P_{31,3}=1$$
$$C_2P_{21,2}+C_3P_{31,2}=C_2$$

four equations in six unknown leaving only two parameters to be specified.

Examination of Structure of P^n

The z transformation defined by Equation B. 24 gives us a powerful technique for finding the n step transition probabilities $P_{j,k}(n)$. If we define, the z transform of the transition probability matrix as the z transform of each element and simiarly for the unconditional probability vector, we can take the transform of the Equation

$$\underline{p}(n+1) = \underline{p}(n)\ \underline{\underline{P}} \tag{B.89}$$

where p(n) is defined by Equation 3.24 and P by Equation 3.18 P=P(1) has no n dependence and as such is constant under a z transformation, p(n) goes to $p(z) = \sum_{n=0}^{\infty} p(n)z^n$ and p(n+1) goes to

$$\sum_{n=0}^{\infty} p(n+1)z^n = \sum_{n=1}^{\infty} p(n)\frac{z^n}{z}$$

$$= \frac{1}{z}\left[\sum_{n=0}^{\infty} p(n)z^n - p(0)\right] = \frac{1}{z}(p(z)-p(0))$$

Therefore, Equation B.89 becomes

$$\frac{1}{z}(\underline{p}(z)-\underline{p}(0)) = \underline{p}(z)\ \underline{\underline{P}} \tag{B.90}$$

This equation can be rearranged to give

$$\underline{p}(z)(\underline{\underline{I}}-z\underline{\underline{P}}) = \underline{p}(0)$$

or $$\underline{p}(z) = \underline{p}(0)(\underline{\underline{I}}-z\underline{\underline{p}})^{-1}$$

If we take the inverse z tranformation we get

$$\underline{p}(n)=\underline{p}(0)\mathcal{Z}[(\underline{\underline{I}}-z\underline{\underline{P}})^{-1}] \tag{B.91}$$

Comparing Equation B.91 with Equation 3.25 we see the important result

$$\underline{\underline{P}}^{n} = \mathcal{Z}[(\underline{\underline{I}}-z\underline{\underline{P}})^{-1}] \tag{B.92}$$

where the inverse z transform is performed on each element of $(\underline{\underline{I}}-z\underline{\underline{P}})^{-1}$. For the 2 state first order Markov chain we can now easily derive Equation 3.29 from Equation 3.27.

$$(I-zP) = \begin{pmatrix} 1-zP_{h,h} - zP_{h,d} \\ -zP_{d,h} - 1-zP_{d,d} \end{pmatrix} = \begin{pmatrix} 1-zP_{h,h} - z(1-P_{h,h}) \\ -z(1-P_{d,d}) \quad 1-zP_{d,d} \end{pmatrix}$$

The determinant of (I-zP) is

$$\begin{aligned} \det(\ ) &= (1-zP_{h,h})(1-zP_{d,d}) - z^2P_{d,h}P_{h,d} \\ &= 1-z(P_{h,h}+P_{d,d}) + z^2(P_{h,h}P_{d,d}-P_{d,h}P_{h,d}) \\ &= 1-z(P_{h,h}+P_{d,d}) + (P_{d,d}+P_{h,h}-1)z^2 \\ &= (1-z)(1-(P_{h,h}+P_{d,d}-1)z) \end{aligned}$$

The inverse of the matrix is

$$(I-zP)^{-1} = \begin{pmatrix} 1-zP_{d,d} & zP_{h,d} \\ zP_{d,h} & 1-zP_{d,d} \end{pmatrix} \quad \frac{1}{(1-z)[1-(P_{h,h}+P_{d,d}-1)z]}$$

We can expand each element by partial fractions. For example the (1,1) element is

$$\frac{1-zP_{d,d}}{(1-z)(1-(P_{h,h}+P_{d,d}-1)z)} = \frac{A}{1-z} + \frac{B}{1-(P_{h,h}+P_{d,d}-1)z}$$

giving $A+B=1$

$$p_{d,d} = A(P_{h,h}+P_{d,d}-1) + B$$

$$A = (1-P_{d,d})/(2-P_{h,h}+P_{d,d})$$

and $$B = 1-A = (1-P_{h,h})/(2-P_{h,h}-P_{d,d})$$

Therefore, we have

$$(I-zP)^{-1} = \frac{1}{2-P_{h,h}-P_{d,d}} \begin{vmatrix} 1-P_{d,d} & 1-P_{h,h} \\ 1-P_{d,d} & 1-P_{h,h} \end{vmatrix} \frac{1}{1-z}$$

$$+ \frac{1}{2-P_{h,h}-P_{d,d}} \begin{vmatrix} 1-P_{h,h} & -(1-P_{h,h}) \\ -(1-P_{d,d}) & 1-P_{d,d} \end{vmatrix} \frac{1}{1-(P_{h,h}+P_{d,d}-1)z}$$

The inverse z transformation is now easily performed since

if $f(n) = \alpha^n$, then $f(z) = \frac{1}{1-\alpha z}$.

$$P^N = \frac{1}{(2-P_{h,h}-P_{d,d})} \begin{vmatrix} 1-P_{d,d} & 1-P_{h,h} \\ 1-P_{d,d} & 1-P_{h,h} \end{vmatrix}$$

$$+ \frac{(P_{h,h}+P_{d,d}-1)^N}{(2-P_{h,h}-P_{d,d})} \begin{vmatrix} (1-P_{h,h}) & -(1-P_{h,h}) \\ -(1-P_{d,d}) & (1-P_{d,d}) \end{vmatrix}$$

which is Equation 3.29 in text.

Since we know from Equation 3.50 and 3.51

$$P_{h,h} = 1-C_d(1-P_{d,d})/(1-C_d)$$

$$\frac{1-P_{d,d}}{(1-P_{d,d})+(1-P_{h,h})} = C_d \tag{B.93}$$

$$\frac{1-P_{h,h}}{2-P_{d,d}-P_{h,h}} = 1-C_d \tag{B.94}$$

and

$$(P_{h,h}+P_{d,d}-1) = \frac{P_{d,d}-C_d}{1-C_d} , \tag{B.95}$$

we obtain

$$P^N = \begin{pmatrix} 1-C_d & C_d \\ 1-C_d & C_d \end{pmatrix} + \left(\frac{P_{d,d}-C_d}{1-C_d}\right)^N \begin{pmatrix} C_d & C_d \\ -(1-C_d) & (1-C_d) \end{pmatrix} \tag{B.96}$$

$$\lim_{N\to\infty} P^N = \begin{pmatrix} 1-C_d & C_d \\ 1-C_d & C_d \end{pmatrix} \tag{B.97}$$

For the two constituent second order Markov chain, the matrix inversion becomes more difficult. For this case

$$P = \begin{pmatrix} P_{hh,h} & P_{hh,d} & 0 & 0 \\ 0 & 0 & P_{hd,h} & P_{hd,d} \\ P_{dh,h} & P_{dh,d} & 0 & 0 \\ 0 & 0 & P_{dd,h} & P_{dd,d} \end{pmatrix} \tag{B.98}$$

where $p(n) = [P_{hh}(n)\ P_{hd}(n)\ P_{dh}(n)\ P_{dd}(n)]$

$$(I-zP) = \begin{pmatrix} 1-z(1-P_{hh,d}) & -zP_{hh,d} & 0 & 0 \\ 0 & 1 & -z(1-P_{hd,d}) & -zP_{hd,d} \\ -z(1-P_{dh,d}) & -zP_{dh,d} & 1 & 0 \\ 0 & 0 & -z(1-P_{dd,d}) & 1-zP_{dd,d} \end{pmatrix}$$

Taking the determinant, after much simplification we get

$$D = \det(I-zP) = 1-z(P_{dd,d}-P_{hh,d}-1)$$

$$+ z^2(P_{dd,d}-P_{dh,d}-P_{dd,d}P_{hh,d}+P_{dh,d}P_{hd,d})$$

$$+ z^3(P_{dh,d}-P_{hh,d}+P_{hh,d}P_{hd,d}+P_{dd,d}P_{dh,d}-2P_{dh,d}P_{hd,d})$$

$$+ z^4(P_{hd,d}P_{dh,d}+P_{hh,d}P_{dd,d}-P_{dh,d}P_{dd,d}-P_{hh,d}P_{hd,d})$$

$$D = (1-z)[1+z(P_{hh,d}-P_{dd,d})+z^2(P_{hh,d}-P_{dh,d}-P_{dd,d}P_{hh,d}+P_{dh,d}P_{hd,d})$$

$$+ z^3(P_{hh,d}P_{hd,d}+P_{dd,d}P_{dh,d}-P_{dd,d}P_{hh,d}-P_{dh,d}P_{hd,d})] \quad \text{(B.99)}$$

D must be factorable to use the expansion by partial fraction. A simple factorization of D does not seem possible. For specific numerical values of $P_{dd,d}$, $P_{dh,d}$, $P_{hd,d}$, and C_d where

$$P_{hh,d} = \frac{C_d(1-P_{dd,d})(1-P_{dh,d})}{1+P_{hd,d}-P_{dd,d}-C_d(P_{hd,d}+2(1-P_{dd,d}))}$$

one can factor D.

$$(I-zP)^{-1} = \frac{1}{D}\begin{pmatrix} a_{11} & a_{12} & a_{13} & a_{14} \\ a_{21} & a_{22} & a_{23} & a_{24} \\ a_{31} & a_{32} & a_{33} & a_{34} \\ a_{41} & a_{42} & a_{43} & a_{44} \end{pmatrix}$$

where

$$a_{11}=1-zP_{dd,d}-z^2(1-P_{hd,d})P_{dh,d}+z^3(P_{dd,d}P_{dh,d}-P_{hd,d}P_{dh,d})$$

$$a_{21}=z^2(1-P_{dh,d})(1-P_{hd,d})+z^3(P_{hd,d}-P_{dd,d}+P_{dh,d}(P_{dd,d}-P_{hd,d})$$

$$a_{31}=z(1-P_{dh,d}) - z^2(1-P_{dh,d})P_{dd,d}$$

$$a_{41}=z^2(1-P_{dh,d})(1-P_{dd,d})$$

$$a_{12}=zP_{hh,d} - z^2P_{hh,d}P_{dd,d}$$

$$a_{22}=1-z(P_{dd,d}-P_{hh,d}+1) + z^2P_{dd,d}(1-P_{hh,d})$$

$$a_{32}=zP_{dh,d}-z^2(P_{dh,d}-P_{hh,d}+P_{dh,d}P_{dd,d}) + z^3[P_{dd,d}(P_{dh,d}-P_{hh,d})]$$

$$a_{42}=z^2P_{dh,d}(1-P_{dd,d})+z^3[P_{hh,d}-P_{dh,d}+P_{dd,d}(P_{dh,d}-P_{hh,d})]$$

$$a_{13}=z^2(1-P_{hd,d})P_{hh,d} + z^3P_{hh,d}(P_{hd,d}-P_{dd,d})$$

$$a_{23}=z(1-P_{hd,d})-z^2(1-P_{hh,d}+P_{dd,d}-2P_{hd,d}+P_{hd,d}P_{hh,d}) + z^3(1-P_{hh,d})(P_{dd,d}-P_{hd,d})$$

$$a_{33}=1-z(P_{dd,d}+1-P_{hh,d})+z^2P_{dd,d}(1-P_{hh,d})$$

$$= a_{22}$$

$$a_{43}=z(1-P_{dd,d}) - z^2(1-P_{dd,d})(1-P_{hh,d})$$

$$a_{14}=z^2P_{hh,d}P_{hd,d}$$

$$a_{24}=zP_{hd,d}-z^2P_{hd,d}(1-P_{hh,d})$$

$$a_{34}=z^2P_{dh,d}P_{hd,d} + z^3P_{hd,d}(P_{hh,d}-P_{dh,d})$$

$$a_{44}=1-z(1-P_{hh,d}) - z^2(1-P_{hd,d})(P_{dh,d})$$

$$+ z^3(1-P_{hd,d})(P_{dh,d}-P_{hh,d})$$

We want to examine this matrix for three cases.

I. First order Markov chain equivalent

$P_{dd,d}=P_{hd,d}$; $P_{hh,d}=P_{dh,d}$
and $P_{hh,d}=C_d(1-P_{dd,d})/(1-C_d)$

II. $P_{dd,d}=P_{dh,d}$; $P_{hh,d}=P_{hd,d}$ and
$P_{hh,d}=C_d(1-P_{dd,d})/(1-C_d)$

III. for $C_d=.5$, $P_{dd,d}=P_{hh,d}$; $P_{dh,d}=P_{hd,d}$
and $P_{dh,d}=1-P_{dd,d}$

Unlike cases I and II, the relationships in case III apply for only a single value of the concentration.

Case I:

$$D=(1-z)(1+z(P_{hh,d}-P_{dd,d})$$

$$=(1-z)(1-z(P_{dd,d}-P_{hh,d}))$$

and

$$a_{11}=1-zP_{dd,d}-z^2(1-P_{dd,d})P_{hh,d}$$

$$a_{21}=z^2(1-P_{hh,d})(1-P_{dd,d})$$

$$a_{31}=z(1-P_{hh,d})-z^2(1-P_{hh,d})P_{dd,d}$$

$$a_{41}=z^2(1-P_{hh,d})(1-P_{dd,d})=a_{21}$$

$$a_{12}=zP_{hh,d}-z^2P_{hh,d}P_{dd,d}$$

$$a_{22}=1-z(P_{dd,d}-P_{hh,d}+1) + z^2P_{dd,d}(1-P_{hh,d})$$

$$a_{32}=zP_{hh,d}-z^2P_{hh,d}P_{dd,d}=a_{12}$$

$$a_{42}=z^2P_{hh,d}(1-P_{dd,d})$$

$$a_{13}=z^2(1-P_{dd,d})P_{hh,d}=a_{42}$$

$$a_{23}=z(1-P_{dd,d})-z^2(1-P_{hh,d}-P_{dd,d}+P_{dd,d}P_{hh,d})$$

$$a_{33}=1-z(1-P_{hh,d}+P_{dd,d})+z^2P_{dd,d}(1-P_{hh,d})=a_{33}$$

$$a_{43}=z(1-P_{dd,d}-z^2(1-P_{dd,d})(1-P_{hh,d})=a_{23}$$

$$a_{24}=zP_{dd,d}-z^2P_{dd,d}(1-P_{hh,d})$$

$$a_{34}=z^2P_{hh,d}P_{dd,d}=a_{14}$$

$$a_{44}=1-z(1-P_{hh,d})-z^2(1-P_{dd,d})P_{hh,d}$$

The expansion by partial fractions is tedious. For example $\frac{a_{11}}{D} = \frac{P_{hh,d}(1-P_{dd,d})}{P_{hh,d}-P_{dd,d}}+\frac{(1-P_{dd,d})(1-P_{hh,d})}{1-P_{dd,d}+P_{hh,d}} \frac{1}{1-z}$

$$+ \frac{P_{hh,d}(1-P_{hh,d})}{(1-P_{dd,d}+P_{hh,d})} \quad \frac{1}{1-(P_{dd,d}-P_{hh,d})z} \quad \frac{1}{(P_{dd,d}-P_{hh,d})}$$

the inverse of this term is

$$\mathcal{J}\left(\frac{a_{11}}{D}\right) = \frac{P_{hh,d}(1-P_{dd,d})}{P_{hh,d}-P_{dd,d}} \quad \delta_{n,0} + \frac{(1-P_{dd,d})(1-P_{hh,d})}{1-P_{dd,d}+P_{hh,d}}$$

$$+ \frac{P_{hh,d}(1-P_{hh,d})}{1-P_{dd,d}+P_{hh,d}} \quad (P_{dd,d}-P_{hh,d})^{n-1}$$

Using the relation between $P_{hh,d}$ and $P_{dd,d}$ for case I we have

$$(1-P_{dd,d}+P_{hh,d}) = (1-P_{dd,d})/(1-C_d)$$

$$(1-P_{hh,d}) = (1-2C_d+C_dP_{dd,d})/(1-C_d)$$

$$(P_{dd,d}-P_{hh,d}) = (P_{dd,d}-C_d)/(1-C_d)$$

therefore,

$$\mathcal{J}\left(\frac{a_{11}}{D}\right) = -\frac{C_d(1-P_{dd,d})^2}{P_{dd,d}-C_d} \quad \delta_{n,0} + {}^{1-2C_d+C_dP_{dd,d}} +$$

$$+ \frac{C_d(1-2C_d+C_dP_{dd,d})}{1-C_d} \left(\frac{P_{dd,d}-C_d}{1-C_d}\right)^{n-1}$$

The inverse has properties

$$\left(\frac{a_{11}}{D}\right) = \begin{cases} 1 & n=0 \\ (1-P_{hh,d}) & n=1 \end{cases}$$

as required, since for no transition (n=0) a state must transition into itself (δ_{ii}) and n=1 give $\underline{\underline{P}}$ again. We can now write, the total inverse in matrix form

$$\rho^n = \frac{\delta_{n,0}}{P_{dd,d}-C_d} \begin{pmatrix} -C_d(1-P_{dd,d})^2 & -C_d P_{dd,d}(1-P_{dd,d}) & C_d(1-P_{dd,d})^2 & C_d P_{dd,d}(1-P_{dd,d}) \\ (1-P_{dd,d})(1-2C_d+C_d P_{dd,d}) & P_{dd,d}(1-2C_d+C_d P_{dd,d}) & -(1-P_{dd,d})(1-2C_d+C_d P_{dd,d}) & -P_{dd,d}(1-2C_d+C_d P_{dd,d}) \\ -P_{dd,d}(1-2C_d+C_d P_{dd,d}) & -C_d P_{dd,d}(1-P_{dd,d}) & P_{dd,d}(1-2C_d+C_d P_{dd,d}) & C_d P_{dd,d}(1-P_{dd,d}) \\ (1-P_{dd,d})(1-2C_d+C_d P_{dd,d}) & C_d(1-P_{dd,d})^2 & -(1-P_{dd,d})(1-2C_d+C_d P_{dd,d}) & -C_d(1-P_{dd,d})^2 \end{pmatrix}$$

$$+ \begin{pmatrix} 1-2C_d+C_d P_{dd,d} & C_d(1-P_{dd,d}) & C_d(1-P_{dd,d}) & C_d P_{dd,d} \\ 1-2C_d+C_d P_{dd,d} & C_d(1-P_{dd,d}) & C_d(1-P_{dd,d}) & C_d P_{dd,d} \\ 1-2C_d+C_d P_{dd,d} & C_d(1-P_{dd,d}) & C_d(1-P_{dd,d}) & C_d P_{dd,d} \\ 1-2C_d+C_d P_{dd,d} & C_d(1-P_{dd,d}) & C_d(1-P_{dd,d}) & C_d P_{dd,d} \end{pmatrix}$$

$$+ \left(\frac{P_{dd,d}-C_d}{1-C_d}\right)^{n-1} \begin{pmatrix} \frac{C_d(1-2C_d+C_d P_{dd,d})}{1-C_d} & \frac{C_d^2(1-P_{dd,d})}{1-C_d} & -C_d(1-P_{dd,d}) & -C_d P_{dd,d} \\ -(1-2C_d+C_d P_{dd,d}) & -C_d(1-P_{dd,d}) & (1-C_d)(1-P_{dd,d}) & (1-C_d)P_{dd,d} \\ \frac{C_d(1-2C_d+C_d P_{dd,d})}{1-C_d} & \frac{C_d^2(1-P_{dd,d})}{1-C_d} & -C_d(1-P_{dd,d}) & -C_d P_{dd,d} \\ -(1-2C_d+C_d P_{dd,d}) & -C_d(1-P_{dd,d}) & (1-C_d)(1-P_{dd,d}) & (1-C_d)P_{dd,d} \end{pmatrix}$$

(B.100)

Case II:

$$D=(1-z)(1-z(P_{dd,d}-P_{hh,d})-z^2(P_{dd,d}-P_{hh,d})+z^3(P_{dd,d}-P_{hh,d})^2$$

$$=(1-z)(1-z(P_{dd,d}-P_{hh,d}))(1-z^2(P_{dd,d}-P_{hh,d})$$

$$=(1-z)(1-z(P_{dd,d}-P_{hh,d}))(1+z\sqrt{P_{dd,d}-P_{hh,d}}) \times (1-z\sqrt{P_{dd,d}-P_{hh,d}})$$

and

$$a_{11}=1-z(P_{dd,d})-z^2(1-P_{hh,d})P_{dd,d}+z^3(P_{dd,d})(P_{dd,d}-P_{hh,d})$$

$$a_{21}=z^2(1-P_{dd,d})(1-P_{hh,d})+z^3(P_{dd,d}-P_{hh,d})(P_{dd,d}-1)$$

$$a_{31}=z(1-P_{dd,d})-z^2(1-P_{dd,d})P_{dd,d}$$

$$a_{41}=z^2(1-P_{dd,d})^2$$

$$a_{12}=z(P_{hh,d})-z^2(P_{hh,d})(P_{dd,d})$$

$$a_{22}=1-z(1+P_{dd,d}-P_{hh,d}) + z^2P_{dd,d}(1-P_{hh,d})$$

$$a_{32}=zP_{dd,d}-z^2(P_{dd,d}-P_{hh,d}+P_{dd,d})+z^3(P_{dd,d})(P_{dd,d}-P_{hh,d})$$

$$a_{42}=z^2P_{dd,d}(1-P_{dd,d})+z^3(P_{dd,d}-P_{hh,d})(P_{dd,d}-1)$$

$$a_{13}=z^2(1-P_{hh,d})P_{hh,d}+z^3(P_{hh,d})(P_{hh,d}-P_{dd,d})$$

$$a_{23}=z(1-P_{hh,d})-z^2(1-3P_{hh,d}+P^2_{hh,d}+P_{dd,d})+z^3(1-P_{hh,d})(P_{dd,d}-P_{hh,d})$$

$$a_{33}=a_{22}$$

$$a_{43}=z(1-P_{dd,d})-z^2(1-P_{dd,d})(1-P_{hh,d})$$

$$a_{14}=z^2P_{hh,d}^2$$

$$a_{24}=zP_{hh,d}-z^2P_{hh,d}(1-P_{hh,d})$$

$$a_{34}=z^2(P_{dd,d})P_{hh,d}+z^3P_{hh,d}(P_{hh,d}-P_{dd,d})$$

$$a_{44}=1-z(1-P_{hh,d})-z^2(1-P_{hh,d})P_{dd,d}+z^3(1-P_{hh,d})(P_{dd,d}-P_{hh,d})$$

For the term

$$a_{ij} = q+rz+sz^2+tz^3$$

the partial fraction expansion is

$$\frac{a_{ij}}{D} = \frac{A}{1-z} + \frac{B}{1-dz} + \frac{C}{1-\sqrt{d}z} + \frac{D}{1+\sqrt{d}z}$$

where $d = P_{dd,d} - P_{hh,d}$

$$A = (r+s+t+q)/(1-d)^2$$

$$B = (qd^3+rd^2+sd+t)/d(1-d)^2$$

$$C = -\frac{(t+rd)+\sqrt{d}(s+dq)}{2d(1-\sqrt{d})^2}$$

$$D' = (\sqrt{d}(s+dq)-(t+rd))/2d(1+\sqrt{d})^2$$

Therefore, for case II, the inverse transform gives

$$P^n = \begin{pmatrix} (1-C_d)^2 & C_d(1-C_d) & C_d(1-C_d) & C_d^2 \\ (1-C_d)^2 & C_d(1-C_d) & C_d(1-C_d) & C_d^2 \\ (1-C_d)^2 & C_d(1-C_d) & C_d(1-C_d) & C_d^2 \\ (1-C_d)^2 & C_d(1-C_d) & C_d(1-C_d) & C_d^2 \end{pmatrix}$$

$$+\left(\frac{P_{dd,d}-C_d}{1-C_d}\right)^n \begin{pmatrix} C_d^2 & -C_d^2 & -C_d^2 & C_d^2 \\ -C_d(1-C_d) & C_d(1-C_d) & C_d(1-C_d) & -C_d(1-C_d) \\ -C_d(1-C_d) & C_d(1-C_d) & C_d(1-C_d) & -C_d(1-C_d) \\ (1-C_d)^2 & -(1-C_d)^2 & -(1-C_d)^2 & (1-C_d)^2 \end{pmatrix}$$

$$+\frac{1}{2}\left(\frac{P_{dd,d}-C_d}{1-C_d}\right)^{n/2}\left[\frac{1}{\left(1-\left(\frac{P_{dd,d}-C_d}{1-C_d}\right)^{\frac{1}{2}}\right)^2}+\frac{(-1)^n}{\left(1+\left(\frac{P_{dd,d}-C_d}{1-C_d}\right)^{\frac{1}{2}}\right)^2}\right] x$$

$$\begin{pmatrix} 0 & \frac{C_d(1-P_{dd,d})}{1-C_d} & \frac{C_d(1-P_{dd,d})}{1-C_d} & 0 \\ 1-P_{dd,d} & \frac{1-2C_d+P_{dd,d}}{1-C_d} & \frac{-2(1-2C_d+C_dP_{dd,d})}{1-C_d} & \frac{-C_d(1-P_{dd,d})}{1-C_d} \\ -(1-P_{dd,d}) & -2P_{dd,d} & \frac{1-2C_d+P_{dd,d}}{1-C_d} & \frac{C_d(1-P_{dd,d})}{1-C_d} \\ 0 & 1-P_{dd,d} & -(1-P_{dd,d}) & 0 \end{pmatrix}$$

$$+\frac{1}{2}\left[\frac{P_{dd,d}-C_d}{1-C_d}\right]\frac{n-1}{2}\left[\frac{1}{\left(1-\left(\frac{P_{dd,d}-C_d}{1-C_d}\right)^{\frac{1}{2}}\right)^2}-\frac{(-1)^n}{\left(1+\left(\frac{P_{dd,d}-C_d}{1-C_d}\right)^{\frac{1}{2}}\right)^2}\right]$$

$$\begin{pmatrix}
\frac{C_d(1-P_{dd,d})^2}{1-C_d} & \frac{C_d P_{dd,d}(1-P_{dd,d})}{1-C_d} & -\frac{C_d(1-P_{dd,d})(1-2C_d+C_d P_{dd,d})}{(1-C_d)^2} & -\frac{C_d^2(1-P_{dd,d})^2}{(1-C_d)^2} \\
-\frac{(1-P_{dd,d})(1-2C_d+C_d P_{dd,d})}{1-C_d} & -2P_{dd,d}+\frac{C_d(1-P_{dd,d}^2)}{1-C_d} & \left(\frac{1-2C_d+C_d P_{dd,d}}{1-C_d}\right)^2+\left(\frac{P_{dd,d}-C_d}{1-C_d}\right) & \frac{C_d(1-P_{dd,d})(1-2C_d+C_d P_{dd,d})}{(1-C_d)^2} \\
P_{dd,d}(1-P_{dd,d}) & P_{dd,d}^2+\left(\frac{P_{dd,d}-C_d}{1-C_d}\right) & -2P_{dd,d}+\frac{C_d(1-P_{dd,d}^2)}{1-C_d} & -\frac{C_d P_{dd,d}(1-P_{dd,d})}{1-C_d} \\
-(1-P_{dd,d})^2 & -P_{dd,d}(1-P_{dd,d}) & (1-P_{dd,d})\left(\frac{1-2C_d+C_d P_{dd,d}}{1-C_d}\right) & \frac{(1-P_{dd,d})^2 C_d}{1-C_d}
\end{pmatrix}$$

(B.101)

For Case III, we have

$$D = (1-z)(1-z^3(1-2P_{dd,d})^2)$$

$$= (1-z)(1-a^{2/3}z)(1+a^{2/3}e^{i\pi/3}z)(1+a^{2/3}e^{-i\pi/3}z)$$

where $a = 1-2P_{dd,d}$

$$a_{11}=1-zP_{dd,d}-z^2P_{dd,d}(1-P_{dd,d})+z^3(2P_{dd,d}-1)(1-P_{dd,d})$$

$a_{21}=z^2P_{dd,d}+z^3P_{dd,d}(1-2P_{dd,d})$

$a_{31}=zP_{dd,d}-z^2P_{dd,d}^2$

$a_{41}=z^2P_{dd,d}(1-P_{dd,d})$

$a_{12}=a_{31}=zP_{dd,d}-z^2P_{dd,d}^2$

$a_{22}=1-z+z^2P_{dd,d}(1-P_{dd,d})$

$a_{32}=z(1-P_{dd,d})-z^2(1-P_{dd,d}-P_{dd,d}^2)+z^3P_{dd,d}(1-2P_{dd,d})$

$a_{42}=z^2(1-P_{dd,d})^2+z^3(1-2P_{dd,d})(P_{dd,d}-1)$

$a_{13}=z^2P_{dd,d}^2+z^3(1-2P_{dd,d})P_{dd,d}=a_{21}$

$a_{23}=zP_{dd,d}+z^2(1-3P_{dd,d}+P_{dd,d}^2)+z^3(1-P_{dd,d})(2P_{dd,d}-1)$

$a_{33}=a_{22}$

$a_{43}=z(1-P_{dd,d})-z^2(1-P_{dd,d})^2$

$a_{14}=z^2P_{dd,d}(1-P_{dd,d})=a_{41}$

$a_{24}=z^2(1-P_{dd,d})-z^2(1-P_{dd,d})^2=a_{43}$

$a_{34}=z^2(1-P_{dd,d})^2-z^3(1-P_{dd,d})(1-2P_{dd,d})$

$a_{44}=1-z(1-P_{dd,d})-z^2P_{dd,d}(1-P_{dd,d})+z^3P_{dd,d}(1-2P_{dd,d})$

for the term $a_{ij}=q+rz+sz^2+tz^3$ the partial fraction expansion for the term $\frac{a_{ij}}{D}$ is

$$\frac{A}{1-z} + \frac{B}{1-dz} + \frac{C}{1+de^{i\pi/3}z} + \frac{D}{1+de^{-i\pi/3}z}$$

where $d = (1-2P_{dd,d})^{2/3}$ and

$$A = \frac{q+r+s+t}{4P_{dd,d}(1-P_{dd,d})}$$

$$B = \frac{t+ds+d^2r+d^3q}{-3d^2(1-d)}$$

$$C = [(t+d^3q)((1-d)(d+2)-(1-d)(1+2d)e^{i\pi/3})+rd^2(-(1-d)^2+(1-d)(d+2)e^{i\pi/3})$$

$$+ sd[-(1-d)^2e^{i\pi/3}-(1-d)(2d+1)]/-3d^2(1-d^3)(e^{i\pi/3}-e^{-i\pi/3})$$

$D = +C^*$ (since d is real)

The inverse transform in rather symbolic form is

$$p^n = \frac{1}{4}\begin{pmatrix} 1 & 1 & 1 & 1 \\ 1 & 1 & 1 & 1 \\ 1 & 1 & 1 & 1 \\ 1 & 1 & 1 & 1 \end{pmatrix}$$

$$+(1-2P_{dd,d})^{\frac{2n}{3}}(B_{ij})+(-(1-2P_{dd,d})^{2/3}e^{i\pi/3})^n(C_{ij})$$

$$+(-(1-2P_{dd,d})^{2/3}e^{-i\pi/3})^n(C^*_{ij}) \qquad \text{(B.102)}$$

where we note that the last two terms can be combined as

$$(-1)^n(1-2P_{dd,d})^{\frac{2n}{3}}\left(C_{ij}e^{\frac{i\pi n}{3}} + C^*_{ij}\, e^{\frac{-i\pi n}{3}}\right)$$

$$=(-1)^n(1-2P_{dd,d})^{\frac{2n}{3}}\, 2\mathrm{Re}\left(C_{ij}e^{i\pi n/3}\right) \qquad \text{(B.103)}$$

Clearly, the long run distributions of constitutents, $C_{\ell,m}$ is completely random, $C_{\ell,m}=(.5)(1-.5)=.25$. Also P^n is always real as we require since imaginary probabilities are meaningless.

Statistical Analysis of Generated Markov Chains

In this section, we will statistically examine the Markov chains we generate to insure the computational accuracy of the computer programs which employ a random number generator. For simplicity, we present the error analysis only for first order Markov chains since P^n is quite complicated for the second order Markov chain. In addition, we will only examine $P_{d,d}(n)$ since the other probabilities give similar results. Using Equations 3.106 and 3.107 in text, we will use a 99% confidence level C, expressed as a certain number of standard deviations,

$$C = a\sigma \qquad \text{(B.104)}$$

the maximum relative error we will tolerate is

$$E = \frac{(\mu+C)-\mu)}{\mu} = \frac{C}{\mu} = a\left(\frac{\sigma}{\mu}\right)$$

From Equations 3.106 and 3.107

$$E = a\frac{[(N\ P_{dd,d}(n)(1-P_{d,d}(n))]^{\frac{1}{2}}}{NP_{d,d}(n)}$$

or $$E = a\sqrt{\frac{1}{N}\left(\frac{1}{P_{d,d}(n)} - 1\right)} \qquad \text{(B.105)}$$

The 99% confidence limit gives a =2.58. Tables B.1, B.2, B.3, and B.4 are for $P_{d,d}$=.1, C_d=.5, and N=1000, 10000, 100000, and 1000000 atom chains respectively. For each case, the n=1 case provides a test of the statistical accuracy of the random number generator.

Table B.1.--Statistic error analysis of a chain with N=1000, C_d=.5, $P_{d,d}$=0.1 compared to 99% confidence limit error of Equation B. 105

n	$P_{d,d}(n)$		Relative Error	
	Calculated	Experimental	Acceptable (Eq. B.105)	Experimental
1	0.1	0.09419	.245	.058
2	0.82	0.82129	.0382	.0016
3	0.244	0.24346	.144	.0022
4	0.7048	0.70423	.0528	.0008
5	0.33616	0.32661	.115	.0284
6	0.63107	0.63306	.0624	.00315
7	0.39514	0.40404	.101	.0225
8	0.58389	0.57374	.0689	.0173
9	0.43289	0.44332	.0934	.0241
10	0.55369	0.55061	.0732	.0056

Table B.2.--Statistic error analysis of a chain with N=100000, C_d=.5, $P_{d,d}$=0.1 compared to the 99% confidence limit error of Equation B.105

n	$P_{d,d}(n)$		Relative Error	
	Calculated	Experimental	Acceptable	Experimental
1	0.1	0.10112	.0774	.0112
2	0.82	.81418	.0121	.0071
3	0.244	.24955	.0454	.0227
4	0.7048	.69678	.0167	.0114
5	0.33616	.34415	.0363	.0238
6	0.63107	.62159	.0197	.0150
7	0.39514	.40313	.0319	.0202
8	0.58389	.57836	.0218	.0095
9	0.43289	.43507	.0295	.0050
10	0.55369	.55322	.0232	.0008

Table B.3.--Statistical error analysis of a chain with N=100,000, C_d=.5, $P_{d,d}$=0.1 compared to the 99% confidence limit error of Equation B.105

n	$P_{d,d}(n)$		Relative Error	
	Calculated	Experimental	Acceptable	Experimental
1	0.1	0.09818	.0245	.0182
2	0.82	.82278	.00382	.00339
3	0.244	.24144	.0144	.0105
4	0.7048	.70787	.00528	.00436
5	0.33616	.33337	.0115	.0083
6	0.63107	.63433	.00624	.00517
7	0.39514	.39190	.0101	.0082
8	0.58389	.58810	.00689	.00721
9	0.43289	.42916	.00934	.00862
10	0.55369	.55811	.00732	.00798

Table B.4.--Statistical error analysis of a chain with N=1,000,000, C_d=.5, $P_{d,d}$=0.1 compared to the 99% confidence limit error of Equation B.105

n	$P_{d,d}(n)$		Relative Error	
	Calculated	Experimental	Acceptable	Experimental
1	0.1	0.09950	.00774	.005
2	0.82	0.81999	.00121	.00001
3	0.244	.24392	.00454	.00033
4	0.7048	.70457	.00167	.00033
5	0.33616	.33562	.00363	.00161
10	0.55369	.55481	.00232	.00202

The table show that the computer routines are clearly generating first order Markov chains. The only two violations which occur at n=8,10 for N=100,000, are out of acceptable error limit by less than .1%, which we do not consider significant. With confidence that the chain generation is correct, we can rearrange Equation B.105 to give another important statistic tool. We might like to generate a chain with C_d=.5 and $P_{d,d}$=0.1; with a 99% confidence that the relative errors will be no greater than 1%. Solving Equation B.105 for N we have

$$N = \frac{a^2}{E^2}\left(\frac{1}{P_{d,d}(n)} - 1\right) \qquad \text{(B.106)}$$

$P_{d,d}$=0.1 is the most severe constraint of any $P_{d,d}(n)$ with E=.01 and a=2.58, we have

$N \geq 599,076 \simeq 600,000$ atoms

We must generate quite long chains to insure a high degree of statistic accuracy in the chains.

From this analysis, we note that, for a given length chain, the C_d=.5, random chain will contain the smallest overall statistical errors of any binary chain. In this case $P_{\ell m}(n)$=.5 for all n, whereas any other concentration and short-range order will give some $P_{\ell,m}(n)<.5$ (ℓ,m=h or d) and therefore insures higher errors. Very low or high concentration of a given constitutent as well as a high degree of correlation will greatly increase overall statistical errors.

Although we have not presented a statistical analysis for other C_d and $P_{d,d}$ and for the second order Markov chain, computer studies have been performed to verify the validity of these computer programs.

APPENDIX C

SHORT-RANGE ORDER PARAMETERS

X-ray and neutron scattering have provided solid state experimentalists with a powerful technique for examining the structure of solids. The differential scattering cross-section per unit solid-angle $\frac{d\sigma}{d\Omega}$ in the Born approximation is given by

$$\frac{d\sigma}{d\Omega} = \frac{k'}{k}\left|\frac{1}{4\pi}\frac{2\mu}{\hbar^2}\int e^{i(\vec{k}-\vec{k}')\cdot\vec{r}}\, V(\vec{r})\, d\vec{r}\right|^2 \qquad (C.1)$$

where $\vec{k}$ is the incident wave vector
$\vec{k}'$ is the reflected wave vector
μ is the reduced mass in the center of mass system
and $V(\vec{r})$ is the interaction between the incident wave and the scattering center.

The interaction $V(\vec{r})$ is the electron density for x-ray scattering, and $V(\vec{r})$ is the nuclear density for neutron scattering. In the case of elastic scattering, we have $k=k'$. We recall that the Born approximation is valid only when the scattering center is quite localized and has a sufficiently small scattering strength.[44]

For the perfect crystal, the scattering potential $V(\vec{r})$ will be periodic or translationally invariant.

$$V(\vec{r}+\vec{\ell}) = V(\vec{r}) \qquad (C.2)$$

where $\vec{\ell} = \ell_1\vec{a}_1+\ell_2\vec{a}_2+\ell_3\vec{a}_3$, ℓ_1,ℓ_2,ℓ_3 are integers, and $\vec{a}_1,\vec{a}_2,\vec{a}_3$ are the basis vectors of the primitive lattice cell.

Rewritting $V(\vec{r})$ as

$$V(\vec{r}) = \sum_{\vec{G}} V_{\vec{G}} e^{i\vec{G}\cdot\vec{r}} \tag{C.3}$$

then

$$V(\vec{r}+\vec{\ell}) = V(\vec{r}) = \sum_{\vec{G}} V_{\vec{G}} e^{i\vec{G}\cdot\vec{r}} e^{i\vec{G}\cdot\vec{\ell}}$$

or

$$\vec{G}\cdot\vec{\ell} = 2\pi n, \quad n=\text{integer} \tag{C.4}$$

$\vec{G}$ is the reciprocal lattice vector of the crystal defined by Equation (C.4).

Using Equation (C.3) in Equation (C.1), we get

$$\frac{d\sigma}{d\Omega} = \frac{k'}{k} \left| \frac{1}{4\pi} \frac{2\mu}{\hbar^2} \sum_{\vec{G}} V_{\vec{G}} \int e^{i(\vec{k}-\vec{k}'+\vec{G})\cdot\vec{r}} d\vec{r} \right|^2$$

$$= \frac{k'}{k} \left| \frac{(2\pi)^3}{4\pi} \frac{2\mu}{\hbar^2} \sum_{\vec{G}} V_{\vec{G}} \delta(\vec{k}-\vec{k}'+\vec{G}) \right|^2 \tag{C.5}$$

or the cross section vanishes unless

$$\vec{k}' = \vec{k}+\vec{G} \tag{C.6}$$

Equation (C.6) is the Bragg reflection law for the perfect crystal.

For the disordered lattice, we must return to Equation (C.1). The integral can be usefully broken into three parts

1. a sum over the lattice sites $\vec{r}_\ell$
2. a sum over the basis $\vec{r}_j'$

3. an integral over the rest of space $\vec{r}''$

$$\int e^{i(\vec{k}-\vec{k}')\cdot\vec{r}} V(\vec{r})\,d\vec{r} = \sum_{\ell,j} \int d\vec{r}'' e^{-i(\vec{\Delta k})\cdot(\vec{r}_\ell+\vec{r}_j+\vec{r}'')} V(\vec{r}'')$$

where $\vec{\Delta k} = \vec{k}'-\vec{k}$

$$= \sum_{\ell} e^{-i\vec{\Delta k}\cdot\vec{r}_\ell} \sum_{j} e^{-i\vec{\Delta k}\cdot\vec{r}_j} \int e^{-i\vec{\Delta k}\cdot\vec{r}''} V(r'')\,d\vec{r}''$$

$$= \sum_{\ell} f(\vec{\Delta k}) e^{-i\vec{\Delta k}\cdot\vec{r}_\ell} \qquad \text{(C.7)}$$

where we define the structure factor by

$$f(\vec{\Delta k}) = \sum_{j} e^{-i\vec{\Delta k}\cdot\vec{r}_j} \int dr'' e^{-i\vec{\Delta k}\cdot\vec{r}''} V(\vec{r}'')$$

The differential scattering cross section is therefore proportional to

$$I\alpha \left| \sum_{\ell} f_\ell(\vec{\Delta k}) e^{i\vec{\Delta k}\cdot\vec{r}_\ell} \right|^2 \qquad \text{(C.8)}$$

This is true for the perfect lattice as well as the disordered one, the only difference is that all $f_\ell(\Delta k)$ are equal for the perfect lattice and can be different for the disordered lattice. For the binary atomic system a lattice point can have a structure factor $f_d(\vec{q})$ or $f_h(\vec{q})$ depending on whether the site is occupied by a defect or a host mass. Rewritting Equation (C.8) we have

$$I\alpha \sum_{\ell\ell'} f_\ell(q) f_{\ell'}(q) e^{i\vec{q}\cdot(\vec{r}_{\ell'}-\vec{r}_\ell)}$$

$$= \sum_{\ell\ell'} f_h^2(q) e^{i\vec{q}\cdot(\vec{r}_{\ell'}-\vec{r}_\ell)}$$

$$+ \sum_{\substack{\ell=d \\ \ell'=h}} [f_h(q) f_d(q) - f_h^2(q)] e^{i\vec{q}\cdot(\vec{r}_{\ell'}-\vec{r}_\ell)}$$

$$+ \sum_{\substack{\ell=h \\ \ell'=d}} [f_h(\vec{q}) f_d(\vec{q}) - f_h^2(\vec{q})] e^{i\vec{q}(\vec{r}_{\ell'}-\vec{r}_\ell)}$$

$$+ \sum_{\substack{\ell=d \\ \ell'=d}} [f_d^2(q) - f_h^2(q)] e^{i\vec{q}\cdot(\vec{r}_{\ell'}-\vec{r}_\ell)} \qquad (C.9)$$

We can further simplify this equation by the introduction of some new quantities

$C_d = \frac{N_d}{N}$ - The concentration of defects where N_d is the number of defects in the system and N is the total number of particles.

$$\theta^d(\vec{\ell}) = \begin{cases} 1 \text{ if atom at site } \vec{\ell} \text{ is a defect} \\ 0 \text{ if atom at site } \vec{\ell} \text{ is a host} \end{cases}$$

$$\theta^h(\vec{\ell}) = \begin{cases} 1 \text{ if atom at site } \vec{\ell} \text{ is a host} \\ 0 \text{ if atom at site } \vec{\ell} \text{ is a defect} \end{cases}$$

Lets examine the function

$$\rho^{i,j}(\vec{L}) = \frac{1}{N_i} \sum_{\vec{\ell}} \theta^i(\vec{\ell}) \theta^j(\vec{L}+\vec{\ell}) \qquad (C.10)$$

in words, $\rho^{i,j}(\vec{L})$ is the number of times there is an atom of kind i, separated from an atom of kind j by a distance $\vec{L}$ in the whole crystal divided by the number of

atoms of type i in the crystal. Clearly, $\rho^{i,j}(\vec{L})$ is defined only for lattice points.

$$\text{Since } \theta^{h}(\vec{\ell}) + \theta^{d}(\vec{\ell}) = 1 \tag{C.11}$$

we have the following relationships

$$\rho^{h,d}(\vec{L}) + \rho^{h,h}(\vec{L}) = 1 \tag{C.12}$$

$$\rho^{d,d}(\vec{L}) + \rho^{d,h}(\vec{L}) = 1 \tag{C.13}$$

Next we look at the following

$$\rho^{j,i}(\vec{L}) = \frac{1}{N_j} \sum_{\ell} \theta^{j}(\vec{\ell})\theta^{i}(\vec{L}+\vec{\ell})$$

$$= \frac{1}{N_j} \sum_{\ell} \theta^{i}(\vec{\ell})\theta^{j}(\vec{\ell}-\vec{L}) \tag{C.14}$$

Comparing Equation (C.14) with Equation (C.10), we get the important result

$$N_i \rho^{i,j}(\vec{L}) = N_j \rho^{j,i}(-\vec{L}) \tag{C.15}$$

If we have an isotropic crystal, then

$$N_i \rho^{i,j}(L) = N_j \rho^{j,i}(L)$$

which, if we divide each side N, gives for the binary chain

$$C_d \rho^{d,h}(L) = C_h \rho^{h,d}(L) \tag{C.16}$$

$\rho^{i,j}(L)$ is also called the conditional pair correlation function between atoms i and j separated by a distance L.

By using the θ function we can eliminate the restricted sums in Equation (C.9) and we get

$$I\alpha \sum_{\vec{\ell}\vec{\ell}'} [f_h^2(q)+\theta^d(\vec{\ell})\theta^h(\vec{\ell}')(f_h(q)f_d(q)-f_h^2(q))$$

$$+\theta^h(\vec{\ell})\theta^d(\vec{\ell}')(f_h(q)f_d(q)-f_h^2(q))$$

$$+\theta^d(\vec{\ell})\theta^d(\vec{\ell}')(f_d^2(q)-f_h^2(q)]e^{i\vec{q}\cdot(\vec{r}_\ell-\vec{r}_{\ell'})}$$

if we take $\vec{r}_\ell-\vec{r}_{\ell'}=\vec{L}$ the sum now goes over $\vec{L}$ and $\vec{\ell}'$. With $\vec{\ell}=(\vec{\ell}'+\vec{L})$, we get

$$I\alpha \sum_{\vec{L}} [\sum_{\vec{\ell}'} f_h^2(q) + \sum_{\ell'} \theta^d(\vec{\ell}+\vec{L})\theta^h(\vec{\ell}')(f_h(q)f_d(q)-f_h^2(q))$$

$$+ \sum_{\ell'} \theta^h(\vec{\ell}'+\vec{L})\theta^d(\vec{\ell}')(f_h(q)f_d(q)-f_h^2(q))$$

$$+ \sum_{\ell'} \theta^d(\vec{\ell}'+\vec{L})\theta^d(\vec{\ell}')(f_d^2(q)-f_h^2(q))]e^{i\vec{q}\cdot\vec{L}}$$

or

$$I\alpha \sum_{L} \{Nf_h^2(q)+N_h\rho^{h,d}(L)[f_h(q)f_d(q)-f_h^2(q)]$$

$$+N_d\rho^{d,h}(L)(f_h(q)f_d(q)-f_h^2(q))$$

$$+N_d\rho^{d,d}(L)(f_d^2(q)-f_h^2(q))\}e^{i\vec{q}\cdot\vec{L}}$$

where Equation (C.10) has been employed. Using Equation (C.16) with Equation (C.13) and dividing by N, we get

$$I\alpha \sum_{\ell} e^{i\vec{q}\cdot\vec{\ell}}(f_h^2(q)+2C_d(1-\rho^{d,d}(\ell))(f_h(q)f_d(q)-f_h^2(q))$$

$$+C_d(f_d^2(q)-f_h^2(q))\rho^{d,d}(\ell)) \qquad (C.17)$$

These pair correlations functions can be expressed in terms of the Warren-Cowley short-range order parameters α as

$$\rho^{d,d}(\ell) = C_d+(1-C_d)\alpha_{0,\ell} \tag{C.18}$$

Equation (C.17) becomes with rearrangement

$$I\alpha \sum_{\ell} e^{i\vec{q}\cdot\vec{\ell}}[(f_h(q)(1-C_d)+f_d(q)C_d)^2+C_d(1-C_d)\alpha_{0,\ell}[f_d(q)-f_h(q)]^2 \tag{C.19}$$

Relationship of the Pair Correlation Function to the Markov Probabilities

Examining Equation (C.10) in the limit as N_i goes to infinity with N_i/N held constant, $\rho^{i,j}(L)$ is the conditional probability that starting at state i,L sites away the site will be occupied by a state j. Specifically, $\rho^{d,d}(n)$ is the conditional probability that starting at a defect, n sites away the site will be occupied by a defect. The relationship between the pair correlation functions and the first order Markov chain probabilities can now be simply expressed. First, to start at a defect, the initial unconditional probability vector is

$$p(0) = [p_h(0)=0,\ p_d(0)=1] \tag{C.20}$$

Then,

$$\rho^{d,d}(n) = p_d(|n|) \tag{C.21}$$

where $p(n) = p(0)P^n$

using Equation (B.96) for P^n, we get

$$[p_h(n), p_d(n)] = [0,1]\begin{pmatrix} 1-C_d & C_d \\ 1-C_d & C_d \end{pmatrix} + [0,1]\begin{pmatrix} C_d & -C_d \\ -(1-C_d) & (1-C_d) \end{pmatrix}\left(\frac{P_{d,d}-C_d}{1-C_d}\right)^n$$

and

$$p_d(|n|) = \rho^{d,d}(n) = C_d + (1-C_d)\left(\frac{P_{d,d}-C_d}{1-C_d}\right)^{|n|} \qquad (C.22)$$

or

$$\rho^{d,d}(n) = P_{d,d}(|n|) \qquad (C.23)$$

Comparing this equation with Equation (C.18) we see

$$\alpha_{0,n} = \left(\frac{P_{d,d}-C_d}{1-C_d}\right)^n = (\alpha_{01})^n \qquad (C.24)$$

where $\alpha_{0,1} = \left(\frac{P_{d,d}-C_d}{1-C_d}\right)$

For the second order Markov chain, the pair correlation functions are not as easily computed. To calculate $\rho^{d,d}(n)$, the initial state must be taken as a linear combination of the states p_{hd} and p_{dd} normalized to unity and is given as

$$(0) = [p_{hh}=0, p_{hd}=C_{hd}/C_d,\ p_{dh}=0, p_{dd}=C_{dd}/C_d] \qquad (C.25)$$

$$= [0, (1-P_{dd,d})/(1+P_{hd,d}-P_{dd,d}), 0,\ P_{hd,d}/(1+P_{hd,d}-P_{dd,d})]$$

where we employ Equations (3.96) and (3.97).

Then,

$$\rho^{d,d}(n) = p_{dd}(|n|)+p_{hd}(|n|)$$

where again $p(n) = p(0)P^n$

Next, we will examine $\rho^{d,d}(n)$ for the three special cases of the second order Markov chain described in Appendix B.

Case 1: First order Markov chain equivalent

$$P_{dd,d}=P_{hd,d};\ P_{hh,d}=P_{dh,d} \text{ and}$$
$$P_{hh,d}=C_d(1-P_{dd,d})/1-C_d)$$

For this case, the initial unconditional probability vector is

$$P(0) = [0,\ (1-P_{dd,d}), 0,\ P_{dd,d}] \qquad (C.26)$$

Using Equation (B.100) for P^n

$$p_{dd}(n)= -\delta_{n,0}(1-P_{dd,d})(P_{dd,d}(1-2C_d+C_dP_{dd,d})$$

$$+\delta_{n,0}(-P_{dd,d})(C_d)(1-P_{dd,d})^2$$

$$+C_d(P_{dd,d})(1-P_{dd,d}+P_{dd,d})$$

$$+\left(\frac{P_{dd,d}-C_d}{1-C_d}\right)^{n-1}(1-C_d)\ (P_{dd,d})(1-P_{dd,d}+P_{dd,d})$$

$$P_{dd}(n) = -\delta_{n,0}\ (1-P_{dd,d})(1-C_d)P_{dd,d}$$

$$+C_d\ P_{dd,d}+\left(\frac{P_{dd,d}-C_d}{1-C_d}\right)^{n-1}(1-C_d)P_{dd,d} \qquad (C.27)$$

$$P_{hd}(n) = \delta_{n,0}(1-P_{dd,d})(P_{dd,d})(1-C_d)$$

$$+C_d(1-P_{dd,d})+\left(\frac{P_{dd,d}-C_d}{1-C_d}\right)^{n-1}(-C_d)(1-P_{dd,d}) \qquad (C.28)$$

Therefore

$$\rho^{d,d}(n) = P_{dd}(|n|) + P_{hd}(|n|) = C_d+\left(\frac{P_{dd,d}-C_d}{1-C_d}\right)^{|n|-1}(P_{dd,d}-C_d)$$

$$\rho^{d,d}(n) = C_d+(1-C_d)\left(\frac{P_{dd,d}-C_d}{1-C_d}\right)^{|n|} \qquad (C.29)$$

For the first-order-equivalent second order chain the Markov transition probabilities $P_{ij,k}$ were chosen to be independent of the first atom i. They therefore simulate the first order chain; thus $P_{dd,d}=P_{hd,d}=P_{d,d}$ in the notation of the first order chain. Using this fact we note that the equivalence between this equation and Equation (C.22) demonstrates that the calculational method of finding $\rho^{d,d}(n)$ for the second order Markov chain is correct.

Case 2. $P_{dd,d}=P_{dh,d}$; $P_{hh,d}=P_{hd,d}$ and
$P_{hh,d}=C_d(1-P_{dd,d})/(1-C_d)$

For this case the initial unconditional probability vector is

$$p(0) = [0,\ 1-C_d, 0, C_d] \tag{C.30}$$

Using Equation (B.101) for P^n, we can write

$$p_{dd}(n)=C_d^2-C_d(1-P_{dd,d})[\tfrac{1}{2}\, a^{n/2}(\frac{1}{(1-\sqrt{a})^2}+\frac{(-1)^n}{(1+\sqrt{a})^2})$$

$$-\tfrac{1}{2}a^{(n-1)/2}(\frac{1}{(1-\sqrt{a})^2}-\frac{(-1)^n}{(1+\sqrt{a})^2})]$$

$$\text{where } a = \frac{(P_{dd,d}-C_d)}{1-C_d}$$

and

$$p_{hd}(n) = C_d(1-C_d)+(1-C_d)(1+P_{dd,d})[\tfrac{1}{2}a^{n/2}(\frac{1}{(1-\sqrt{a})^2}+\frac{(-1)^n}{(1+\sqrt{a})^2})]$$

$$+(C_d-2P_{dd,d}+C_dP_{dd,d})[\tfrac{1}{2}a^{(n-1)/2}(\frac{1}{(1-\sqrt{a})^2}-\frac{(-1)^n}{(1+\sqrt{a})^2}]$$

Therefore, after some simplification

$$\rho^{d,d}(n)=C_d+(1-2C_d+P_{dd,d})[\tfrac{1}{2}a^{|n|/2}(\frac{1}{(1-\sqrt{a})^2}+\frac{(-1)^{|n|}}{(1+\sqrt{a})^2})]$$

$$+(C_d-P_{dd,d})a^{(|n|-1)/2}[\frac{1}{(1-\sqrt{a})^2}-\frac{(-1)^{|n|}}{(1+\sqrt{a})^2}]$$

$$\rho^{d,d}(n)=C_d+(1-C_d)(\frac{P_{dd,d}-C_d}{1-C_d})^{|n|/2}\tfrac{1}{2}[1+(-1)^{|n|}] \tag{C.31}$$

Comparing this equation with (C.18), we see

$$\alpha_{0,2\ell+1} = 0$$

$$\alpha_{0,2\ell} = \left(\frac{P_{dd,d}-C_d}{1-C_d}\right)^{|\ell|} \tag{C.32}$$

The Fourier transform of Equation (C.32) is

$$\alpha(q) = \sum_{\ell=-\infty}^{\infty} e^{iq\ell a}\alpha_{o,\ell} = \sum_{\ell=-\infty}^{\infty} e^{iq2\ell a}\left(\frac{P_{dd,d}-C_d}{1-C_d}\right)^{|\ell|}$$

$$= 1+2\sum_{\ell=1}^{\infty} \cos(2q\ell a)(\alpha_2)^{\ell}$$

where $\alpha_2 = (P_{dd,d}-C_d)/(1-C_d)$

Therefore,

$$\alpha(q) = \frac{1-\alpha_2^2}{1-2\alpha_2\cos(2qa)+\alpha_2^2} \tag{C.33}$$

Case 3: $P_{dd,d}=P_{hh,d}$; $P_{hd,d}=P_{dh,d}=1-P_{dd,d}$ and $C_d=.5$

For this case, the initial uncondition probability vector is

$$p(0) = [0,\ \tfrac{1}{2},\ 0,\ \tfrac{1}{2}] \tag{C.34}$$

Since in Equation (B.102) we have not explicitly written out P^n, we will solve explicitly for the elements we need. Since $p(n) = p(0)\ P^n$ and we require only $p_{dd}(n)$ and $p_{hd}(n)$, we need to solve for only four elements of the matrix (2,2), (2,4), (4,2) and (4,4).

If for convenience we let an element of P^n be given by Q_{ij}, then

$$p_{dd}(n) = \tfrac{1}{2}\ (Q_{42}+Q_{44})$$

$$p_{hd}(n) = \tfrac{1}{2}\ (Q_{22}+Q_{24})$$

The pair correlation function is

$$\rho^{d,d}(n) = \tfrac{1}{2}(Q_{22}+Q_{24}+Q_{42}+Q_{44})$$

Now, instead of writing out each Q_{ij} needed, an examination of the B_{ij} and C_{ij} coefficients in Equation (B.102) shows a running sum of the four Q_{ij} will greatly simplify the results. In fact, we get

$$\Sigma(B_{ij}) = 1/3$$

and

$$\Sigma(C_{ij}) = 1/3\ e^{i\pi n/3}$$

Finally

$$\rho^{d,d}(n) = \tfrac{1}{2}+\tfrac{1}{2}[1/3(1-2P_{dd,d})^{2n/3}(1+2(-1)^{n}\cos(\tfrac{\pi n}{3}))] \qquad (C.35)$$

We next examine three cases for Equation (C.35)

Case 1: $\rho^{d,d}(3n-2)=\tfrac{1}{2}+\tfrac{1}{2}(1/3(1-2P_{dd,d})^{(6n-4)/3}(1+2(-1)^{3n-2}\cos(\frac{\pi(3n-2)}{3})$

but

$$\cos(n\pi-\tfrac{2\pi}{3}) = \cos(n\pi)\cos(\tfrac{2\pi}{3}) \text{ since } \sin(n\pi)=0$$

$$= (-1)^{n}(-\tfrac{1}{2})=\tfrac{1}{2}(-1)^{n+1}$$

therefore

$$2(-1)^{3n-2}\tfrac{1}{2}(-1)^{n+1} = (-1)^{4n}(-1) = -1$$

and

$$\rho^{d,d}(3n-2) = \tfrac{1}{2} \qquad \text{(C.36a)}$$

Case 2: $\rho^{d,d}(3n-1) = \tfrac{1}{2}+\tfrac{1}{2}[1/3(1-2P_{dd,d})^{(6n-2)/3}(1+2(-1)^{3n-1}\cos(\frac{\pi(3n-1)}{3})$

again

$$\cos(\pi n - \tfrac{\pi}{3}) = \cos\pi n \cos\tfrac{\pi}{3} = \tfrac{1}{2}(-1)^n$$

and

$$\rho^{d,d}(3n-1) = \tfrac{1}{2} \qquad \text{(C.36b)}$$

Case 3: $\rho^{d,d}(3n) = \tfrac{1}{2}+\tfrac{1}{2}(1/3(1-2P_{dd,d})^{2n}(1+2(-1)^{3n}\cos(\pi n))$

since $(-1)^{3n}\cos(n\pi) = (-1)^{4n} = 1$

$$\rho^{d,d}(3n) = \tfrac{1}{2}+\tfrac{1}{2}(1-2P_{dd,d})^{2n} \qquad \text{(C.36c)}$$

Comparing these equations with Equation (C.18) for $C_d=\tfrac{1}{2}$, we see

$$\begin{aligned} \alpha_{0,3\ell-2} &= 0 \\ \alpha_{0,3\ell-1} &= 0 \qquad \text{(C.37)} \\ \alpha_{0,3\ell} &= (1-2P_{dd,d})^{2|\ell|} \end{aligned}$$

If we take the Fourier transformation, we have

$$\alpha(q) = \sum_{\ell=-\infty}^{\infty} e^{iq\cdot\ell a}\alpha_{0,\ell} = \sum_{\ell=-\infty}^{\infty} e^{3iq\ell a}(1-P_{dd,d})^{2|\ell|}$$

$$= 1+2\sum_{\ell=1}^{\infty}\cos(3q\ell a)\alpha_3^{\ell}$$

$$\alpha(q) = \frac{1-\alpha_3^2}{1-2\alpha_3\cos 3qa+\alpha_3^2} \qquad \text{(C.38)}$$

where $\alpha_3 = (1-P_{dd,d})^2$

APPENDIX D

NUMERICAL COMPUTATION OF EIGENVECTORS OF CHAINS

Given an eigenvalue of a matrix one can calculate the corresponding eigenvector. By the method of bisection described in Appendix A, we can compute the eigenvalue of the linear chain to any desired accuracy. For a computed eigenvalue, λ, the computation of the corresponding eigenvector seems at first almost trival. Using Equation A.1, we can write

$$X_{i+1} = \frac{1}{b_{i+1}} [(\lambda - a_i) X_i - b_i X_{i-1}] \qquad (D.1)$$

where $X_i = \sqrt{m_i}\, U_i$ (U_i is the displacement of the i^{th} atom)

$$b_{i+1} = -\gamma / \sqrt{m_i m_{i+1}}$$

and $$a_i = \frac{2\gamma}{m_i}$$

Equation D.1 requires initial conditions to be complete. For fixed boundary conditions, $X_o = 0$. Arbitrarily, we take $X_1 = 1$, since $X_1 = 0$ would give all $X_i = 0$. Then, Equation D.1 allows us to compute all X_i's and correspondingly the U_i's. In terms of the leading principle minors

$$X_r = (-1)^{r-1} P_{r-1}(\lambda) / b_2 b_3 \ldots b_r \quad (r = 2, \ldots, n) \qquad (D.2)$$

Unfortunately eigenvectors computed in this manner can be completely wrong. The procedure will in fact work when the exact eigenvalue is given and exact computations are performed. However, although we compute on eigenvalue

to 8 significant digits, it is not exact. In fact, the computation of X_{N+1} will not usually give 0 as specified by the fixed boundary condition but

$$b_{N+1}X_{N+1} = \delta = -b_N X_{n-1} + (\lambda - a_N)X_N \neq 0 \tag{D.3}$$

In the matrix form of Equation A.1, we have

$$(\underline{\underline{B}} - \lambda \underline{\underline{I}})\ \underline{X} = \delta \underline{e}_n \tag{D.4}$$

where e_n is the n^{th} column of the identity matrix. For simplicity, we can renormalize X to give

$$(\underline{\underline{B}} - \lambda \underline{\underline{I}})\ \underline{X} = \underline{e}_n$$

or

$$\underline{X} = (\underline{\underline{B}} - \lambda \underline{\underline{I}})^{-1} \underline{e}_n \tag{D.5}$$

Next for $\lambda_1 > \lambda_2 > \lambda_3 >> \lambda_N$, the approximate eigenvalue is almost λ_k or $(\lambda - \lambda_k)$ "small" and $(\lambda - \lambda_i)(i \neq k)$ "not small". Let $\underline{V}_1, \underline{V}_2, \ldots, \underline{V}_N$ be the exact set of eigenvectors of $\underline{\underline{B}}$ corresponding to $\lambda_1, \lambda_2, \ldots, \lambda_N$. We can expand the vector $\underline{e}_n$ in terms of these eigenvectors

$$\underline{e}_n = \sum_{i=1}^{N} \gamma_i \underline{V}_i \tag{D.6}$$

where $\sum_{i=1}^{N} \gamma_i^2 = 1$.

Rewriting Equation D.5, we have

$$\underline{X} = \sum_{i=1}^{N} \frac{\gamma_i \underline{V}_i}{\lambda_i - \lambda} = \frac{\gamma_k \underline{V}_k}{\lambda_k - \lambda} + \sum_{i \neq k} \gamma_i \underline{V}_i / (\lambda_i - \lambda) \qquad (D.7)$$

For $\underline{X}$ to be a good approximation to $\underline{V}_k$ we require

$$\frac{\gamma_k}{\lambda_k - \lambda} >> \frac{\gamma_i}{(\lambda_i - \lambda)} \quad (i \neq k). \qquad (D.8)$$

Often, $\lambda_k - \lambda >> \gamma_k$ and Equation D.8 is not fulfilled. Solving Equation D.6 for γ_k we have

$$\gamma_k = \underline{V}_k^T e_n \qquad (D.9)$$

Therefore, any time, the last (N^{th}) component of the eigenvector is >>1, the eigenvector $\underline{X}$ calculated by this procedure will usually be incorrect. The procedure would work if we computed the eigenvalue and carried all computations to greater accuracy by five or six digits than the value of the N^{th} component of V_k. Given $\underline{V}_k \underline{V}_k^T = 1$, and $(\underline{V}_k)_N = 10^{-20}$, then computations to 26-30 digits would give accurate results. In practice, this method fails on disordered linear chains working to 18 digit accuracy for chains of length N>30.

If we knew apriori that the r^{th} component of $\underline{V}_k$ was <u>not</u> small, we could take $X_r = 1$ instead of $X_1 = 1$, and reiterate the Equation D.1 to a correct solution.

A more satisfactory method of computing eigenvectors is that of inverse reiteration. First, consider the set of equations

$$(\underline{\underline{B}}-\lambda\underline{\underline{I}})\ \underline{X} = \underline{C} \tag{D.10}$$

where $\underline{C}$ is an arbitrary vector normalized to one. We can, as before, write $\underline{C}$ in terms of the exact eigenvectors $\underline{V}$ of $\underline{\underline{B}}$,

$$\underline{C} = \sum_{i=1}^{N} \gamma_i \underline{V}_i \tag{D.11}$$

For λ close to λ_k, Equation D.7 shows that $\underline{X}$ is much richer in the $\underline{V}_k$ than is $\underline{C}$, namely by a factor $\frac{1}{\lambda-\lambda_k} >> 1$, since Equation D.11 gives

$$\gamma_k = \underline{V}_k^T \underline{C} \tag{D.12}$$

Next, we solve the equation

$$(\underline{\underline{B}}-\lambda\underline{\underline{I}})\underline{Y} = \underline{X} \tag{D.13}$$

$\underline{Y}$ can similarly be expanded in terms of the eigenvectors of $\underline{\underline{B}}$.

$$\underline{Y} = \sum_i \delta_i \underline{V}_i/(\lambda-\lambda_i) \tag{D.14}$$

where

$$\delta_k = \underline{V}_k^T\ \underline{X} = \frac{\gamma_k}{\lambda-\lambda_k} = \frac{\underline{V}_k^T \underline{C}}{\lambda-\lambda_k} \tag{D.15}$$

Therefore,

$$\underline{y} = (\underline{V}_k^T \underline{C})\ V_k/(\lambda-\lambda_k)^2 + \sum_{i\neq k} \delta_i \underline{V}_i/(\lambda-\lambda_i) \qquad (D.16)$$

This process can be reiterated to any desired accuracy for $\underline{V}_k$. If, for example, we take $(\lambda-\lambda_k)=10^{-8}$ with $\gamma_k=10^{-12}$, the first reiteration gives $\gamma_k/(\lambda-\lambda_k)=10^{-4}$ or $\underline{X}$ is very deficient in V_k but the second reiteration gives $\sigma_k/(\lambda-\lambda_k)^2=10^4$ or $\underline{y}$ is quite a good approximation to $\underline{V}_k$. As long as $\underline{C}$ is not orthogonal to $\underline{V}_k$ the method will always work given $(\lambda-\lambda_k)$ "small" compared to $(\lambda-\lambda_i)(i\neq k)$.

Applying this approach requires the inversion of the matrix $(\underline{B}-\lambda\underline{I})$. Since this matrix is tridiagonal, the method of triangularization, also called Gaussian elimination with partial pivoting, is the most efficient. We look at the elements in Equation D.10 as follows

$$\left(\begin{array}{ccccccc|c}
a_1-\lambda & b_2 & & & & & & C_1 \\
b_2 & a_2-\lambda & b_3 & & & 0 & & C_2 \\
 & b_3 & a_3-\lambda & b_4 & & & & C_3 \\
 & & \ddots & \ddots & \ddots & & & \vdots \\
 & & & & & b_n & a_n-\lambda & C_n
\end{array}\right) \qquad (D.17)$$

We start by comparing the elments in the first column,

1. if $|b_2| > a_i-\lambda$, we exchange the elements of rows one and two; otherwise, we do nothing. Denoting the nonzero elements in row one by U_1, V_1, w_1, and d_1 and those in row two by X_2, y_2, z_2, and d_2', we have

$$U_1 = b_2,\ V_1 = \alpha_2-\lambda,\ w_1 = b_3,\ d_1 = C_2$$

and $$X_2 = a_1-\lambda,\ y_2 = b_2,\ z_2 = 0,\ d_2' = C_1$$

for $|b_2| > (a_1-\lambda)$, or

$$U_1 = a_1-\lambda,\ V_1 = b_2,\ w_1 = 0,\ d_1 = C_1$$

and $$X_2 = b_2,\ y_2 = \alpha_2-\lambda,\ z_2 = b_3,\ d_2' = C_2,$$

otherwise,

2. we compute

$m_2 = X_2/U_1$ and replace X_2 by zero.

3. compute

$$P_2 = y_2-m_2V_1$$

$$q_2 = z_2-m_2w_1$$

$$C_2' = d_2'-m_2d_1$$

then, replace

y_2 by P_2,

z_2 by q_2

and d_2' by C_2'

Matrix D.17 looks like

$$m_2 \left(\begin{array}{ccccc|c} U_1 & V_1 & w_1 & & & d_1 \\ 0 & P_2 & q_2 & & 0 & C_2' \\ & b_3 & a_3-\lambda & b_4 & \cdot & C_3 \\ & & \cdot & \cdot & \cdot & \\ & & & \cdot & ; & \\ & 0 & & b_n & a_n-\lambda & C_n \end{array} \right) \qquad \text{(D.18)}$$

For the r^{th} step, we proceed as follows

1. If $|b_{r+1}|>P_r$, we interchange the r and r+1 rows. If $|b_{r+1}|>P_r$, we have $U_r=b_{r+1}$, $V_r=a_{r+1}-\lambda$, $w_r=b_{r+2}$, $d_r=C_{r+1}$, and $X_{r+1}=P_r$, $y_{r+1}=q_r$, $z_{r+1}=0$, $d_{r+1}'=C_r'$

otherwise

$U_r = P_r$, $U_r = q_r$, $w_r = 0$, $d_r = C_r'$

and $X_{r+1}=b_{r+1}$, $y_{r+1}=a_{r+1}-\lambda$, $z_{r+1}=b_{r+2}$, $d_{r+1}'=C_{r+1}$

2. We compute $m_{r+1}=X_{r+1}/U_r$ and replace X_{r+1} by zero.

3. Compute

$$P_{r+1} = y_{r+1}-m_{r+1}V_r$$

$$q_{r+1} = z_{r+1}-m_{r+1}w_r$$

$$C'_{r+1} = d'_{r+1}-m_{r+1}d_r$$

and replace

y_{r+1} by P_{r+1}

z_{r+1} by q_{r+1}

d'_{r+1} by C'_{r+1}

The r^{th} principle minor of $(\underline{B}-\lambda\underline{I})$ is, (also given by Equation A.3)

$$P_i(\lambda) = (-1)^{k_i} U_1U_2U_3\cdots U_{i-1}P_i \qquad (D.19)$$

where k_i is the total number of row interchanges occurring to the end of (i-1) steps. Therefore, the process of triangularization could also be used to determine eigenvalues.

We can now solve for the eigenvector $\underline{X}$ given by Equation D.10

$$X_N = C'_N/P_N$$

$$X_{N-1} = (d_{N-1}-X_N V_{N-1})/U_{N-1} \qquad (D.20)$$

$$X_i = (d_i-X_{i+1}V_i-X_{i+2}w_i)/U_i$$

$$(1\leq i\leq N-2)$$

If λ is the exact eigenvalue P_N would be zero. Usually, it is not zero, however, if it is we need only to take $P_N<<1$.

On the first reiteration, since C, is an arbitrary initial vector, we can pick $\underline{d}$ saving a calculation of $\underline{d}$ from $\underline{C}$. We take all $d_i=\frac{1}{\sqrt{N}}$. This choice is not necessarily the best for all cases but it works in every case we have encountered. Once we have $(\underline{B}-\lambda\underline{I})$ in triangular form, it does not have to be recalculated on successive reiterations. We therefore only have to compute $\underline{d}$ from the initial vector $\underline{X}$. From step 1 in the reiteration we notice that $w_r=0$ if no exchange took place in the r^{th} step; otherwise, $w_r\neq 0$. Therefore, we have

1. If $w_r=0$, we compute $d_r=X_r$ and $d_{r+1}=X_{r+1}-m_{r+1}d_r$.
2. If $w_r\neq 0$, we interchange the elements X_r and X_{r+1}, then calculate $d_r=X_{r+1}$ and $d_{r+1}=X_r-m_{r+1}d_r$.

Then, we can reapply Equation D.20.

Once, we get the eigenvector of $(\underline{\underline{B}}-\lambda\underline{\underline{I}})$, we must finally return to the displacements

$$U_i = X_i/\sqrt{m_i} \qquad (D.21)$$

and renormalize $\underline{U}$ to unity.

APPENDIX E

GREEN'S FUNCTION FOR THE MONATOMIC CHAIN

We will examine the Green's function of a monatomic linear chain in the harmonic approximation in two ways. First, we will explicitly calculate the general Green's function $g(\ell,\ell';\omega)$ from the k space transformation given by Equation (5.12). Next, since diagonal elements or near diagonal elements of $g(\ell,\ell',\omega^2)$ are all that are usually required in calculation of thermodynamic quantities, we will examine a simple method of calculating these from the inverse Green function. Since this method does not require a k space transformation, it will be useful for calculating the impurity mode frequencies of defect clusters in a host medium and for calculating the density of states of an n site periodic system. These applications will be described in the next two appendices.

Using Equation (1.10) for the monatomic lattice, we can rewrite Equation (5.12) as

$$g(k,k';\omega) = \frac{\delta_{k,k'}}{\omega^2-\omega_m^2\sin^2(\frac{ka}{2})} \qquad (E.1)$$

where $\omega_m^2 = \frac{4\gamma}{m}$

The transformation into real space gives

$$g(\ell,\ell';\omega^2) = \frac{1}{Nm}\sum_k \frac{e^{ikLa}}{\omega^2-\omega_m^2\sin^2(\frac{ka}{2})} \qquad (E.2)$$

where $L = \ell - \ell'$ and

$$k = \frac{2\pi}{aN}(n), \quad n=0,1,2..;N-1$$

For N , the sum over k can be converted to an integral,

$$\sum_k \to \frac{Na}{2\pi} \int_0^{\frac{2\pi}{a}} dk \tag{E.3}$$

Therefore,

$$g(L,\omega^2) = \frac{a}{2\pi m} \int_0^{\frac{2\pi}{a}} \frac{e^{ikLa} dk}{\omega^2 - \omega_m^2 \sin^2 \frac{ka}{2}} \tag{E.4}$$

Let $z = e^{\pm ika}$ for $L(\gtrless)0$ (E.5)

$$g(L;\omega^2) = \pm \frac{2}{i\pi m} \oint \frac{z^{|L|} dz}{\omega_m^2 z^2 + (4\omega^2 - 2\omega_m^2) z + \omega_m^2} \tag{E.6}$$

where the integral is around the unit circle (clockwise (-), counterclock wise (+))

The only contributions to the integral will be from poles of the integrand inside the unit circle. These poles are

$$z_\pm = -2\left(\frac{\omega}{\omega_m}\right)^2 + 1 \pm 2\sqrt{\left(\frac{\omega}{\omega_m}\right)^2}\sqrt{\left(\frac{\omega}{\omega_m}\right)^2 - 1} \tag{E.7}$$

$$= -2y+1 \pm 2\sqrt{y}\ \sqrt{y-1} \qquad \text{where } y = \left(\frac{\omega}{\omega_m}\right)^2$$

For $y \geq 1$, we have

$$z(1) = -1$$

and $$z(\infty) = \lim_{y\to\infty} \left(-2y-1 \pm 2y\left(1-\tfrac{1}{2}\,\frac{1}{y}+0\left(\frac{1}{y^4}\right)\right)\right)$$

$$z(\infty) = \begin{cases} 0 & (+) \\ \infty & (-) \end{cases} \qquad \text{(E.8)}$$

Clearly only the + root is inside the contour and

$$g(L;\omega^2) = \frac{(\pm 2)}{i\pi m\omega_m^2}\,(\pm 2\pi i)\,\mathrm{Res}\left(\frac{z^{|L|}}{(z-z_2)}\right)_{z=z_1}$$

where

$$z_{\substack{1\\2}} = -2y+1 \pm 2\sqrt{y}\,\sqrt{y-1}$$

$$g(L;\omega^2) = \frac{4}{m\omega_m^2}\left(\frac{-2y+1+2\sqrt{y}\sqrt{y-1}}{4\sqrt{y}\,\sqrt{y-1}}\right)^{|L|} \quad (y\geq 1)$$

or

$$g(L;\omega^2) = \frac{(-1)^{|L|}}{m\omega_m^2}\,\frac{(\sqrt{y}-\sqrt{y-1})^{2|L|}}{\sqrt{y}\,\sqrt{y-1}} \quad (y\geq 1) \qquad \text{(E.8)}$$

For $y<1$

$$z = -2y+1 \pm i\,2\sqrt{y}\sqrt{1-y}$$

and $$|z| = (z\cdot z^*)^{\frac{1}{2}} = 1\ . \qquad \text{(E.9)}$$

Both poles are on the contour and the integral has no precise value. However, since we need $g(L,(\omega \pm i\varepsilon)^2)$, we can calculate these directly. First $\omega\to\omega\pm i\varepsilon$ implies $y\to y\pm i\delta$ as long as $\varepsilon<<1$. Therefore,

$$z_{\pm}(y\overset{+}{-}i\delta)=-2(y\overset{+}{-}i\delta)+1\pm 2\sqrt{y\overset{+}{-}i\delta}\ \sqrt{(y\pm i\delta)-1}$$

$$=-2y+1\overset{-}{+}2i\delta\pm 2\left[\sqrt{y}\ \sqrt{y-1}\overset{+}{-}\frac{i\delta(2y-1)}{\sqrt{y}\ \sqrt{y-1}}\right]$$

to first order in δ. For $y<1$, we must show the imaginary parts explicitly, i.e. $\sqrt{y-1}=i\sqrt{1-y}$

$$z_{\pm}(y\overset{+}{-}i\delta)=-2y+1\pm(\overset{+}{-})\ \frac{\delta(2y-1)}{\sqrt{y}\ \sqrt{1-y}}+2i(\pm\sqrt{y}\ \sqrt{1-y}\overset{-}{+}\delta)$$

and

$$|z_{\pm}(y\overset{+}{-}i\delta)|^2=(4y^2-4y+1+4y-4y^2)\pm(\overset{-}{+}(\frac{2\delta(2y-1)^2}{\sqrt{y}\ \sqrt{1-y}}+\delta\sqrt{y}\ \sqrt{1-y})$$

$$|z_{\pm}(y\overset{+}{-}i\delta)|^2=1\pm(\overset{-}{+}2\delta)(1/(\sqrt{y}\ \sqrt{1-y}))$$

For $\omega+i\varepsilon$, z_+ is inside the contour and

for $\omega-i\varepsilon$, z_- is inside the contour.

$$g(L,(\omega+i\varepsilon)^2)=\frac{4}{m\omega_m^2}\ \frac{(-2y+1+2\sqrt{y}\ \sqrt{y-1})^{|L|}}{4\sqrt{y}\ \sqrt{y-1}}$$

$$=\frac{(-1)^L}{m\omega_m^2}\ \frac{(\sqrt{y}-\sqrt{y-1})^{2|L|}}{\sqrt{y}\ \sqrt{y-1}} \qquad \text{(E.10)}$$

or

$$g(L,(\omega+i\varepsilon)^2)=\frac{(-1)^L}{m\omega_m^2}\ \frac{(\sqrt{y}-i\sqrt{1-y})^{2|L|}}{i\sqrt{y}\ \sqrt{1-y}}\ (Y<1) \qquad \text{(E.11)}$$

showing the explicit imaginary part.

Similarly,

$$g(L,(\omega-i\varepsilon)^2)=\frac{(-1)^L}{m\omega_m^2}\,\frac{(\sqrt{y}+i\sqrt{1-y})^{2|L|}}{-i\sqrt{y}\ \sqrt{1-y}} \tag{E.12}$$

$$y=(\frac{\omega}{\omega_m})^2<1$$

In the band $g(0,(\omega\pm i\varepsilon)^2)$ is purely imaginary and outside the band purely real. We can calculate the density of states using Equation (5.18) with $s=1$ and compare the results with Equation (1.11b).

$$D(\omega^2) = \frac{-1}{N\pi}\ \mathrm{Im\ tr}\ (mg(0,(\omega+i\varepsilon)^2)$$

$$= \frac{-1}{\pi}\ \mathrm{Im}\ \frac{1}{\omega_m^2}\ \frac{1}{i\sqrt{(\frac{\omega}{\omega_m})^2}\sqrt{1-(\frac{\omega}{\omega_m})^2}}$$

$$= \frac{1}{\pi}\ \mathrm{Re}(\frac{1}{\sqrt{\omega^2}\sqrt{\omega_m^2-\omega^2}}) \tag{E.13}$$

Inside the band we can rewrite the Green's function in an alternate form. First, define

$$\theta = \sin^{-1}\ \sqrt{y} \tag{E.14}$$

Then $\cos\theta = \sqrt{1-y}$

and $(\sqrt{y}\pm i\sqrt{1-y})^{2|L|}= \pm i(i\ \sin\theta\pm\cos\theta)^{2|L|}$

$$(\pm i)^{2|L|}e^{\mp 2i(L)\theta}=(-1)^{|L|}e^{\mp 2i|L|}$$

Therefore

$$g(L,(\omega\pm i\varepsilon)^2)=2(\mp i)\ \frac{e^{\pm 2i|L|\theta}}{m\omega^2\sin 2\theta} \tag{E.15}$$

Using this form the spectral density is

$$J_L(\omega^2) = \frac{i(g(L,(\omega+i\varepsilon)^2)-g(L,(\omega-i\varepsilon)^2))}{e^{\hbar\omega/\tau}-1}$$

$$= \frac{4}{m\omega_m^2} \frac{\cos(2|L|\theta)}{\sin(2\theta)(e^{\hbar\omega/\tau}-1} \qquad \text{(E.16)}$$

and the pair displacement correlation function is

$$F_L(t) = \frac{4\hbar}{m\omega_m^2} \int e^{i\omega t} \frac{\cos(2|L|\theta)\ d\omega}{\sin(2\theta)(e^{\hbar\omega/\tau}-1)} \qquad \text{(E.17)}$$

with the autocorrelation being

$$F_0 = \frac{2\hbar}{m} \int \frac{e^{i\omega t}\ d\omega}{\omega\sqrt{\omega_m^2-\omega^2}\ (e^{\hbar\omega/\tau}-1)} \qquad \text{(E.18)}$$

Alternative Green's Function Derivation

From Equation (5.8) we can define an inverse Green's function for the perfect monatomic crystal in the harmonic approximation as

$$G^{-1}(\ell,\ell';\omega^2) = (m\omega^2-2\gamma)\delta_{\ell,\ell'}+\gamma\delta_{\ell,\ell'\pm1} \qquad \text{(E.19)}$$

In matrix form, we have an infinite tridiagonal matrix, i.e.

$$G^{-1}(\ell\ell';\omega^2) = \begin{pmatrix} \ddots & & & & \\ & m\omega^2-2\gamma & \gamma & & \\ & \gamma & m\omega^2-2\gamma & \gamma & \\ & & \gamma & m\omega^2-2\gamma & \gamma \\ & & & \gamma & \ddots \end{pmatrix} \qquad \text{(E.20)}$$

If we wish to know $G(\ell,\ell';\omega^2)$ for all ℓ,ℓ' we have to invert this infinite matrix, an impossible job. However, we can find matrix elements of $G(\ell,\ell';\omega^2)$ for $|\ell-\ell'|$ of the order of unity relatively easily. In fact for $L=|\ell-\ell'|$, we have to invert an $(L+1)x(L+1)$ matrix. We will first calculate $g(0,\omega^2)$. We partition the matrix as follows,

$$G^{-1}(\ell,\ell';\omega^2)\quad G(\ell,\ell';\omega^2) = \underline{\underline{1}}$$

$$\left(\begin{array}{c|c|c} \begin{matrix}(a)\\ \gamma\\ \gamma & m\omega^2-2\gamma\end{matrix} & \begin{matrix}(b)\\ o\\ \gamma\end{matrix} & \begin{matrix}(c)\\ o\end{matrix} \\ \hline \begin{matrix}o\\ (d)\end{matrix}\ \gamma & \begin{matrix}m\omega^2-2\gamma\\ (e)\end{matrix} & \gamma\ \begin{matrix}(f)\\ o\end{matrix} \\ \hline & \begin{matrix}\gamma\\ o\end{matrix} & \begin{matrix}m\omega^2-2\gamma & \gamma\\ \gamma & o\\ (i)\end{matrix} \\ \begin{matrix}o\\ (g)\end{matrix} & (h) & \end{array}\right) \left(\begin{array}{c|c|c} A & B & C \\ \hline D & E & F \\ \hline G & H & I \end{array}\right) = \underline{\underline{1}} \qquad (E.21)$$

where G^{-1} and G are similarly partitioned. Notice that $E=G(0,\omega^2)$. We can write the matrix equations

$$\underline{\underline{a}}\ \underline{\underline{B}} + \underline{\underline{b}}\ \underline{\underline{E}} = 0 \Rightarrow \underline{\underline{B}} = -\underline{\underline{a}}^{-1}\underline{\underline{b}}E$$

$$\underline{\underline{d}}\ \underline{\underline{B}} + \underline{\underline{e}}\ \underline{\underline{E}} + \underline{\underline{f}}\ \underline{\underline{H}} = \underline{\underline{1}}$$

$$\underline{\underline{h}}\ \underline{\underline{E}} + \underline{\underline{i}}\ \underline{\underline{H}} = 0 \Rightarrow H = -\underline{\underline{i}}^{-1}\underline{\underline{h}}\underline{\underline{E}}$$

Therefore

$$(\underline{\underline{e}} - \underline{\underline{d}}\underline{\underline{a}}^{-1}\underline{\underline{b}} - \underline{\underline{f}}\underline{\underline{i}}^{-1}\underline{\underline{h}})\underline{\underline{E}} = 1 \qquad (E.22)$$

If we denote the (m,m) element of a^{-1} as the last element of $\underline{\underline{a}}^{-1}$, then $\underline{\underline{d}}\underline{\underline{a}}^{-1}\underline{\underline{b}}=\gamma^2(a^{-1}_{m,m})\delta_{\ell,o}\delta_{\ell',o}$ and $\underline{\underline{f}}\underline{\underline{i}}^{-1}\underline{\underline{h}} = \gamma^2(i^{-1}_{1,1})$ $\delta_{\ell,n}\delta_{\ell',n}$ where ℓ,ℓ' are the element descriptors $e_{\ell,\ell'}$ and n,n the last element of $\underline{\underline{e}}$. For n=1 we have

$$(\underline{\underline{e}}-\gamma^2(a^{-1}_{m,m})-\gamma^2(i^{-1}_{1,1}))\underline{\underline{E}} = \underline{\underline{1}} \qquad \text{(E.23)}$$

Next, we look at $\underline{\underline{a}}^{-1}$, using

$\underline{\underline{a}}\ \underline{\underline{a}}^{-1} = \underline{\underline{1}}$ we have

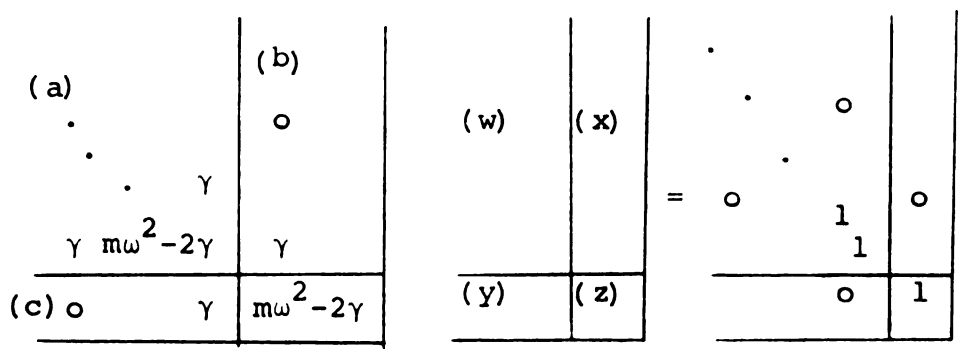

since $\underline{\underline{a}}$ is semi-infinite the partitioning of $\underline{\underline{a}}$ as shown gives $\underline{a}$ as one of its submatrices and we have

$$\underline{\underline{a}}\ \underline{x} + \underline{\underline{b}}\ z = 0 = \underline{x} \Rightarrow -\underline{\underline{a}}^{-1}\underline{\underline{b}}\underline{z}$$

$$\underline{\underline{c}}\ \underline{x} + (m\omega^2-2\gamma)z = 1$$

$$(-\underline{\underline{c}}\ \underline{\underline{a}}^{-1}\underline{\underline{b}} + (m\omega^2-2\gamma)z = 1$$

where $\underline{\underline{c}}\ \underline{\underline{a}}^{-1}\ \underline{\underline{b}} = \gamma^2 a^{-1}_{m,m}$

Since $z = a^{-1}_{m,m}$ we have

$$(-\gamma^2\ a^{-1}_{m,m} + (m\omega^2-2\gamma))a^{-1}_{m,m} = 1$$

or

$$a^{-1}_{m,m} = \frac{(m\omega^2-2\gamma) \pm \sqrt{(m\omega^2-2\gamma)^2-4\gamma^2}}{2\gamma^2} \qquad \text{(E.24)}$$

Next, if we similarly partition $\underline{\underline{i}}\ \underline{\underline{i}}^{-1} = 1$

we find

$$i^{-1}_{1,1} = a^{-1}_{m,m} \qquad \text{(E.25)}$$

and from Equation (E.24) we have,

$$g(o,\omega^2)=E= \frac{1}{m\omega^2-2\gamma-(m\omega^2-2\gamma-\sqrt{(m\omega^2-2\gamma)^2-4\gamma^2})}$$

$$g(o,\omega^2) = \frac{1}{m\sqrt{(\omega^2)}\sqrt{\omega^2-\omega_m^2}} \qquad \text{(E.26)}$$

where $\omega_m^2=\frac{4\gamma}{m}$ and we took the negative square root.
The only difficulty lies in the sign of the root of a^{-1}_{mm} we take. As Equation (E.26) is defined, it is $g(o,(\omega+i\varepsilon)^2)$. If we wanted $g(1,\omega^2)$ the matrix $\underline{\underline{e}}$ in Equation (E.22) will need to be a 2 by 2 and the matrix $\underline{\underline{E}}$ is given by

$$\underline{\underline{E}} = \begin{pmatrix} m\omega^2-2\gamma-\gamma^2 a^{-1}_{mm} & \gamma \\ \gamma & m\omega^2-2\gamma-\gamma^2 i^{-1}_{11} \end{pmatrix}^{-1}$$

$$= \begin{pmatrix} \frac{(m\omega^2-2\gamma)+\sqrt{m\omega^2(m\omega^2-4\gamma)}}{2} & \gamma \\ \gamma & \frac{m\omega^2-2\gamma+\sqrt{m\omega^2(m\omega^2-4\gamma)}}{2} \end{pmatrix}^{-1}$$

where we take the negative square root.

The determinant of $\underline{\underline{E}}$ is

$$\det(\underline{\underline{E}}) = \frac{m^2}{2}\sqrt{\omega^2(\omega^2-\omega_m^2)}\left[\sqrt{\omega^2(\omega^2-\omega_m^2)}+(\omega^2-\frac{\omega_m^2}{2})\right]$$

$$E = \begin{pmatrix} \dfrac{1}{m\sqrt{\omega^2(\omega^2-\omega_m^2)}} & \dfrac{-\omega_m^2}{2m\sqrt{\omega^2(\omega^2-\omega_m^2)}\sqrt{\omega^2(\omega^2-\omega_m^2)+(\omega^2-\frac{\omega_m^2}{2})}} \\ \dfrac{-\omega_m^2}{2m\omega\sqrt{\omega^2-\omega_m^2}(\omega\sqrt{\omega^2-\omega_m^2}+\omega^2-\frac{\omega_m^2}{2}} & \dfrac{1}{m\sqrt{\omega^2(\omega^2-\omega_m^2)}} \end{pmatrix}$$

(E.27)

Clearly, E_{11} and E_{22} are $g(o,\omega^2)$ as before. First, using Equation (E.8) with $\ell=1$ we have

$$g(1,\omega^2) = +\frac{2}{m\omega_m^2}\,\frac{-(\omega^2-\frac{\omega_m^2}{2})+\sqrt{\omega^2(\omega^2-\omega_m^2)}}{\sqrt{\omega^2}\sqrt{\omega^2-\omega_m^2}}$$

if we rationalize E_{12}, we have

$$E_{12} = \frac{2}{m\omega_m^2}\,\frac{-(\omega^2-\frac{\omega_m^2}{2})+\sqrt{\omega^2(\omega^2-\omega_m^2)}}{\sqrt{\omega^2(\omega^2-\omega_m^2)}}$$

$$= g(1,\omega^2) \qquad \text{Q.E.D.}$$

Comparing E_{12} with Equation (E.10), we see we again generate $g(1,(\omega+i\varepsilon)^2)$. For $g(2,\omega^2)$, we need to invert a 3x3.

In this case

$$E=\begin{pmatrix} g(0) & g(1) & g(2) \\ g(1) & g(0) & g(1) \\ g(2) & g(1) & g(0) \end{pmatrix} = \begin{pmatrix} m\omega^2-2\gamma-\gamma^2 a^{-1}_{mm} & \gamma & 0 \\ \gamma & m\omega^2-2\gamma & \gamma \\ 0 & \gamma & m\omega^2-2\gamma-\gamma^2 i^{-1}_{11} \end{pmatrix}^{-1}$$

This procedure can get quite messy for large L.

APPENDIX F

ISOLATED DEFECT CLUSTERS EMBEDDED IN A HOST CHAIN

If a light mass or cluster of light masses is embedded in a heavy mass chain, vibrational modes often appear in region forbidden to the pure host lattice. In Appendix I, we will look in detail at the single defect in a host chain. In this appendix, we will look at the impurity modes.

For the light defect mass, we define

$$\varepsilon = \frac{m-m'}{m} \tag{F.1}$$

where m is the mass of host chain atoms
and m' is the impurity mass.

For the single defect at the origin we can easily solve the Dyson equation

$$G = P + PCG \tag{F.2}$$

where $C(\ell,\ell') = \varepsilon m\omega^2 \delta_{\ell,0}\delta_{\ell',0}$
and P is the monatomic chain Green function. Upon reiteration we have

$$G(\ell\ell',\omega^2) = P(\ell,\ell',\omega^2) + \frac{\varepsilon\omega^2 m P(\ell,0,\omega) P(0,\ell',\omega)}{1-\varepsilon m\omega^2 P(0,0,\omega^2)} \tag{F.3}$$

We can find the local mode frequency from the pole of $G(00,\omega^2)$.

$$G(0,0,\omega^2) = P(0,0,\omega^2)/(1-\varepsilon m\omega^2 P(0,0,\omega^2)) \tag{F.4}$$

An impurity mode occurs at frequencies satisfying

$$1-\varepsilon m\omega^2 P(0,0;\omega^2) = 0 \qquad (F.5)$$

In Appendix E, we found

$$P(0,0;(\omega+i\varepsilon)^2) = \frac{1}{m\sqrt{\omega^2}\sqrt{\omega^2-\omega_m^2}}$$

and we have an impurity mode at

$$\omega^2 = \frac{\omega_m^2}{1-\varepsilon^2} \qquad (F.6)$$

for a mass ratio $\frac{m}{m'} = 2$, $\varepsilon=\frac{1}{2}$ and

$$\omega^2 = \frac{4}{3}\omega_m^2 = 2\,\frac{2}{3} \text{ for } \omega_m^2=2 \qquad (F.7)$$

Alternately, we could have found $G(0,0,\omega^2)$, by the inversion of $P^{-1}(\ell,\ell,\omega^2)$ with the element at the origin replaced by $m\omega^2(1-\varepsilon)-2\gamma$ in this case,

$$g(0,\omega^2) = (m\omega^2(1-\varepsilon)-2\gamma-\gamma^2 a_{mm}^{-1}-\gamma^2 i_{11}^{-1})^{-1} \qquad (F.8)$$

by using Equation (E.21) and

$$mg(0,\omega^2) = [\sqrt{\omega^2(\omega^2-\omega_m^2)}-\omega^2\varepsilon]^{-1} \qquad (F.9)$$

again, the impurity mode occurs at

$$\sqrt{\omega^2(\omega^2-\omega_m^2)}-\omega^2\varepsilon = 0$$

or

$$\omega^2 = \frac{\omega_m^2}{1-\varepsilon^2}$$

The utility of the inversion method becomes evident for the two defect cluster. The Dyson equation method becomes cumbersome at best whereas we can write the diagonal Green's functions for the cluster by matrix inversion almost by inspection. For the 2 defect cluster we have

$$E = \begin{pmatrix} m\omega^2(1-\varepsilon)-2\gamma-\gamma^2 a_{mm}^{-1} & \gamma \\ \gamma & m\omega^2(1-\varepsilon)-2\gamma-\gamma^2 i_{11}^{-1} \end{pmatrix}^{-1} \qquad \text{(F.10)}$$

For convenience, since $a_{mm}^{-1} = i_{11}^{-1}$ for the host chain, we will take

$$A = \gamma^2 a_{m,m}^{-1} = \gamma^2 i_{1,1}^{-1} = \frac{m\omega^2-2\gamma-\sqrt{m\omega^2(m\omega^2-4\gamma)}}{2} \qquad \text{(F.11)}$$

$$G(0,0,(\omega+i\varepsilon)^2) = G(1,1,(\omega+i\varepsilon)^2)$$

$$= \frac{-\omega^2\varepsilon + \frac{\omega^2-\frac{\omega_m^2}{2}+\sqrt{\omega^2(\omega^2-\omega_m^2}}{2}}{m\left[\left(-\omega^2\varepsilon + \frac{\omega^2-\frac{\omega_m^2}{2}+\sqrt{\omega^2(\omega^2-\omega_m^2)}}{2}\right)^2-\left(\frac{\omega_m^2}{4}\right)^2\right]} \qquad \text{(F.12)}$$

The denominator vanishes for

$$\omega^2 = \omega_m^2/[4\varepsilon\ (1-\varepsilon)] \tag{F.13}$$

and for

$$\omega^2 = \frac{\omega_m^2}{8(\varepsilon)(1-\varepsilon)}\ ((4\varepsilon-1)+\sqrt{1+8\varepsilon}) \tag{F.14}$$

for $\varepsilon=\frac{1}{2}$ Equation (F.13) gives $\omega^2=\omega_m^2$ and is not of much interest since the perfect chain has a zero denominator in the Green's function at $\omega^2=\omega_m^2$. However, for larger mass ratios ($\varepsilon>\frac{1}{2}$), a second mode emerges into the impurity band. Equation (F.14) gives for $\varepsilon=\frac{1}{2}$

$$\omega^2 = \frac{\omega_m^2}{2}(1+\sqrt{5}) = 1+\sqrt{5} \text{ for } \omega_m^2=2 \tag{F.15}$$

$$= 3.236068$$

For a three defect cluster two possible cluster configurations are present namely, d-d-d and d-h-d. For these cases

$$E = \begin{pmatrix} m(1-\varepsilon_1)\omega^2-2\gamma-A & \gamma & 0 \\ \gamma & m\omega^2(1-\varepsilon_2)-2\gamma & \gamma \\ 0 & \gamma & m(1-\varepsilon_1)\omega^2-2\gamma-A \end{pmatrix}^{-1} \tag{F.16}$$

where $\varepsilon_1 = \varepsilon$ and $\varepsilon_2 = 0$ or ε

and the determinant of $\underline{\underline{E}}$ gives the poles of the Green's function.

$$0 = \det(E) = (m\omega^2(1-\varepsilon)-2\gamma-A)((m(1-\varepsilon)\omega^2-2\gamma-A)(m\omega^2(1-\varepsilon_2)-2\gamma)-2\gamma^2)$$

The poles are at

$$\omega^2 = \omega_m^2 \left(\frac{\varepsilon+\sqrt{\varepsilon}}{4\varepsilon(1-\varepsilon)}\right) \qquad \text{(F.17)}$$

and

$$4\omega^6(1-\varepsilon_1)^2\varepsilon(\varepsilon-1))+2\omega^4\omega_m^2(1-\varepsilon_1)(3-(\varepsilon_1+2\varepsilon))\varepsilon$$

$$+ \frac{\omega_m^4\omega^2}{4}[(\varepsilon_1+2\varepsilon)^2-(1+8\varepsilon)]+\frac{\omega_m^6}{4} = 0 \qquad \text{(F.18)}$$

Equation (F.18) is cubic in ω^2 and we will solve it only for specific values of $\varepsilon, \varepsilon_1$ and ω_m^2. First, Equation (F.14) will introduce a mode into the impurity band for $\varepsilon > \frac{1}{4}$ or a mass ratio $\frac{M_H}{M_L} > 4/3$. For $\varepsilon = \frac{1}{2}$ and $\omega_m^2 = 2$ Equation (F.17) gives

$$\omega^2 = 1+\sqrt{2} = 2.414214 \qquad \text{(F.19)}$$

independent of the values of ε_1 indicating that the middle atom does not participate in this mode. For $\varepsilon_1 = 0$ (d-h-d), $\varepsilon = \frac{1}{2}$, $\omega_m^2 = 2$, we get

$$\omega^6-4\omega^4+4\omega^2-2 = 0$$

or $$\omega^2 = 2.8392868 \qquad \text{(F.20)}$$

for $\varepsilon_1=\frac{1}{2}$, $\varepsilon=\frac{1}{2}$ and $\omega_m^2=2$, we get

$$\omega^6-6\omega^4+11\omega^2-8 = 0 \qquad \text{(F.21)}$$

or $$\omega^2 = 3.5213797$$

This method with some algebra can be extended to many site defect clusters. For sake of brevity we will stop at three site defect clusters since n site defect clusters requires us to solve an n^{th} order polynomial for its roots.

APPENDIX G

DENSITY OF STATES OF PERIODIC LINEAR CHAINS WITH ALL FORCE CONSTANTS EQUAL

For a periodic linear chain, we can calculate the density of states using Equation (1.8) and

$$D(\omega^2) = \frac{1}{2\omega} \frac{a}{\pi} \frac{dk}{d\omega}. \tag{G.1}$$

For the monatomic chain, we get Equation (1.11) derived in text. For a two-site periodic system only the h-d binary chain is possible and Equation (1.8) gives

$$\begin{aligned} \omega^2\sigma_1 &= +\frac{2\gamma}{m_1}\sigma_1 - 2\gamma\cos(ka)\sigma_2/\sqrt{m_1m_2} \\ \omega^2\sigma_2 &= -\frac{2\gamma}{m_2}\sigma_2 - 2\gamma\cos(ka)\sigma_1/\sqrt{m_1m_2} \end{aligned} \tag{G.2}$$

The determinant of coefficients must vanish for a solution to exist, or

$$\begin{vmatrix} (\omega^2 - \frac{2\gamma}{m_1}) & \frac{2\gamma}{\sqrt{m_1m_2}}\cos ka \\ \frac{2\gamma}{\sqrt{m_1m_2}}\cos ka & \omega^2 - \frac{2\gamma}{m_2} \end{vmatrix} = 0$$

or

$$\frac{4\gamma^2}{m_1m_2}\sin^2 ka = (2\gamma(\frac{1}{m_1} + \frac{1}{m_2})\omega^2 - \omega^4) \tag{G.3}$$

$$k = \frac{1}{a}\sin^{-1}[\sqrt{\frac{m_1m_2}{4\gamma^2}}(\omega^2 2\gamma(\frac{1}{m_1} + \frac{1}{m_2}) - \omega^4)^{\frac{1}{2}}]$$

Then

$$\frac{dk}{d\omega} = \frac{1}{a}\sqrt{\frac{m_1 m_2}{\gamma}}\left(\frac{\gamma\left(\frac{1}{m_1}+\frac{1}{m_2}\right)-\omega^2}{\sqrt{\left(2\gamma\left(\frac{1}{m_1}+\frac{1}{m_2}\right)-\omega^2\right)\left[1-\frac{m_1 m_2}{4\gamma^2}\omega^2\left(2\gamma\left(\frac{1}{m_1}+\frac{1}{m_2}\right)-\omega^2\right)\right]}}\right.$$

upon simple factoring

$$D(\omega^2) = \frac{1}{\pi}\,\mathrm{Re}\left(\frac{\left(\gamma\left(\frac{1}{m_1}+\frac{1}{m_2}\right)-\omega^2\right)}{\sqrt{\omega^2}\sqrt{\left(2\gamma\left(\frac{1}{m_1}+\frac{1}{m_2}\right)-\omega^2\right)}\sqrt{\omega^2-\frac{2\gamma}{m_1}}\sqrt{\omega^2-\frac{2\gamma}{m_2}}}\right) \qquad \text{(G.4)}$$

For $m_1=m_2$, Equation (G.4) reduces to Equation (1.11).

For $m_1=2m_2$ and $\frac{\gamma}{m_2} = 1$,

$$D(\omega^2) = \frac{1}{\pi}\,\mathrm{Re}\left(\frac{(1.5-\omega^2)}{\sqrt{\omega^2}\sqrt{3-\omega^2}\sqrt{\omega^2-1}\sqrt{\omega^2-2}}\right. \qquad \text{(G.5)}$$

Figure 2.9 gives the comparative numerical frequency spectrum.

For a three-site periodic system, Equation (1.8) gives

$$\omega^2\sigma_1 = + \frac{2\gamma}{m_1}\sigma_1 - \frac{\gamma e^{ika}}{\sqrt{m_1 m_2}}\sigma_2 - \frac{\gamma e^{-ika}}{\sqrt{m_1 m_3}}\sigma_3$$

$$\omega^2\sigma_2 = \frac{2\gamma}{m_2}\sigma_2 - \frac{\gamma e^{-ika}}{\sqrt{m_2 m_1}}\sigma_1 - \frac{\gamma e^{ika}}{\sqrt{m_2 m_3}}\sigma_3 \qquad \text{(G.6)}$$

$$\omega^2\sigma_3 = \frac{2\gamma}{m_3}\sigma_3 - \frac{\gamma e^{ika}}{\sqrt{m_1 m_3}}\sigma_1 - \frac{\gamma e^{-ika}}{\sqrt{m_2 m_3}}\sigma_2$$

Again the determinant of coefficients must vanish for a non-zero solution to exist.

$$\begin{vmatrix} \omega^2 - \frac{2\gamma}{m_1} & \frac{\gamma e^{ika}}{\sqrt{m_1 m_2}} & \frac{\gamma e^{-ika}}{\sqrt{m_1 m_3}} \\ \frac{\gamma e^{-ika}}{\sqrt{m_1 m_2}} & \omega^2 - \frac{2\gamma}{m_2} & \frac{\gamma e^{ika}}{\sqrt{m_2 m_3}} \\ \frac{\gamma e^{ika}}{\sqrt{m_1 m_3}} & \frac{\gamma e^{-ika}}{\sqrt{m_2 m_3}} & \omega^2 - \frac{2\gamma}{m_3} \end{vmatrix} = 0$$

or

$$\omega^6 - \omega^4 2\gamma\left(\frac{1}{m_1} + \frac{1}{m_2} + \frac{1}{m_3}\right) + \omega^2\, 3\gamma^2\left(\frac{1}{m_1 m_2} + \frac{1}{m_1 m_3} + \frac{1}{m_2 m_3}\right)$$

$$+ \frac{2\gamma^3}{m_1 m_2 m_3}(-2)\sin^2\left(\frac{3ka}{2}\right) = 0$$

Therefore

$$k = \frac{2}{3a}\sin^{-1}\left[\sqrt{\frac{m_1 m_2 m_3}{4\gamma^3}}\ \sqrt{\omega^2}\ \sqrt{\omega^4 - \omega^2 2\gamma\left(\frac{1}{m_1} + \frac{1}{m_2} + \frac{1}{m_3}\right) + 3\gamma^2\left(\frac{1}{m_1 m_2} + \frac{1}{m_1 m_3} + \frac{1}{m_2 m_3}\right)}\ \right]$$

$$\frac{dk}{d\omega} = \frac{2}{3a}\sqrt{\frac{m_1 m_2 m_3}{4\gamma^3}}\left(3\omega^4 - 4\gamma\left(\frac{1}{m_1} + \frac{1}{m_2} + \frac{1}{m_3}\right)\omega^2 + 3\gamma^2\left(\frac{1}{m_1 m_2} + \frac{1}{m_2 m_3} + \frac{1}{m_1 m_3}\right)\right) /$$

$$\left[\sqrt{\omega^4 - \omega^2 2\gamma\left(\frac{1}{m_1} + \frac{1}{m_2} + \frac{1}{m_3}\right) + 3\gamma^2\left(\frac{1}{m_1 m_2} + \frac{1}{m_1 m_3} + \frac{1}{m_2 m_3}\right)}\right.$$

$$\times \sqrt{1-\omega^2\frac{m_1m_2m_3}{4\gamma^3}(\omega^4-2\gamma\omega^2(\frac{1}{m_1}+\frac{1}{m_2}+\frac{1}{m_3})+3\gamma^2(\frac{1}{m_1m_2}+\frac{1}{m_1m_3}+\frac{1}{m_2m_3})}\,]$$

$\frac{dk}{d\omega}$ has zeros at

$$\omega^2=\frac{2\gamma}{3}(+(\frac{1}{m_1}+\frac{1}{m_2}+\frac{1}{m_3})\pm\sqrt{\frac{4}{m_1^2}+\frac{4}{m_2^2}+\frac{4}{m_3^2}-(\frac{1}{m_1m_2}+\frac{1}{m_1m_3}+\frac{1}{m_2m_3})})$$
$$2$$

which we designate $\omega^2_{r+}, \omega^2_{r-}$

and poles at

$$\omega^2 =\gamma(\frac{1}{m_1}+\frac{1}{m_2}+\frac{1}{m_3}\pm\sqrt{\frac{1}{m_1^2}+\frac{1}{m_2^2}+\frac{1}{m_3^2}-(\frac{1}{m_1m_2}+\frac{1}{m_1m_3}+\frac{1}{m_2m_3})}$$

which we designate ω^2_{p+} and ω^2_{p-}

$$D(\omega^2) =\frac{1}{\pi}\,\mathrm{Re}\Bigg(\frac{(\omega^2-\omega^2_{r+})(\omega^2-\omega^2_{r-})}{\sqrt{\omega^2}\sqrt{\omega^2-\omega^2_{p+}}\sqrt{\omega^2-\omega^2_{p-}}\sqrt{\frac{4\gamma^3}{m_1m_2m_3}-3\gamma^2\omega^2(\frac{1}{m_1m_2}+\frac{1}{m_1m_3}+\frac{1}{m_2m_3})+}}$$

$$\sqrt{2\gamma\omega^4(\frac{1}{m_1}+\frac{1}{m_2}+\frac{1}{m_3})-\omega^6}\Bigg) \qquad (G.7)$$

For $m_1=m_2=m_3$ we again get Equation (1.11) as a check to our calculations. There are two other unique combination both with $m_1=m_3$,

Case 1: $m_1 = 2m_2$ and Case 2: $m_2 = 2m_1$

For Case 1, $\frac{\gamma}{m_2} = 1$ and the density of states has zeros at

$$\omega^2 = \frac{4}{3}\left(1\pm\frac{\sqrt{19}}{8}\right) = .60685,\ 2.05986$$

and poles at $0,\ \tfrac{1}{2},\ 2\pm\tfrac{1}{2},\ \tfrac{1}{4}(7\pm\sqrt{17})$

$$= 0,\ .5,\ .719224,\ 1.5,\ 2.5,\ 2.78078.$$

and

$$D(\omega^2)=\frac{1}{\pi}\,\mathrm{Re}\left(\frac{(\omega^2-.60685)(\omega^2-2.05986)}{\sqrt{\omega^2}\sqrt{\omega^2-1.5}\sqrt{\omega^2-2.5}\ \sqrt{.5-\omega^2}\ \sqrt{\omega^2-.71922}\ \sqrt{\omega^2-2.78078}}\right) \tag{G.8}$$

Figure (G.1) gives a numerical spectrum for Case 1 (h-d-h).

For Case 2; $\frac{\gamma}{m_1} = 1$ and we have zeros in $D(\omega^2)$ at

$$\omega^2 = \frac{1}{3}(5\pm\sqrt{7}) = .78475,\ 2.54858$$

and poles at

$$\omega^2 = 0,\ 1,\ \tfrac{1}{2}\ (5\pm1),\ (2\pm\sqrt{2})$$

$$= 0,\ 1,\ 2,\ 3,\ .585786,\ 3.41421$$

and

$$D(\omega^2) = \frac{1}{\pi}\,\mathrm{Re}\left(\frac{(\omega^2-.78475)(\omega^2-2.54858)}{\sqrt{\omega^2}\sqrt{\omega^2-1}\sqrt{\omega^2-2}\sqrt{\omega^2-3}\sqrt{.585786-\omega^2}\sqrt{\omega^2-3.41421}}\right) \tag{G.9}$$

Figure (G.2) gives the corresponding numerical spectrum.

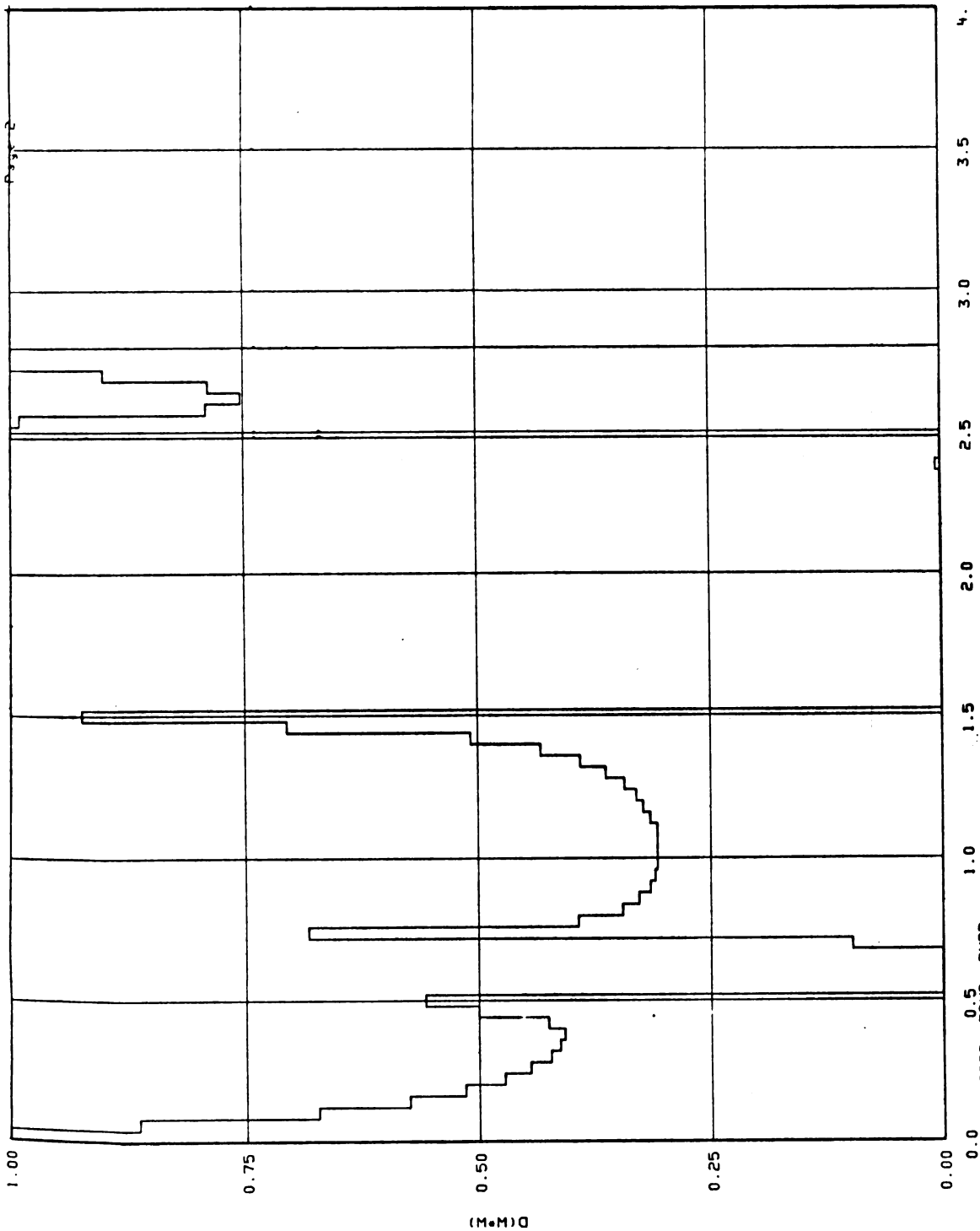

FIGURE G.1.--Density of states for 3 site-periodic system, h-h-d, and mass ratio 2/1.

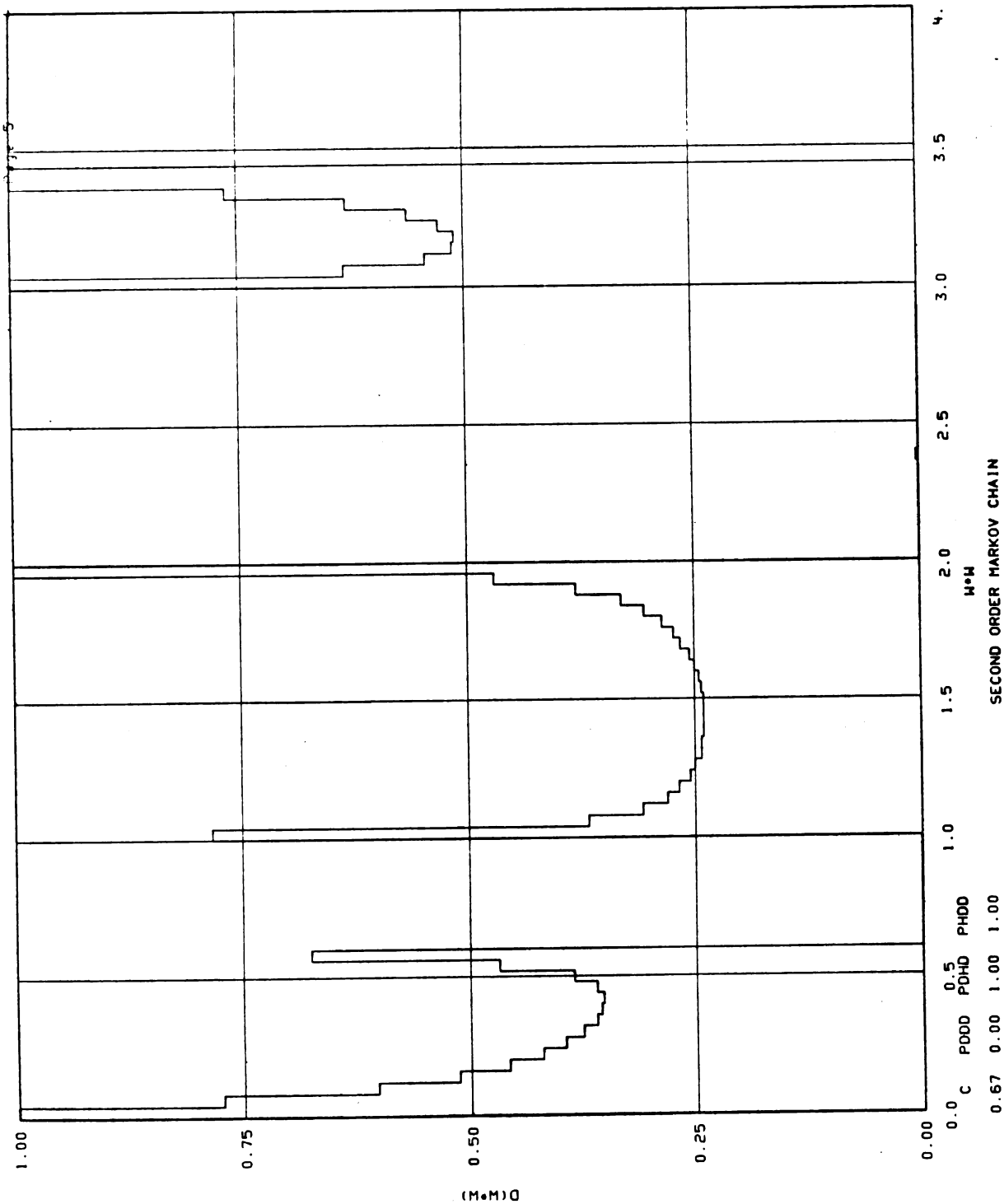

FIGURE G.2.--Density of states for a 3 site periodic system, d-d-h, and mass ratio 2/1.

Alternative Approach

A very useful alternative approach to the calculation of density of states for an n site periodic system is available. By the method of matrix inversion as described in Appendix E, we can generate the diagonal Green's functions for the system. The density of states is

$$D(\omega^2)=\frac{-1}{n\pi}\ \mathrm{Im}\ \sum_{\alpha=1}^{n} m_\alpha g_{\alpha\alpha}(0,0,(\omega^2+i\varepsilon)^2 \qquad \text{(G.9a)}$$

where α refers to atoms in the basis of an n site periodic system.

This approach is much simplier than at first it may seem for several basic reasons. First, the diagonal elements can be written in terms of continued fractions of the inverse matrix; also, the procedure is easily adaptable to computer calculation.

An additional benefit is we calculate the Green's function itself and can relatively easily calculate near off diagonal elements. The inverse Green's function for a two site periodic system is

$$G^{-1}_{\alpha\beta}(\ell,\ell',\omega^2)=\begin{pmatrix} \gamma & m_1\omega^2-2\gamma & \gamma & & & \\ & \gamma & m_2\omega^2-2\gamma & \gamma & & \\ & & \gamma & m_1\omega^2-2\gamma & \gamma & \\ & & & \gamma & m_2\omega^2-2\gamma & \gamma \\ & & & & \gamma & \end{pmatrix} \qquad \text{(G.10)}$$

Partitioning $G^{-1}G=1$ as we did in Equation (E.19) where $\underline{e}$ is now a 2x2 matrix, we find

$$\underline{\underline{E}} = \begin{pmatrix} m_1\omega^2-2\gamma-\gamma^2\, a_{mm}^{-1} & \gamma \\ \gamma & m_2\omega^2-2\gamma-\gamma^2 i_{11}^{-1} \end{pmatrix}^{-1} \tag{G.11}$$

where, following the arguments in Appendix E,

$$a_{mm}^{-1} = \begin{pmatrix} m_1\omega^2-2\gamma-\gamma^2 a_{mm}^{-1} & \gamma \\ \gamma & m_2\omega^2-2\gamma \end{pmatrix}^{-1}_{2,2} \tag{G.12}$$

and

$$i_{11}^{-1} = \begin{pmatrix} m_1\omega^2-2\gamma & \gamma \\ \gamma & m_2\omega^2-2\gamma-\gamma^2 i_{1,1}^{-1} \end{pmatrix}^{-1}_{1,1} \tag{G.13}$$

Therefore: $$a_{mm}^{-1} = \frac{1}{m_2\omega^2-2\gamma-\dfrac{\gamma^2}{m_1\omega^2-2\gamma-\gamma^2 a_{mm}^{-1}}}$$

and $$i_{1,1}^{-1} = \frac{1}{m_1\omega^2-2\gamma-\dfrac{\gamma^2}{m_2\omega^2-2\gamma-\gamma^2 i_{11}^{-1}}}$$

$$a_{mm}^{-1} = \frac{1}{2\gamma^2}\left(m_1\omega^2-2\gamma-\sqrt{\frac{m_1\omega^2-2\gamma}{m_2\omega^2-2\gamma}(\omega^2)\,(m_1m_2\omega^2-2\gamma(m_1+m_2))}\right)$$

$$i_{1,1}^{-1} = \frac{1}{2\gamma^2}\left(m_2\omega^2-2\gamma-\sqrt{\frac{m_2\omega^2-2\gamma}{m_1\omega^2-2\gamma}(\omega^2)\,[\,(m_1m_2\omega^2-2\gamma(m_1+m_2)\,]}\right)$$

Notice $a_{m,m}^{-1}$ and $i_{1,1}^{-1}$ are no longer equal.

$$G_{11}(0,0,(\omega+i\varepsilon)^2) = \frac{1}{m_1\omega^2-2\gamma-\gamma^2 a^{-1}_{mm} - \dfrac{\gamma^2}{m_2\omega^2-2\gamma-\gamma^2 i^{-1}_{11}}}$$

$$= \frac{1}{m_1} \frac{(\omega^2-\frac{2\gamma}{m_2})}{\sqrt{\omega^2}\sqrt{\omega^2-2\gamma(\frac{1}{m_1}+\frac{1}{m_2})}\ \sqrt{\omega^2-\frac{2\gamma}{m_1}}\sqrt{\omega^2-\frac{2\gamma}{m_2}}} \qquad (G.14)$$

$$G_{22}(0,0,(\omega+i\varepsilon)^2) = \frac{1}{m_2\omega^2-2\gamma-\gamma^2 i^{-1}_{11} - \dfrac{\gamma^2}{m_1\omega^2-2\gamma-\gamma^2 a^{-1}_{mm}}}$$

$$= \frac{1}{m_2} \frac{(\omega^2-\frac{2\gamma}{m_1})}{\sqrt{\omega^2}\sqrt{\omega^2-2\gamma(\frac{1}{m_1}+\frac{1}{m_2})}\ \sqrt{\omega^2-\frac{2\gamma}{m_1}}\sqrt{\omega^2-\frac{2\gamma}{m_2}}} \qquad (G.15)$$

The density of states from Equation (G.9a) is

$$D(\omega^2) = \frac{1}{\pi}\,\mathrm{Re}\,\frac{(\gamma(\frac{1}{m_1}+\frac{1}{m_2})-\omega^2)}{\sqrt{\omega^2}\sqrt{2\gamma(\frac{1}{m_1}+\frac{1}{m_2})-\omega^2}\sqrt{\omega^2-\frac{2\gamma}{m_1}}\sqrt{\omega^2-\frac{2\gamma}{m_2}}}$$

which is identical to Equation (G.4).

We can set up the three site (or the n site) periodic system Green's function by inspection! Being more explicit than necessary we have

$$\underline{\underline{E}} = \begin{pmatrix} m_1\omega^2-2\gamma-\gamma^2 a^{-1}_{m,m} & \gamma & 0 \\ \gamma & m_2\omega^2-2\gamma & \gamma \\ 0 & \gamma & m_3\omega^2-2\gamma-\gamma^2 i^{-1}_{1,1} \end{pmatrix}^{-1} \qquad (G.16)$$

where

$$a_{mm}^{-1} = \begin{pmatrix} m_1\omega^2-2\gamma-\gamma^2 a_{mm}^{-1} & \gamma & 0 \\ \gamma & m_2\omega^2-2\gamma & \gamma \\ 0 & \gamma & m_3\omega^2-2\gamma \end{pmatrix}^{-1}_{3,3} \tag{G.17}$$

and

$$i_{1,1}^{-1} = \begin{pmatrix} m_1\omega^2-2\gamma & \gamma & 0 \\ \gamma & m_2\omega^2-2\gamma & \gamma \\ 0 & \gamma & m_3\omega^2-2\gamma-\gamma^2 i_{11}^{-1} \end{pmatrix}^{-1}_{1,1} \tag{G.18}$$

In continued fractions, we would write

$$G_{11}(0,0,(\omega+i\varepsilon)^2) = \cfrac{1}{m_1\omega^2-2\gamma-\gamma^2 a_{mm}^{-1} - \cfrac{\gamma^2}{m_2\omega^2-2\gamma- \cfrac{\gamma^2}{m_3\omega^2-2\gamma-\gamma^2 i_{1,1}^{-1}}}} \tag{G.19}$$

$$G_{22}(0,0,(\omega+i\varepsilon)^2) = \cfrac{1}{m_2\omega^2-2\gamma-\cfrac{\gamma^2}{m_1\omega^2-2\gamma-\gamma^2 a_{mm}^{-1}} - \cfrac{\gamma^2}{m_3\omega^2-2\gamma-\gamma^2 i_{1,1}^{-1}}} \tag{G.20}$$

$$G_{33}(0,0,(\omega+i\varepsilon)^2)=\cfrac{1}{m_3\omega^2-2\gamma-\gamma^2 i_{11}^{-1}-\cfrac{\gamma^2}{m_2\omega^2-2\gamma-\cfrac{\gamma^2}{m_1\omega^2-2\gamma-\gamma^2 a_{m,m}^{-1}}}} \tag{G.21}$$

where

$$\gamma^2 a_{m,m}^{-1}=\cfrac{\gamma^2}{m_3\omega^2-2\gamma-\cfrac{\gamma^2}{m_2\omega^2-2\gamma-\cfrac{\gamma^2}{m_1\omega^2-2\gamma-\gamma^2 a_{m,m}^{-1}}}} \tag{G.22}$$

and

$$\gamma^2 i_{1,1}^{-1}=\cfrac{\gamma^2}{m_1\omega^2-2\gamma-\cfrac{\gamma^2}{m_2\omega^2-2\gamma-\cfrac{\gamma^2}{m_3\omega^2-2\gamma-\gamma^2 i_{1,1}^{-1}}}} \tag{G.23}$$

We can solve these equations relatively easily by hand and almost trivally by numerical computer techniques. For the three site periodic system, we have shown that $m_1=m_3\neq m_2$ give all possible spectra that can result from a three site periodic system except for the trival case, $m_1=m_2=m_3$, the monatomic lattice which is really a one site periodic system. For $m_1=m_3$, $\gamma^2 a_{m,m}^{-1} = \gamma^2 i_{1,1}^{-1}$ (only true for this special condition), and $G_{11}(0,0,\omega^2)=G_{33}(0,0,\omega^2)$.

$$G_{11}(0,0,(\omega+i\varepsilon)^2) = G_{33}(0,0(\omega+i\varepsilon)^2)$$

$$= \frac{1}{m_1}\left(\frac{-(\omega^4-2\gamma(\frac{1}{m_1}+\frac{1}{m_2})\omega^2+\frac{3\gamma^2}{m_1m_2})}{\sqrt{\omega^2}\sqrt{\omega^2-\omega_{r1}^2}\sqrt{\omega^2-\omega_{r2}^3}\sqrt{\omega^2-\omega_{r3}^2}\sqrt{\omega^2-\omega_{r4}^2}\sqrt{\omega^2-\omega_{r5}^2}}\right) \qquad \text{(G.24)}$$

where

$$\omega_{r1}^2 = \frac{\gamma}{m_1}$$

$$\omega^2_{\substack{r2\\r3}} = \gamma\left(\frac{2}{m_1}+\frac{1}{m_2} \pm \sqrt{\left(\frac{1}{m_1}-\frac{1}{m_2}\right)^2}\right)$$

$$\omega^2_{\substack{r4\\r5}} = \frac{\gamma}{2}\left(\frac{3}{m_1}+\frac{2}{m_2} \pm \sqrt{\left(\frac{9}{m_1^2}+\frac{4}{m_2^2}-\frac{4}{m_1m_2}\right)}\right)$$

$$G_{22}(0\rho,(\omega+i\varepsilon)^2) = \frac{1}{m_2}\frac{-(\omega^4-\frac{4\gamma}{m_1}\omega^2+\frac{3\gamma}{m_1^2})}{\sqrt{\omega^2}\sqrt{\omega^2-\omega_{r1}^3}\sqrt{\omega^2-\omega_{r2}^2}\sqrt{\omega^2-\omega_{r3}^2}\sqrt{\omega^2-\omega_{r4}^2}\sqrt{\omega^2-\omega_{r5}^2}}$$

(G.25)

The density of states is

$$D(\omega^2)=\frac{-1}{3\pi}\,\mathrm{Im}(2m_1G_{11}(0,0,(\omega+i\varepsilon)^2)+m_2G_{22}(0,0,(\omega+i\varepsilon)^2))$$

$$= \frac{1}{\pi}\,\mathrm{Re}\left(\frac{(\omega^2-\omega_+^2)(\omega^2-\omega_-^2)}{\sqrt{\omega^2}\sqrt{\omega_{r1}^2-\omega^2}\sqrt{\omega^2-\omega_{r2}^2}\sqrt{\omega^2-\omega_{r3}^2}\sqrt{\omega^2-\omega_{r4}}\sqrt{\omega^2-\omega_{r5}}}\right)$$

(G.26)

Where

$$\omega_{\pm}^2 = \frac{\gamma}{3}\left(\frac{4}{m_1}+\frac{2}{m_2} \pm \sqrt{\frac{7}{m_1^2} + \frac{4}{m_2^2} - \frac{2}{m_1 m_2}}\right)$$

This is identical with Equation (G.7) with $m_1=m_3$.

APPENDIX H

SELF-CONSISTENT SINGLE SITE APPROXIMATION

D. Taylor in 1968 first derived, the results we will now present. We present this derviation for two reasons. First, it is necessary for the sake of completeness of this thesis and, second, the published papers all contain misprints. From Equation (5.49) in text, we can write the self consistent condition

$$\langle \underline{\underline{t}}_s \rangle = 0 = C_d \underline{\underline{t}}_{ds}^{d} + (1-C_d)\underline{\underline{t}}_s^{h} \tag{H.1}$$

where

$$\underline{\underline{t}}_s^{\delta} = (1-(\underline{\underline{C}}_s^{\delta}-\underline{\underline{\sigma}}_s)\underline{\underline{R}})^{-1}(\underline{\underline{C}}_s^{\delta}-\underline{\underline{\sigma}}_s) \tag{H.2}$$

The subscripts indicate a site representation where the matrix $\underline{\underline{Q}}_s$ is zero except at the site (s,s). For the single site,

$$\underline{\underline{C}}_s^{d} = m\omega^2(1-\varepsilon) \tag{H.3}$$

$$\underline{\underline{C}}_s^{h} = 0 \tag{H.4}$$

For convenience, we take

$$\underline{\underline{\sigma}}_s = m\omega^2(1-\bar{\varepsilon}) \tag{H.5}$$

For a single site, the matrices can be treated as scalars; whereupon Equation (H.1) becomes

$$0 = \frac{C_d(\varepsilon-\bar{\varepsilon})}{(1-m\omega^2(\varepsilon-\bar{\varepsilon})R_{00})} + \frac{(1-C_d)(-\bar{\varepsilon})}{(1+m\omega^2\bar{\varepsilon}R_{00})}$$

We can rearrange and solve for R_{00}, getting

$$R_{oo} = \frac{\bar{\varepsilon}-C_d\varepsilon}{(\varepsilon-\bar{\varepsilon})\bar{\varepsilon}m\omega^2} \tag{H.6}$$

Now, we must solve for R_{00} and substitute into Equation (H.6). Since

$$\underline{\underline{R}}^{-1} = \underline{\underline{P}}^{-1} - \underline{\underline{g}} \tag{H.7}$$

where $\underline{\underline{P}}$ is the perfect chain Green's function and $\underline{\underline{g}}$ is diagonal. We can take the k space transformation since $\underline{\underline{R}}$ possesses the symmetry of the monatomic crystal.

$$R(k) = (P^{-1}(k)-\omega^2\bar{\varepsilon})^{-1} \tag{H.8}$$

Since $P(k) = \frac{1}{\omega^2-\omega_j^2(k)}$,

$$R(k) = \frac{1}{\omega^2(1-\bar{\varepsilon})-\omega_j^2(k)} \tag{H.9}$$

The inverse transform is now obvious when we look at the perfect monatomic chain Green's function derivation in Appendix G.

$$R(\ell,\ell',\omega^2) = P(\ell,\ell',\omega^2(1-\bar{\varepsilon})) \tag{H.10}$$

and

$$R(0,0,\omega+i\delta)^2) = \frac{1}{m} \frac{1}{(\omega^2(1-\bar{\varepsilon}))^{\frac{1}{2}}(\omega^2(1-\bar{\varepsilon})-\omega_m^2)^{\frac{1}{2}}} \tag{H.11}$$

Alternatively, we could have derived $R(0,0(\omega+i\delta)^2)$ by the real space inversion of an Equation (H.7). Using the methods of Appendix E, we have

$$R(0,0;(\omega+i\delta)^2) = \frac{1}{m\omega^2-2\gamma-\sigma-2\gamma^2 A} \tag{H.12}$$

where

$$A = \frac{1}{m\omega^2-2\gamma-\sigma-\gamma^2 A} \tag{H.13}$$

or

$$A = \frac{1}{2\gamma^2}(m\omega^2-2\gamma-\sigma-\sqrt{(m\omega^2-2\gamma-\sigma)^2-4\gamma^2}) \tag{H.14}$$

and

$$R(0,0(\omega+i\delta)^2) = \frac{1}{(m\omega^2-\sigma)^{\frac{1}{2}}(m\omega^2-\sigma-4\gamma)^{\frac{1}{2}}}$$

substituting $\sigma=m\omega^2\bar{\varepsilon}$ and $\frac{4\gamma}{m} = \omega_m^2$, we get Equation (H.11).

Substituting $R(0,0(\omega+i\delta)^2)$ into Equation (H.6) and squaring to remove the radical, we get

$$\frac{(\varepsilon-\bar{\varepsilon})^2\bar{\varepsilon}^2\omega^2}{(\bar{\varepsilon}-C_d\varepsilon)^2} = (1-\bar{\varepsilon})(\omega^2(1-\bar{\varepsilon})-\omega_m^2)$$

First dividing each side by ω_m^2 and defining $x = \frac{\omega^2}{\omega_m^2}$, we, then, collect terms in powers of $\bar{\varepsilon}$.

$$\bar{\varepsilon}^3[2x(1-\varepsilon(1-C_d))-1]$$

$$+\bar{\varepsilon}^2[x(\varepsilon^2(1-C_d^2)-(1+4\varepsilon C_d))+1+2\varepsilon C_d]$$

$$+\bar{\varepsilon}[C_d\varepsilon(\varepsilon C_d-2(1+C_d\,\varepsilon)(1-x))]$$

$$+C_d^2\varepsilon^2(1-x) = 0 \qquad \text{(H.15)}$$

This equation has three roots, all three will be real or one will be real and the others complex conjugate numbers. When all three roots are real, the Green's function will always be real, i.e., the density of states will be zero. The single real root, we can discard as unphysical. To get $R(\omega+i\delta)^2$ we have to take the complex root with the negative imaginary part. Then, the density of states is

$$D(\omega^2) = -\frac{1}{\pi}\,\mathrm{Im}\,R(0,0;\omega^2) \qquad \text{(H.16)}$$

Finally, we wish to examine two special cases of Equation (H.15). First, for $C_d=0$ or equivalently, $\varepsilon=0$, we get $\bar{\varepsilon}=0$ which gives $\underline{\underline{R}}=\underline{\underline{P}}$, the perfect chain Green function. Second, for $C_d=1$, we get $\bar{\varepsilon}=\varepsilon$ which gives

$$R = \frac{1}{m}\,\frac{1}{(\omega^2(1-\varepsilon))^{\frac{1}{2}}(\omega^2(1-\varepsilon)-\omega_m^2)^{\frac{1}{2}}} \qquad \text{(H.17)}$$

This is the Green's function of the chain with mass $m(1-\varepsilon)$ where $\omega_m^2 = \omega_m^2/(1-\varepsilon)$. Therefore, the self-consistent method presented in this thesis is exact in both limits $C_d \to 0\,(\varepsilon\to 0)$ and $C_d \to 1$.

APPENDIX I

ISOLATED DEFECT IN A MONATOMIC HOST CHAIN

In this appendix, we will briefly examine the eigenvectors and localization parameter for a monatomic chain and a diatomic ordered binary chain of length, N. Next, we will explore, the effect a single defect, either lighter or heavier than the host mass, has on the eigenfrequencies and eigenvectors of a monatomic chain. For the monatomic chain the equations of motion are

$$U_{n+1} = (2-\frac{m}{\gamma}\omega^2)U_n - U_{n-1} \qquad (I.1)$$

In text, we showed that we could diagonalize this coupled set of equations by expanding in running waves

$$U_n = U\, e^{\pm ikna} \qquad (I.2)$$

This solution for the eigenvector is valid for an infinite chain and for chains with periodic boundary conditions. For fixed boundary conditions, we can expand in a linear combination of outgoing and incoming waves.

$$U_n = U\, e^{ikna} + U^* e^{-ikna} \qquad (I.3)$$

where $U \equiv U^{(1)} + iU^{(2)}$

subject to the boundary condition $U_n = 0$ and $U_{N+1} = 0$.

For $U_0 = 0$ we have

$$U = -U^{(2)}$$

and

$$U_n = U \sin(kna) \tag{I.4}$$

For $U_{N+1} = 0$

$$U \sin(k(N+1)a) = 0$$

or

$$k = \frac{\pi r}{(N+1)a} \text{ , r-integer} \tag{I.5}$$

Substituting Equation (I.4) into Equation (I.1), we get

$$\omega^2 = \omega_m^2 \sin^2(\frac{ka}{2}) \tag{I.6}$$

where

$$\omega_m^2 = \frac{4\gamma}{m}$$

and $$k = \frac{\pi r}{(N+1)a} \quad r = 1, 2 \ldots, N \tag{I.7}$$

Equation I.6 is identical to the equation in text. The eigenvector for a given value of r is

$$U_n = U \sin(\frac{\pi rn}{N+1}) \tag{I.8}$$

The localization parameter α is

$$\alpha = \frac{\sum_{n=1}^{N} |U_n|^4}{\left(\sum_{n=1}^{N} |U_n|^2\right)^2} \qquad (I.9)$$

First, since

$$\sum_{q=1}^{N} \sin^2(qx) = \frac{N}{2} - \frac{\cos[(N+1)x]\sin(Nx)}{2\sin(x)} \quad (1.351.1)^{39}$$

we will want to evaluate

$$\sum_{n=1}^{N+1} |U_n|^2 \equiv \sum_{n=1}^{N} U_n^2 \quad (\text{since } U_{N+1} \equiv 0)$$

$$= \sum_{n=1}^{N+1} U^2 \sin^2\left(\frac{\pi rn}{N+1}\right) = \left(\frac{N+1}{2} - \frac{\cos\left(\frac{(N+2)r\pi}{N+1}\right)\sin(\pi r)}{2\sin\left(\frac{\pi r}{N+1}\right)}\right) U^2$$

$$= \frac{N+1}{2} U^2 \qquad (I.10)$$

Since $\sin(\pi r) = 0$ for all r.

Next since

$$\sum_{q=1}^{N} \sin^4(qx) = \frac{1}{8}\{3N + \cos[2(N+1)x]\sin(2Nx)\operatorname{cosec}(2x)$$

$$-4\cos[(N+1)x]\sin(Nx)\operatorname{cosec}(x)\}$$

we again add the N+1 term to the sum

$$\sum_{n=1}^{N+1} (U_n)^4 = \sum_{n=1}^{N+1} U^4 \sin^4\left(\frac{\pi rn}{N+1}\right) = \frac{3(N+1)}{8} U^4 \qquad (I.11)$$

since $\sin(2\pi r) = \sin(\pi r) = 0$

Therefore $$\alpha = \frac{3}{2}\frac{1}{N+1} \tag{I.12}$$

For N=100, $\alpha = .01485$

and For N=1000, $\alpha = .0014985$

For the ordered binary chain, the equations of motion are

$$\begin{aligned} U_{2n+1} &= (2-\frac{m_1}{\gamma}\omega^2)U_{2n}-U_{2n-1} \\ U_{2n+2} &= (2-\frac{m_2}{\gamma}\omega^2)U_{2n+1}-U_{2n} \end{aligned} \tag{I.13}$$

where for a fixed boundary conditions n takes on the values 1 to N/2. We take the eigenvectors to have the form

$$U_{2n} = U \sin(ka2n) \tag{I.14}$$

$$U_{2n+1} = U \sin(ka(2n+1)) \tag{I.15}$$

From the boundary conditions, we have

$U_0=0$ satisfied by Equation (I.15) with (n=0) and $U_{N+1}=0$ giving

$$k = \frac{\pi r}{N+1} \text{ (r integer)} \tag{I.16}$$

as before. Using Equations (I.14) and (I.15) in Equations (I.14), we have

$$2U\cos(ka) = (2 - \frac{m_1}{\gamma}\omega^2)U'$$

$$2U'\cos(ka) = (2 - \frac{m_2}{\gamma}\omega^2)U$$

And from (G.3)

$$\omega^2 = \frac{\gamma}{m_1} + \frac{\gamma}{m_2} \pm \sqrt{(\frac{\gamma}{m_1}+\frac{\gamma}{m_2})^2 - 4(\frac{\gamma^2}{m_1 m_2})\sin^2 ka} \qquad (I.17)$$

For each value of k, we get two eigenvalues and eigenvectors; therefore, for

$$k = \frac{\pi r}{(N+1)a}, \quad r=1, 2, \ldots, \frac{N}{2} \qquad (I.18)$$

will give all eigenvalues.

For our case $\frac{m_2}{m_1} = 2$, $\frac{\gamma}{m_1} = 1$, and $\frac{\gamma}{m_2} = \frac{1}{2}$ and we have

$$\omega_{\pm}^2 = \frac{3}{2} \pm \sqrt{\frac{9}{4} - 2\sin^2(\frac{\pi r}{N+1})} \qquad (I.19)$$

$$U_{2n} = U \frac{(-1 \pm \sqrt{9-8\sin^2(\frac{\pi r}{N+1})})}{2\cos(\frac{\pi r}{N+1})} \sin(\frac{\pi r 2n}{N+1}) \qquad (I.20)$$

$$U_{2n+1} = U \sin(\frac{\pi r(2n+1)}{N+1}) \qquad (I.21)$$

We can find approximate localization values near the band edges fairly easily. First, for r=1 and N large, we take

$$\sin(\frac{\pi}{N+1}) \simeq 0$$

and $$\cos\frac{\pi}{N+1} \simeq 1$$

The two eigenvalues are

$$\omega^2 \simeq 0,3 \tag{I.22}$$

For $\omega^2 \simeq 0$, the eigenvector is

$$U_{2n} \simeq U \sin\left(\frac{\pi}{N+1} 2n\right)$$

$$U_{2n+1} = U \sin\left(\frac{\pi}{N+1}(2n+1)\right)$$

or $$U_n = U \sin\left(\frac{\pi n}{N+1}\right) \tag{I.23}$$

Near $\omega^2=0$ the localization α is nearly the same value as in the monatomic chain.

For $\omega^2 \simeq 3$, $U_{2n} = -2U \sin\left(\frac{\pi 2n}{N+1}\right)$

$$U_{2n+1} = U \sin\left(\frac{\pi(2n+1)}{N+1}\right) \tag{I.24}$$

or the light masses are vibrating in opposite direction of the heavy masses with twice the amplitude of the heavy masses. Then we have

$$\sum_{n=1}^{N} U^2_n = \sum_{n=1}^{N/2} U^2_{2n} + \sum_{n=1}^{N/2} U^2_{2n+1}$$

$$= 4U^2 \sum_{n=1}^{N/2} \sin^2\left(\frac{\pi 2n}{N+1}\right) + U^2 \sum_{n=1}^{N/2} \sin^2\left(\frac{\pi(2n+1)}{N+1}\right)$$

$$\simeq U^2\left(5\ \frac{N}{4}\right)$$

and $\sum_{n=1}^{N} U_n^4 \simeq \frac{17}{8}(\frac{3N}{2})\ U^4$

and $\alpha = \frac{51}{25}\frac{1}{N}$, (I.25)

For N = 100, $\alpha \simeq .0204$

and for N=1000, $\alpha \simeq .00204$

Whether we should take N or N+1 in the above equation is questionable but doesn't matter within the error of the approximation.

For $r=\frac{N}{2}$, we take

$\sin\ (\frac{\pi}{2}\ \frac{N}{N+1}) \simeq 1$

and $\cos\ (\frac{\pi}{2}\ (\frac{N}{N+1})) \simeq 0$

The eigenvalues are $\omega^2 = 1,2$ (I.26)

For $\omega^2 = 1$, $U_{2n} \simeq 0$

and $U_{2n+1} = U \sin(\pi(2n+1)(\frac{N}{N+1})$ (I.27)

for $\omega^2 = 2$, $U_{2n+1} = 0$

$U_{2n} = U' \sin(\pi 2n(\frac{N}{N+1}))$ (I.28)

Within our approximation, these two eigenvectors will have the same localization, α.

$$\alpha = \frac{\sum_{n=1}^{N} U_n^4}{\left| \sum_{n=1}^{N} U_n^2 \right|^2} \simeq \frac{3}{N} \qquad \text{(I.29)}$$

For N=100, α =.03

and for N=1000, α = .003.

Before looking at the single defect, we will examine the eigenvector of the monatomic chain in greater detail. For small eigenvalues, r=1, 2 .. the eigenvector is a sine wave with period $2(\frac{N+1}{r})$. For large eigenvalues (N+1)-p, p = 1,2,3...

$$U_n = U \sin\left(\frac{(N+1)-p\ \pi n}{N+1}\right) = -\cos(n\pi)\sin\left(\frac{n\pi p}{N+1}\right)$$

$$U_n = (-1)^{n+1} \sin\left(\frac{n\pi p}{N+1}\right) \qquad p=1,2,3\ ..$$

This is the product of a wave where all the atoms are vibrating in opposite directions and an envelope function $\sin(\frac{n\pi p}{N+1})$.

Increasing p, increases the number of nodes in the envelope function and therefore decreases the number of nodes of the alternating chain giving lower frequency. If N is odd, then N+1 is even and atom at (N+1)/2 will be at a node for all r or p odd. Other atoms in the chain can also be at nodes. If N is even, then N+1 is odd. First if N+1 is a prime number, then no atom can ever be at a node. If (N+1) is odd but not prime, then no atom can be at a node at p or $r = 2^j$, $j=0,1,2,\ldots,{}^{\ln(N)}/_{\ln(2)}$.

If we place a single heavy defect in a light chain, Rayleigh's theorem says that all eigenfrequencies may decrease but not more than to the next lowest eigenvalue of the perfect chain. For an almost infinite heavy mass placed at or as close as possible to the center of the chain, we can easily demonstrate this theorem. First, if N is even the heavy defect is placed at N/2, dividing the chain into one even chain of length N/2 and one odd chain of length N/2-1. The heavy mass almost acts like a fixed boundary. The eigenvalues of the short chain are

$$\omega_s^2 \simeq \omega_m^2 \sin^2\left(\frac{\pi r'}{N}\right) \tag{I.30}$$

$$r' = 1,2 \ldots N/2-1$$

And the eigenvalues of the longer chain are

$$\omega_L^2 = \omega_m^2 \sin^2\left(\frac{\pi r''}{N+2}\right) \tag{I.31}$$

$$r'' = 1, 2, 3 \ldots N/2$$

compared to Equation (I.7) for the monatomic chain. First, we see we lose the lowest frequency mode $\omega^2 \simeq 0$, r=1 for the infinite defect. For a very heavy defect, this mode will be the only mode to propagate throughout the chain. The r=even modes become the modes of the longer chain ($r=2r''$) and the energy shift is

$$\Delta\omega_r^2 = \omega_m^2[\sin^2(\frac{\pi r''}{N+1}) - \sin^2(\frac{\pi r''}{N+2})]$$

$$= \omega_m^2 \sin[(\pi r'')\frac{2N+3}{(N+1)(N+2)}]\sin[(\pi r'')\frac{1}{(N+1)(N+2)})] \quad (I.32)$$

$$r = 1, 2, \ldots N/2$$

The r=odd modes become the modes of the shorter chain with frequency shift ($r=2r'+1$)

$$\Delta\omega_{r'}^2 = \omega_m^2[\sin^2(\frac{(2r'+1)\pi}{2(N+1)}) - \sin^2(\frac{\pi r'}{N})]$$

$$r' = 1, 2, 3, \ldots N/2-1$$

$$\Delta\omega_{r'}^2 = \omega_m^2 \sin(\pi\frac{4r'N+N+2r'}{2N(N+1)})\sin(\pi\frac{N-2r'}{2N(N+1)}) \quad (I.33)$$

The long chain frequency shift increases with increasing r'' and the short chain frequency shift decreases for increasing r'. Therefore, we expect the modes to cluster in groups of 2 near $\omega^2=0$ and ω_m^2 and be well separated from one another for $\omega^2 \simeq \omega_m^2/2$.

If N is odd, the heavy defect is placed at $\frac{N+1}{2}$ dividing the chain into two equal chains of length $(N-1)/2$ separated by the heavy defect. If the heavy defect is infinite, we have two identical short chains with two fold degenerate eigenvalues at

$$\omega^2 = \omega_m^2 \sin^2(\frac{\pi r'}{N+1}) \quad (I.34)$$

$$r' = 1, 2, \ldots, \frac{N-1}{2} .$$

For this case, the even modes of the perfect chain remain unchanged with the odd modes shifting as far as Rayleigh's theorem allows; that is, the r odd modes have an energy decrease of exactly the spacing between the eigenfrequencies of the perfect chain. The non-shift in r even modes is not surprizing when we recall that for N odd (N+1, even) the atom at $\frac{N+1}{2}$ is stationary for the r even modes; therefore, the heavy defect cannot affect these modes giving the same eigenvector as the perfect chain. For the r odd modes, where the atom at $\frac{N+1}{2}$ is at an antinode for the perfect chain, the heavy atom chokes this displacement giving a mode symmetric about $(\frac{N+1}{2})$ instead of the antisymmetric r-even mode.

$$U_n = U \sin\left(\frac{r\pi n}{N+1}\right)$$

for r-even modes

and
$$U_n = U \sin \frac{r'\pi n}{N+1} \qquad n=0,\ 1,\ \ldots\ \frac{N+1}{2}$$
$$= -U \sin\left(\frac{r'\pi n}{N+1}\right) \qquad n=\frac{N+1}{2},\ \ldots,\ N$$

for distorted r-odd modes.

These modes can also be found by symmetry considerations as the modes of two identical length chains placed side by side.

To consider the case of one light impurity in a heavy chain, we look at an impurity of almost zero mass.

The isolated frequency in the impurity band occurs near $\omega^2=\infty$. The almost zero light mass creates an unusual boundary between the two light chains. We are therefore restricted to a qualitative analysis versus a quantitative approach. For N odd (N+1 even) the light mass divides the chain into two identical small chain of length $(\frac{N-1}{2})$. The r even modes (eigenvalues and eigenvectors) of the perfect heavy chain will remain unchanged since the atom at $\frac{N+1}{2}$ is at a node for r even. For r odd, the atom at $\frac{N+1}{2}$ is at an antinode for the perfect chain. For r small, we have

$$U_{\frac{N-1}{2}} \simeq U_{\frac{N+1}{2}} \simeq U_{\frac{N+3}{2}}$$

and the light mass at $U_{\frac{N+1}{2}}$ will not greatly effect this mode. For r large ($\simeq$N), we have

$$U_{\frac{N-1}{2}} \simeq -U_{\frac{N+1}{2}} \simeq U_{\frac{N+3}{2}}$$

for the perfect chain. The effect of the light mass ($\simeq$0) at $U_{\frac{N+1}{2}}$ will be to make

$$U_{\frac{N+3}{2}} \simeq U_{\frac{N-1}{2}} \simeq 0$$

causing a frequency shift to the next highest frequency of the perfect lattice. For r large, the zero mass

defect acts much like the infinite mass defect but for r small, the zero mass defect hardly disturbs the perfect system.